ZooKeys 833: 1–20 (2019)
doi: 10.3897/zookeys.833.30689
http://zookeys.pensoft.net

RESEARCH ARTICLE

A peer-reviewed open-access journal
ZooKeys
Launched to accelerate biodiversity research

Discovery of *Neonrosella vitiata* (Darwin) and *Newmanella spinosus* Chan & Cheang (Balanomorpha, Tetraclitidae) from the Andaman Sea, eastern Indian Ocean

Woranop Sukparangsi[1], Ashitapol Pochai[2], Chinnakit Wongkunanusorn[3], Salinee Khachonpisitsak[1]

1 *Department of Biology, Faculty of Science, Burapha University, 169 Long-Hard Bangsaen Road, Saen Suk, Mueang, Chon Buri, 20131 Thailand* **2** *Takuapa Senanukul School, 15 Phet Kasem Road, Bang Nai Si, Takua Pa, Phang-Nga, 82110 Thailand* **3** *Biology Program, Department of Biology, Faculty of Science, Burapha University, 169 Long-Hard Bangsaen Road, Saen Suk, Mueang, Chon Buri, 20131 Thailand*

Corresponding author: *Salinee Khachonpisitsak* (salineek@go.buu.ac.th)

Academic editor: *Kai Horst George* | Received 19 October 2018 | Accepted 1 March 2019 | Published 25 March 2019

http://zoobank.org/7716B2EA-10C2-4F95-A4A2-702ACD17D57A

Citation: Sukparangsi W, Pochai A, Wongkunanusorn C, Khachonpisitsak S (2019) Discovery of *Neonrosella vitiata* (Darwin) and *Newmanella spinosus* Chan & Cheang (Balanomorpha, Tetraclitidae) from the Andaman Sea, eastern Indian Ocean ZooKeys 833: 1–20. https://doi.org/10.3897/zookeys.833.30689

Abstract

In this present study, distantly related acorn barnacle species in the subfamily Newmanellinae (Cirripedia, Thoracica, Tetraclitidae), including *Neonrosella vitiata* (Darwin, 1854) and *Newmanella spinosus* Chan & Cheang, 2016, were discovered in the Andaman Sea of Thailand. *Neo. vitiata* can be readily distinguished from other newmanellids by shell plate and operculum morphology (external shell, tergum geometry, and pattern of parietal tube) and arthropodal characters (presence of basi-dorsal point at base of penis and triangular spines on cirri, setal type, and mouth parts). Both species were found to share overlapping territories on rocks at the rockweed zone, an area submerged under seawater most of the time throughout the year. This study highlights the first discovery of *Neonrosella* in the eastern Indian Ocean, whose ultrastructure compared to *Newmanella* is redescribed and illustrated here based on scanning electron microscopy.

Keywords

Acorn barnacle, Cirripedia, Crustacea, Newmanellinae, Sessilia

Copyright *Woranop Sukparangsi et al.* This is an open access article distributed under the terms of the Creative Commons Attribution License (CC BY 4.0), which permits unrestricted use, distribution, and reproduction in any medium, provided the original author and source are credited.

Introduction

The genus *Neonrosella* Jones, 2010 contains only one species, *Neonrosella vitiata* (Darwin, 1854). This species was placed and repositioned in different taxa of family Tetraclitidae. Originally, it was described in the genus *Tetraclita* Schumacher, 1817 belonging to subfamily Tetraclitinae Gruvel, 1903, as *Tetraclita vitiata* by Darwin (1854). For more details of description of *T. vitiata*, see Rosell (1972). Ikeya and Yamaguchi (1993) then placed *T. vitiata* alongside with *T. coerulescens* (Spengler, 1970) into the genus *Newmanella* Ross, 1969 (Ikeya and Yamaguchi 1993).

Later, a revision of species of the superfamily Tetraclitoidea Gruvel, 1903 was done by Ross and Perreault (1999). Based on the difference in shell morphology compared with species of the genus *Newmanella*, they moved *Newmanella vitiata* (Darwin, 1854) to a newly proposed genus *Yamaguchiella* Ross & Perreault, 1999, and established this barnacle as a new subgenus *Yamaguchiella* (*Rosella*) Ross & Perreault, 1999. Thus, this species was renamed as *Yamaguchiella* (*Rosella*) *vitiata* (Darwin, 1854). In addition, they also placed both genera *Newmanella* and *Yamaguchiella* in a newly proposed subfamily Newmanellinae Ross & Perreault, 1999.

Afterwards, Jones (2010) proposed *Neonrosella* Jones, 2010 to replace *Rosella*, as that name was already assigned to a genus of curculionid beetles (Insecta, Coleoptera) by Whitehead (1977; in Clark et al. 1977). Thus, Jones (2010) renamed this species as *Yamaguchiella* (*Neonrosella*) *vitiata* (Darwin, 1854).

Recently, the subgenus *Neonrosella* was elevated to generic level by Chan and Cheang (2016) based on a phylogenetic analysis to clearly separate *Yamaguchiella* (*Yamaguchiella*), which is closer related to *Tetraclita singaporensis* Chan, Tsang & Chu, 2007, from *Yamaguchiella* (*Neonrosella*), which is closer related to *Tetraclita ehsani* Shahdadi, Chan & Sari, 2011 (Tsang et al. 2015). The subspecies *Yamaguchiella* (*Neonrosella*) *vitiata* was thus elevated to species status as *Neonrosella vitiata* (Chan and Cheang 2016).

The genus *Newmanella* was established by Ross (1969) for a group of low intertidal to subtidal tetraclitid barnacles with *Balanus radiata* Bruguière, 1789 as the type species (Ross, 1969: 242), later known as *Newmanella radiata* (Bruguière, 1789) and recently redescribed by Chan and Cheang (2016). Ross and Perreault (1999) proposed the classification for the subfamily Newmanellinae and placed *Newmanella* into that subfamily as well as described a new species *Newmanella Kolosvaryi* Ross & Perreault, 1999 from the east coast of Panama in the western Atlantic. Recently, *Newmanella spinosus* was described as a new species from the western Pacific (Taiwan) by Chan and Cheang (2016). Hence, the genus *Newmanella* is currently represented by four species: *New. hentscheli* Kolosvary, 1942, *New. Kolosvaryi*, Ross & Perreault, 1999, and *New. radiata* (Bruguière, 1789) from the Atlantic waters of South America (Bruguière 1789; Kolosvary 1942; Ross and Perreault 1999) and *New. spinosus* Chan & Cheang, 2016 from the western Pacific and the Andaman Sea, eastern Indian Ocean (Chan and Cheang 2016; Pochai et al. 2017, respectively).

A recent examination of acorn barnacle specimens from the Andaman Sea, southern Thailand, recognized two morphologically similar newmanellin species from the same area of the Na-Tai rocky shore (Phang-Nga Province); *Neonrosella vitiata* is new to Thailand and *Newmanella spinosus* is found next to *Neo. vitiata* at lowest low tide

point. Both species are redescribed herein, based on shell plate morphology and arthropodal characters using scanning electron microscopy (SEM). This is also the first illustration of *Neo. vitiata* in its ultrastructure, providing clear observation of this barnacle for taxonomic identification. Both species are compared with the detailed redescription of *New. radiata* provided by Chan and Cheang (2016).

Materials and methods

This study is based upon material collected from the Andaman Sea at Na-Tai rocky shore, Phang-Nga Province, southern Thailand, in March 2018. Samples were collected by hand picking and were transferred into plastic containers containing 95% ethanol. In the laboratory, specimens were transferred into clean 95% ethanol for storage. Specimens were examined under a compound microscope and stereomicroscope and later selected for dissection. All taxonomically important characters, shell plate morphology, and arthropodal characters were dissected and investigated with LEO 1450 VP scanning electron microscope on gold-coated specimens at Microscopic Center, Faculty of Science, Burapha University.

Specimens are preserved in 95% ethanol and have been deposited in the Zoological Collections of Burapha University, Thailand (ZCBUU).

The general terminology of the shell morphology and arthropodal characters follows Ross (1969), Rosell (1972), Ross and Perreault (1999), and Chan and Cheang (2016). The final images were processed with Adobe Photoshop CS6 and Adobe Illustrator CS6. Abbreviations used to denote shell morphology and arthropodal characters are explained directly in figure captions.

Museum and collection acronyms

NMNS National Museum of Natural Science, Taichung, Taiwan
ZCBUU Zoological Collections of Burapha University, Thailand

Taxonomy

Order Sessila Lamarck, 1818
Suborder Balanomorpha Pilsbry, 1916
Superfamily Tetraclitoidea Gruvel, 1903
Family Tetraclitidae Gruvel, 1903
Subfamily Newmanellinae Ross & Perreault, 1999

Genus *Neonrosella* Jones, 2010, monotypic

Type species. *Neonrosella vitiata* (Darwin, 1854)

Redescription of *Neonrosella vitiata* (Darwin, 1854)
Figs 1–4

Tetraclita vitiata Darwin, 1854: 340–341, Pl. 11, fig. 3a-e; Hoek 1913: 256; Broch 1922: 339–341, text fig. 73a-c; Hiro 1936: 635; 1937: 67, text fig. 13a & d.
Tetraclita (*Tetraclita*) *vitiata*: Rosell 1972: 214.
Newmanella vitiata (Darwin, 1854) Yamaguchi, in Ikeya and Yamaguchi 1993: 93; Jones et al. 1990: 14.
Yamaguchiella (*Rosella*) *vitiata* (Darwin, 1854): Ross and Perreault 1999: 5.
Yamaguchiella (*Neonrosella*) *vitiata* (Darwin, 1854): Jones 2010: 14.

Material examined. 13 specimens, southern Thailand, Andaman Sea in the eastern Indian Ocean, Phang-Nga Province, Na-Tai District, Na-Tai rocky shore, 20 Mar 2018, A Pochai leg. ZCBUU-CP-024-036.

Diagnosis. Parietes white with dark orange spots or longitudinal stripes. Tergum with broad spur. Area with lateral tergal depressor crests on basal margin long and carrying numerous and deep crests. Lateral scutal depressor crests numerous and deep. Cirrus II with equal rami. Cirrus III antenniform in both rami; lesser curvature with hook-like spines. Lesser curvature of cirrus IV without spines. Maxillule with two large spines and two smaller spines before notch; five pairs of spines and a cluster of 12 spines after notch. Mandible with five teeth; the third teeth tridentate; the fourth teeth quadridentate and the fifth teeth close to the fourth teeth; seven smaller setae on lower margin; without setae under inferior angle. Labrum with three canine-like teeth on each cutting margin. Penis with basi-dorsal point.

Description. Peduncle absent. Body length 2–3 cm. Shell white with orange longitudinal lines; low conic; composed of four shell plates including one carina, two laterals, and one rostrum (Fig. 1A, D, E). Base calcareous with parietal tubes; two rows of irregular shape and size of parietal tubes; inner laminar compartment carrying larger parietal tubes that its intraparietal septum radiating to the outer laminar; outer laminar compartment carrying three smaller and horizontal parietal tubes between larger tubes from inner laminar (Fig. 1B, C). External shell plate ornamented with rough and white with orange longitudinal striation; some exhibited decolouration or erosion of shell plate but carina always possesses 4–5 remnants of orange spots close to the orifice (Fig. 1D). Basal margin of each shell plate irregularly undulated. Internal shell plate smooth and white; interior part close to orifice oranges and with horizontal striation (Fig. 1E). Orifice kite-shaped or pentagonal (Fig. 1F). External surface of opercular plates white with irregular orange-brown spots (Fig. 1F, G). Internal surface of opercular plates mostly white with orange (Fig. 1F, H). Tergum smaller than scutum (Fig. 1G, H). Tergum triangular to polygonal shaped; dorsal surface with horizontal lines; longitudinal furrow on dorsal side broad. Spur of tergum broad with rounded tip. Scutal margin smooth without teeth. Basal margin of tergum longer than carina margin or area with lateral depressor muscle crests thick (ten crests). Tergal articular ridge with broad width but low ridge and thus when articulated, tergum occupies small area of scutum (Fig. 1I–L). Scutum triangular with height similar to width. External sur-

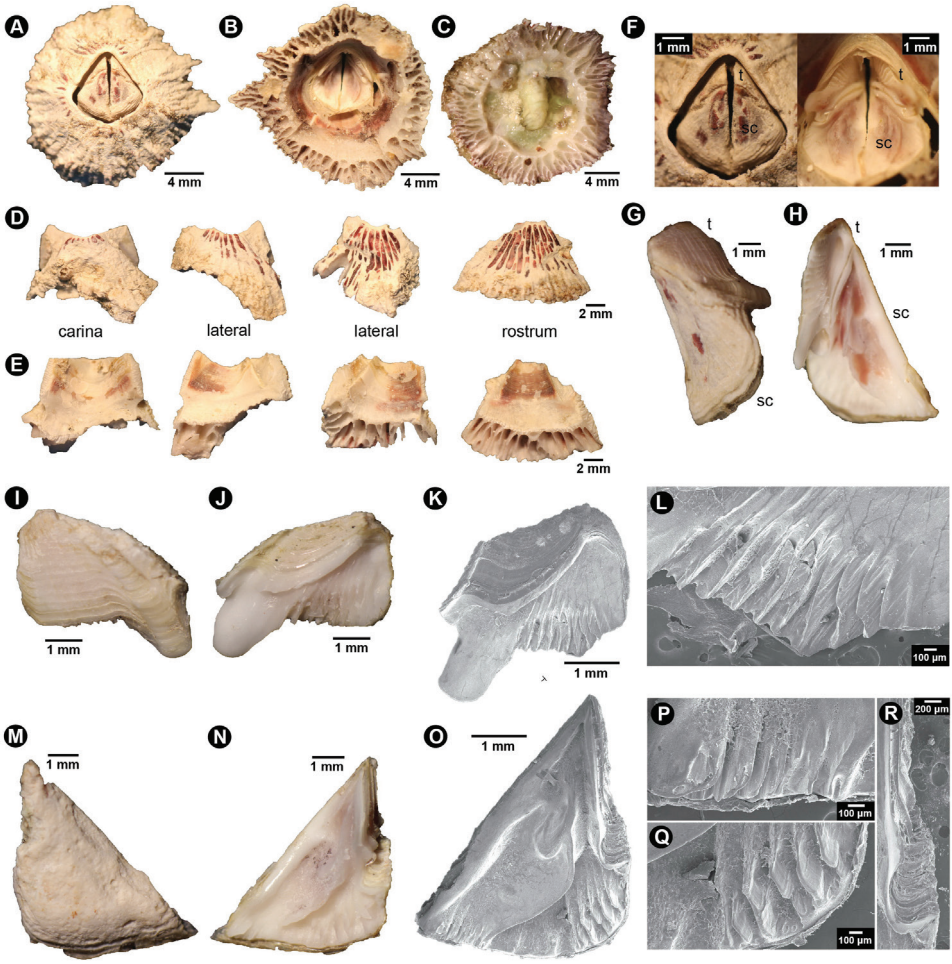

Figure 1. Shell plate and operculum morphology of *Neonrosella vitiata* (Darwin, 1854) **A** anterior view of shell **B** basal view of shell without body tissue **C** basal view of shell with body tissue intact **D** external view of individual shell plates (parietes) **E** internal view of individual shell plates **F** (left) close-up on external view of operculum (right) internal view of intact operculum **G** external view of operculum (one side of both tergum and scutum) **H** internal view of operculum (one side of both tergum and scutum) **I–L** tergum **I** external view **J** internal view **K** SEM of internal view **L** close-up on crests for lateral tergal depressor muscle M)–R) scutum **M** external view **N** internal view **O** SEM of internal view **P** close-up of crests at edge of basal margin (bm) close to occludent margin (om) **Q** close-up of crests for lateral scutal depressor muscle **R** close-up of articular ridge (ar).

face of scutum without horizontal striation. Ventral surface of scutum with long adductor ridge. Lateral scutal depressor crests deep and numerous (five crests) (Fig. 1M–R).

Cirrus I with unequal rami; anterior ramus (20-segmented) length longer than that of posterior ramus (10-segmented), approximately 2.5 times (Fig. 2A); intermediate segments of posterior ramus normal or not protuberant; greater and lesser curvature of both rami

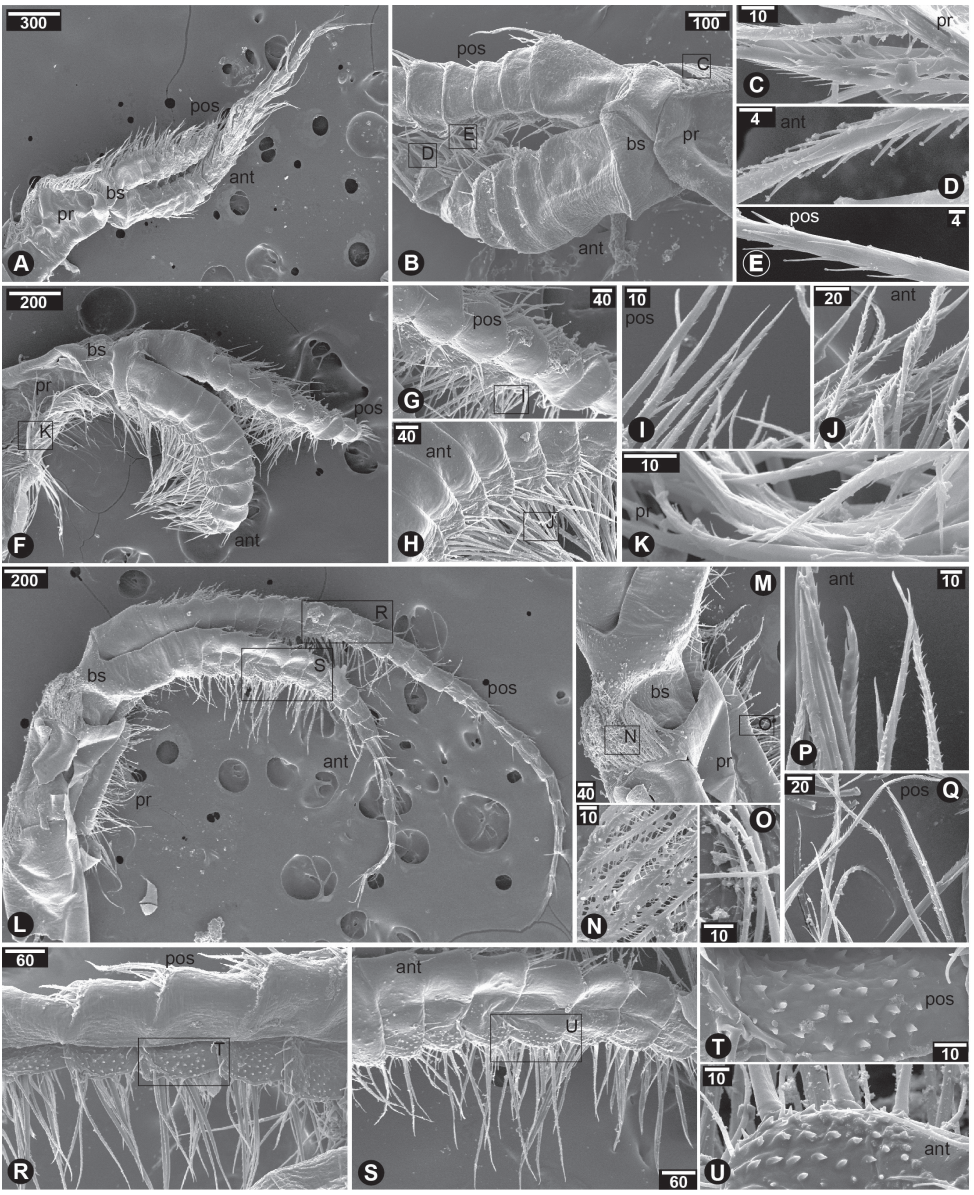

Figure 2. SEM showing cirral morphology of *Neonrosella vitiata* (Darwin, 1854) **A–E** cirrus I **A** overview of cirrus I morphology **B** close-up at proximal region of cirrus I **C** serrulated seta on posterior side of protopod **D** serrulated seta on anterior ramus **E** serrulated seta on posterior ramus **F–K** cirrus II **F** overview of cirrus II morphology **G** posterior ramus **H** anterior ramus **I** serrulated seta on posterior ramus **J** serrulated setae on anterior ramus **K** serrulated seta on anterior side of protopod **L–U** cirrus III **L** overview of cirrus III morphology **M** close-up on basipod and protopod **N** plumose seta on posterior side of basipod **O** plumose seta on anterior side of protopod **P** anterior seta on anterior ramus **Q** posterior seta on posterior ramus **R** posterior ramus **S** anterior ramus **T** close-up on posterior ramus showing spines on lesser curvature **U** close-up on anterior ramus showing spines on lesser curvature. Abbreviations: pr, protopod; bs, basipod; pos, posterior ramus; ant, anterior ramus. Scale bars in μm.

without spine; basipod without spines; protopod with serrulated setae on the posterior side; serrulated setae found in both rami (Fig. 2B–E). Cirrus II with equal rami and similar length (both rami with 10-segmented) (Fig. 2F); lesser curvature of both rami without spines (Fig. 2G–H); posterior ramus with serrulated setae (Fig. 2I); anterior ramus with serrulated setae along the entire length from apex to basipod and bi-pinnate setae on distal segments near apex (Fig. 2J); protopod with long serrulated setae on anterior side (Fig. 2K). Cirrus III with unequal rami; posterior ramus (27-segmented) longer than anterior ramus (19-segmented) about 1.5 fold; both rami antenniform (Fig. 2L); basis without spine (Fig. 2M); basis with plumose setae on posterior side (Fig. 2N); protopod with plumose setae on anterior side (Fig. 2O); serrulated and bidentate setae found in both rami (Fig. 2P, Q); lesser curvature of proximal region of both rami carrying spines (7-segmented on anterior ramus and 4-segmented on posterior ramus) (Fig. 2R, S); spines on both rami with hook-like shaped and thick (Fig. 2T, U). Cirrus IV–VI with equal and long rami (Fig. 3A, H, O); basis of cirrus IV–VI carrying triangular and slender spines (Fig. 3B, C, K, S); only first proximal segment of greater curvature of posterior ramus carrying triangular and slender spines (Fig. 3E, J, T). Cirrus IV, anterior ramus 17-segmented, posterior ramus 18-segmented (Fig. 3A). Cirrus V–VI, anterior ramus 22-segmented, posterior ramus 22-segmented (Fig. 3H, O). Lesser curvature of Cirrus IV–VI without spines and carrying two pairs of long serrulated setae and one pair of shorter simple setae (Fig. 3F, G, L, M, N, U, V).

Maxilla bi-lobate; upper lobe covered with densely packed serrulated setae; lower lobe with a few serrulated setae carrying more packed setules (Fig. 4A–C). Maxillule with U-shaped notch; two large spines and two small spines before notch; five pairs of small and slender spines after notch (Fig. 4D); cutting edge after notch carrying another 12 smaller spines followed by a cluster of serrulated setae (Fig. 4E). Mandible with five teeth; the first teeth largest; the second teeth bidentate; the third teeth tridentate; the fourth teeth quadridentate; the fifth teeth only single close to the fourth teeth; lower margin narrow with a pack of seven small setae followed by three larger setae close to inferior angle; no setae under inferior angle; simple setae scattered on surface of mandible (Fig. 4F–H). Labrum with V-shaped notch; three canine-shaped teeth with densely packed simple setae on each side of cutting margin (Fig. 4I–L). Mandibular palp rectangular with serrulated setae on superior margin (Fig. 4M, N). Penis long with annulation with basi-dorsal point on the dorsal side of penis base (Fig. 4O inset); a few simple setae scattered randomly along whole length; two bundles of simple and long setae found at the tip of penis (Fig. 4O–Q).

Habitat. *Neonrosella vitiata* was collected only during the lowest tide (March) of the year and at the lowest littoral zone, an area submerged most of the time throughout the year. It was found on rocks covered with seaweed, densely packed green and red algae, hydroids, sponges, limpets, other acorn barnacles including *Tetraclita* species at the algal crust zone of the intertidal region. The barnacles were found mostly in solitary form, in connection with *Newmanella spinosus*, or with conspecifics as small colonies of only two or three individuals per colony.

Distribution. Great Barrier Reef (Raine's Islet), Australia (Darwin 1854); Lucipara Islands, Banda Sea (Hoek 1913), Zamboanga, Philippines (Broch 1922); Goram Island (Hiro 1936); Oropusyakaru and Madarai Islands (Hiro 1937); Philippines

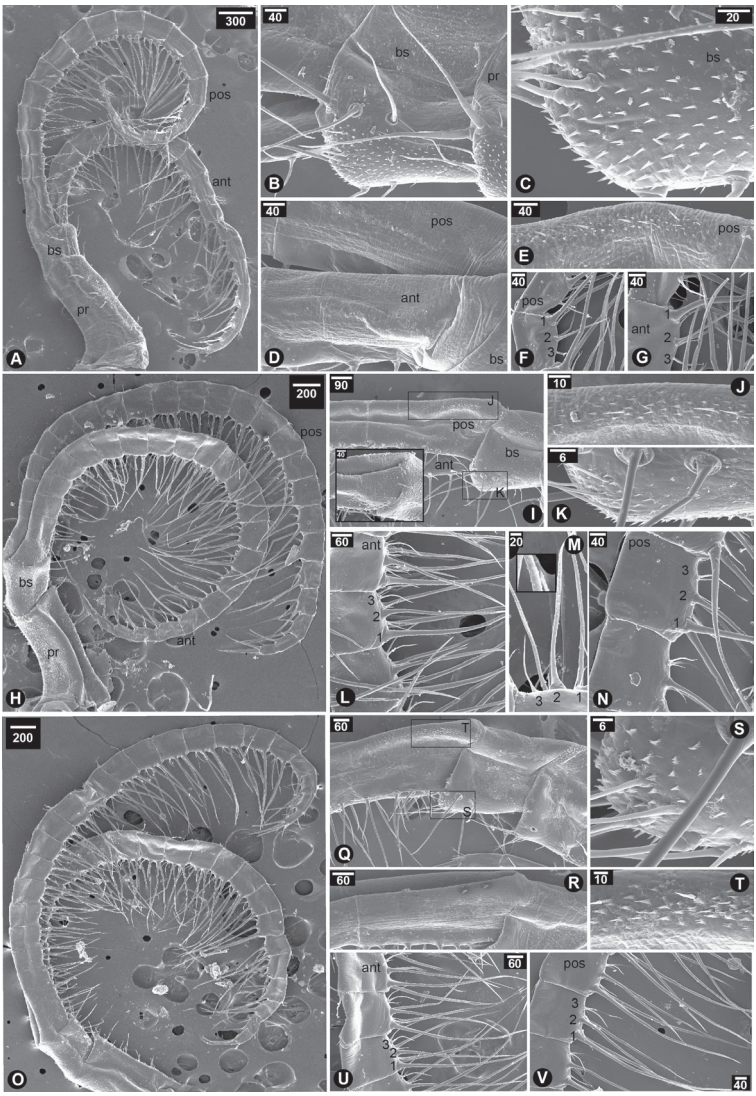

Figure 3. SEM showing cirral morphology of *Neonrosella vitiata* (Darwin, 1854) **A–G** cirrus IV **A** overview of cirrus IV morphology **B** close-up at basis and protopod **C** basipod with spines **D** greater curvature of both rami **E** close-up on spines on posterior ramus **F** lesser curvature of posterior ramus (1, 2 and 3 indicating first pair of long serrulated setae-longest, second pair of serrulated setae-second longest and third pair of simple setae-shortest, respectively) **G** lesser curvature of anterior ramus (number described as F) **H–N** cirrus V **H** overview of cirrus V morphology **I** proximal region showing greater curvature of both rami **J** close-up on greater curvature of posterior ramus carrying spines **K** basipod with spines **L** lesser curvature of anterior ramus **M** close-up on a segment on lesser curvature of anterior ramus showing type of setae (inset showing serrulated setae and number as described in F) **N** lesser curvature of posterior ramus (number as described in F) **O–V** cirrus VI **O** overview of cirrus VI morphology **Q** greater curvature of posterior ramus **R** greater curvature of both rami **S** basipod with spines **T** close-up on spines on posterior ramus **U** lesser curvature of anterior ramus **V** lesser curvature of posterior ramus (number described as F). Abbreviations: pr, protopod; bs, basipod; pos, posterior ramus; ant, anterior ramus. Scale bars in μm.

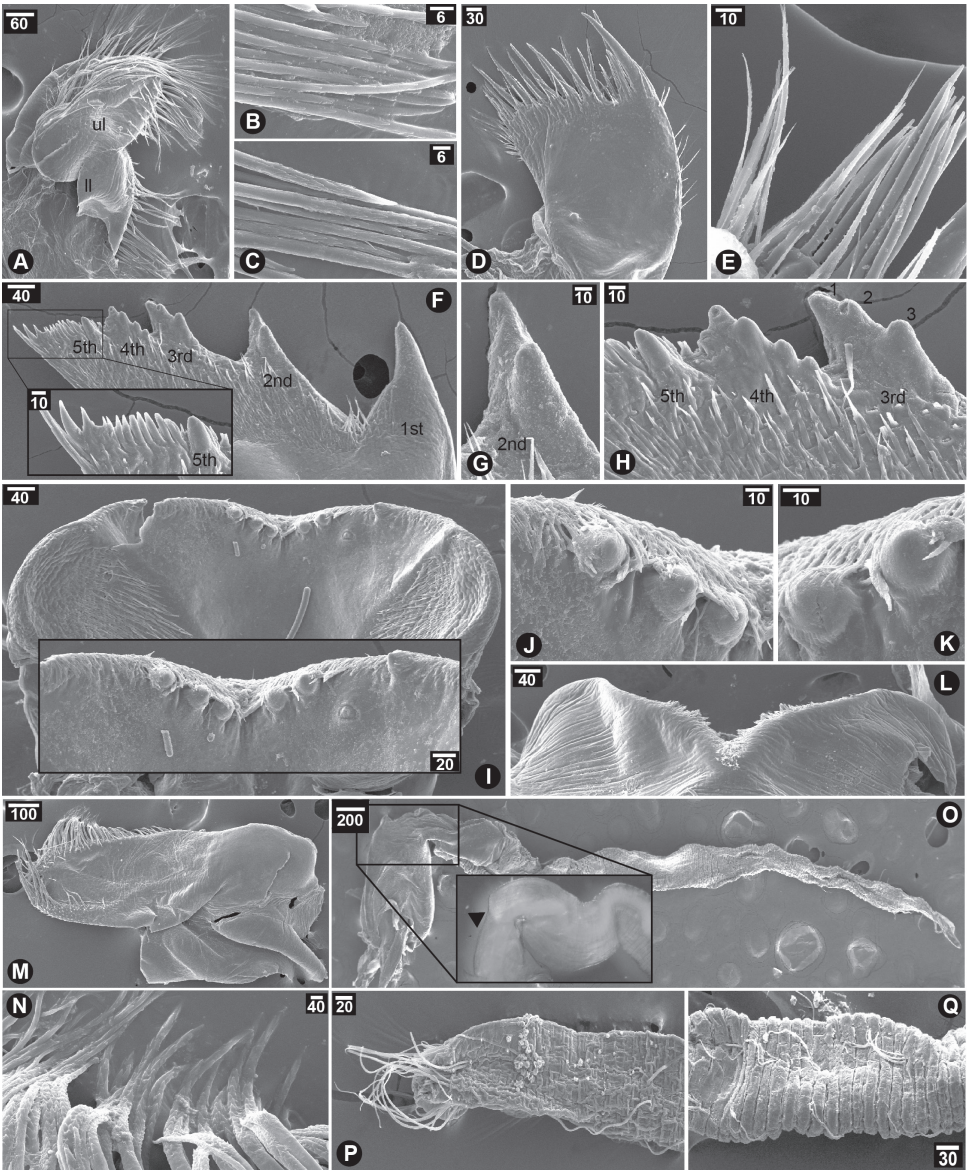

Figure 4. SEM showing mouth parts of *Neonrosella vitiata* (Darwin, 1854) **A–C** maxilla **A** overview of maxilla morphology **B** serrulated setae on upper lobe **C** serrulated setae on lower lobe **D–E** maxillule **D** overview **E** spines and serrulated setae on inferior angle **F–H** mandible **F** overview of mandible morphology and inset showing close-up of lower margin **G** bidentate 2nd teeth **H** tridentate 3rd teeth, quadridentate 4th teeth and single 5th teeth **I–L** labrum **I** overview of labrum morphology of interior labrum and inset showing close-up of teeth on labrum **J** close-up of teeth on right side of labrum **K** close-up on teeth on left side of labrum **L** exterior side of labrum **M–N** mandibular palp **M** overview of mandibular palp morphology **N** serrulated setae on superior margin **O–Q** penis **O** overview of whole penis on side view and inset showing basi-dorsal point (arrow head) on base of the penis **P** close-up on apex of penis **Q** annulation along penis. Abbreviations: ul, upper lobe of maxilla; ll, lower lobe of maxilla. Scale bars in µm.

(Rosell 1972); Singapore (Jones and Hosie 2016) and Andaman Sea of eastern Indian Ocean, Phang-Nga Province, southern Thailand (new record).

Genus *Newmanella* Ross, 1969

Type species. *Newmanella radiata* (Bruguière, 1789). Additional species: *New. hentscheli* Kolosvary, 1942, *New. Kolosvaryi* Ross & Perreault, 1999, *New. spinosus* Chan & Cheang, 2016.

Redescription of *Newmanella spinosus* Chan & Cheang, 2016

Figs 5–8

Newmanella radiata. Chan et al. 2009: 199, fig. 170; Shuto and Hayashi 2013: 159, fig. 3c (non *New. radiata* (Bruguière 1789).
Newmanella sp. Tsang et al. 2015: 325, fig. 1A, 327 fig. 2.
Newmanella spinosus Chan & Cheang, 2016: 212–220, figs 9–15.

Type. NMNS-006535-00001, deposited in NMNS (not examined).

Material examined. 17 specimens, southern Thailand, Andaman Sea in the eastern Indian Ocean, Phang-Nga Province, Na-Tai District, Na-Tai rocky shore, 20 Mar 2018, A Pochai leg. ZCBUU-CP-007-023.

Diagnosis. Parietes and opercular plates green on external and internal surfaces. External shell plate with numerous radiating or longitudinal lines extending from apex to base. Scutal margin of tergum with serrated teeth and broad spur with cutting edges. Cirrus II with equal rami and slight curvature of both rami carrying triangular spines. Basis of cirri IV–VI without spines. Greater curvature of both anterior ramus and posterior ramus of Cirrus IV with triangular spines. Mandible with five teeth, the third teeth bidentate, the fourth teeth with serrations and small teeth along the edge, and the fifth teeth sits on the middle of lower margin surrounded by other small spines. Labrum with four teeth on each cutting margin. Penis without basi-dorsal point.

Description. Peduncle absent. Body length 2–3 cm. Shell green with longitudinal folds or lines from orifice toward base or radiating lines; low conic; composed of four shell plates including one carina, two laterals and one rostrum. Base calcareous with parietal tubes; three rows of irregular shape and size of parietal tubes (Fig. 5A–F). External shell plate with longitudinal fold or striation from apex to base; some exhibited decolouration or erosion of shell plate. Basal margin of each shell plate irregularly undulated (Fig. 5E). Internal shell plate smooth and white to pale green; interior part close to orifice green and with some white horizontal striations (Fig. 5F). Orifice pentagonal (Fig. 5G). External surface of opercular plates white with irregular green spots or lines (Fig. 5G). Internal surface of opercular plates mostly white with green, in par-

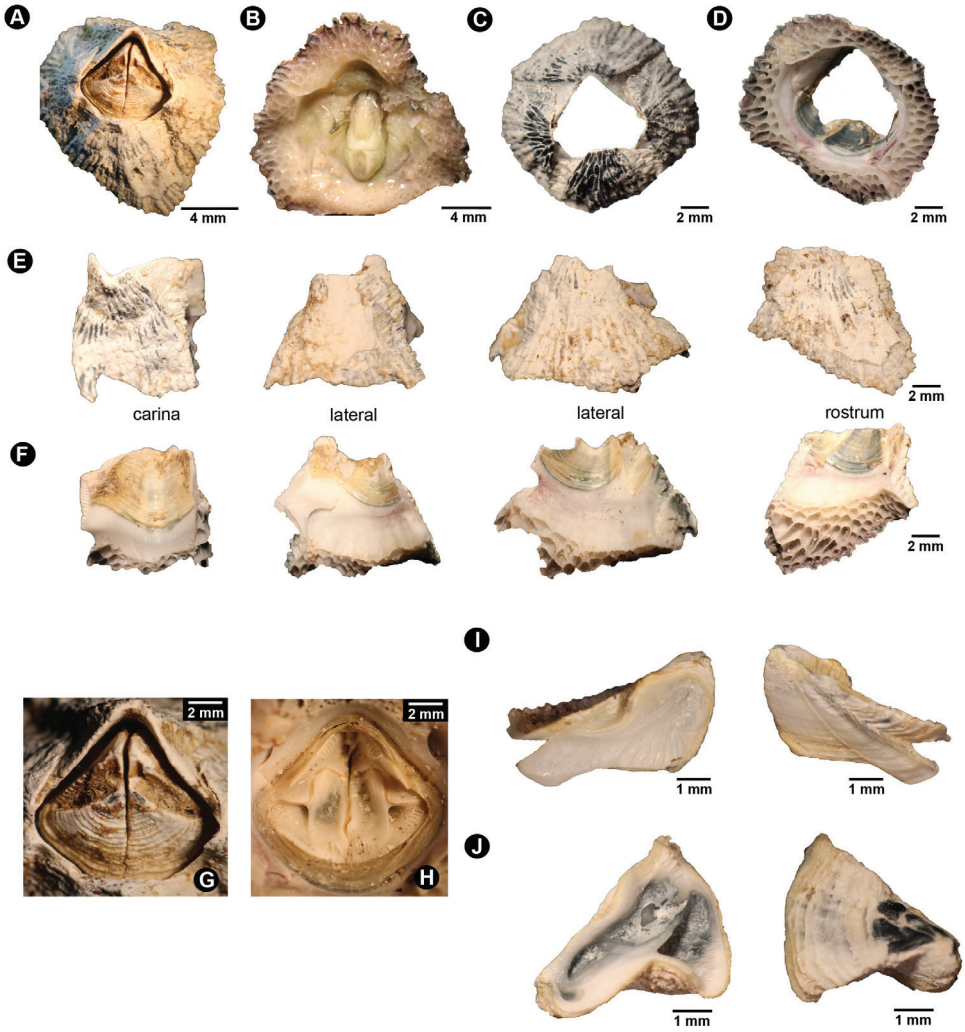

Figure 5. Shell plate and operculum morphology of *Newmanella spinosus* Chan & Cheang, 2016 **A** anterior view of shell **B** basal view of shell with body tissue **C** external and anterior view of shell without body tissue **D** internal and basal view of shell plates showing parietal tubes **E** external view of parietes **F** internal view of parietes **G** close-up on orifice and exterior opercular plates **H** internal view of operculum without intact tissues **I** internal view (left) and external view (right) of tergum **J** internal view (left) and external view (right) of scutum.

ticular scutum (Fig. 5H). Tergum smaller than scutum (Fig. 5I, J). Tergum triangular with clear spur protruding from basal margin; dorsal surface with horizontal lines; longitudinal furrow on dorsal side broad connected to spur. Spur of tergum broad with cutting edge tip. Scutal margin with serrated teeth. Basal margin of tergum with lateral depressor muscle crests thick (9–10 crests); tergal articular ridge with narrow width (Fig. 5I). Scutum triangular with height 1.3 times base. External surface of scutum with horizontal lines. Lateral depressor crest deep and numerous (5–8 crests) (Fig. 5J).

Cirrus I with unequal rami; anterior ramus (21-segmented) length approx. twice as long as posterior ramus (10-segmented) (Fig. 6A); intermediate segments of posterior ramus normal or not protuberant (Fig. 6B); greater and lesser curvature of both rami without spines (Fig. 6C, D); basipod without spines; serrulated setae found in both anterior and posterior rami (Fig. 6F, G); protopod on the posterior side with plumose setae (Fig. 6H). Cirrus II with equal rami and similar length (both rami with 10-segmented) (Fig. 6I); greater curvature of posterior ramus with serrulated setae (Fig. 6J, K); lesser curvature of posterior ramus with hook-like triangular spines (Fig. 6L) and lesser curvature of anterior ramus with slender spines and serrulated setae (Fig. 6M); apex of posterior ramus with long serrulated setae (Fig. 6N, O); apex of anterior ramus with bi-pinnate setae (Fig. 6P). Cirrus III with unequal rami; posterior ramus (26-segments) longer than anterior ramus (22-segmented, approximately 1.2 times; both rami antenniform (Fig. 6Q); basipod with spines (Fig. 6R) and anterior side of basipod with serrulated setae (Fig. 6S); weak curvature of both rami with hook-like triangular spines (Fig. 6T, U); greater curvature of anterior ramus with short spines (Fig. 6V); Both rami with serrulated setae and bidentate setae (Fig. 6W–Y). Cirrus IV–VI with semi-equal and long rami (Fig. 7A, G, K); basis of cirrus IV–VI without spines, only denticles observed (Fig. 7E, J, N). Cirrus IV, anterior ramus 20-segmented posterior ramus 21-segmented (Fig. 7A); Greater curvature of posterior ramus with slender spines (Fig. 7B, C); Greater curvature of anterior ramus with broad triangular spines (Fig. 7B, D); each segment carries two pairs of long serrulated setae and one pair of shorter simple setae (Fig. 7F). No spine on each segment at lesser curvature side. Cirrus V, anterior ramus 19-segmented posterior ramus 20-segmented (Fig. 7G); Greater curvature of posterior ramus with slender spines (Fig. 7H) while no spines on anterior ramus (Fig. 7I). Cirrus VI, anterior ramus 24-segmented, posterior ramus 26-segmented (Fig. 7K); greater curvature of both rami with slender spines (Fig. 7L, M).

Maxilla bi-lobate; both lobes covered with serrulated setae (Fig. 8A, B, C). Maxillule with V-shaped notch; two large spines and five smaller spines before notch; six pairs of long slender spines and following seven smaller spines closed to inferior angle after notch (Fig. 8D); cutting edge after notch carrying a cluster of serrulated setae (Fig. 8E). Mandible with five teeth; the first teeth largest; the second and the third teeth bidentate; the fourth teeth serrated; the fifth teeth only single in the middle of lower margin surrounded by small and slender spines; lower margin narrow with a pack of 12 spines (irregular length); no setae under inferior angle (Fig. 8F). Labrum with V-shaped notch; four teeth with densely packed simple setae on each side of cutting margin (Fig. 8H–J). Mandibular palp rectangular carrying densely packed serrulated setae on superior margin (Fig. 8K–L). Penis long and annulated without basi-dorsal point (Fig. 8M inset); a few simple setae scattered randomly along whole length; at the tip of penis carrying two clusters of simple and long setae (Fig. 8M–P).

Habitat. The specimens were collected only during the lowest tide (March) of the year at the lowest tide littoral zone, the same habitat as *Neonrosella vitiata*.

Distribution. Western Pacific from Taiwan (type locality) and Philippines (Chan and Cheang 2016) and Andaman Sea of eastern Indian Ocean (Phang-Nga Province, southern Thailand).

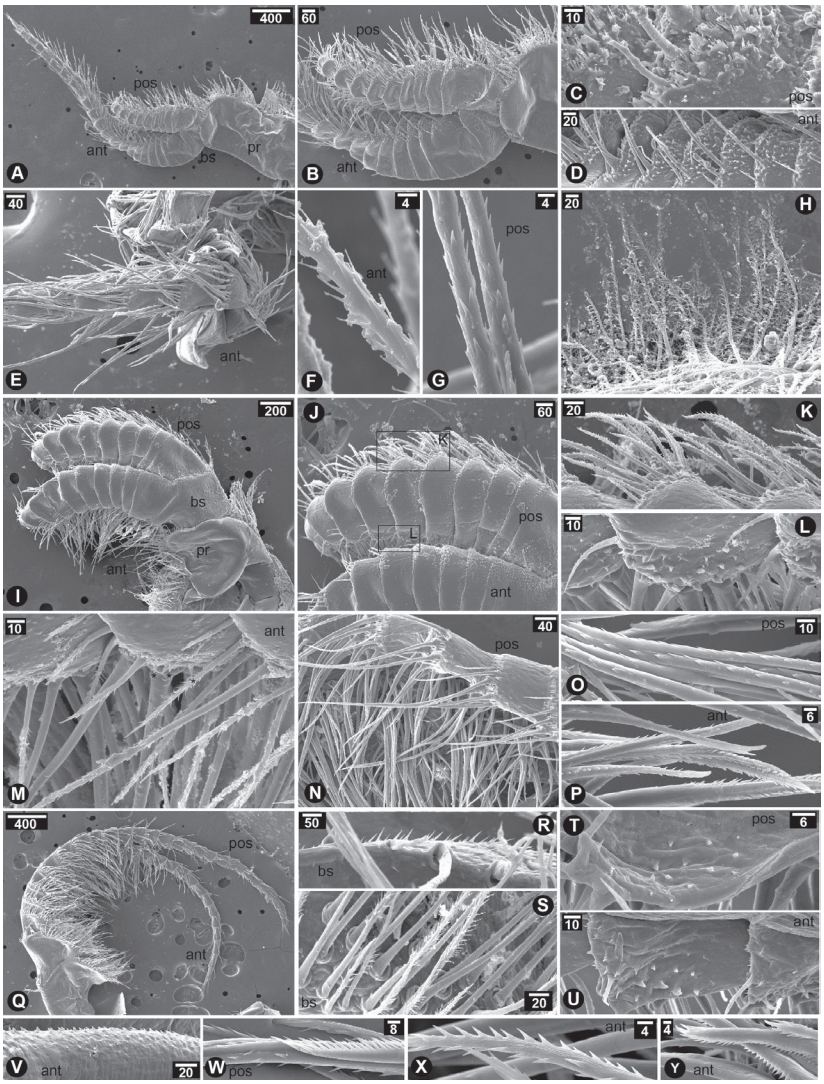

Figure 6. SEM showing cirral morphology of *Newmanella spinosus* Chan & Cheang, 2016 **A–H** cirrus I **A** overview of cirrus I morphology **B** close-up at proximal region of cirrus I **C** close-up on posterior ramus **D** close-up on anterior ramus **E** apex of anterior ramus **F** serrulated setae on anterior ramus **G** serrulated setae on posterior ramus **H** plumose setae on posterior side of protopod **I–P** cirrus II **I** overview of cirrus II morphology **J** proximal region of cirrus II **K** serrulated and bidentate setae on greater curvature of posterior ramus **L** hook-like triangular spines on lesser curvature of posterior ramus **M** spines (asterisks) on lesser curvature of anterior ramus **N** close-up on apex on posterior ramus **O** serrulated setae on posterior ramus **P** serrulated and bidentate setae on anterior ramus **Q–Y** cirrus III **Q** overview of cirrus III morphology **R** slender spines on basipod **S** plumose setae on anterior side of basipod **T** hook-like triangular spines on lesser curvature of posterior ramus **U** hook-like triangular spines on lesser curvature of anterior ramus **V** greater curvature of anterior ramus with spines **W** serrulated setae and bidentate setae on posterior ramus **X** serrulated setae on anterior ramus **Y** bidentate setae on anterior ramus. Abbreviations: pr, protopod; bs, basipod; pos, posterior ramus; ant, anterior ramus. Scale bars in μm.

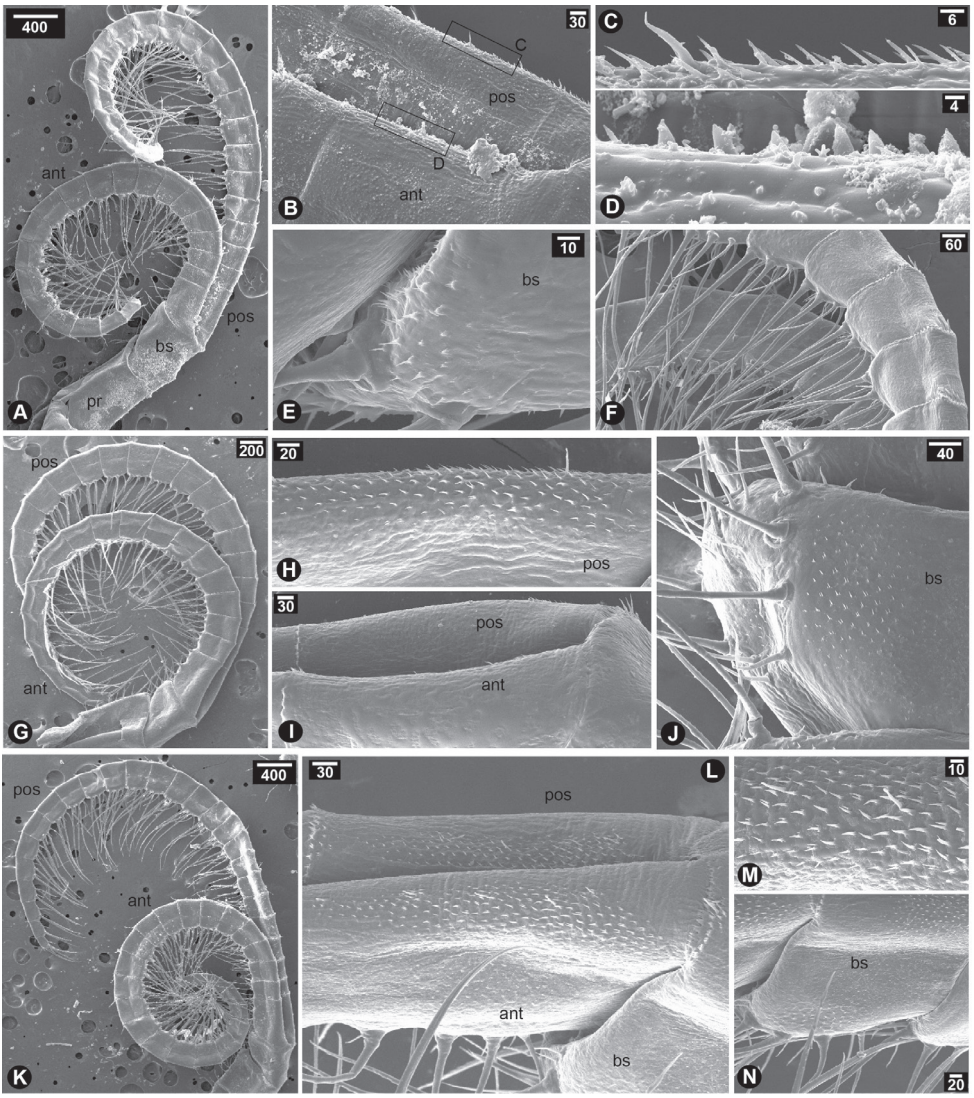

Figure 7. SEM showing cirral morphology of *Newmanella spinosus* Chan & Cheang, 2016 **A–F** cirrus IV **A** overview of cirrus IV morphology **B** close-up on proximal region of greater curvature **C** slender spines on greater curvature of posterior ramus **D** triangular spines on greater curvature of anterior ramus **E** close-up on basipod showing denticles without spine **F** lesser curvature of both rami showing two pairs of long serrulated setae and a pair of simple setae **G–J** cirrus V **G** overview of cirrus V morphology **H** greater curvature of posterior ramus showing spines **I** greater curvature of both rami (the other side) without spine **J** close-up on basipod without spine (only denticles) **K–N** Cirrus VI **K** overview of cirrus VI morphology **L** greater curvature of both rami **M** close-up on slender spines on greater curvature of anterior ramus **N** close-up on basipod without spine. Abbreviations: pr, protopod; bs, basipod; pos, posterior ramus; ant, anterior ramus. Scale bars in μm.

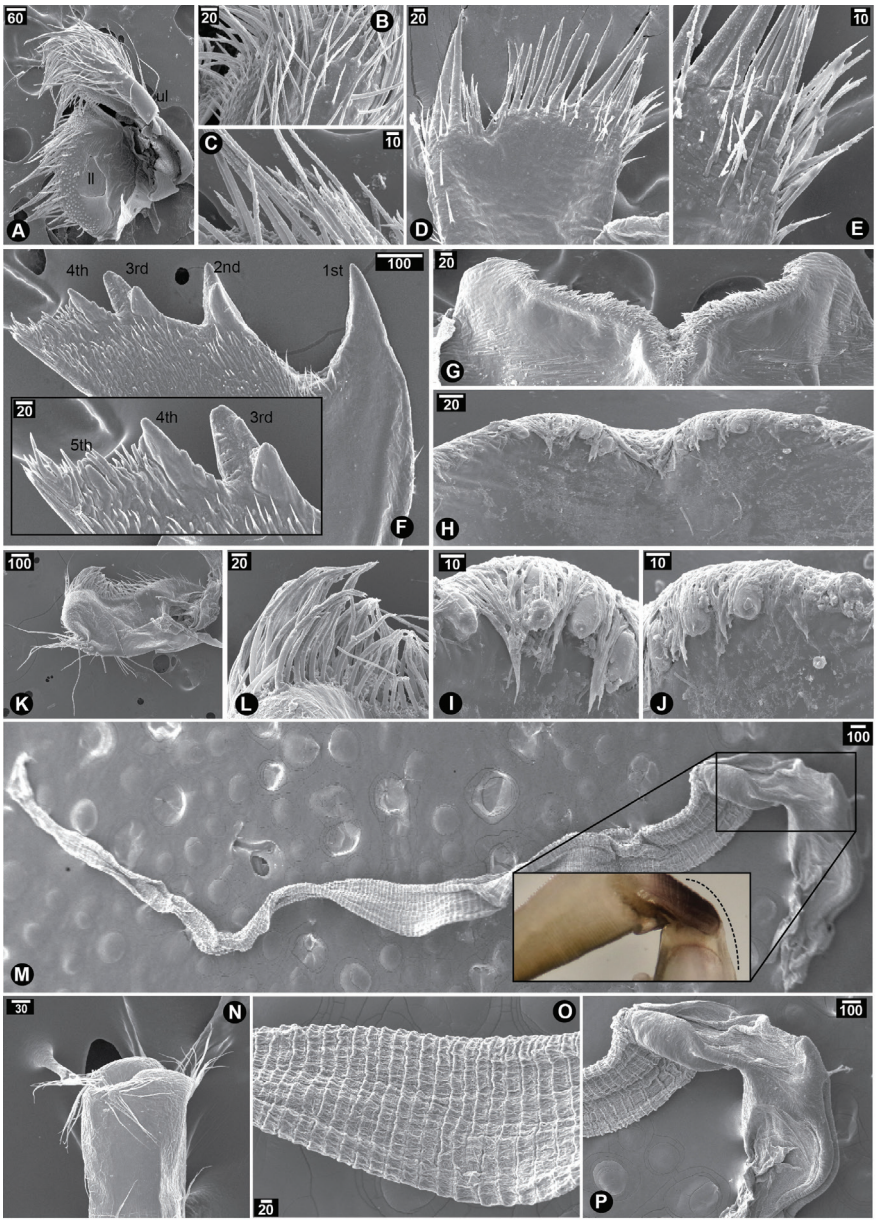

Figure 8. SEM showing mouth parts of *Newmanella spinosus* Chan & Cheang, 2016 **A–C** maxilla **A** overview of maxilla morphology showing upper lobe (ul) and lower lobe (ll) **B** serrulated setae on upper lobe **C** serrulated setae on lower lobe **D–E** maxillule **D** overview of maxillule morphology **E** serrulated setae on inferior angle of maxillule **F** mandible (inset showing close up of third-fifth teeth of mandible) **G–J** labrum **G** exterior view of labrum **H** interior view of labrum **I** teeth on labrum (left margin from H) **J** teeth on labrum (right margin from H) **K** mandibular palp **L** close-up on superior side showing serrulated setae on mandibular palp **M–P** penis **M** overview of whole penis on side view and inset showing smooth dorsal side (dash line) on the base of the penis without basi-dorsal point **N** apex of penis carrying setae **O** penis with annulation **P** base of penis. Abbreviations: ul, upper lobe of maxilla; ll, lower lobe of maxilla. Scale bars in μm.

Key to the western Pacific and the Andaman Sea of eastern Indian Ocean species of subfamily Newmanellinae

1 Low-conic shell plate on calcareous base with four parietes; two layers of parietal tubes (inner laminar with radiating large tubes and outer laminar with three horizontal tubes) (Fig. 1B, C); cirrus IV without triangular spines (Fig. 3D); mandible with five teeth (Fig. 4F); penis with basi-dorsal point (Fig. 4O) ....***Neonrosella vitiata***

– Low-conic shell plate on calcareous base with four parietes; multiple layers of parietal tubes; cirrus IV with triangular spines (see Fig.7D and Chan and Cheang 2016: fig. 5G); mandible with five teeth; penis without basi-dorsal point (Fig. 8) **2**

2 External shell plate white and longitudinal fold from apex to base without colour spots; tergum with narrow spur (see Chan and Cheang 2016: fig. 2); the third teeth of mandible bidentate, the fourth teeth bidentate with cutting edge serrated and small teeth, and the fifth teeth close to the fourth (see Chan and Cheang 2016: fig. 7G, H); five teeth on each side of labrum (see Chan and Cheang 2016: fig. 8E).....***Newmanella radiata***

– External shell plate green; scutal margin of tergum serrated (Fig. 5I); the third teeth of mandible bidentate, four serrated and small teeth close to base of the fourth teeth, the fifth teeth in the middle of pectin (Fig. 8F); four teeth on each side of labrum (Fig. 8H) ..... ***Newmanella spinosus***

Discussion

The present study represents the first discovery of *Neonrosella vitiata*, sharing overlapping habitat with *Newmanella spinosus* in the Andaman Sea, eastern Indian Ocean. We previously reported a list of new record acorn barnacles in Thailand (the Gulf of Thailand and the Andaman Sea) and *New. spinosus* was also observed in the low-tide intertidal zone at Na-Tai District, Phang-Nga Province, southern Thailand (Pochai et al. 2017). The collection of new batches of specimens further down the rockweed at this region uncovered the presence of two newmanellin species (clearly recognized by their low conical shell plate with four parietes): one with white-background shell plates carrying decorations of dark orange spots and one with green shell plates. The white newmanellin species were thought to be *Newmanella radiata* redescribed in Chan and Cheang (2016). However, based on the shell morphology characters (white shell plate with radiating orange stripes and two-layered and unequal-sized parietal tubes, tergum with broad spur and longer basal margin carrying extensive lateral depressor crests than that of *New. radiata*), this provides a possible clue for the occurrence of *Neonrosella*. By observation under the conical shell plate, *New. spinosus* is easily distinguished from *Neonrosella* in that they possess multiple layers (three or more) of parietal tubes in honeycombed pattern. Based on ex-

Table 1. Summary of shell plate morphology and anatomical characters used to diagnose *Neonrosella vitiata* from two morphologically related *Newmanella* species *New. radiata* and *New. spinosus*. Diagnostic characters to distinguish these three species are marked in bold.

Characters	***Neonrosella vitiata* (Darwin, 1854)**	***Newmanella radiata* (Bruguière, 1789)** As redescribed in Chan and Cheang (2016)	***Newmanella spinosus* Chan & Cheang, 2016** As redescribed in Chan and Cheang (2016) and the present study
Shell plates	Low conical; white with irregular longitudinal dark orange/brownish stripes	Low conical; white with radiating lines	Low conical; **green** with radiating lines
Parietal tube	Two layers: inner laminar with larger parietal tubes; outer laminar with three smaller parietal tubes between large parietal tubes from inner laminar	Two layers with irregular size of holes	**Three layers**
Tergum	Broad spur with rounded tip; ten lateral depressor crests on long basal margin; scutal margin without serrated teeth	**Narrow spur**; 4–5 lateral depressor crests on basal margin; scutal margin without serrated teeth	Broad spur with cutting edge; 9–10 Lateral depressor crests on basal margin; scutal margin **with serrated teeth**
Scutum	Triangular; height and width equal; deep and numerous lateral scutal depressor crests	Triangular; height and width equal; deep and numerous lateral scutal depressor crests	Triangular; height **longer than width** by 1.5 times; deep and numerous lateral scutal depressor crests
Cirrus I	1. Unequal rami; anterior ramus longer than posterior ramus 2.5 fold	1. Unequal rami; anterior ramus longer than posterior ramus 2/3 fold	1. Unequal rami; anterior ramus longer than posterior ramus
	2. Posterior ramus normal/**not protuberant**	2. Posterior ramus protuberant	2. Posterior ramus protuberant
Cirrus II	1. Equal rami	1. **Unequal rami**; posterior ramus longer 1.5 fold than anterior ramus	1. Equal rami
	2. Greater/lesser curvature of both rami without triangular spines	2. Greater/lesser curvature of both rami without triangular spines	2. Lesser curvature of both rami **with spines**
Cirrus III	1. Unequal rami; both antenniform	1. Unequal rami; only **posterior ramus antenniform**	1. **Semi-equal rami**; both antenniform
	2. Lesser curvature of anterior (only 7-segmented) and posterior rami (only 4-segmented) with triangular spines	2. Lesser curvature of anterior (entire) and posterior rami (not 3 distal segments) with triangular spines	2. Lesser curvature of anterior and posterior with triangular spines
	3. Greater curvature of anterior ramus without spines	3. Greater curvature of anterior ramus without spines	3. Greater curvature of anterior ramus with spines
Cirrus IV–VI	Basis with triangular spines	Basis with triangular spines	Basis **without triangular spines**
Cirrus IV	**No triangular spines** at greater curvature of anterior ramus	Triangular spines at greater curvature of anterior ramus	Triangular spines at greater curvature of anterior ramus
Mandible	Five teeth: 1^{st}(1)+2^{nd}(2)+ **3^{rd}(3)**+4^{th}(3-4/serrated) +5^{th}(1)+7 small setae+3 larger setae at lower margin	Five teeth:1^{st}(1)+2^{nd}(2)+3^{rd}(2)+4 th(2/serrated)+5^{th}(1)+16 setae at lower margin	Five teeth: 1^{st}(1)+2^{nd}(2)+3^{rd}(2)+4th (1/serrated)+5^{th}(1)+12 setae at lower margin
Labrum	Three teeth on each side of cutting margin	Five teeth on each side of cutting margin	Two large teeth right side and five teeth on left side (in this study – 4 large teeth on right and left sides)
Penis	Penis long and annulated **with basi-dorsal point** and at the tip of penis carrying two clusters of simple and long setae	Penis long and annulated **without basi-dorsal point**	Penis long and annulated **without basi-dorsal point**

amination of arthropodal characters by scanning electron microscopy, *Neo. vitiata* carried different morphologies of cirri I–VI in the presence and absence of triangular spines on greater and/or lesser curvature of the anterior and/or posterior rami. Additionally, *Neo. vitiata* and *New. spinosus* exhibited unequal rami in cirri I and III but equal in others, as described in Table 1. Unique characters among several body parts were found in the mandible and labrum. In the mandible of *Neo. vitiata*, the third and fourth teeth are tridentate and quadridentate while both teeth are bidentate in *New. radiata*. There are three teeth on each V-shaped cutting edge of *Neo. vitiata* but five in *New. radiata*. The obvious difference between *Neonrosella* and *Newmanella* is found in their intromittent organ or penis, in that *Neo. vitiata* carries basi-dorsal point on the base of penis while both *New. spinosus* and *New. radiata* have smooth dorsal surface of penis base.

Neo. vitiata in this study exhibited some similarities in shell plate morphology to *Tetraclita vitiata* Darwin, 1854 found in Philippines and Indo-west Pacific water, as described in Rosell (1972) as following: i) white conical shell plate ii) a few layers of irregular parietal tubes iii) long basal margin of tergum with several lateral depressor crests. However, our redescription of *Neo. vitiata* here report more distinct feature in following terms: colouration of external and internal shell plate with dark orange spots/lines and other arthropodal characters, including less number of cirral segments, the presence of serrulated and bipinnate setal types, the presence of triangular spines on both anterior and posterior ramus in cirri III, cirri IV–VI with three pairs of unequal setae, and in particular penis carrying hair tuft-like in group of two with basi-dorsal point.

Across all regions we examined in both the Gulf of Thailand and the Andaman Sea, *Neo. vitiata* was found only at the rocky shore-rockweed interface of the intertidal zone during the lowest tides, and the only one site for sample collection is Na-Tai, Phang-Nga. However, further investigations of more sampling areas at deeper depths of the intertidal zone are required and they may reveal a subtidal distribution of this species. In addition, the presence of *Neo. vitiata* in eastern Indian Ocean provides a possible scenario that before sea levels fluctuated by glaciation during the Pleistocene (e.g., Voris 2000), *Neo. vitiata* was already distributed across the Pacific Ocean towards the Indian Ocean.

Acknowledgements

This work was financially supported by the Research Grant of Burapha University through the National Research Council of Thailand (Grant no. 27/2560). We would like to express our heartfelt gratitude to Prof Frederick William Henry Beamish (Burapha University, Thailand) for his comments and reading through an earlier draft of this paper. We appreciate great review of this manuscript and careful consideration of correct taxonomic identification by Prof Benny KK Chan (Academia Sinica, Biodiversity Research Center, Taiwan). Thanks are due to the Microscopic Center, Faculty of Science, Burapha University for preparation of material for the SEM studies.

References

Broch H (1922) Studies on Pacific Cirripedes. Papers from Dr Th. Mortensen's Pacific Expedition 1914–1916 (10). Videnskabelige Meddelelser fra Dansk Naturhistorisk Forening i København 73: 215–358.

Bruguière M (1789) Balanite. In: Encyclopedia methodique: Histoire naturelle des Vers, 1, Panckoucke, Paris, 158–173.

Chan BKK, Cheang CC (2016) First discovery of a new species of *Newmanella* Ross, 1969 (Balanomorpha: Tetraclitidae) in the western Pacific, with a note on the new status of *Neonrosella* Jones, 2010. Zootaxa 4098(2): 201–226. https://doi.org/10.11646/zootaxa.4098.2.1

Chan BKK, Prabowo RE, Lee KS (2009) Crustacean fauna of Taiwan: Barnacles, Vol 1-Cirripedia: Thoracica excluding the Pyrgomatidae and Acastinae. National Taiwan Ocean University Press, Keelung, Taiwan, 298 pp.

Clark WE, Whitehead DR, Warner RE (1977) Classification of the weevil subfamily Tychinae, with a new genus and species, new combinations and new synonymy in *Lignyodini* (Coleoptera: Curculionidae). The Coleopterists Bulletin 31: 1–18.

Darwin C (1854) A monograph on the subclass Cirripedia with figures of all the species. The Ray Society, London, 684 pp. https://doi.org/10.5962/bhl.title.2104

Hiro F (1936) Report on the Cirripedia collected in the Malayan waters by the ship 'Zhuiho-Maru'. Japanese Journal of Zoology 6(19): 621–636.

Hiro F (1937) Studies on the cirripedian fauna of Japan. II. Cirripeds found in the vicinity of the Seto Marine Biological Laboratory. Memoirs of the College of Science, Kyoto University, Series B, 12, 385–478.

Hoek PPC (1913) The Cirripedia of the Siboga Expedition. B. Cirripedia sessilia. Siboga Expedition Monograph 31b: 129–275.

Ikeya N, Yamaguchi T (1993) An Introduction to Crustacean Paleobiology (UP Biology Series 93). University of Tokyo Press, Tokyo, 148 pp. [In Japanese]

Jones DS (2010) The littoral and shallow-water barnacles (Crustacea: Cirripedia) of south-eastern Queensland. In: Davie PJF, Phillips JA (Eds) Proceedings of the Thirteenth International Marine Biological Workshop, The Marine Fauna and Flora of Moreton Bay, Queensland. Memoirs of the Queensland Museum-Nature 54(3): 199–233.

Jones DS, Anderson JT, Anderson, DT (1990) Checklist of the Australian Cirripedia (Thoracica, Acrothoracica). Technical Reports of the Australian Museum 3: 1–28. https://doi.org/10.3853/j.1031-8062.3.1990.76

Jones DS, Hosie AM (2016) A checklist of the barnacles (Cirripedia: Thoracica) of Singapore and neighbouring waters. Raffles Bulletin of Zoology 34: 241–311.

Kolosvary G (1942) Studien an Cirripedien. Zoologischer Anzeiger 137: 138–150.

Pochai A, Kingtong S, Sukparangsi W, Khachonpisitsak S (2017) The diversity of acorn barnacles (Cirripedia, Balanomorpha) across Thailand's coasts: The Andaman Sea and the Gulf of Thailand. Zoosystematics and Evolution 93(1): 13–34. https://doi.org/10.3897/zse.93.10769

Rosell NC (1972) Some barnacles (Cirripedia Thoracica) of Puerto Galera found in the vicinity of the U.P. Marine Biological Laboratory. National and Applied Science Bulletin 24(4): 104–283.

Ross A (1969) Studies on the Tetraclitidae (Cirripedia, Thoracica). Revision of *Tetraclita*. Transactions of the San Diego Society of Natural History 15: 237–251. https://doi.org/10.5962/bhl.part.12058

Ross A, Perreault RT (1999) Revision of the Tetraclitellinae and description of a new species of *Newmanella* Ross from the tropical western-Atlantic Ocean (Cirripedia: Tetraclitoidea). Sessile Organisms 15: 1–8. https://doi.org/10.4282/sosj.15.2_1

Shuto T, Hayashi R (2013) Floating castles in the ocean: the barnacles of two giant fish aggregating devices from Okinawa, Japan. Landscape and Ecological Engineering 9(1): 157–163. https://doi.org/10.1007/s11355-012-0190-7

Tsang LM, Chu KH, Achituv Y, Chan BKK (2015) Molecular phylogeny of the acorn barnacle family Tetraclitidae (Cirripedia: Balanomorpha: Tetraclitoidea): validity of shell morphology and arthropodal characteristics in the systematics of Tetraclitid barnacles. Molecular Phylogenetics and Evolution 82: 324–329. https://doi.org/10.1016/j.ympev.2014.09.015

Voris HK (2000) Maps of Pleistocene sea levels in Southeast Asia: shorelines, river systems and time durations. Journal of Biogeography 27: 1153–1167. https://doi.org/10.1046/j.1365-2699.2000.00489.x

ZooKeys 833: 21–40 (2019)
doi: 10.3897/zookeys.833.26164
http://zookeys.pensoft.net

RESEARCH ARTICLE

A peer-reviewed open-access journal
ZooKeys
Launched to accelerate biodiversity research

Geometric morphometric analysis of the pronotum and elytron in stag beetles: insight into its diversity and evolution

Mengna Zhang[1,2], Yongying Ruan[2], Xia Wan[3], Yijie Tong[1], Xingke Yang[1], Ming Bai[1]

1 *Key Laboratory of Zoological Systematics and Evolution, Institute of Zoology, Chinese Academy of Sciences, Box 92, Beichen West Road, Chaoyang District, Beijing, 100101, China* **2** *School of Applied Chemistry and Biological Technology, Shenzhen Polytechnic, Shenzhen, 518055, China* **3** *Department of Ecology, School of Resources & Engineering, Anhui University, Hefei 230601, China*

Corresponding authors: *Xingke Yang* (yangxk@ioz.ac.cn); *Ming Bai* (baim@ioz.ac.cn)

Academic editor: *A. Frolov* | Received 25 April 2018 | Accepted 2 January 2019 | Published 25 March 2019

http://zoobank.org/AAE7F761-EF57-4ADC-9327-53D30F77AE95

Citation: Zhang M, Ruan Y, Wan X, Tong Y, Yang X, Bai M (2019) Geometric morphometric analysis of the pronotum and elytron in stag beetles: insight into its diversity and evolution. ZooKeys 833: 21–40. https://doi.org/10.3897/zookeys.833.26164

Abstract

Stag beetles (Coleoptera, Scarabaeoidea, Lucanidae) have received extensive attention from researchers in behavioral ecology and evolutionary biology. There have been no previous quantitative analyses, particularly using a geometric morphometric approach based on a large sample of data, to shed light on the morphological diversity and evolution of Lucanidae. Thoracic adaptation and ecological differentiation are intimately related, and the pronotum bears important muscles and supports the locomotion of prothoracic legs. The elytron is an autapomorphy of the Coleoptera. To reconstruct and visualize the patterns of evolutionary diversification and phylogenetic history of shape change, an ancestral groundplan can be reconstructed by mapping geometric morphometric data onto a phylogenetic tree. In this study, the morphologies of the pronotum and elytron in 1303 stag beetles (Lucanidae), including approximately 99.2% of all globally described species, were examined, thus revealing several aspects of morphological diversity and evolution. First, on the basis of geometric morphometric analysis, we found significant morphological differences in the pronotum or elytron between any two Lucanidae subfamilies. And we subsequently reconstructed the ancestral groundplans of the two structures in stag beetles and compared them with those of extant species (through cladistic and geometric morphometric methods). The ancestral groundplan of Lucanidae was found to be most similar to extant Nicagini in both the pronotum and

Copyright *Mengna Zhang et al.* This is an open access article distributed under the terms of the Creative Commons Attribution License (CC BY 4.0), which permits unrestricted use, distribution, and reproduction in any medium, provided the original author and source are credited.

elytron, according to Mahalanobis distances. Furthermore, we analyzed species richness and morphological diversity of stag beetles and the relationships between them and found that the two parameters were not always correlated. Aesalinae was found to be the most diverse subfamily in both the pronotum and elytron, despite its poor species richness, and the diversity of the pronotum or elytron was not superior in Lucaninae, despite its high species richness. Our study provides insights into the morphological variations and evolutionary history of the pronotum and elytron in four subfamilies of stag beetles, and it illuminates the relationship between morphological diversity and species richness. Intriguingly, our analysis indicates that morphological diversity and species richness are not always correlated. These findings may stimulate further studies in this field.

Keywords

Elytron, geometric morphometrics, morphological diversity, pronotum, species richness, stag beetle

Introduction

Stag beetles (Lucanidae) comprise more than 1300 described species, which are grouped into over 100 genera and exist in all zoogeographical regions except Antarctica (Fujita 2010; Kim and Farrell 2015). Owing to their sexual dimorphism, male polymorphism, and unique behaviors, stag beetles have received extensive attention from coleopterists and evolutionary biologists.

In recent years, multiple aspects of stag beetle morphology have been studied, and numerous evolutionary interpretations have been proposed. For instance, a study of the evolution of the Lucanidae has suggested that negative wing allometry may reflect a morphological cost of evolving oversized mandibles (Kawano 1997), and finite-element modeling has revealed force modulation of jaw adductors in stag beetles (Goyens et al. 2014). In addition, some studies have attempted to address evolutionary questions in specific subfamilies, such as Penichrolucaninae (Ratcliffe, 1984). Hosoya and Araya (2005, 2006) have inferred the phylogeny and evolution of Japanese stag beetles from morphological characters and 16S mtrRNA gene sequences, and the same team has investigated the phylogeny of the genus *Dorcus* and its allied genera by using allozyme or molecular data (Hosoya et al. 2002, 2003; Hosoya 2011). Furthermore, a new genus has been proposed, and a phylogenetic tree of Lucanidae based on two gene regions of ribosomal DNA has indicated the monophyly of four subfamilies (Paulsen 2013). Both morphological diversity and species richness are important in the study of diversity. The species richness of stag beetles has been revealed through various monographs (Fujita 2010; Maes and Pinratana 2003; Paulsen 2010), descriptions of new species (Okuda 2012b; Nguyen 2013) and reviews of certain taxa (Paulsen and Mondaca 2006; Huang and Chen 2012).

Among the morphological characters of stag beetles previous research was focused on the mandibles (Kawano 2003; Knell et al. 2004; Knight 2014), allometry (Kawano 2000; Tatsuta et al. 2001; Hardersen et al. 2011), sexual dimorphism or male polymorphism (Kawano 2006; Iguchi 2013), and genitalia (Tatsuta et al. 2001; Imura 2007). The pronotum and elytron have typically been used as indexes for body size (Tatsuta et al. 2004; Chiari et al. 2014), both of which contain important information about the evolution of the Lucanidae. Thoracic adaptation and ecological differentiation are inti-

mately related and, differences in size, structure and function in the prothorax are readily perceived and correlated with physical demands of various environments (Hlavac 1972). As a part of the prothorax, the pronotum bears important muscles and supports the locomotion of the prothoracic legs (Evans 1977). In fact, the muscles in the prothorax of a stag beetle are hypertrophied to help raise the head while lifting opponents (Goyens et al. 2015). The elytron is an autapomorphy of the Coleoptera, which was being transformed into elytra in the Permian (Beutel and Leschen 2005; Ponomarenko 2004). These two traits are also correlated to mandibles in morphology. The mandibles of most males are highly developed, thus contributing to the morphological diversity of the stag beetles. The species with relatively large mandibles have proportionally enlarged prothorax and smaller wings, which may be developmental integration trade-offs generated by resource competition between characters (Kawano 1997; Okada and Miyatake 2009). As mandible shape has wide variation even within the same species between large and small males in stag beetles, this study focuses on the pronotum and elytron, which are relatively conservative within species and more feasible for a large sample size.

However, no quantitative analyses have been conducted, especially through a geometric morphometric approach (Bai et al. 2012, 2014b; Friedman 2010), to reveal the morphological diversity and evolution of Lucanidae on the basis of a large sample size. Additionally, the relationship remains unclear between the species richness and morphological diversity of the subfamilies of Lucanidae . To reconstruct and visualize the phylogenetic history of shape change, the phylogeny can be projected into the shape tangent space, and provides intuitive graphical displays that show, as far as it is possible to infer from the shape information of terminal taxa, how specific clades diversified and spread through the space of morphometric variables (Klingenberg and Marugán-Lobón 2013).

Three major aspects of pronotum and elytron morphology of stag beetles were investigated in this study. First, the morphological variations in the pronotum and elytron of 1303 stag beetles were analyzed through a geometric morphometric approach. Second, the ancestral groundplans of the pronotum and elytron of the subfamilies of Lucanidae were reconstructed, and the evolution of the two structures was inferred and discussed. Furthermore, the species richness and morphological diversity of four subfamilies were compared.

Methods

Taxa examined

This study analyzed 1447 species including 1303 lucanid species and 144 outgroup species. All four subfamilies (Aesalinae, Lampriminae, Lucaninae, and Syndesinae), all 105 lucanid genera, and 1303 lucanid species (approximately 99.2% of all described lucanid species) from around the world were included as the inner group, and the outgroups consisted of 4 Diphyllostomatidae species, 16 Hybosoridae species, 16 Geotrupidae (Geotrupinae+Bolboceratinae) species, 11 Passalidae (Passalinae+Aulacocyclinae)

species, 6 Glaresidae species, 19 Ochodaeidae species, 43 Scarabaeidae species, 9 Trogidae species, 12 Silphidae species, and 8 Histeridae species. The measurements of all lucanid species and most outgroup species were based on published images (photographs or specimen drawings) (Dallwitz 1980; Dallwitz et al. 1993, 1995, 2000; Sakai and Nagai 1998; Bunalski 1999; Král 2001; Arnett et al. 2002; Ocampo 2006; Mondaca and Smith 2008; Schenk 2008; Nikolajev 2009; Bomans 2010; Fujita 2010; Imura 2010, 2011, 2012; Boilly 2011; Kobayashi and Matsumoto 2011; Okajima and Araya 2012; Okuda 2012a; Palestrini et al. 2012; Paulsen and Ocampo 2012; Ballerio 2013; Král et al. 2013; Paulsen 2013; Bezborodov and Koshkin 2014), and those of the Passalidae species were based on the specimens housed in the Institute of Zoology of the Chinese Academy of Sciences (Suppl. material 1: Table S1). In consideration of sexual dimorphism and male polymorphism in Lucanidae, images of the male specimens were selected in this study, as they are more accessible in publications, and medium-sized specimens were chosen if there were images of different body sizes available.

Data analysis

Geometric morphometric analysis of the variations in the pronotum and elytron were based on one curve for each structure (Fig. 1), and the curves for the pronotum or elytron were resampled by length after 25 and 50 semi-landmarks (SLM), respectively. The curves were digitized with TPS-DIG 2.05 (Rohlf 2006), and the data file was modified as .txt file to convert the semi-landmarks to landmarks (MacLeod 2017). The two lines with the curve number and point number were deleted, and the landmark number was replaced by the point number. This approach was used earlier by Bai et al. (2014a) and Li et al. (2016). The landmark configurations were scaled, translated, and rotated against the consensus configuration by using the Procrustes superimposition method (Bookstein 1991). The differences in the shapes and diversity indexes of the pronotum and elytron were inferred on the basis of principal component analysis (PCA) in MORPHOJ 1.06a (Klingenberg 2011) (Figs 2, 3, 8, 9, Table 1, Suppl. material 1: Table S10). The diversity index was quantified as Procrustes variance, which measures the dispersion of all observations around the mean shape of the respective taxa (Zelditch et al. 2004; Sherratt et al. 2014). The association of morphological diversity with species richness at genus-level was measured using Pearsons correlation coefficient, r in PAST 3.01 software (Sherratt et al. 2014; Hammer et al. 2001) (Suppl. material 1: Table S10, S11).

A phylogenetic tree was visualized in MESQUITE 2.72 (Maddison and Maddison 2011) on the basis of earlier molecular analysis (Kim and Farrell 2015), and the aligned landmark data were entered into MESQUITE 2.72 as a continuous matrix and linked to the tree (Figs 4, 5). Because the branch lengths (Grafen 1989) were missing, we followed the evaluation proposed by Klingenberg and Marugán-Lobón (Klingenberg and Marugán-Lobón 2013) and assigned an equal length to all branches (i.e., an evolutionary model with the same expected amount of morphological change on every branch was assumed).

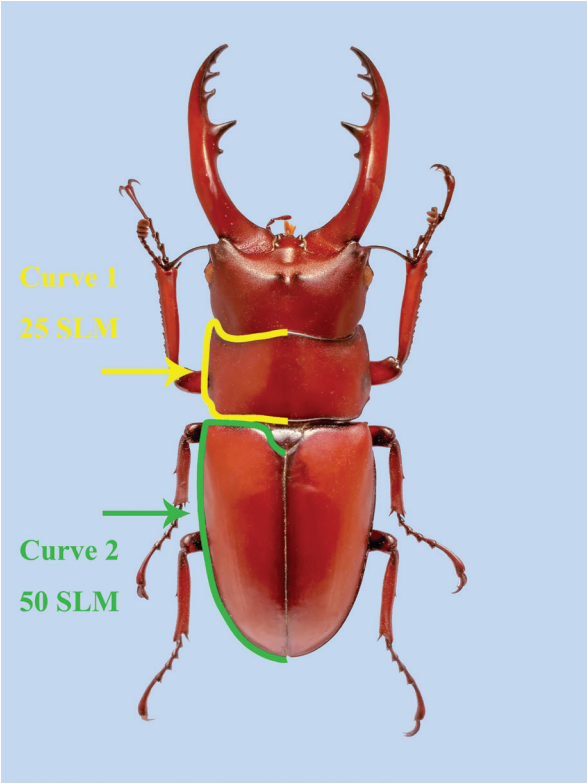

Figure 1. Description of the curves used in geometric morphometric analysis. The positions selected for the pronotum and elytron curves are represented by *Prosopocoilus* sp. in dorsal view. The curves were resampled in 25 or 50 semi-landmarks (SLM).

Table 1. Species richness and morphological diversity of the pronotum and elytron at the subfamily level.

Subfamily	Species number	Total variance	
		Pronotum	Elytron
Aesalinae	47	0.0158	0.0044
Lampriminae	11	0.0030	0.0007
Lucaninae	1220	0.0111	0.0025
Syndesinae	25	0.0123	0.0008

The ancestral groundplans of the Lucanidae pronotum and elytron were reconstructed by combining the landmark data with the phylogenetic tree, and the ancestral groundplans of all nodes were reconstructed by using the trace-all-characters and/or landmark-drawing modules of the RHETENOR package in MESQUITE. The ancestral states of all nodes were calculated and exported, and the data computed for the nodes were integrated with the original landmark data for the two characteristics from the 1303 stag beetles in EXCEL and NTSYS-PC (Rohlf 2007), respectively. The thin-plate splines showing the deformation of the landmarks compared with the original computed by MESQUITE were mapped onto the phylogenetic tree (Figs 4, 5).

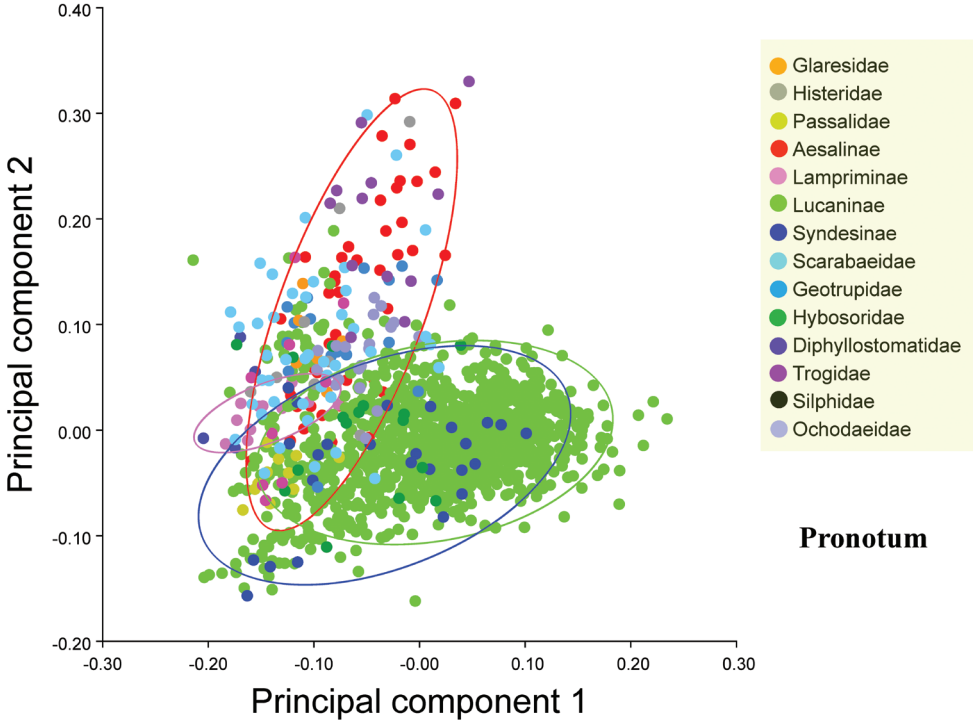

Figure 2. Differences in pronotum shape between outgroups and Lucanidae, on the basis of principal component analysis at the species level. The four circles are 90%-equal frequency ellipses of Lucanidae subfamilies.

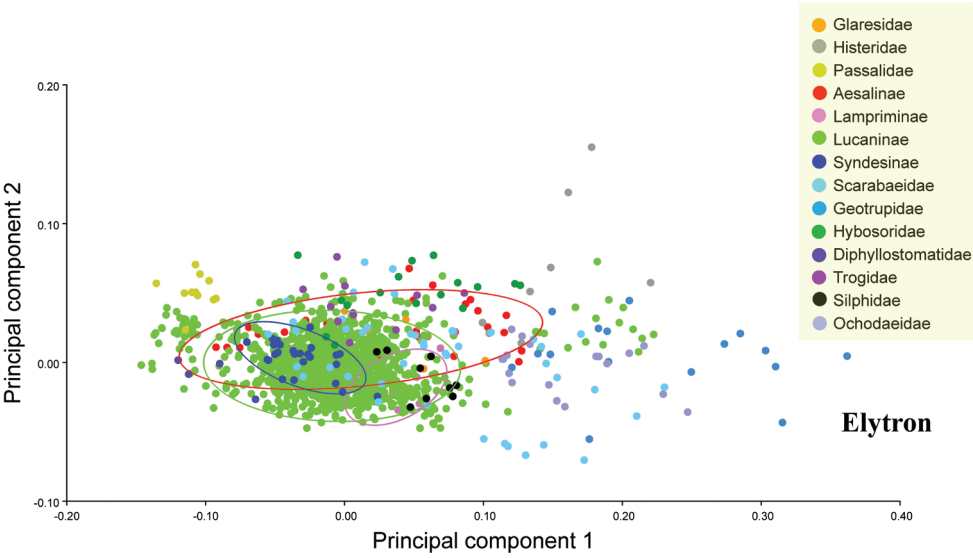

Figure 3. Differences in elytron shape between outgroups and Lucanidae, on the basis of principal component analysis at the species level. The four circles are 90%-equal frequency ellipses of Lucanidae subfamilies.

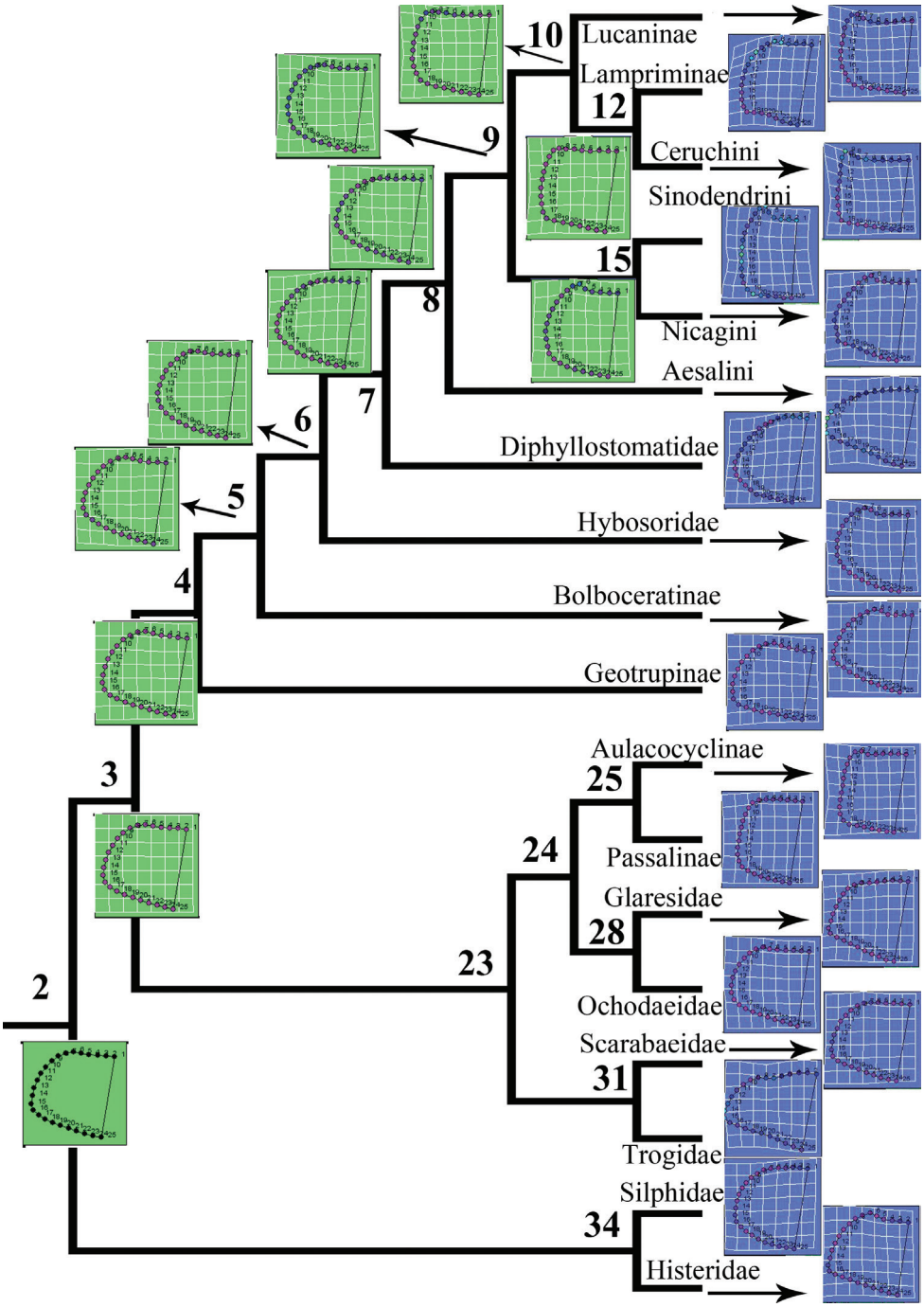

Figure 4. Reconstruction of ancestral groundplans of the pronotum in Lucanidae and the outgroups. The splines indicate deformation of the shapes relative to the reference configuration. The phylogenetic tree was summarized and reconstructed from earlier molecular results (Kim and Farrell 2015).

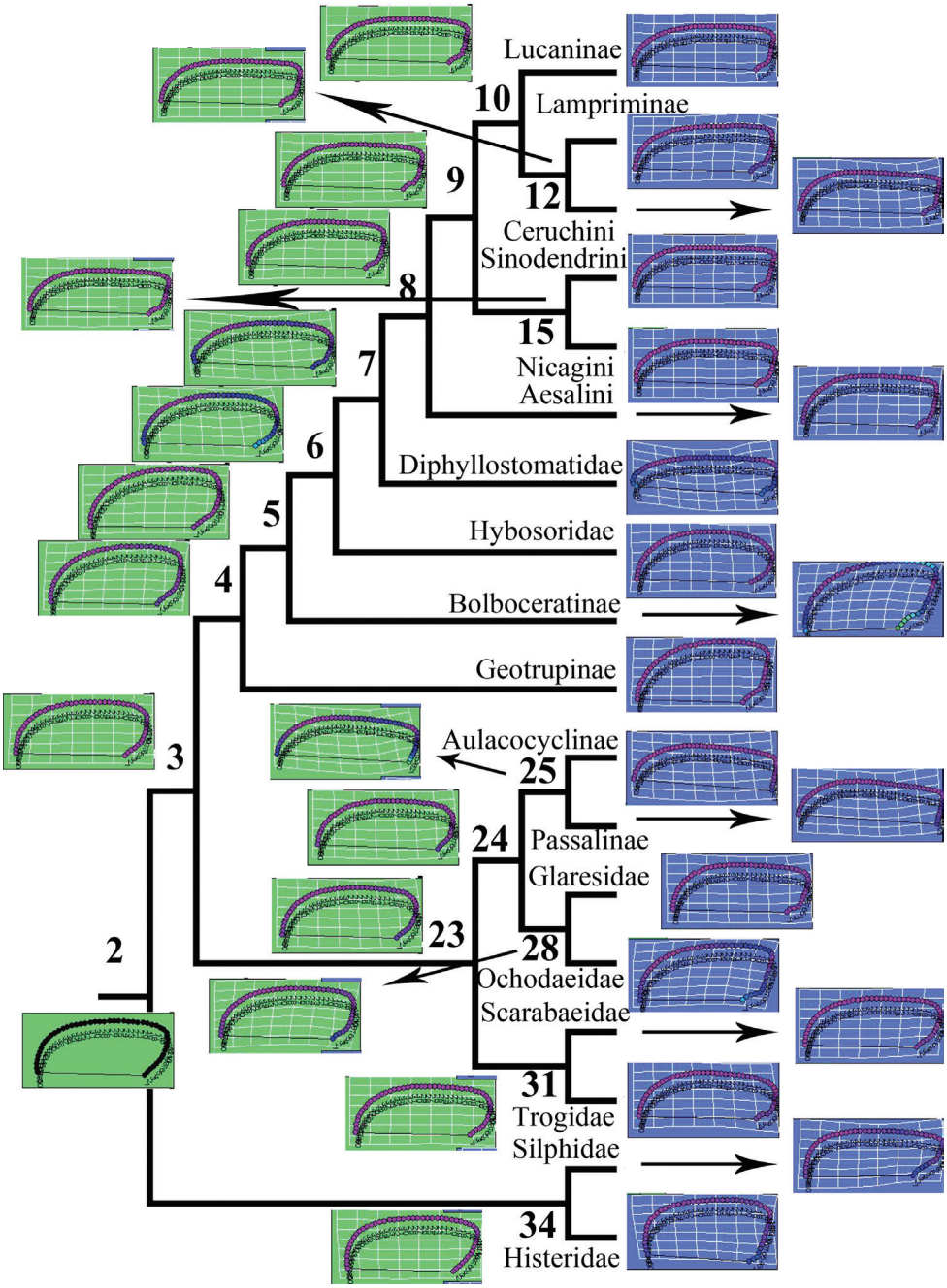

Figure 5. Reconstruction of ancestral groundplans of the elytron in Lucanidae and the outgroups. The splines indicate the deformation of the shapes relative to the reference configuration. The phylogenetic tree was summarized and reconstructed from earlier molecular results (Kim and Farrell 2015).

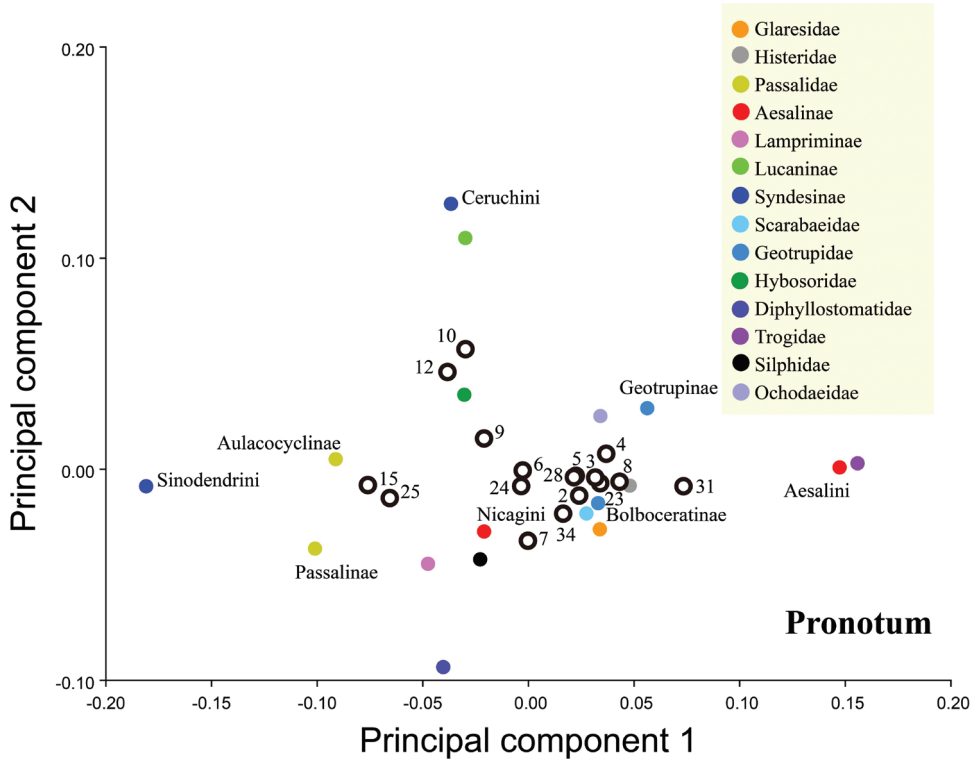

Figure 6. Differences in pronotum shape among each branch and ancestor, on the basis of principal component analysis. Empty dots indicate the number of the node on the phylogenetic tree; solid dots indicate the average shape of the extant subfamily/tribe of each branch.

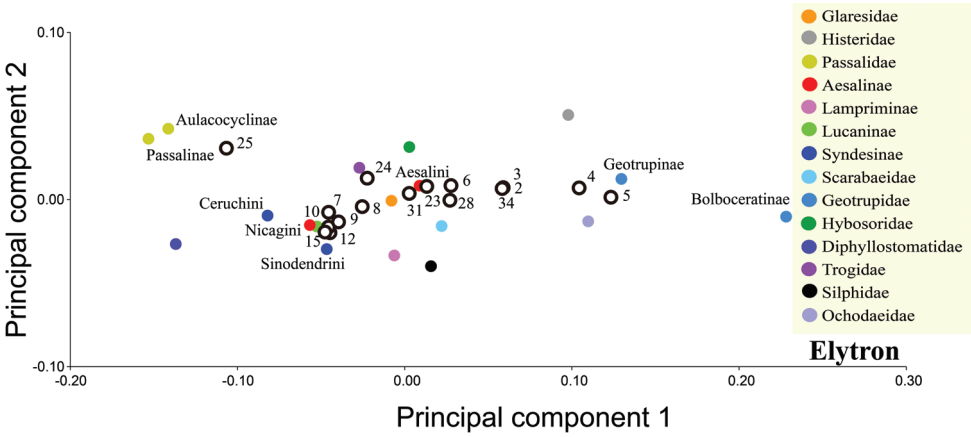

Figure 7. Differences in elytron shape among each branch and ancestor, on the basis of principal component analysis. Empty dots indicate the number of the node on the phylogenetic tree; solid dots indicate the average shape of the extant subfamily/tribe of each branch.

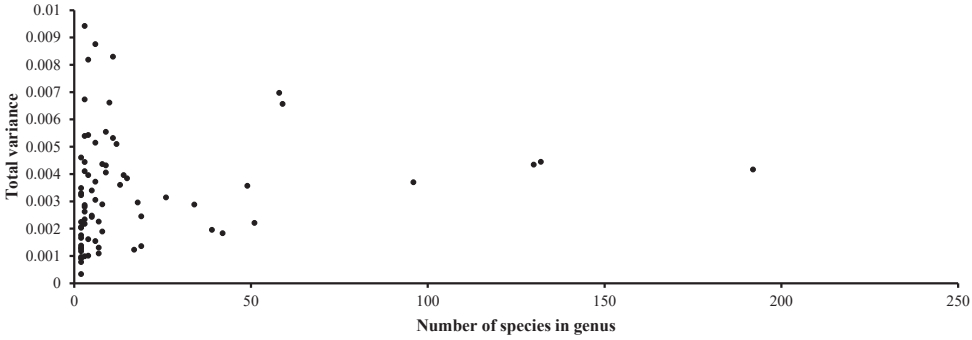

Figure 8. Species richness and morphological diversity of the pronotum at the genus level.

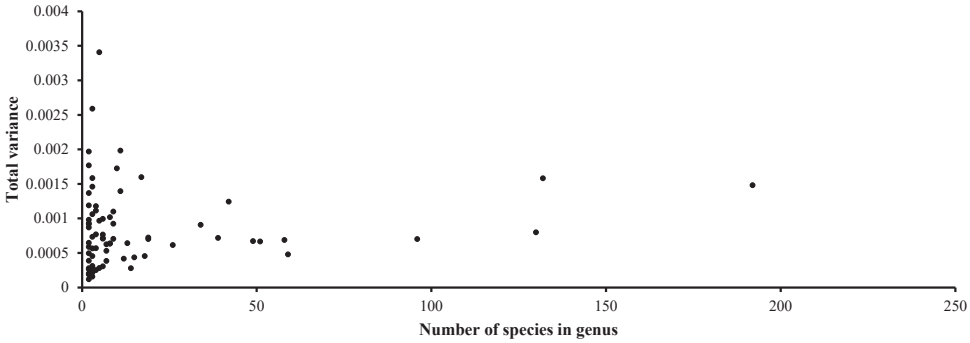

Figure 9. Species richness and morphological diversity of the elytron at the genus level.

In this case, the differences in the shapes of the pronotum and elytron among extant and extinct Lucanidae were inferred on the basis of PCA in MORPHOJ 1.06a and PAST 3.01 (Figs 6, 7). The canonical variate analysis (CVA) and discriminant function analysis (DFA) of the landmark data were based on MORPHOJ 1.06a (Suppl. material 1: Tables S2–S9, S12, S13).

Results

Comparison of pronotum/elytron morphology among lucanid subfamilies

The first two principal components of the pronotum and elytron from all 1447 species accounted for 77.37% and 88.40% of the variation among the species, respectively. The first two principal components were plotted to indicate variation along the two axes, which provided 90% equal frequency ellipses containing approximately 90% of the data points of each group (Figs 2, 3). The pronotum morphologies of the outgroups were mostly within the entire morphological variation of the Lucanidae (Fig. 2).

All the *p*-values obtained from the permutation tests (10000 permutation rounds) for both Mahalanobis distances and Procrustes distances between any two Lucanidae subfamilies were less than 0.05 for both the pronotum and elytron. Most of the *p*-values for the pronotum and elytron Mahalanobis or Procrustes distances between the Lucanidae subfamilies and outgroups were less than 0.05, except for some of the distances between the Aesalinae or Lampriminae and the outgroups.

There were significant differences in both the pronotum and elytron between any two of the Lucanidae subfamilies (Suppl. material 1: Table S3, S5, S7, S9). For the pronotum, there was a significant difference between Lampriminae, Lucaninae, or Syndesinae and the outgroups; the Lucanidae and the outgroups partly overlapped, because the pronotum morphology of Aesalinae could not be distinguished from that of Geotrupidae, Glaresidae, Ochodaeidae, and Histeridae (Suppl. material 1: Table S3, S5). However, the differences in the pronotum among these four pairs were not equivalent. On the basis of the Procrustes distance, a measure of the absolute magnitude of the deviation in shape that indicates the extent of the differences between the average group shapes, the differences in the pronotum between Aesalinae and Geotrupidae, Glaresidae, Ochodaeidae, and Histeridae were 0.0512, 0.0637, 0.0488 and 0.0659, respectively (Table S4). For the elytron, there was a significant difference between Lucaninae or Syndesinae and the outgroups, but the morphology of Aesalinae and Lampriminae could not be distinguished from the morphologies of Glaresidae, Scarabaeidae, or Trogidae (Table S7, S9). There was greater overlap in the pronotum morphology of the Lucanidae subfamilies and outgroups than the elytron morphology (Suppl. material 1: Table S2, S6).

Ancestral reconstruction of the pronotum and elytron

In a comparison of the ancestor of Lucanidae and all outgroups (node 2 in Fig. 4), the anterior angle of the pronotum of the ancestor of Lucanidae (node 8 in Fig. 4) is more obtuse (landmarks 4–12 at the splines in Fig. 4). It is shown in Figure 6 that a clear divergence between the two lineages of Lucanidae, the Aesalini lineage and lineage I (node 9 in Fig. 4), is primarily in the direction of the first principal component. Moreover, within lineage I, there is continued diversification in the direction of the first principal component (the horizontal direction in Fig. 6). The pronotum morphology of Lampriminae and Ceruchini showed clear changes in different directions, almost in the inverse direction of the second principal component (the vertical direction in Fig. 6), particularly in the anterior angle (landmarks 4–12 at the splines in Fig. 4).

The elytron of the ancestor of Lucanidae (node 8 in Fig. 5) is more slender than that of the outgroups (node 2 in Fig. 5) (the ratios of the length to the greatest width are 1.571 and 1.235, respectively) and narrower at the end (landmarks 35–50 at the splines in Fig. 5), but it is much wider than that of Diphyllostomatidae (the ratios of the length to the greatest width are 1.571 and 2.170, respectively). The elytron of Aesalini is wider than in lineage I (node 9 in Fig. 5) (the ratios of the length to the greatest width are 1.313 and 1.571, respectively), thus illustrating the major differ-

ences in the elytron between the two Lucanidae lineages. The humeral angle is narrower in the ancestor of Sinodendrini and Nicagini (node 15 in Fig. 5) than in the ancestor of Lucaninae, Lampriminae and Ceruchini (node 10 in Fig. 5) (landmarks 10–18 at the splines in Fig. 5).

Species richness and pronotum and elytron morphology

In terms of the species richness, Lucaninae is the largest subfamily of Lucanidae, comprising more than 90% (1220) of the species of stag beetles, followed by Aesalinae, Syndesinae, and Lampriminae, which have fewer than 50 species each (47, 25, 11). However, morphological diversity of the pronotum and elytra shape does not correspond with species richness (Table 1). Aesalinae, with fairly low species richness, was found to be the most diverse subfamily in both pronotum and elytron morphology, whereas Lucaninae exhibited low morphological diversity (both in the pronotum and elytron). This is an unexpected result considering its extremely high species richness.

In 73 genera (all Lucanidae genera with more than one species), similarly to the subfamily data, the morphological diversity of neither the pronotum nor the elytron was consistent with species richness. There is no significant correlation between morphological diversity and species richness in pronotum at genus-level (Procrustes variance $r = 0.15$, $P = 0.21$), nor a relationship between morphological diversity and species richness in elytron at genus-level (Procrustes variance $r = 0.11$, $P = 0.33$). The total morphological variances in extremely species-rich genera, such as *Aegus*, *Dorcus*, *Lucanus*, and *Prosopocoilus*, were not predominant.

Discussion

Evolution of the pronotum and elytron in Lucanidae

According to the Mahalanobis distances from the DFA (Suppl. material 1: Table S12, S13), all lucanid ancestors (nodes 8–10, 12, and 15) most resemble Nicagini in their pronotum and elytron morphology. Procrustes distances indicated that the pronotum of the ancestor of Lucanidae (node 8) is closest to that of Scarabaeidae, and the elytron is closest to that of Glaresidae. The common ancestor of Lucaninae, Lampriminae, Syndesinae, and Nicagini (node 9) most resembles Hybosoridae in the pronotum and Lucaninae in the elytron, and the ancestor of Lampriminae and Ceruchini (node 12) most resembles Hybosoridae in the pronotum and Sinodendrini in the elytron. The ancestor of Lucaninae, Lampriminae, and Ceruchini (node 10) is most similar to Lucaninae in both the pronotum and elytron, and as shown by both Mahalanobis and Procrustes distances, the ancestor of Sinodendrini and Nicagini (node 15) most resembles Nicagini in the pronotum as well as the elytron.

The ancestral pronotum and elytra were reconstructed, which could be combined with fossil materials to uncover the ancestors' habitat as well as evolution procedure. There is still a lack of sufficient data as well as studies of the functional morphology of the pronotum and the elytron in Lucanidae, but the functional morphology of other insect clades may allow for certain interpretations. Broad pronotum and elytra of stag beetles may provide advantages during locomotion and hunting prey, like ground beetles (Evans 1977; Forsythe 1981). The diversity of pronotum may reflect occupancy of diverse habitats and niches, as in the case of grylloblattids (Bai et al. 2010).

The inconsistency between morphological diversity and species richness

Morphological and taxonomic diversity provide insight into the expansion and contraction of major taxa, and the nature of the relationship between these two aspects of diversity has important implications in evolutionary mechanisms (Foote 1993). Lampriminae has the lowest pronotum and elytron diversity as well as species richness, but species richness and morphological diversity do not always vary consistently in Lucanidae subfamilies. Despite having many more species than the other three subfamilies combined, the subfamily Lucaninae has little morphological diversity. Furthermore, the results from the genus-level data reveal the same pattern in which some of the largest genera are not as diverse as the small groups in terms of either pronotum or elytron morphology.

The theory that species richness generates a variety of forms has been tested and supported in various studies (Williams and Humphries 1996; Roy and Foote 1997; Bell and Barnes 2001), thus suggesting that the relationship between morphological and species diversity should be monotonic or at least positive.

In contrast, numerous studies have indicated that richness and morphology do not always follow a common trend. Foote (1993) has found that morphological variety and taxonomic richness often increase together during the initial diversification of a clade, but two major patterns have been observed as clades decline. In Blastoidea, Trilobita, Libristoma, and Asaphina, morphological diversity continued to increase even in the face of striking decreases in taxonomic richness, but in Phacopida, Scutelluina, and to some extent in Proetida, morphological diversity decreased along with taxonomic diversity. Roy et al. (2001), using data from a large group of Indo-Pacific gastropods (family Strombidae), have shown that the species richness of a region is a poor predictor of morphological diversity. Areas with only a few species may harbor an impressive array of morphologies, and in contrast, morphological diversity in the most species-rich regions is no higher than that in regions with half the taxonomic diversity. Bell and Barnes (2002) have found no significant correlation between species richness and morphological diversity in cave or boulder habitats, although these variables are significantly correlated in coral reef and soft substratum habitats. In another scenario (Mohedano-Navarrete et al. 2008), the morphological diversity and species richness of *Porites* corals has been found to vary independently; some regions with few species had

remarkably high morphological diversity, including peripheral areas such as Polynesia and East Africa. In a study of 107 families of passerine birds, morphological space was weakly related to the number of species in a family, i.e., the higher species richness of the order Passeriformes in the tropics compared with temperate regions was not matched by increased morphological diversity (Ricklefs 2012).

Conclusion

Our results showed significant differences in both pronotum and elytron morphology between any two lucanid subfamilies; in other words, the four subfamilies could be statistically separated and determined based on the two characters. On the basis of cladistic and geometric morphometric methods, the ancestral groundplans of the pronotum and elytron of extant Lucanidae were reconstructed and compared with those of extant species. The ancestor of Lucanidae is most similar to extant Nicagini in both pronotum and elytron morphology, according to Mahalanobis distances, but Procrustes distances indicated that the pronotum of the ancestor of Lucanidae is most similar to that of extant Scarabaeidae and that the elytron is most similar to that of extant Glaresidae. On the basis of a comparison of the four subfamilies as well as an analysis of Lucanidae genera, species richness and morphological diversity do not generally correlate. Lampriminae has the poorest morphological diversity in the pronotum and elytron as well as the poorest species richness, whereas Aesalinae is the most diverse subfamily with respect to both the pronotum and elytron, despite its small number of species.

However, the analyses are relatively limited, as there is morphological variation within species especially in male polymorphic stag beetles, and only one image per species was sampled during the procedure. In addition, as our results were limited to the morphological characters of the pronotum and elytron from the dorsal view, the investigation of more traits and groups should improve the understanding of the relationship between morphological diversity and species richness in beetles.

Acknowledgements

We thank the Group of Morphology and Evolution of Beetles of IZCAS for providing the platform of this research. The staff from the Beetle Collection of IZCAS is acknowledged for supplying materials for this study. We extend our sincere appreciation to all of the scholars and colleagues who encouraged and supported the first authors to accomplish this paper. We are also grateful to Mrs Xiaoyan Hu, Dr Menglei Zhang and Dr Sha Li for assisting with a portion of the previous stage of this research.

This research was supported by the National Natural Science Foundation of China (No. 31672345; 31572311), Research Equipment Development Project of Chinese Academy of Sciences (YZ201509), and by a Humboldt Fellowship (M.B.) from Alexander von Humboldt Foundation.

References

Arnett, RH Jr, Thomas MC, Skelley PE, Frank JH (2002) American Beetles. Volume 2. Polyphaga: Scarabaeoidea through Curculionoidea. CRC Press LLC, Boca Raton, 861 pp.

Bai M, Beutel RG, Liu WG, Li S, Zhang MN, Lu YY, Song KQ, Ren D, Yang XK (2014a) Description of a new species of Glaresidae (Coleoptera: Scarabaeoidea) from the Jehol Biota of China with a geometric morphometric evaluation. Arthropod Systematics & Phylogeny 72: 223–236.

Bai M, Beutel RG, Song KQ, Liu WG, Malqin H, Li S, Hu XY, Yang XK (2012) Evolutionary patterns of hind wing morphology in dung beetles (Coleoptera: Scarabaeinae). Arthropod Structure & Development 41: 505–513. https://doi.org/10.1016/j.asd.2012.05.004

Bai M, Jarvis K, Wang SY, Song KQ, Wang YP, Wang ZL, Li WZ, Wang W, Yang XK (2010) A second new species of ice crawlers from China (Insecta: Grylloblattodea), with thorax evolution and the prediction of potential distribution. PLoS ONE 5(9): e12850. https://doi.org/10.1371/journal.pone.0012850

Bai M, Yang XK, Li J, Wang WC (2014b) Geometric Morphometrics, a super scientific computing tool in morphology comparison. Chinese Science Bulletin 59: 887–894. https://doi.org/10.1360/972012-1561

Ballerio A (2013) Revision of the Australian Ceratocanthinae (Coleoptera, Scarabaeoidea, Hybosoridae). ZooKeys 339: 67–91. https://doi.org/10.3897/zookeys.339.6033

Bezborodov VG, Koshkin ES (2014) A review of Bolboceratidae (Coleoptera, Scarabaeoidea) species from the Russian Far East. Entomological Review 94: 1313–1319. https://doi.org/10.1134/s0013873814090127

Bell JJ, Barnes DKA (2001) Sponge morphological diversity: a qualitative predictor of species diversity. Aquatic Conservation: Marine and Freshwater Ecosystems 11(2): 109–121. https://doi.org/10.1002/aqc.436

Bell JJ, Barnes DKA (2002) Modelling sponge species diversity using a morphological predictor: a tropical test of a temperate model. Journal for Nature Conservation 10(1): 41–50. https://doi.org/10.1078/1617-1381-00005

Benesh B (1960) Coleopterorum Catalogus. Pars 8. Lucanidea. Junk, The Hague, 178 pp.

Beutel RG, Leschen RAB (2005) Handbook of Zoology, Vol. IV, Part 38, Coleoptera, Beetles. Vol. 1: Morphology and Systematics (Archostemata, Adephaga, Myxophaga, Polyphaga partim). Walter de Gruyter, Berlin, New York, 567 pp.

Boilly O (2011) Les Bolboceratidae de Guyane. ACOREP, Coléoptères de Guyane 4: 19–31.

Bomans HE (2010) Description of a new species of *Figulus* Macleay, 1819 from Micronesia. (108th contribution on Lucanidae, Coleoptera). Lambillionea 110(3): 338–339.

Bookstein FL (1991) Morphometric Tools for Landmark Data: Geometry and Biology. Cambridge University Press, Cambridge, 435 pp.

Bouchard P, Bousquet Y, Davies AE, Alonso-Zarazaga MA, Lawrence JF, Lyal CH, Newton AF, Reid CA, Schmitt M, Slipiński SA, Smith AB (2011) Family-group names in Coleoptera (Insecta). ZooKeys 88: 1–972. https://doi.org/10.3897/zookeys.88.807

Bunalski M (1999) Die Blatthornkäfer Mitteleuropas. Coleoptera, Scarabaeoidea. Bestimmung - Verbreitung - Ökologie. Slamka, Bratislava, 80 pp.

Chiari S, Zauli A, Audisio P, Campanaro A, Donzelli PF, Romiti F, Svensson GP, Tini M, Carpaneto GM (2014) Monitoring presence, abundance and survival probability of the stag beetle, *Lucanus cervus*, using visual and odour-based capture methods: implications for conservation. Journal of Insect Conservation 18: 99–109. https://doi.org/10.1007/s10841-014-9618-8

Dallwitz MJ (1980) A general system for coding taxonomic descriptions. Taxon 29: 6–41. https://doi.org/10.2307/1219595

Dallwitz MJ, Paine TA, Zurcher EJ (1993) User's Guide to the DELTA System: a General System for Processing Taxonomic Descriptions. 4th edition. http://delta-intkey.com

Dallwitz MJ, Paine TA, Zurcher EJ (1995) User's Guide to Intkey: a Program for Interactive Identification and Information Retrieval. http://delta-intkey.com

Dallwitz MJ, Paine TA, Zurcher EJ (2000) Principles of interactive keys. http://delta-intkey.com

Didier R, Seguy E (1953) Catalogue illustré des Lucanides du globe. Texte. Encyclopédie Entomologique (A) 27: 1–223.

Evans MEG (1977) Locomotion in the Coleoptera Adephaga especially Carabidae. Journal of Zoology 181: 189–226. https://doi.org/10.1111/j.1469-7998.1977.tb03237.x

Foote M (1993) Discordance and concordance between morphological and taxonomic diversity. Paleobiology 19(02): 185–204. https://doi.org/10.1017/s0094837300015864

Forsythe TG (1981) Running and pushing in relationship to hind leg structure in some Carabidae (Coleoptera). Coleoptera Bulletin 35: 353–378.

Friedman M (2010) Explosive morphological diversification of spiny-finned teleost fishes in the aftermath of the end-Cretaceous extinction. Proceedings of the Royal Society B: Biological Sciences 277(1688): 1675–1683. https://doi.org/10.1098/rspb.2009.2177

Fujita H (2010) The Lucanid beetles of the world. Mushi-Sha's Iconographic Series of Insects. Mushisha, Tokyo, 472 pp.

Goyens J, Dirckx J, Aerts P (2015) Stag beetle battle behavior and its associated anatomical adaptations. Journal of Insect Behavior 28: 227–244. https://doi.org/10.1007/s10905-015-9495-3

Goyens J, Dirckx J, Dierick M, Van Hoorebeke L, Aerts P (2014) Biomechanical determinants of bite force dimorphism in *Cyclommatus metallifer* stag beetles. Journal of Experimental Biology 217(7): 1065–1071. https://doi.org/10.1242/jeb.091744

Grafen A (1989) The phylogenetic regression. Philosophical transactions of the Royal Society B326: 119–157. https://doi.org/10.1098/rstb.1989.0106

Hammer Ø, Harper DAT, Ryan PD (2001) PAST: Paleontological statistics software package for education and data analysis. Palaeontologia Electronica 4: 1–9.

Hardersen S, Macagno ALM, Sacchi R, Toni I (2011) Seasonal constraints on the mandible allometry of *Lucanus cervus* (Coleoptera: Lucanidae). European Journal of Entomology 108(3): 461–468. https://doi.org/10.14411/eje.2011.059

Hlavac TF (1972) The prothorax of Coleoptera: origin, major features of variation. Psyche 79(3): 123–149. https://doi.org/10.1155/1972/31579

Hosoya T (2011) Phylogenetic relationships of the genus *Dorcus* and its related genera (Coleoptera, Lucanidae): a reanalysis of allozyme data. Elytra 1(2): 199–209.

Hosoya T, Araya K (2005) Phylogeny of Japanese stag beetles (Coleoptera: Lucanidae) inferred from 16S mtrRNA gene sequences, with reference to the evolution of sexual dimorphism of mandibles. Zoological Science 22(12): 1305–1318. https://doi.org/10.2108/zsj.22.1305

Hosoya T, Araya K (2006) Phylogeny and evolution of sexual dimorphism of mandibles in Japanese stag beetles (Coleoptera, Lucanidae). Gekkan-Mushi 426: 41–49.

Hosoya T, Araya K, Shirota Y (2002) Molecular phylogeny of Japanese and Taiwanese stag beetles of the genus *Dorcus* and allied genera (Coleoptera, Lucanidae) based on random amplified polymorphic DNA. Giornale Italiano di Entomologia 10(50): 133–140.

Hosoya T, Araya K, Shirota Y (2003) Molecular phylogeny of Japanese stag beetles of the genus *Dorcus* (Coleoptera, Lucanidae) and its allied genera inferred from mitochondrial COI gene sequences. Elytra 31(1): 127–142.

Huang H, Chen CC (2012) A review of the genera *Prismognathus* Motschulsky and *Cladophyllus* Houlbert (Coleoptera: Scarabaeoidea: Lucanidae) from China, with the description of two new species. Zootaxa 3255: 1–36.

Iguchi Y (2013) Male mandible trimorphism in the stag beetle *Dorcus rectus* (Coleoptera: Lucanidae). European Journal of Entomology 110(1): 159–163. https://doi.org/10.14411/eje.2013.022

Imura Y (2007) Endophallic structure of the genus *Platycerus* (Coleoptera, Lucanidae) of Japan, with descriptions of two new species. Elytra 35(2): 471–489.

Imura Y (2010) A new *Platycerus* (Coleoptera, Lucanidae) from the Baotianman Nature Reserve in western Henan, Central China. Elytra 38(2): 227–232.

Imura Y (2011) Two new taxa of the genus *Platycerus* (Coleoptera, Lucanidae) from China. In: Kawai S (Ed.) Masumushi: entomological papers dedicated to Dr. Kimio Masumoto on the occasion of his retirement 1: 131–141.

Imura Y (2012) Description of a new *Platycerus* (Coleoptera, Lucanidae) from Sichuan, southwest China, with records of two other species belonging of the same genus. Elytra 2(1): 61–68.

Kawano K (1997) Cost of evolving exaggerated mandibles in stag beetles (Coleoptera: Lucanidae). Annals of the Entomological Society of America 90(4): 453–461. https://doi.org/10.1093/aesa/90.4.453

Kawano K (2000) Genera and allometry in the stag beetle family Lucanidae, Coleoptera. Annals of the Entomological Society of America 93(2): 198–207. https://doi.org/10.1603/0013-8746(2000)093[0198:gaaits]2.0.co;2

Kawano K (2003) Character displacement in stag beetles (Coleoptera: Lucanidae). Annals of the Entomological Society of America 96(4): 503–511. https://doi.org/10.1603/0013-8746(2003)096[0503:cdisbc]2.0.co;2

Kawano K (2006) Sexual dimorphism and the making of oversized male characters in beetles (Coleoptera). Annals of the Entomological Society of America 99(2): 327–341. https://doi.org/10.1603/0013-8746(2006)099[0327:sdatmo]2.0.co;2

Kim SI, Farrell BD (2015) Phylogeny of world stag beetles (Coleoptera: Lucanidae) reveals a Gondwanan origin of Darwin's stag beetle. Molecular Phylogenetics and Evolution 86: 35–48. https://doi.org/10.1016/j.ympev.2015.02.015

Klingenberg CP (2011) MorphoJ: an integrated software package for geometric morphometrics. Molecular Ecology Resources 11: 353–357. https://doi.org/10.1111/j.1755-0998.2010.02924.x

Klingenberg CP, Marugán-Lobón J (2013) Evolutionary covariation in geometric morphometric data: analyzing integration, modularity, and allometry in a phylogenetic context. Systematic Biology 62: 591–610. https://doi.org/10.1093/sysbio/syt025

Knell RJ, Pomfret JC, Tomkins JL (2004) The limits of elaboration: curved allometries reveal the constraints on mandible size in stag beetles. Proceedings of the Royal Society B: Biological Sciences 271(1538): 523–528. https://doi.org/10.1098/rspb.2003.2641

Knight K (2014) Stag beetle males compensate for massive mandibles. Journal of Experimental Biology 217(7): 1009. https://doi.org/10.1242/jeb.105213

Kobayashi H, Matsumoto T (2011) Atlas of Japanese Scarabaeoidea, Volume 3: Phytophagous Group II. Roppon-Ashi Entomological Books, Tokyo. 178 pp.

Král D (2001) Revision of the genera *Odontotrypes* and *Phelotrupes* (Coleoptera: Geotrupidae). Folia Heyrovskyana Supplementum 8: 1–178.

Král D, Hillert O, Drožová D, Šípek P (2013) *Lethrus* (*Lethrus*) *schneideri* sp n. (Coleoptera, Geotrupidae) from Greece. ZooKeys 339: 93–106. https://doi.org/10.3897/zookeys.339.6132

Lawrence JF, Newton Jr AF (1995) Families and subfamilies of Coleoptera. In: Pakaluk J, Slipinski SA (Eds) Biology, Phylogeny, and Classification of Coleoptera: Papers Celebrating the 80th Birthday of Roy A. Crowson. Muzeum I Instytut Zoologii PAN, Warszawa, 559–1092.

Li S, Ricchiardi E, Bai M, Yang X (2016) A taxonomy review of *Oreoderus* Burmeister, 1842 from China with a geometric morphometric evaluation (Coleoptera, Scarabaeidae, Valgini). Zookeys 552: 67–89. https://doi.org/10.3897/zookeys.552.6096

MacLeod N (2017) Morphometrics: history, development methods and prospects. Zoological Systematics 42: 4–33. https://doi.org/10.11865/zs.201702

Maddison WP, Maddison DR (2011) Mesquite: a Modular System for Evolutionary Analysis Version 2.75. http://mesquiteproject.org

Maes JM, Pinratana A (2003) Lucanidae of Thailand. Sunrise Printing, Bangkok, 447 pp.

Mohedano-Navarrete A, Reyes-Bonilla H, López-Pérez RA (2008) Species richness and morphological diversity of the Genus *Porites* in the Pacific Ocean. Proceedings of the 11th International Coral Reef Symposium, Fort Lauderdale, Florida, 7–11.

Mondaca J, Smith ABT (2008) A revision of the southern South American genus *Bolborhinum* Boucomont (Coleoptera: Geotrupidae: Bolboceratinae). Zootaxa. 1–48. https://doi.org/10.5281/zenodo.182603

Nguyen TQ (2013) Description of a new species of the genus *Neolucanus* Thomson, 1862 (Coleoptera: Lucanidae) from central Vietnam. Zootaxa 3741(3): 377–384. https://doi.org/10.11646/zootaxa.3741.3.6

Nikolajev GV (1999) On the polyphyly of the subfamily Penichrolucaninae (Coleoptera, Lucanidae) with the erection of the new monotypic tribe Brasilucanini. Tethys Entomological Research 1: 171–172.

Nikolajev GV (2009) Ochodaeidae species of the Palaearctic's Asia. Euroasian Entomological Journal 8(2): 205–211.

Ocampo FC (2006) Phylogenetic analysis of the scarab family Hybosoridae and monographic revision of the New World subfamily Anaidinae (Coleoptera: Scarabaeidae). Bulletin of the University of Nebraska State Museum 19: 13–177.

Okada K, Miyatake T (2009) Genetic correlations between weapons, body shape and fighting behaviour in the horned beetle *Gnatocerus cornutus*. Animal Behaviour 77(5): 1057–1065. https://doi.org/10.1016/j.anbehav.2009.01.008

Okajima S, Araya K (2012) The Standard of Scarabaeoid Beetles in Japan. Gakken Publishing Co. Ltd, Tokyo, 445 pp.

Okuda N (2012a) A new species of the genus *Nigidius* MacLeay from Kon Tum Province, Central Vietnam. Kogane 13: 143–146.

Okuda N (2012b) Two new species of *Aegus* MacLeay (Coleoptera, Lucanidae) from south Sulawesi province, Indonesia. Gekkan-Mushi 493: 25–28.

Palestrini C, Roggero A, Hernandez Nova LK, Giachino PM, Rolando A (2012) On the evolution of shape and size divergence in Nebria (Nebriola) ground beetles (Coleoptera, Carabidae). Systematics and Biodiversity 10: 147–157. https://doi.org/10.1080/14772000.2012.685775

Paulsen MJ (2010) The stag beetles of southern South America (Coleoptera: Lucanidae). Bulletin of the University of Nebraska State Museum 24: 1–147.

Paulsen MJ (2013) A new genus for the Neotropical species of *Aesalus* Fabricius, with descriptions of eight new species (Coleoptera: Lucanidae: Aesalinae). Insecta Mundi 25: 1–25.

Paulsen MJ, Mondaca EJ (2006) Revision of the South American Ceratognathini (Coleoptera: Lucanidae: Aesalinae) with the description of a new genus and a new species. Zootaxa 1191: 1–19.

Paulsen MJ, Ocampo FC (2012) The Ochodaeidae of Argentina (Coleoptera, Scarabaeoidea). ZooKeys 174: 7–30. https://doi.org/10.3897/zookeys.174.2668

Ponomarenko AG (2004) Beetles (Insecta, Coleoptera) of the late Permian and early Triassic. Paleontological Journal 38(Supplement 2): S185–S196.

Ratcliffe BC (1984) A review of the Penichrolucaninae with analyses of phylogeny and biogeography, and description of a second New World species from the Amazon Basin (Coleoptera: Lucanidae). Quaestiones Entomologicae 20(2): 60–87.

Ricklefs RE (2012) Species richness and morphological diversity of passerine birds. Proceedings of the National Academy of Sciences 109(36): 14482–14487. https://doi.org/10.1073/pnas.1212079109

Rohlf FJ (2006) tps-DIG, Digitize Landmarks and Outlines, Version 2.05. [Software and Manual]. Department of Ecology and Evolution, State University of New York at Stony Brook, New York. http://life.bio.sunysb.edu/morph/

Rohlf FJ (2007). NTSYS-pc Numerical Taxonomy and Multivariate Analysis System, Version 2.20 for Windows [Software and Manual]. Exeter Software, New York.

Roy K, Balch DP, Hellberg ME (2001) Spatial patterns of morphological diversity across the Indo-Pacific: analyses using strombid gastropods. Proceedings of the Royal Society B: Biological Sciences 268(1485): 2503–2508. https://doi.org/10.1098/rspb.2000.1428

Roy K, Foote M (1997) Morphological approaches to measuring biodiversity. Trends in Ecology & Evolution 12(7): 277–281. https://doi.org/10.1016/s0169-5347(97)81026-9

Sakai K, Nagai S (1998) The Cetoniine Beetles of the World. Mushi-Sha, Tokyo, 421 pp.
Schenk KD (2008) Lucanidae vom Arunachal Pradesh, Indien und beschreibung von zwei neuen Arten. Entomologische Zeitschrift 118(4): 175–178.
Sherratt E, Gower DJ, Klingenberg CP, Wilkinson M (2014) Evolution of cranial shape in caecilians (Amphibia: Gymnophiona). Evolutionary Biology 41: 528–545. https://doi.org/10.1007/s11692-014-9287-2
Tatsuta H, Mizota K, Akimoto SI (2001) Allometric patterns of heads and genitalia in the stag beetle *Lucanus maculifemoratus* (Coleoptera: Lucanidae). Annals of the Entomological Society of America 94(3): 462–466. https://doi.org/10.1603/0013-8746(2001)094[0462:apohag]2.0.co;2
Tatsuta H, Mizota K, Akimoto SI (2004) Relationship between size and shape in the sexually dimorphic beetle *Prosopocoilus inclinatus* (Coleoptera: Lucanidae). Biological Journal of the Linnean Society 81: 219–233. https://doi.org/10.1111/j.1095-8312.2003.00279.x
Van Roon G (1910) Lucanidae. In: Schenkling S (Ed.) Coleopterorum Catalogus. W. Junk, Berlin, 7–8.
Williams PH, Humphries CJ (1996) Comparing character diversity among biotas. In: Gaston KJ (Ed.) Biodiversity: a Biology of Numbers and Differences. Blackwell Science, Oxford, 54–76.
Zelditch ML, Swiderski DL, Sheets HD, Fink WL (2004) Geometric Morphometrics for Biologists: a Primer. Elsevier, San Diego, 428 pp.

Supplementary material 1

Geometric morphometric data

Authors: Mengna Zhang, Yongying Ruan, Xia Wan, Yijie Tong, Xingke Yang, Ming Bai
Data type: morphometric data
Explanation note: Tables S1–S12.
Copyright notice: This dataset is made available under the Open Database License (http://opendatacommons.org/licenses/odbl/1.0/). The Open Database License (ODbL) is a license agreement intended to allow users to freely share, modify, and use this Dataset while maintaining this same freedom for others, provided that the original source and author(s) are credited.
Link: https://doi.org/10.3897/zookeys.833.26164.suppl1

ZooKeys 833: 41–58 (2019)
doi: 10.3897/zookeys.833.32837
http://zookeys.pensoft.net

RESEARCH ARTICLE

A peer-reviewed open-access journal
ZooKeys
Launched to accelerate biodiversity research

On the clawed lobsters of the genus *Nephropsis* Wood-Mason, 1872 recently collected from deep-sea cruises off Taiwan and the South China Sea (Crustacea, Decapoda, Nephropidae)

Su-Ching Chang[1], Tin-Yam Chan[1,2]

1 *Institute of Marine Biology, National Taiwan Ocean University, Keelung 20224, Taiwan* **2** *Center of Excellence for the Oceans, National Taiwan Ocean University, Keelung 20224, Taiwan*

Corresponding author: *Tin-Yam Chan* (tychan@mail.ntou.edu.tw)

Academic editor: *S. De Grave* | Received 4 January 2019 | Accepted 13 February 2019 | Published 25 March 2019

http://zoobank.org/2309E59F-5CB1-471F-8C00-73008352A515

Citation: Chang S-C, Chan T-Y (2019) On the clawed lobsters of the genus *Nephropsis* Wood-Mason, 1872 recently collected from deep-sea cruises off Taiwan and the South China Sea (Crustacea, Decapoda, Nephropidae). ZooKeys 833: 41–58. https://doi.org/10.3897/zookeys.833.32837

Abstract

Recent deep-sea cruises using Taiwanese research vessels off Taiwan and in the South China Sea yielded seven species of the clawed lobster genus *Nephropsis* Wood-Mason, 1872. Four species are new records for Taiwan (*Nephropsis acanthura* Macpherson, 1990, *N. holthuisi* Macpherson, 1993, *N. serrata* Macpherson, 1993, and *N. suhmi* Bate, 1888) and three species are new records of Dongsha (under the jurisdiction of Taiwan) in the South China Sea (*N. ensirostris* Alcock, 1901, *N. stewarti* Wood-Mason, 1872, and *N. suhmi*). Altogether, five and four species of this genus are now known from Taiwan and Dongsha, respectively. The diagnostic characters and coloration are illustrated for most, if not all, of these species.

Keywords

New records, synonym, taxonomy, West Pacific

Introduction

Members of the genus *Nephropsis* Wood-Mason, 1872 represent the common clawed lobster found in the deep sea world-wide (Macpherson 1990; Holthuis 1991; Chan 1997; Alves-Júnior et al. 2016). At present, 15 species of this genus are recognized (Chan 2010), and with nine of them distributed in the Indo-West Pacific (Macpherson 1990, 1993; Griffin and Stoddart 1995; Holthuis 1991; Chan 1997; Watabe and Ii-

Copyright *Su-Ching Chang, Tin-Yam Chan.* This is an open access article distributed under the terms of the Creative Commons Attribution License (CC BY 4.0), which permits unrestricted use, distribution, and reproduction in any medium, provided the original author and source are credited.

zuka 1999; Zarenkov 2006). In Taiwanese waters, only one species, *Nephropsis stewarti* Wood-Mason, 1872, has been formally reported (Chan and Yu 1988, 1993), and this species can often been caught by commercial deep-sea trawlers although never in large numbers. Recent deep-sea cruises using Taiwanese research vessels off Taiwan and the South China Sea have yielded many species of *Nephropsis*. Amongst them, *N. serrata* Macpherson, 1993 had been listed in a molecular phylogenetic study (Tshudy et al. 2009). Close examination of this *Nephropsis* material reveals seven species, including four new Taiwanese records (*N. acanthura* Macpherson, 1990, *N. holthuisi* Macpherson, 1993, *N. serrata*, and *N. suhmi* Bate, 1888) and three new records (*N. ensirostris* Alcock, 1901, *N. suhmi*, and *N. stewarti*) around Dongsha (Pratas, under the jurisdiction of Taiwan) in the South China Sea. The present work reports these findings. The two other Indo-West Pacific species those are still not known in Taiwan and adjacent areas are *N. carpenteri* Wood-Mason, 1885, and *N. malhaensis* Borradaile, 1910. Both of them appear to be restricted in the Indian Ocean (Macpherson 1990).

Materials and methods

Specimens are deposited in the National Taiwan Ocean University, Keelung (**NTOU**). The station (stn) designation is preceded by a prefix indicating the actual type of collecting equipment, as follows: Le Drezen type solo hard bottom 12.4 m otter trawl (CD), 4 m French beam trawl (CP), 2.5 m French beam trawl (PCP), and 3 m ORE beam trawl (OCP). Carapace length (cl) is measured along the dorsal midline from the orbital margin to the posterior margin of the carapace. Morphological terminology mainly follows Macpherson (1990). The synonymy provided is restricted to important taxonomic works of the species and previous Taiwanese and South China Sea records.

Taxonomy

Family Nephropidae Dana, 1852
Genus *Nephropsis* Wood-Mason, 1872

***Nephropsis acanthura* Macpherson, 1990**
Figs 1A, B, 3

Nephropsis acanthura Macpherson, 1990: 311, figs 5d, 9d–f, 11a, b, 16d (type locality: Philippines); Holthuis 1991: 35, figs 61, 62; Chan 1997: 413; 2010: 156; Poore 2004: 166, fig. 43b; Zarenkov 2006: 85, fig. 3; Poore et al. 2008: 34.

Material examined. TAIWAN 2003, stn CD210, 24°28.99'N, 122°12.79'E, 500–1183 m, 1 Jun 2003, 1 female cl 10.6 mm (NTOU M00951). TAIWAN 2006, stn PCP343, 22°15.699'N, 120°2.131'E, 945–1059 m, 8 Mar 2006, 1 female cl 8.9 mm (NTOU M00952).

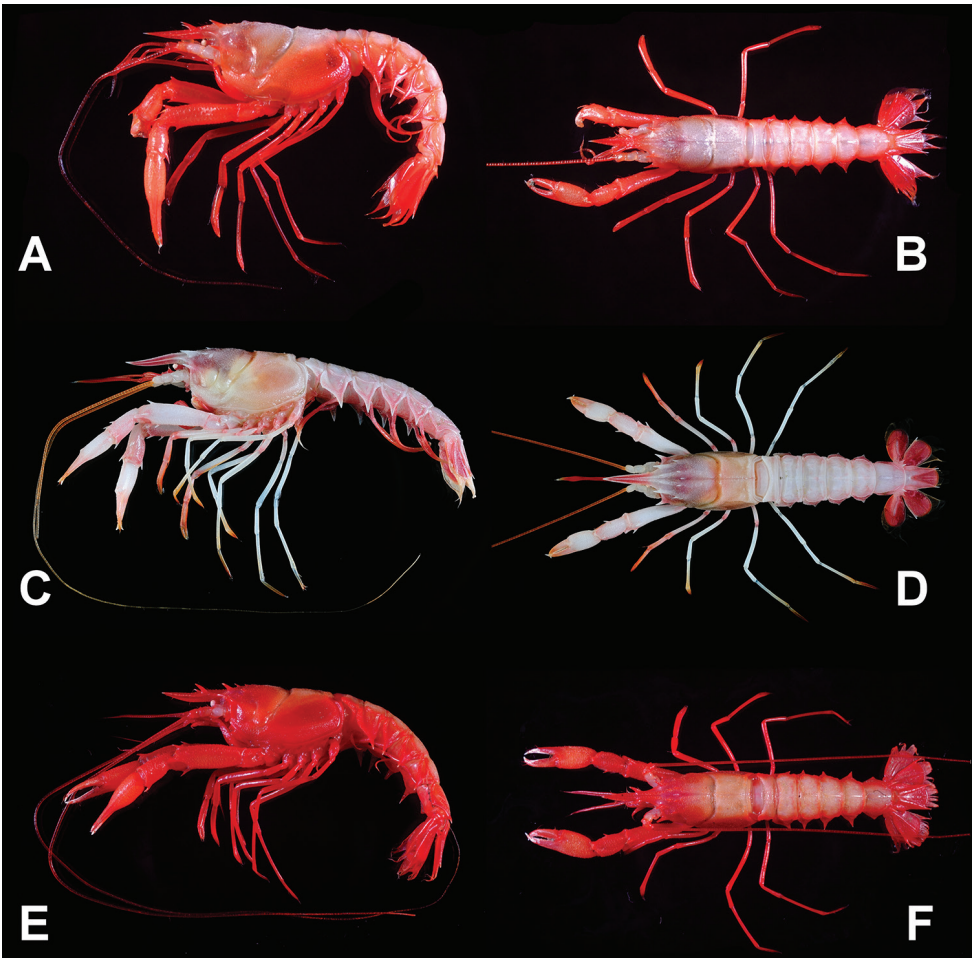

Figure 1. *Nephropsis acanthura* Macpherson, 1990, stn CD210, female cl 10.6 mm (NTOU M00951) (**A, B**); *N. ensirostris* Alcock, 1901, stn CP4137, female cl 14.6 mm (NTOU M02071) (**C, D**); *N. holthuisi* Macpherson, 1993, stn CP214, male cl 15.2 mm (NTOU M02160) (**E, F**).

Diagnosis. Carapace finely granulate. Rostrum longer than half carapace length, bearing a pair of strong lateral spines. Median groove on rostrum extending anteriorly beyond lateral rostral spines. Subdorsal carinae granulate. Supraorbital spines well developed. Postcervical groove passing dorsal midline of carapace. Distance between orbital border and postcervical groove slightly less than twice distance between postcervical groove and posterior border of carapace.

Abdomen with tergites II–VI bearing conspicuous median carina. Anterior border of pleuron II convex and bearing some spinules, terminating in long, acute point. Anterior border of pleura III–V less convex and also terminating in long, acute point. Strong erect dorsal spine present near base of telson. Uropodal exopod with complete diaeresis.

Carpus of cheliped I with strong anterordorsal spine; outer surface without spine; inner border with a spine somewhat at middle of carpus. Carpus of pereiopod II

shorter than palm. Carpus of pereiopod III approximately 2/3 palm length. Dactyli of pereiopods IV and V slightly longer than half propodus length.

Color in life. Body generally reddish with dorsal carapace and abdomen whitish. Eyes whitish.

Distribution. Widely distributed in the Indo-West Pacific: Madagascar, Indonesia, Australia, Coral Sea, New Caledonia, Tasman Sea, Chesterfield Islands, the Philippines, southern Japan (Macpherson 1990; Holthuis 1991; Griffin and Stoddart 1995; Chan 1997; Poore 2004; Zarenkov 2006; Poore et al. 2008), and now Taiwan. The bathymetric depth ranges from 500–1305 m.

Remarks. *Nephropsis acanthura* is reported from Taiwan for the first time. This species and *N. occidentalis* Faxon, 1893 are the only two species in the genus bearing an erect spine near the base of the telson (Macpherson 1990; Holthuis 1991). The two Taiwanese specimens fit well with the characteristics of *N. acanthura* in the carapace bearing numerous small granules, the rostrum longer than half carapace length, and the abdominal pleura II-V terminating in a long, acute point (see Macpherson 1990; Holthuis 1991). Nevertheless, there are some variations noticed in the present material compared with those reported by Macpherson (1990). In the Taiwanese specimens, the dactyli of pereiopods IV and V (Fig. 3C) are slightly longer than half propodus length (vs. less than half). The median groove on the rostrum extends beyond the lateral rostral spines (vs. terminating at the level of lateral rostral spines). The distance between the orbital border and postcervical groove is slightly less (vs. slightly more) than twice the distance between the postcervical groove and posterior border of carapace. Additionally, it is reported that the carapace is less granular in the Indonesian material (Chan 1997).

Nephropsis ensirostris Alcock, 1901

Figs 1C, D, 4

Nephropsis ensirostris Alcock, 1901: 158, pl. 1-fig. 2 (type locality: north of the Laccadives, Arabian Sea); Macpherson 1990: 303, figs 5a, 6, 8a, b, 16a; Holthuis 1991: 41, figs 71, 72; Chan 1997: 414; 2010: 157.

Material examined. Zhongsha 2015, stn CP4137, 19°53.059'N, 114°21.678'E, 536–524 m, 23 Jul 2015, 1 male cl 12.1 mm (NTOU M01831), 1 female cl 14.6 mm (NTOU M02071).

Diagnosis. Carapace finely granulate. Rostrum more than half carapace length, without lateral spine. Median groove reaching or overreaching midpoint of rostrum. Each subdorsal carina with none or two spines and several granules. Gastric tubercle located closer to orbital border than to postcervical groove. Supraorbital and postsupraorbital spines present. Postcervical groove deep, passing dorsal midline of carapace. Pair of dorsal spines located just behind postcervical groove. Distance between orbital border and postcervical groove less than twice distance between postcervical groove and posterior border of carapace.

Abdominal tergites I–V with conspicuous transverse grooves. Dorsal median carina present on tergites II–VI. Anterior borders of pleura II–V granulated, spineless, terminating in a long, acute point. Anterior border of pleuron II more convex than those of other pleura. Uropodal exopod with distinct but incomplete diaeresis.

Cheliped I with little pubescence; carpus with well-developed anterodorsal spine, outer spine on terminal half and inner spine at about mid-length. Carpus of pereiopod II slightly longer than palm. Carpus of pereiopod III more than half palm length. Dactyli of pereiopods IV and V approximately 2/3 propodus length.

Color in life. Body generally pinkish to whitish, with rostrum, tail fan, and antennal and antennular flagella reddish. Eyes whitish.

Distribution. This species has been reported in the Indian Ocean along Gulf of Aden, Laccadive Sea, Bay of Bengal to Andaman Sea. In the western Pacific it is only known from Indonesia and the Philippines. The present material extends its distribution to near Dongsha in the South China Sea. Bathymetric depth ranges from 315 to 1314 m (Macpherson 1990; Holthuis 1991; Chan 1997; Zarenkov 2006).

Remarks. *Nephropsis ensirostris* can be readily distinguished from other species of the genus by lacking a lateral spine on the rostrum. The two small specimens collected off west of Dongsha agree well with the description of Macpherson (1990), except for the spines on the subdorsal carina are missing in the male (Fig. 4B; see also Chan 1997). These spines are present in Macpherson's (1990) material as well as in the female specimen reported here (Figs 1D, 4A).

Nephropsis holthuisi **Macpherson, 1993**

Figs 1E, F, 5

Nephropsis holthuisi Macpherson, 1993: 55, figs 1–3 (except fig 3B), fig. 6B (erroneously as *N. serrata*) (type locality: Ashmore Reef, northwest Australia); Griffin and Stoddart 1995: 234; Chan 1997: 414; 2010: 157; Watabe and Iizuka 1999: 372, figs 1, 2; Poore 2004: 166, fig. 43c.

Nephropsis macphersoni Watabe & Iizuka, 1999: 376, figs 3, 4 (type locality: east of Terrigal, southeastern Australia); Poore 2004: 166, fig. 43d.

Material examined. TAIWAN 2001, stn CD132, 22°20.98'N, 120°6.73'E, 690–700 m, 21 Nov 2001, 1 female cl 18.7 mm (NTOU M02159). TAIWAN 2003, stn CP214, 24°28.59'N, 122°12.66'E, 490–1027 m, 27 Aug 2003, 1 female cl 11.3 mm, 3 males cl 13.6–14.1 mm (NTOU M02158); 1 male cl 15.2 mm (NTOU M02160).

Diagnosis. Carapace sparsely granulate. Rostrum 0.6–0.8 times carapace length, with pair of lateral spines. Median groove on rostrum reaching or overreaching lateral rostral spines. Subdorsal carinae with 1–4 spines posterior to supraorbital spines. Supraorbital spine well-developed, followed by distinct post-supraorbital spine. Distance between level of supraorbital spine and gastric tubercle approximately 0.4 times the distance between gastric tubercle and postcervical groove. Postcervical groove passing

dorsal midline of carapace. Distance between orbital border and postcervical groove 1.5–1.9 times distance between postcervical groove and posterior border of carapace.

Abdominal tergites II–VI with distinct dorsal median carina. Anterior border of each pleuron spineless, more convex in pleuron II, and terminating in long, sharp point on pleura II–V. Uropodal exopod with complete diaeresis.

Cheliped I sparsely granulate. Carpus shorter than palm, with anterodorsal spine, a spine on inner dorsal border at midlength, and without any accessory spines or granules. Carpus of pereiopod II somewhat shorter than palm. Carpus of pereiopod III 0.6 times palm length. Dactyli of pereiopods IV and V approximately half propodus length.

Color in life. Body generally vermilion red, with dorsal surface of posterior carapace and abdomen pinkish orange. Tips of large chelae and eyes whitish.

Distribution. Indo-West Pacific: Indonesia, Australia, Japan, and now Taiwan, at depths of 350–1135 m (Macpherson 1993; Griffin and Stoddart 1995; Chan 1997; Watabe and Iizuka 1999; Poore 2004).

Remarks. This species is similar to *Nephropsis rosea* Bate, 1888 from the West Atlantic. They both have one pair of rostral lateral spines, one pair of post-supraorbital spines, a median carina on tergites II–VI, and a complete diaeresis on uropodal exopods. These two species mainly differ in the position of the gastric tubercle (see Macpherson 1993). The Taiwanese material fits the characteristics of *N. holthuisi* in the distance between the supraorbital spine and gastric tubercle being less than half (vs. approx. 2/3 in *N. rosea*) the distance between the gastric tubercle and postcervical groove. Watabe and Iizuka (1999) argued that *N. holthuisi* can be readily distinguished from *N. rosea* by the large spine at the midlength of the inner dorsal border of carpus of cheliped I does not have any accessory spines or granules (vs. 1–3 accessory spines in *N. rosea*). The present specimens also agree in this character.

There are variations in the development of the subdorsal spines in the type series of *N. holthuisi* from rather granulate in the holotype to distinct in the paratype (Macpherson 1993). The present six specimens from Taiwan all have 1–4 distinct spines on the subdorsal carina (Figs 1F, 5). Watabe and Iizuka (1999) considered such difference as specific and treated the paratype of *N. holthuisi* as a distinct species *N. macphersoni* Watabe & Iizuka, 1999. However, all other differences proposed to distinguish *N. macphersoni* from *N. holthuisi* by Watabe and Iizuka (1999), such as pereiopods "less pubescent" or "more robust", abdominal tergite "more strongly granulated", are rather vague. Therefore, for the time being *N. macphersoni* is treated as a synonym of *N. holthuisi* as already stated by Chan (2010) until more evidence (e.g., from molecular analysis) is available to support that the former is a distinct species.

Nephropsis serrata **Macpherson, 1993**

Figs 2A, B, 6

Nephropsis serrata Macpherson, 1993: 59, figs 4–6 (type locality: northwestern Australia); Chan 1997: 414; 2010: 157; Poore 2004: 166, fig. 42b.

Nephropsis hamadai Watabe & Ikeda, 1994: 102, figs 1–2 (type locality: Japan).
Nephropsis lyra Zarenkov, 2006: 87, figs 8–11 (type locality: off northwestern Australia).
Nephropsis pseudoserrata Zarenkov, 2006: 91, figs 15–18 (type locality: northeastern Sumatra).

Material examined. TAIWAN 2003, stn CD210, 24°28.99'N, 122°12.79'E, 500–1183 m, 1 Jun 2003, 3 females cl 9.6–17.3 mm (NTOU M02156); stn CP214, 24°28.59'N, 122°12.66'E, 490–1027 m, 27 Aug 2003, 6 females cl 12.2–23.4 mm, 1 ovig. female cl 18.4 mm, 2 males cl 14.1, 22.5 mm (NTOU M02157); 3 females cl 17.7–20.5 mm, 1 ovig. female cl 17.9 mm (NTOU M00157); 3 females cl 10.7–25.3 mm, 2 ovig. females cl 19.7, 20.1 mm, 5 males cl 9.7–20.7 mm (NTOU M02150). TAIWAN 2006, stn CP371, 24°28.521'N, 122°12.821'E, 582–613 m, 26 Aug 2006, 1 female cl 12.9 mm (NTOU M02151); 1 female cl 13.7 mm, 1 ovig. female cl 17.7 mm, 1 male cl 16.9 mm (NTOU M02154). TAIWAN 2012, stn CP463, 24°28.775'N, 122°12.719'E, 474–647 m, 30 Jun 2012, 2 females cl 11.8, 21.7 mm, 1 ovig. female cl 18.1 mm, 1 male with damaged carapace (NTOU M02152); 1 male cl 10.6 mm (NTOU M02153); 4 females cl 15.6–21.2 mm, 2 ovig. females cl 18.4, 21.7 mm, 3 males cl 13.1–20.3 mm (NTOU M02155).

Diagnosis. Carapace slightly granulate. Rostrum 0.4–0.8 times carapace length, with pair of lateral spines. Median groove reaching lateral rostral spines. Each subdorsal carinae with 2–6 distinct spines and some granules. Supraorbital spine well-developed, without post-supraorbital spine. Postcervical groove passing midline of carapace. Distance between orbital margin and postcervical groove 1.5–1.9 times distance between postcervical groove and posterior margin of carapace.

Abdominal tergites smooth, sometimes with some granules on large specimens, without median dorsal carina. Anterior margins of pleura II–V without spines, usually ending in a long, acute point. Uropodal exopod with complete diaeresis.

Cheliped I sparsely granulated, covered with dense hairs. Carpus with anterodorsal spine, 0–1 spine (rarely 0) on inner dorsal border at midlength, and an anteroventral spine on inner margin. Carpus of pereiopod II more or less as long as palm. Carpus of pereiopod III 0.6 times palm length. Dactyli of pereiopods IV and V 0.5–0.6 times propodus length.

Color in life. Body generally whitish with rostrum, distal parts of pereiopods, maxilliped III, antennular and antennal flagella, abdominal pleura, uropods and distal part of telson pinkish red to reddish. Eyes whitish. Eggs greyish yellow.

Distribution. Recorded from Indonesia, Australia, Japan, and now Taiwan, at depths of 390–1430 m (Macpherson 1993; Watabe and Ikeda 1994; Chan 1997; Poore 2004; Zarenkov 2006).

Remarks. One of the specimens from the lot NTOU M00157 was used and listed in a recent molecular phylogenetic work (Tshudy et al. 2009: table 1), which is the first literature record of this species from Taiwan. *Nephropsis serrata* is very similar to *N. stewarti*. They both lack median dorsal carina on the abdomen and mainly differ in the presence or absence of spines on the subdorsal carina (Macpherson 1993). The other

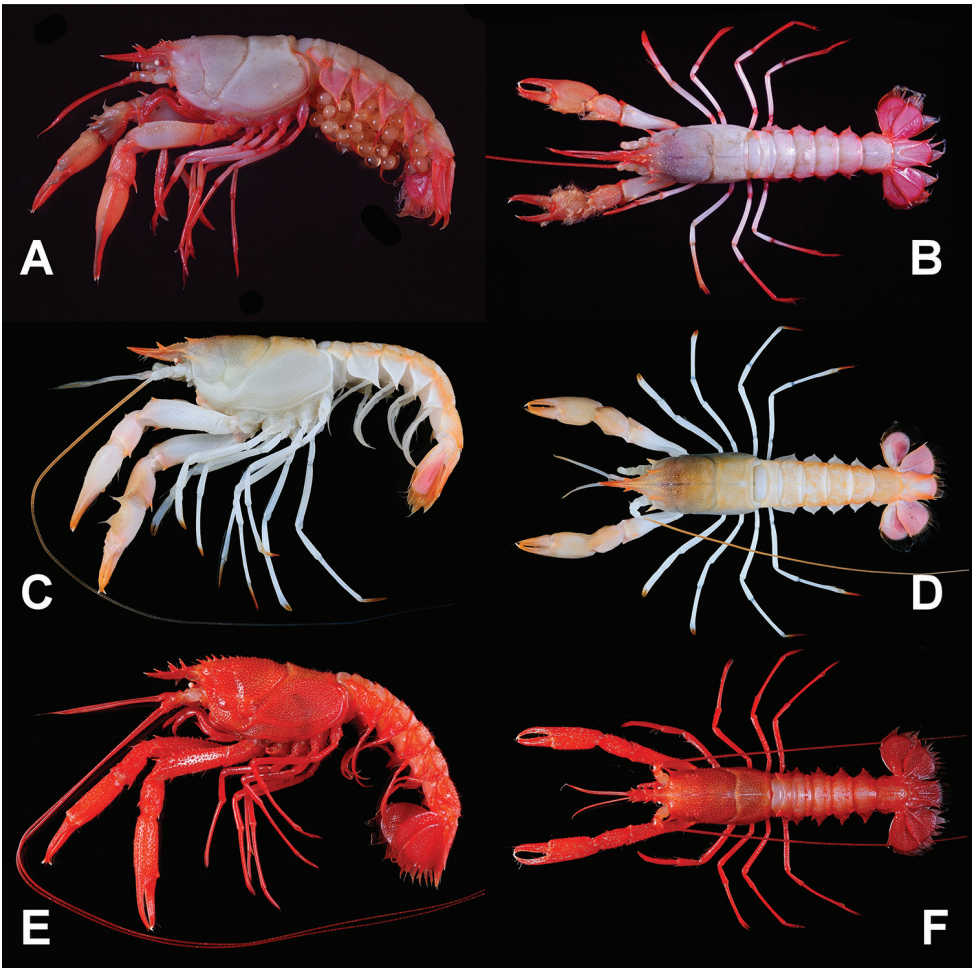

Figure 2. *Nephropsis serrata* Macpherson, 1993 (**A, B**), stn CP214, ovig. female cl 17.9 mm (NTOU M00157) (**A**); stn CD210, female cl 17.3 mm (NTOU M02156) (**B**). *N. stewarti* Wood-Mason, 1872, stn CP4155, female cl 25.2 mm (NTOU M02162) (**C, D**); *N. suhmi* Bate, 1888, stn OCP280, female 32.4 mm (NTOU M02134) (**E, F**).

distinguishing characters mentioned by Macpherson (1993), such as *N. serrata* having more elongate lateral rostral spines than supraorbital spines, a slightly shorter rostrum, and a less elongate large chela, are difficult to use (see Macpherson 1993: Figs 7, 8). The Taiwanese specimens all bear distinct spines on the subdorsal carinae and agree well with the original description of the species (Macpherson 1993), except for the carpus of the large cheliped bearing 0–1 (mostly one) rather than two spines on the inner dorsal border at mid-length. Moreover, an ovigerous female (NTOU M02154) is abnormal in having two spines on the right side of the rostrum.

Three recently described species, namely *N. hamadai* Watabe & Ikeda, 1994, *N. lyra* Zarenkov, 2006, and *N. pseudoserrata* Zarenkov, 2006, are treated under the synonyms

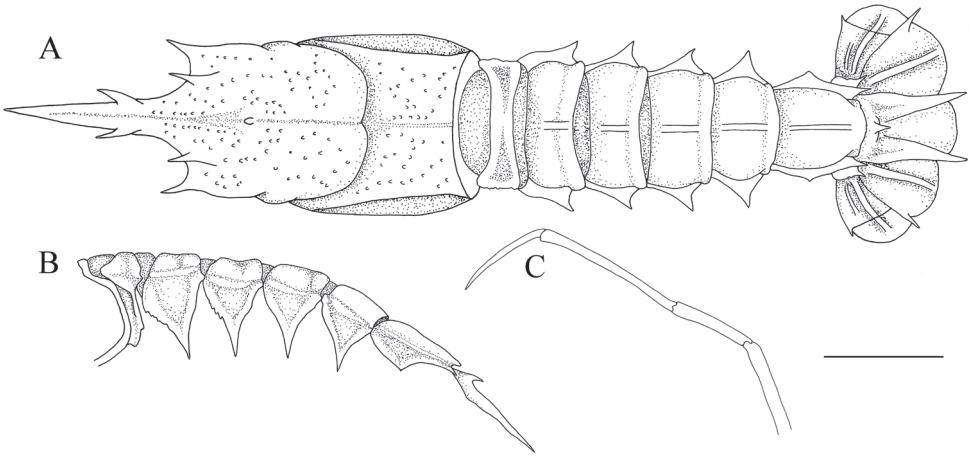

Figure 3. *Nephropsis acanthura* Macpherson, 1990, stn CD 210, female cl 10.6 mm (NTOU M00951). Dorsal habitus (**A**); abdomen, lateral view (**B**); left pereiopod V, lateral view (**C**). Scale bar: 0.5 cm.

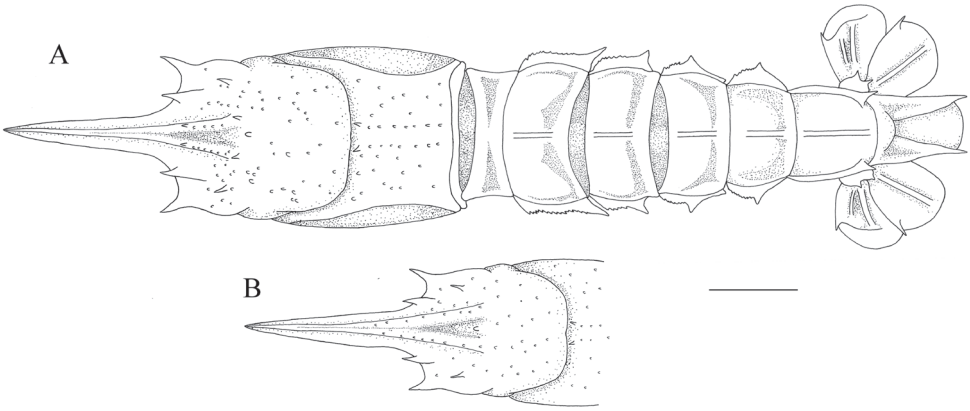

Figure 4. *Nephropsis ensirostris* Alcock, 1901, stn CP4137. Female cl 14.6 mm (NTOU M02071), dorsal habitus (**A**); male cl 12.1 mm (NTOU M01831), anterior carapace, dorsal view (**B**). Scale bar: 0.5 cm.

of *N. serrata* by Chan (1997, 2010). Some of the differences between *N. hamadai* and *N. serrata* proposed by Watabe and Ikeda (1994) have been shown to be inappropriate by Chan (1997). The present Taiwanese material also reflects such an opinion, except for the inner dorsal border of the carpus of the large cheliped always being armed with fewer than two spines at the mid-length (two spines in *N serrata* by Macpherson 1993 and one spine in *N. hamadai* by Watabe and Ikeda 1994). In the original description of *N. lyra*, Zarenkov (2006) argued that this species is closest to *N. stewarti* and *N. grandis* Zarenkov 2006. However, *N. lyra* is actually most similar to *N. serrata* in bearing 3–4 distinct spines on the subdorsal carina. Since no distinct difference is observed between

the original illustrations of *N. lyra* (Zarenkov 2006: figs 8–11) from *N. serrata*, and the type localities of both species are from the same area (i.e., off northwestern Australia), these two species are considered as synonyms pending more evidence to support their separation. Another species, *N. pseudoserrata* described by Zarenkov (2006), based on a single specimen from Sumatra, is also closest to *N. serrata* in having 1–2 spines on the subdorsal carina. However, Zarenkov (2006) claimed that *N. serrata* differs from *N. pseudoserrata* in the subdorsal carina being smooth. As this separation is based on a misinterpretation and the other differences proposed by Zarenkov (2006: table 4) on the armature of the large cheliped are rather variable in this genus, *N. pseudoserrata* is not recognized as a species distinct from *N. serrata*.

Nephropsis stewarti Wood-Mason, 1872

Figs 2C, D, 7

Nephropsis stewarti Wood-Mason, 1872: 60 (type locality: Ross Island, Andaman Sea); Chan and Yu 1988: 8, pl. 1A; 1993: 83, unnumbered photo; Macpherson 1990: 312, figs 5e, 10, 11c, d, 16e; 1993: 63; Holthuis 1991: 45, figs 80, 81; Chan 1997: 415; 2010: 157; Zarenkov 2006: 93, fig. 19; Poore et al. 2008: 34.

Nephropsis grandis Zarenkov, 2006: 86, figs 5–7 (type locality: off Arnhem Land, northern Australia).

Material examined. Zhongsha 2015, stn CP4137, 19°53.059'N, 114°21.678'E, 536–524 m, 23 Jul 2015, 1 male cl 15.9 mm (NTOU M02161); stn CP4155, 16°13.60'N, 115°01.61'E, 526–510 m, 28 Jul 2015, 1 female cl 25.2 mm (NTOU M02162), 1 male cl 12.8 mm (NTOU M02163). Yilan County, Dasi fishing port, 10 Sept 1984, 1 female cl 44.8 mm (NTOU M02165); Sept 1992, 2 females cl 39.7, 39.8 mm, 1 male cl 45.3 mm (NTOU M02171); Aug 2003, 1 male cl 38.9 mm (NTOU M00505); 29 May 2008, 1 male cl 41.9 mm (NTOU M02177); 12 Apr 2012, 1 female cl 32.4 mm (NTOU M02178); 14 Aug 2013, 1 male cl 19.8 mm (NTOU M02179). Yilan County, Nanfang-ao fishing port, 2 May 1985, 1 female cl 40.7 mm, 1 male with damaged carapace (NTOU M02166); 20 Apr 1988, 1 female cl 40.5 mm, 1 male cl 28.2 mm (NTOU M02167); 12 Nov 2004, 1 male cl 31.8 mm (NTOU M02176). Pingtung County, Donggang fishing port, Jul 1975, 1 male cl 23.4 mm (NTOU M02164); 3 Mar 1991, 6 females cl 19.5–20.2 mm, 1 male cl 21.1 mm (NTOU M02168); 14 May 1991, 2 males cl 19.2, 21.7 mm (NTOU M02169); 4 Jun 1995, 1 male cl 22.4 mm (NTOU M02173); 27 Dec 1997, 2 males cl 29.0, 32.7 mm (NTOU M02174), 1 male cl 21.8 mm (NTOU M02175); 2 Oct 2014, 1 male cl 25.6 mm (NTOU M01898). Taiwan, locality not specified, 1993, 2 females cl 30.2, 40.6 mm, 1 male cl 31.1 mm (NTOU M02172). Dongsha, Jun 1991, 1 female cl 45.9 mm (NTOU M02170).

Diagnosis. Carapace nearly smooth, sometimes with some granules. Rostrum with pair of lateral spines. Median groove overreaching lateral rostral spines. Subdorsal carinae granulate, without spines. Supraorbital spines well developed, without post-

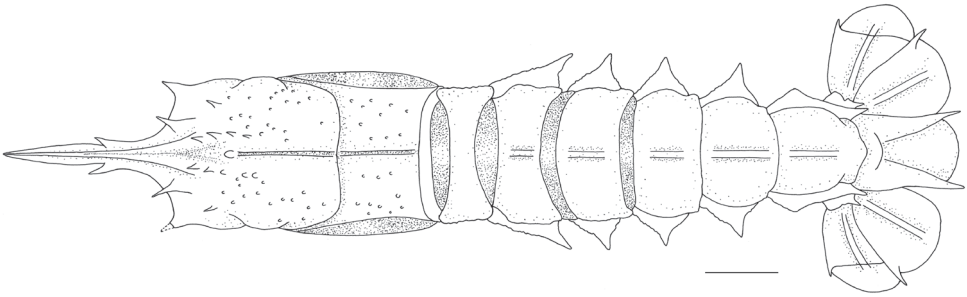

Figure 5. *Nephropsis holthuisi* Macpherson, 1993, stn CP132, female cl 18.7 mm (NTOU M02159), dorsal habitus. Scale bar: 0.5 cm.

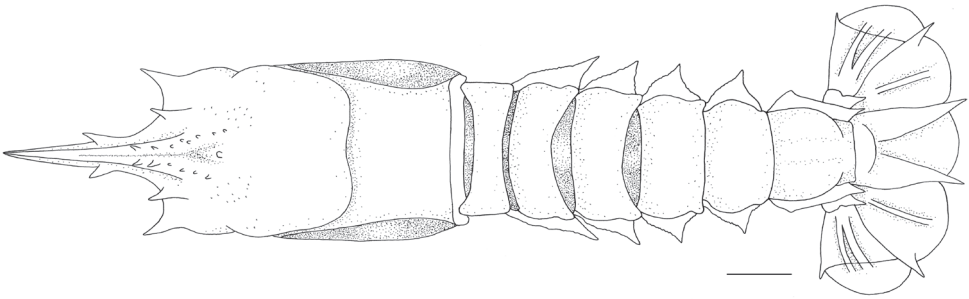

Figure 6. *Nephropsis serrata* Macpherson, 1993, stn CP463, female cl 21.7 mm (NTOU M02152), dorsal habitus. Scale bar: 0.5 cm.

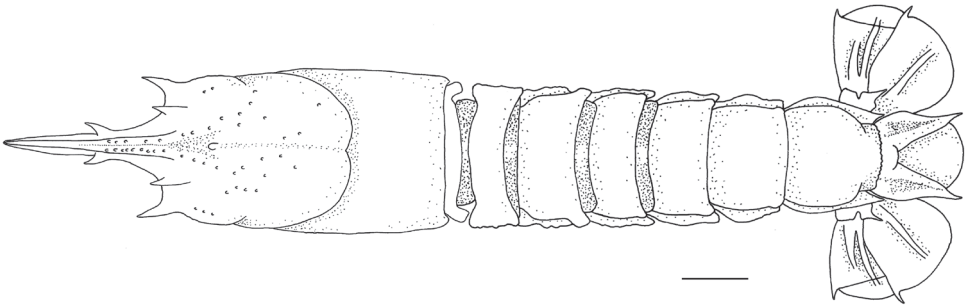

Figure 7. *Nephropsis stewarti* Wood-Mason, 1872, Dasi fishing port, Yilan County, male cl 38.9 mm (NTOU M00505), dorsal habitus. Scale bar: 1 cm.

supraorbital spine. Distance between orbital margin and postcervical groove more than 1.5 times distance between postcervical groove and posterior margin of carapace.

Abdominal tergites II–V without dorsal median carina. No spines on anterior margin of each pleuron. Anterior margin of pleuron II convex, generally ending in long,

sharp point (but rather short and blunt in large specimens). Anterior margins of pleura III–V less convex, each ending in long, sharp point. Uropodal exopod with distinct and complete diaeresis.

Cheliped I densely pubescent. Carpus with anterodorsal and anteroventral spines, and 0–4 dorsal spines on outer margin. Carpus of pereiopod II slightly shorter than palm. Carpus of pereiopod III more than half palm length. Dactyli of pereiopods IV and V approximately half propodus length.

Color in life. Body generally whitish with antennular and antennal flagella, anterior segment of large chelae, dorsal carapace, and abdomen somewhat pale orange. Rostrum, tips of pereiopods II to V, and tail fan pinkish red. Eyes whitish. Pubescence on body light grey and eggs whitish.

Distribution. Widely distributed in the Indo-West Pacific and has been reported from Madagascar, Natal, Mozambique, Kenya, Gulf of Aden, Andaman Sea, Bay of Bengal, Indonesia, Australia, the Philippines, Japan, Taiwan, and now the South China Sea, at depths of 170 to more than 1060 m (Macpherson 1990, 1993; Chan 1997; Zarenkov 2006; Poore et al. 2008).

Remarks. The present material collected by Taiwanese research vessels were from the South China Sea; near Dongsha (NTOU M02161, M02170) or the center of the South China Sea (NTOU M02162, M02163).

Nephropsis grandis Zarenkov, 2006 was described based on a single specimen from northern Australia, and is extremely similar to *N. stewarti* in the subdorsal carina lacking a spine and the abdomen without any dorsal median carina. These two species were differentiated only by the carpus of the large cheliped, which is more spiny in *N. grandis* (cf. Zarenkov 2006: table 4). As there are generally large intraspecific variations in the spination on the large cheliped in *Nephropsis* (e.g., in the present abundant material there are 4–15 distinct spines on the carpus of the large cheliped), more comprehensive studies with molecular genetic comparisons are necessary to verify if large cheliped spination is indeed a good character in separating the species of this genus. Therefore, for the time being *N. grandis* is treated as a synonym of *N. stewarti* as stated by Chan (2010).

Nephropsis suhmi **Bate, 1888**

Figs 2E, F, 8

Nephropsis suhmi Bate, 1888: 181, pl. 23-fig. 3, pl. 24-fig. 2 (type locality: Aru Islands, Indonesia); Macpherson 1990: 306, figs 5b, 7d-f, 8c, d, 16b; 1993: 64; Holthuis 1991: 46, figs 60b, 82; Griffin and Stoddart 1995: 234; Poore 2004: 166, fig. 43e; Zarenkov 2006: 93; Chan 2010: 157; Yaldwyn and Webber 2011: 198.

Nephropsis meteor Zarenkov, 2006: 90, figs 12–14 (type locality: Gulf of Aden).

Material examined. TAIWAN 2002, stn CP189, 21°39.91'N, 118°20.94'E, 1649–1629 m, 27 Aug 2002, 1 female cl 26.6 mm (NTOU M02131). TAIWAN

2004, stn CD238, 25°12.28'N, 123°1.85'E, 1689–1650 m, 23 Jul 2004, 1 male cl 17.8 mm (NTOU M02132). TAIWAN 2005, stn CP278, 24°23.63'N, 122°14.13'E, 1222–1239 m, 14 Jun 2005, 1 female cl 17.9 mm (NTOU M02133); stn OCP280, 24°23.71'N, 122°14.22'E, 1213–1261 m, 14 Jun 2005, 1 female 32.4 mm, 1 male cl 28.1 mm (NTOU M02134). TAIWAN 2006, stn CP372, 24°23.619'N, 122°14.138'E, 1220–1280 m, 26 Aug 2006, 1 female cl 12.9 mm (NTOU M02135). NanHai 2014, stn CP4106, 10°19.1500'N, 114°14.2530'E, 1292–1321 m, 6 Jan 2014, 1 female cl 18.5 mm (NTOU M02136); stn CP4108, 10°23.3701'N, 114°23.2672'E, 1707–1799 m, 6 Jan 2014, 1 female cl 35.7 mm (NTOU M02137), 1 male cl 38.3 mm (NTOU M02138), 1 male cl 34.8 mm (NTOU M02139). Dongsha 2014, stn CP4122, 21°34.976'N, 118°14.2792'E, 1713–1624 m, 30 Apr 2014, 1 female cl 40.4 mm (NTOU M02140). — Zhongsha 2015, stn CP4134, 19°55.837'N, 116°25.368'E, 1128–1278 m, 22 Jul 2015, 1 female cl 16.8 mm, 1 male cl 16.7 mm (NTOU M02141); stn CP4141, 18°54.31'N, 113°58.27'E, 1151–1286 m, 24 Jul 2015, 1 female cl 16.1 mm (NTOU M02142); stn CP4157, 19°52.593'N, 116°27.145'E, 1205–1389 m, 29 Jul 2015, 1 female cl 28.8 mm, 2 males cl 12.7, 16.0 mm (NTOU M02143); stn CP4163, 21°38.534'N, 118°19.179'E, 1683–1643 m, 31 Jul 2015, 1 female cl 46.8 mm (NTOU M02144); 1 female cl 39.4 mm, 1 male cl 19.9 mm (NTOU M02145); stn CP4167, 22°6.125'N, 119°7.775'E, 1756–1306 m, 1 Aug 2015, 1 male cl 13.2 mm (NTOU M02146). Cold Seep Cruise 2016, stn CST 11, 22°8.830'N, 119°15.681'E, 1319–1176 m, 27 Apr 2016, 1 female with damaged carapace (NTOU M02147); stn CST 17, 22°3.791'N, 118°58.804'E, 1483 m, 1 May 2016, 1 male cl 16.0 mm (NTOU M02148). Dongsha, 1256 m, 25 Apr 1996, 1 male cl 23.1mm (NTOU M02149).

Diagnosis. Carapace covered with numerous granules of varying sizes (more developed in adults). Rostrum 0.4–0.6 times carapace length (somewhat longer in smaller specimens), bearing two (rarely three) lateral spines on each side, sometimes with one additional spine. Median groove reaching or almost reaching distal pair of lateral rostral spines. Each subdorsal carina with 0–7 (usually 3–5) spines and some granules. Gastric tubercle closer to supraorbital spine than to postcervical groove. Supraorbital spine well developed. Post-supraorbital spine present, usually followed by 1–2 spines. Postcervical groove deep, crossing dorsal midline. Distance between orbital border and postcervical groove 1.5–1.9 times distance between postcervical groove and posterior border of carapace.

Abdomen covered with granules. Tergites I–V each with distinct transverse groove interrupted medially. Pleura II–V slightly convex, each terminating in long, acute point which occasionally absent on pleuron V. Anterior border of pleura II and III usually bearing one strong spine (sometimes two) and some additional spinules. Anterior border of pleuron IV sometimes with a spine as well. Posterobasal border of pleuron V usually unarmed but occasionally bearing a single large spine. Dorsal surface of tail fan granulate; uropodal exopod lacking diaeresis.

Cheliped I bearing numerous granules; carpus with well-developed anterodorsal spine; outer surface bearing several spines (sometimes only 1–2 distinct spines in smaller specimens); inner surface with anteroventral spine and 1–2 (rarely 0) spines medi-

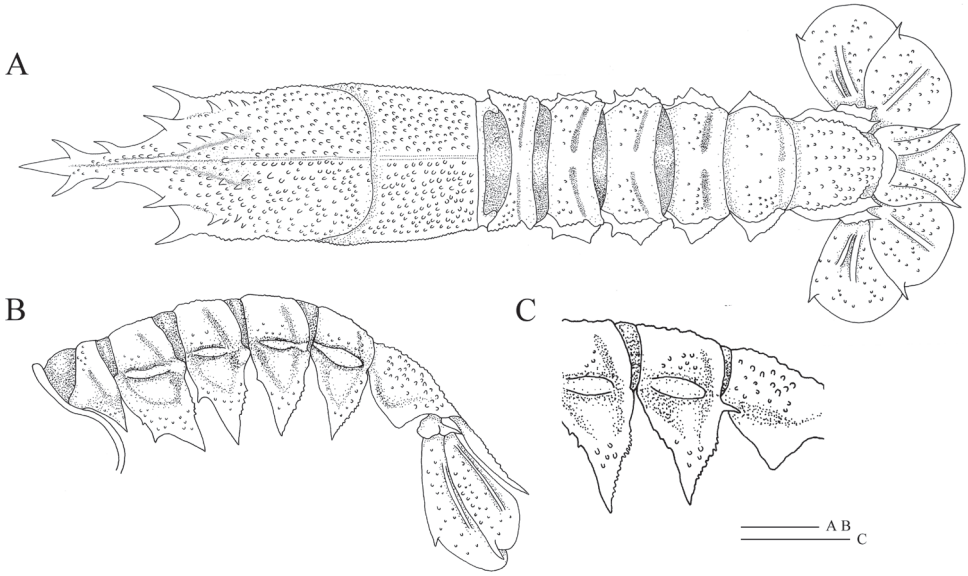

Figure 8. *Nephropsis suhmi* Bate, 1888, stn CP4163. Female cl 39.4 mm (NTOU M02145) (**A, B**); stn CP4108, female cl 38.3 mm (NTOU M02138) (**C**). Dorsal habitus (**A**); abdomen, lateral view (**B**); abdomen somite V, lateral view (**C**). Scale bar: 1 cm.

ally; dorsal surface of merus lined with spines. Carpus of pereiopod II 0.6–0.9 times palm length. Carpus of pereiopod III slightly more than half palm length. Dactyli of pereiopods IV and V approximately half propodus length.

Color in life. Entire body vermilion red, except tips of large chelae, eyes, most dorsal parts of abdominal tergites I to V, and basal parts of antennular peduncles whitish.

Distribution. Widely distributed in the Indo-West Pacific and recorded from Madagascar, Gulf of Aden, Maldive Sea, Arabian Sea, Indonesia, Australia, New Caledonia, western Tasman Sea, New Zealand, at 786–2029 m deep (Macpherson 1990, 1993; Griffin and Stoddart 1995; Poore 2004; Zarenkov 2006; Yaldwyn and Webber 2011). This species is reported for the first time from Taiwan and the South China Sea (including Dongsha).

Remarks. *N. suhmi* from the Indo-West Pacific and *N. agassizii* A. Milne-Edwards, 1880 from the West Atlantic (Macpherson 1990; Alves-Júnior et al. 2016) are the only two known species of *Nephropsis* lacking a diaeresis on uropodal exopods. The present material fits well with the concept of *N. suhmi* in having the dactylus of pereiopod V approximately half the propodus length (vs. distinctly less than half in *N. agassizii*; Holthuis 1974: fig. 19; Macpherson 1990: fig. 7c; Alves-Júnior et al. 2016: fig. 1A). The only discrepancy may be that in two (female of NTOU M02134; NTOU M02138) of the present 24 specimens there is a large posterior spine at the base of the pleuron V (Fig. 8C).

Nephropsis meteor Zarenkov, 2006 is closely related to *N. suhmi* and was described based on a single specimen from the Gulf of Aden (Zarenkov 2006). The characters

separating *N. meteor* from *N. suhmi* are the merus of large cheliped with two instead of one rows of spines, the postcervical groove dorsally armed with a pair of dorsal spines (vs. no dorsal spines), and the anterior margin of abdominal pleura III–V each bearing two spines instead of one spine (Zarenkov 2006: table 3). However, in the original description and illustration of *N. meteor* (Zarenkov 2006: 90, fig. 13B), the anterior margins of pleura IV and V each bearing only one and not two spines as listed in the table of distinguishing characters given by Zarenkov (2006: table 3). In the present material, there are 0–2 distinct spines on the anterior margin of each of the abdominal pleura III–V. The spination on the postcervical groove and merus of large cheliped are also rather variable in the abundant material examined in this study (i.e., 1–2 rows of spines on the merus of the large cheliped and 0–2 distinct spines on the dorsal part of postcervical groove). Thus, *N. meteor* should be considered as a synonym of *N. suhmi* as stated by Chan (2010) until there is more evidence to support their separation.

Nephropsis sulcata Macpherson, 1990

Fig. 9

Nephropsis sulcata Macpherson, 1990: 319, figs 13e–g, 14a, b, 15a, b, 16g (type locality: Philippines); 1993: 64; Holthuis 1991: 47, figs 84, 85; Griffin and Stoddart 1995: 235, fig. 1; Chan 1997: 415; 2010: 157; Zarenkov 2006: 94, fig. 20A.
Nephropsis atlantica: Bruce 1966: 223. **non** Norman, 1882

Material examined. Dongsha 2014, stn CP4130, 20°17.971'N, 116°07.966'E, 795–822 m, 2 May 2014, 1 male cl 16.6 mm (NTOU M02130).

Diagnosis. Carapace generally smooth, with some small granules. Rostrum more than half carapace length, bearing two strong lateral spines. Median groove overreaching distal pair of lateral rostral spines. Posterior portion of subdorsal carina armed with several small spines. Postorbital and post-supraorbital spines present. Postcervical groove crossing midline of carapace. Distance between orbital margin and postercervical groove approximately 1.5 times distance between postcervical groove and posterior margin of carapace.

Abdominal tergites II–VI with distinct median carina. Anterior border of pleura II–V convex, each terminating in long, acute point. A single strong spine and 1–3 additional spines on anterior border of pleuron II. Anterior border of pleuron III with two small spines. Posterior border of pleuron V armed with a strong spine. Uropodal exopod with complete diaeresis.

Cheliped I bearing numerous granules on all articles. Carpus with anterodorsal and anteroventral spines; two spines on inner surface; outer surface with one spine on distal half. Carpus of pereiopod III 0.79 times palm length.

Color in life. Unknown.

Distribution. Widely distributed in the Indo-West Pacific from Madagascar, Laccadive Sea, Indonesia, South China Sea, northwestern and eastern Australia, Coral Sea, Chesterfield Islands, New Caledonia, and the Philippines, at depths of 200–1115 m

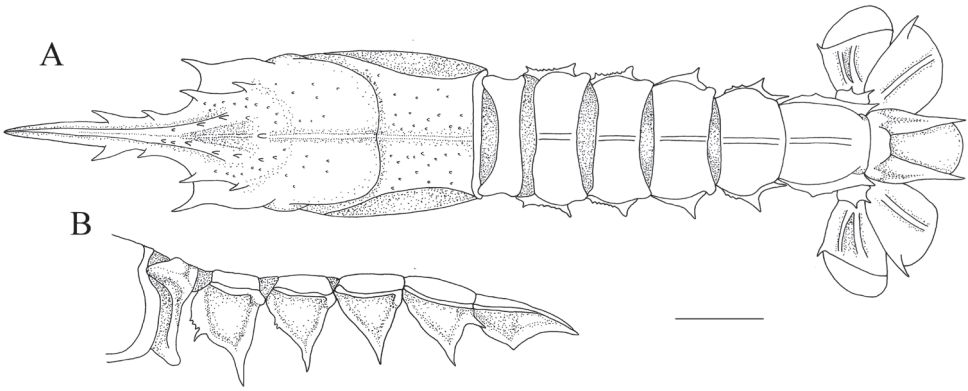

Figure 9. *Nephropsis sulcata* Macpherson, 1990, stn CP4130, male cl 16.6 mm (NTOU M02130). Dorsal habitus (**A**); abdomen, lateral view (**B**). Scale bar: 0.5 cm.

(Macpherson 1990, 1993; Holthuis 1991; Griffin and Stoddart 1995; Chan 1997; Zarenkov 2006).

Remarks. The present specimen was collected off Dongsha in the South China Sea and the presence of *N. sulcata* off Dongsha has been reported before (Bruce 1966, as *N. atlantica* Norman, 1882; see Macpherson 1990). *Nephropsis sulcata* can be distinguished from the closely related Atlantic species *N. atlantica* by the carpus of the pereiopod II being longer than the palm, and usually bearing a spine on the posterior border of the abdominal pleuron V (Fig. 9B; see also Chan 1997). Even though both sides of pereiopod II are missing in the present specimen, its remaining part agrees well with the description of *N. sulcata* by Macpherson (1990).

Key to species of *Nephropsis* off Taiwan and Dongsha

1 Rostrum without lateral spines.....***N. ensirostris***
– Rostrum with lateral spines.....**2**
2 Exopod of uropod without diaeresis.....***N. suhmi***
– Exopod of uropod with diaeresis.....**3**
3 Rostrum with 2 pairs of lateral spines .....***N. sulcata***
– Rostrum with 1 pair of lateral spines.....**4**
4 Dorsal surface of telson with well-developed proximal median spine.....
.....***N. acanthura***
– Dorsal surface of telson without median spine **5**
5 Abdominal tergites with dorsal median carina.....***N. holthuisi***
– Abdominal tergites without dorsal median carina **6**
6 Subdorsal carinae of rostrum with distinct spines.....***N. serrata***
– Subdorsal carinae of rostrum without distinct spines .....***N. stewarti***

Acknowledgements

This work was supported by grants from the Ministry of Science and Technology, Taiwan, ROC, and the Center of Excellence for the Oceans (National Taiwan Ocean University), which is financially supported by The Featured Areas Research Center Program within the framework of the Higher Education Sprout Project by the Ministry of Education in Taiwan, ROC.

References

Alcock A (1901) A descriptive catalogue of the Indian deep-sea Crustacea Decapoda Macrura and Anomala in the Indian Museum. Being a revised account of the deep-sea species collected by the Royal Indian Marine Survey Ship Investigator. The Trustees of the Indian Museum, Calcutta, 286 pp. https://doi.org/10.5962/bhl.title.16083

Alves-Júnior FdA, Araújo MDSLCD, Souza-Filho JF (2016) Distribution of two species of *Nephropsis* Wood-Mason, 1872 (Crustacea, Decapoda, Nephropidae) from northeastern Brazil. Zootaxa 4114: 90–94. https://doi.org/10.11646/zootaxa.4114.1.8

Bate CS (1888) Report on the Crustacea Macrura collected by HMS Challenger during the years 1873–1876, Zoology. Neill and Company, Edinburgh, 942 pp. https://doi.org/10.5962/bhl.title.6513

Bruce AJ (1966) *Hymenopenaeus halli* sp. nov., a new species of penaeid prawn from the South China Sea (Decapoda, Penaeidae). Crustaceana 11: 216–224. https://doi.org/10.1163/156854066X00388

Chan TY (1997) Crustacea Decapoda: Palinuridae, Scyllaridae and Nephropidae collected in Indonesia by the KARUBAR Cruise, with an identification key for the species of *Metanephrops*. In: Crosnier A, Bouchet P (Eds) Rèsultats des Campagnes MUSORSTOM. Volume 16. Mèmoires du Musèum national d'Histoire naturelle, Paris, 409–431. http://www.documentation.ird.fr/hor/fdi:010010306

Chan TY (2010) Annotated checklist of the world's marine lobsters (Crustacea: Decapoda: Astacidea, Glypheidea, Achelata, Polychelida). The Raffles Bulletin of Zoology supplement: 153–181. https://lkcnhm.nus.edu.sg/rbz/supplement-no-23/

Chan TY, Yu HP (1988) Clawed lobsters (Crustacea: Decapoda: Nephropidae) of Taiwan. Bulletin of the Institute of Zoology, Academia Sinica 27: 7–12.

Chan TY, Yu HP (1993) The Illustrated Lobsters of Taiwan. SMC Publishing, Taipei, 247 pp. [figs 1–74]

Griffin DJG, Stoddart HE (1995) Deep-water decapod Crustacea from eastern Australia: lobsters of the families Nephropidae, Palinuridae, Polychelidae and Scyllaridae. Records of the Australian Museum 47: 231–263. https://doi.org/10.3853/j.0067-1975.47.1995.239

Holthuis LB (1991) Marine Lobsters of the World. An Annotated and Illustrated Catalogue of Species of Interest to Fisheries known to Date. FAO Species Catalogue, FAO, Rome, 292 pp. http://www.fao.org/3/t0411e/t0411e00.htm

Macpherson E (1990) Crustacea Decapoda: on a collection of Nephropidae from the Indian Ocean and Western Pacific. In: Crosnier A (Ed) Résultats des campagnes MUSORSTOM, vol. 6 (Crustacés de la Nouvelle Calédonie). Mémoires du Muséum national d'Histoire naturelle. Série A, Zoologie, Paris, 289–329. http://www.documentation.ird.fr/hor/fdi:42400

Macpherson E (1993) New records for the genus *Nephropsis* Wood-Mason (Crustacea, Decapoda, Nephropidae) from northern Australia, with the description of two new species. Beagle: Records of the Museums and Art Galleries of the Northern Territory 10: 55–66. https://reurl.cc/G4j0y

Poore GCB (2004) Marine decapod Crustacea of southern Australia: a guide to identification. CSIRO publishing, Melbourne, 574 pp. https://doi.org/10.5860/CHOICE.42-4032

Poore GCB, McCallum AW, Taylor J (2008) Decapod Crustacea of the continental margin of southwestern and central Western Australia: preliminary identifications of 524 species from FRV *Southern Survey* voyage SS10-2005. Museum Victoria Science Reports 11: 1–106. https://doi.org/10.24199/j.mvsr.2008.11

Tshudy D, Robles R, Chan TY, Ho KC, Chu KH, Ahyong ST, Felder DL (2009) Phylogeny of marine clawed lobster families Nephropidae Dana 1852 and Thaumastochelidae Bate 1888 based on mitochondrial genes. In: Martin JW, Crandall KA, Felder DL (Eds) Decapod Crustacean Phylogenetics. CRC Press, Boca Raton, Florida, 357–368. https://doi.org/10.1201/9781420092592-c18

Watabe H, Ikeda H (1994) *Nephropsis hamadai*, a new nephropid lobster (Decapoda: Nephropidae) from bathyal depth in Sagami Nada, central Japan. Crustacean Research 23: 102–107. https://doi.org/10.18353/crustacea.23.0_102

Watabe H, Iizuka E (1999) A new species of the bathyal lobster genus *Nephropsis* (Crustacea: Decapoda: Nephropidae) from Australian waters, with a redescription of *N. holthuisi*. Species Diversity 4: 371–380. https://doi.org/10.12782/specdiv.4.371

Wood-Mason J (1872) VII. On *Nephropsis Stewarti*, a new genus and species of macrurous crustaceans, dredged in deep water off the Eastern coast of the Andaman Islands. Annals and Magazine of Natural History 12: 59–64. https://doi.org/10.1080/00222937308680697

Yaldwyn JC, Webber WR (2011) Annotated checklist of New Zealand Decapoda (Arthropoda: Crustacea). Tuhinga 22: 171–272. https://reurl.cc/67vnb

Zarenkov NA (2006) Nephropid lobsters from the Indian Ocean with descriptions of four new species (Crustacea: Decapoda: Nephropidae). Senckenbergiana Maritima 36: 83–98. https://doi.org/10.1007/BF03043703

ZooKeys 833: 59–74 (2019)
doi: 10.3897/zookeys.833.30592
http://zookeys.pensoft.net

RESEARCH ARTICLE

A peer-reviewed open-access journal
ZooKeys
Launched to accelerate biodiversity research

Molecular and morphological evidence for the identity of two nominal species of *Astegopteryx* (Hemiptera, Aphididae, Hormaphidinae)

Qiang Li[1], Jiamin Yao[1], Lingda Zeng[1], Xiaolan Lin[1], Xiaolei Huang[1]

1 *State Key Laboratory of Ecological Pest Control for Fujian and Taiwan Crops, College of Plant Protection, Fujian Agriculture and Forestry University, Fuzhou 350002, China*

Corresponding author: *Xiaolei Huang* (huangxl@fafu.edu.cn)

Academic editor: *R. Blackman* | Received 16 October 2018 | Accepted 25 January 2019 | Published 25 March 2019

http://zoobank.org/017B191A-82E0-45A4-BA6E-785CB853F1A0

Citation: Li Q, Yao J, Zeng L, Lin X, Huang X (2019) Molecular and morphological evidence for the identity of two nominal species of *Astegopteryx* (Hemiptera, Aphididae, Hormaphidinae). ZooKeys 833: 59–74. https://doi.org/10.3897/zookeys.833.30592

Abstract

The morphology of many insect species is usually influenced by environmental factors and therefore high phenotypic variation exists even within a species. This causes difficulty and uncertainty in species taxonomy, which can be remedied by using molecular data and integrative taxonomy. *Astegopteryx bambusae* and *A. bambucifoliae* are currently regarded as two closely related aphid species with similar bamboo hosts and overlapping distributions in the oriental region. However, in practice it is hard to distinguish between them. By incorporating molecular data from four mitochondrial and nuclear genes as well as morphological information from an extensive collection of live specimens, the present study indicates that *A. bambucifoliae* is a junior synonym of *A. bambusae*. The data also indicate that large-scale geographic patterns of population differentiation may exist within this species.

Keywords

DNA barcoding; Hormaphidinae; integrative taxonomy; species delimitation

Introduction

For many insect groups, morphology is influenced by environmental factors. For example, aphids are a plant-feeding group with extremely high phenotypic plasticity across space and time, which can be influenced by different factors such as host plant (Wool

Copyright *Qiang Li et al.* This is an open access article distributed under the terms of the Creative Commons Attribution License (CC BY 4.0), which permits unrestricted use, distribution, and reproduction in any medium, provided the original author and source are credited.

and Hales 1997; Margaritopoulos et al. 2000), associated ant species (Yao 2012), climate and temperature (Blackman and Eastop 1994), as well as geography (Madjdzadeh and Mehrparvar 2009). In traditional insect taxonomy, species identification depends heavily on specimen morphology, and many species are first described based on only a small number of samples (Winston 1999; Eastop and Blackman 2005). However, for species with high intraspecific morphological variation, small samples from restricted areas and times cannot represent the complete range of morphological variation. This can cause difficulty and uncertainty in species delimitation, so that synonymies inevitably occur in taxonomy (Eastop and Blackman 2005; Meier 2017). Fortunately, new types of data yielded by new technologies such as DNA barcoding (Hebert et al. 2003; Foottit et al. 2008) and integrative taxonomic practices (Schlick-Steiner et al. 2010) can help to solve these problems and improve the quality and efficiency of taxonomy (Turčinavičienė and Rakauskas 2009; Jensen et al. 2010; Heethoff et al. 2011).

The genus *Astegopteryx* is an oriental aphid group with more than twenty species, and is the largest genus in the tribe Cerataphidini (Hemiptera, Aphididae, Hormaphidinae) (Blackman and Eastop 2018; Favret 2018). Some species of *Astegopteryx* have host alternation between their primary host plants, *Styrax* (Styracaceae) trees, on which they form multiple-cavity galls, and secondary host plants, mainly bamboos and palms (Kurosu and Aoki 1991; Aoki and Kurosu 2010; Huang et al. 2012; Blackman and Eastop 2018). However, many species can live exclusively on their secondary host plants with parthenogenetic reproduction (Blackman and Eastop 2018) and display variable morphology (Noordam 1991; Stern et al. 1997). In the taxonomic history of this genus, due to morphological variation between generations on different host plants (e.g. primary and secondary hosts) and even within generations (Aoki and Kurosu 2010), as well as species description on the basis of limited sampling, many synonyms have been created (Blackman and Eastop 1994; Favret 2018). Two currently valid species, *A. bambusae* (Buckton, 1893) and *A. bambucifoliae* (Takahashi, 1921), occur simultaneously on similar bamboo hosts and have overlapping distributions in the oriental region (Noordam 1991; Blackman and Eastop 1994; Qiao et al. 2018). These species have been distinguished mainly by differences in color and appearance in life, as well as some differences in morphology of antennae and wax glands in mounted specimens (Blackman and Eastop 1994). *Astegopteryx bambusae* was originally described as *Oregma bambusae* by Buckton (1893) based on samples on *Bambusa arundinacea* in Dehra Dun, India, with the erection of the genus *Oregma*, now a junior synonym of *Astegopteryx* (Buckton 1893; Blackman and Eastop 2018). The original description of the oval-shaped apterous viviparous female was obscure and simple when judged by today's criteria. Moreover, the description as "color greenish brown, more or less mottled with black" in Buckton (1893) may have been based on dead specimens (Blackman and Eastop 2018). Takahashi (1921) originally described *A. bambucifoliae* (as *Oregma bambucifoliae*) attacking *Bambusa* spp. in Taiwan Island, with yellowish or fresh green body and a distinct character, "a pair of longitudinal dark green patches on the dorsum, which are often interrupted at mid-length" (Takahashi 1921). Later other morphological characters observed in mounted specimens such as the morphology of the wax glands were introduced to distinguish these two species

(Noordam 1991; Qiao et al. 2018). For example, in the key to species of *Astegopteryx* of Qiao et al. (2018), wax cells tightly connected or not, and wax cells discernible or not, were used to separate these two species. However, in practice it is still hard to distinguish them due to overlap of morphological characters of different populations. We also observed many times in the field that the occurrence of wax and dark green patches varied across populations in both *A. bambusae* and *A. bambucifoliae*. This indicates that the stability of proposed morphological diagnostic characters for these two species with similar habitats and times of occurrence is uncertain (Blackman and Eastop 2018), leading to doubts about their validity. Further detailed study including wider sampling is necessary to understand more about the morphological variation in both species, and molecular data analysis is crucial to clarify any distinction between them. In addition, considering that the mounting process of aphid slides may discard some useful morphological information, we think that the appearance of live specimens is helpful to understand morphological variation within or between species.

In the present study, based on an extensive sampling effort in subtropical China as well as molecular data from four mitochondrial and nuclear gene markers (cytochrome c oxidase subunit I, COI; cytochrome b, Cytb; tRNA/COII; elongation factor-1α, EF-1α), we aimed to show the spatial and temporal morphological diversity of both species, and test the validity of the two species by integrating the molecular and morphological data.

Materials and methods

Sampling

We did extensive field collections in subtropical China (including Fujian, Guangdong, Hainan, Guangxi, Yunnan provinces, ca. 18°15'–27°19'N, 100°15'–120°12'E) from 2015 to 2017. During the field work, photographs of live individuals were taken for all samples using a digital camera (Cannon EOS 7D plus Canon EF 100mm f/2.8L Macro IS USM Lens). Collected specimens were preserved in 95% ethanol and stored at -20 °C for further molecular experiments. The voucher specimens were stored at the Fujian Agriculture and Forestry University. For the final analyses, 37 specimens were chosen to represent the diversity of geography and time as clearly as possible. In accordance with the original descriptions of the two nominal species (Buckton 1893; Takahashi 1921) and other references (Noordam 1991; Blackman and Eastop 2018; Qiao et al. 2018), sixteen samples with an obvious pair of longitudinal dark green patches on the dorsum and relatively narrower body shape were tentatively identified as *A. bambucifoliae*, while 21 samples with relatively broader pear-shaped body and more wax were tentatively determined as *A. bambusae*. Based on current knowledge about the species relationships among this genus and related groups from previous literature (Aoki and Kurosu 1995; Stern et al. 1997; Blackman and Eastop 2018), two specimens of the closely-related but distinct species *A. formosana* were used as outgroups for phylogenetic tree reconstruction. Detailed specimen information including host plant, collection locality, voucher number, and GenBank accession number are shown in Table 1.

Table 1. Samples used in this study, with collection information and GenBank accession numbers.

Species (putative designation)	Host plant	Location	Voucher number	Accession number			
				COI	Cytb	EF	tRNA/COII
Astegopteryx bambucifoliae	bamboo	Fujian, Fuzhou	HL20160326_4	MH821567			
	bamboo	Fujian, Fuzhou	HL20160326_5	MH821568			
	bamboo	Fujian, Fuzhou	HL20160409_11	MH821537			
	bamboo	Fujian, Fuzhou	HL20160417_7	MH821538			
	bamboo	Fujian, Fuzhou	HL20160512_1	MH821539	MK028307	MK028325	MK372350
	bamboo	Fujian, Fuzhou	HL20161127_3	MH821542			
	bamboo	Fujian, Fuzhou	HL20161127_4	MH821543	MK028308	MK028331	MK372351
	bamboo	Fujian, Fuzhou	HL20161228_18	MH821544			
	bamboo	Guangdong, Shenzhen	HL20170205_7	MH821545	MK028309	MK028332	MK372352
	bamboo	Guangdong, Shenzhen	HL20170205_8	MH821546			
	bamboo	Fujian, Fuding	HL20170403_10	MH821549	MK028310	MK028333	MK372353
	bamboo	Fujian, Fuzhou	HL20170409_2	MH821551			
	bamboo	Fujian, Fuzhou	HL20170409_3	MH821554	MK028311		MK372354
	bamboo	Fujian, Fuzhou	HL20170419_4	MH821556			
	bamboo	Fujian, Fuzhou	HL20170926_23	MH821559	MK028312	MK028334	MK372355
	bamboo	Guangxi, Chongzuo	HLzld20171102_15	MH821571	MK028313		MK372356
A. bambusae	bamboo	Fujian, Fuzhou	HL20150416_14	MH821562			
	bamboo	Fujian, Fuzhou	HL20150510_2	MH821570			
	bamboo	Fujian, Fuzhou	HL20150530_4	MH821561			
	bamboo	Fujian, Xiamen	HL20160131_8	MH821563	MK028314	MK028335	MK372357
	bamboo	Hainan, Sanya	HL20160217_1	MH821565	MK028315		MK372358
	bamboo	Fujian, Fuzhou	HL20160308_1	MH821566			
	bamboo	Fujian, Fuzhou	HL20160412_5	MH821569	MK028316	MK028336	MK372359
	bamboo	Fujian, Ningde	HL20161004_1	MH821540	MK028317	MK028337	MK372360
	bamboo	Guangdong, Shenzhen	HL20170205_9	MH821548	MK028318	MK028338	MK372361
	bamboo	Fujian, Fuzhou	HL20170226_3	MH821560			
	bamboo	Fujian, Fuzhou	HL20170318_3	MH821547			
	bamboo	Fujian, Fuding	HL20170403_13	MH821550			
	bamboo	Fujian, Fuzhou	HL20170409_4	MH821555			
	bamboo	Fujian, Fuzhou	HL20170606_8	MH821557			
	bamboo	Yunnan, Kunming	HL20170806_1	MH821558	MK028319		MK372362
	bamboo	Guangxi, Chongzuo	HLzld20171103_22	MH821572			
	bamboo	Yunnan, Kunming	HLzld20171108_6	MH821573	MK028320	MK028326	MK372363
	bamboo	Yunnan, Kunming	HLzld20171108_7	MH821574			
	bamboo	Yunnan, Kunming	HLzld20171111_3	MH821576	MK028321	MK028327	MK372364
	bamboo	Yunnan, Dali	HLzld20171126_6	MH821577			
	bamboo	Yunnan, Dali	HLzld20171126_7	MH821578	MK028322	MK028328	
A. formosana	bamboo	Guangxi, Chongzuo	HLzld20171102_16	MH821579	MK028323	MK028329	
	bamboo	Guangxi, Chongzuo	HLzld20171103_19	MH821582	MK028324	MK028330	MK372365
*A. bambucifoliae**		Guizhou	ZMIOZ13322	JN032708		DQ493848	
*A. bambusae**	*Bambusa tulda*	India, Karnataka	ORP-2010-61	HQ112196			
		Guangxi	ZMIOZ 14592	JX282768	JX282692	JX282849	
	Bambusa tulda	India, Bangalore	KBRIIHR-172	JX051408			
	Bambusa tulda	India, Karnataka	KBRIIHR-149	JX051385			
	Bambusa tulda	India, Karnataka	KBRIIHR-148	JX051384			
	Bambusa tulda	India, Karnataka	KBRIIHR-147	JX051383			
	Bambusa tulda	India, Karnataka	KBRIIHR-146	JX051382			
A. bambucifoliae	Poaceae	Taiwan, Puli					L27324
*A. formosana**	Poaceae	Taiwan, Sun Moon Lake					L27326

* indicates the sequences downloaded from the GenBank.

DNA extraction, PCR, and sequencing

We used DNeasy Blood &Tissue Kit (QIAGEN, GERMANY) to extract total genomic DNA from one individual per sample. The primers LepF (5'-ATTCAACCAATCATAAAGATATTGG-3') and LepR (5'-TAAACTTCTGGATGTCCAAAAAATCA-3') (Foottit et al. 2008) were used to amplify COI barcode region. The primers for amplification of Cytb were CP1 (5'-GATGATGAAATTTTGGATC-3') and CP2 (5'-CTAATGCAATAACTCCTCC-3') (Harry et al. 1998). EF-1α sequences were amplified based on EF3 (5'-GAACGTGAACGTGGTATCAC-3') and EF2 (5'-ATGTGAGCAGTGTGGCAATCCAA-3') (Palumbi 1996; von Dohlen et al. 2002). tRNA/COII sequences were amplified based on mt2793 + (5'-ATACCTCGACGTTATTCAGA) and mt3660- (5'- CCACAAATTTCTGAACATTGACCA) (Stern 1994). The PCR was performed in 30 μl reaction volumes: 20 μl ddH2O, 3 μl 10Xbuffer, 2.4 μl dNTP, 0.6 μl forward and reverse primer (10 μM), 0.4 μl of Taq DNA polymerase (5U/μl) and 3 μl of template DNA. All polymerase chain reactions included an initial denaturation step for 5 min at 95 °C and final extension step for 10 min at 72 °C. The cycling conditions of COI included 35 cycles of denaturation at 94 °C for 20s, annealing at 50 °C for 30s and extension at 72 °C for 2 min. The cycling conditions for Cytb were: 35 cycles of 1 min at 92 °C, 1.5 min at 48 °C and 1 min at 72 °C. The thermal setup for EF-1α was: 35 cycles of 30s at 95 °C, 1 min at 51 °C and 1 min at 72 °C. The cycling conditions for tRNA/COII were 34 cycles of 30s at 95 °C, 1 min at 54 °C and 1 min at 72 °C. Detection of the PCR products was performed on a 1% agarose gel. The eligible products were bidirectionally sequenced using the same PCR primer pairs by Sangon Biotech (Shanghai).

Sequence and phylogenetic analyses

Thirty-nine COI sequences were successfully obtained from the 37 ingroup samples and two *A. formosana* outgroups. In addition, eight COI sequences including one of *A. bambucifoliae* and seven of *A. bambusae* were downloaded from GenBank (accession numbers: JN032708, HQ112196, JX282768, JX051408, JX051385, JX051384, JX051383 and JX051382) for further phylogenetic analyses (Table 1). Based on the topology of the COI tree, sixteen ingroup samples were selected for Cytb, tRNA/COII, and EF-1α amplification. Finally, a total of 16 Cytb sequences, 12 EF-1α sequences and 15 tRNA/COII sequences were successfully generated. We downloaded several Cytb (accession number: JX282692) and EF-1α (accession numbers: DQ493848, JX282849) sequences of both species from the GenBank. Furthermore, as *A. bambucifoliae* was originally described from Taiwan, we downloaded two tRNA/COII sequences L27324 (*A. bambucifoliae*) and L27326 (*A. formosana*), which were obtained from Taiwanese samples from GenBank to test the relationships between them and our sequences (Table 1). For all the sequences obtained

in this study, the raw forward and reverse sequences were corrected based on the chromatograms and assembled using BioEdit software (Hall 1999). Subsequently, the sequences were aligned by MAFFT (Kazutaka and Standley 2013) and trimmed to the same length with BioEdit. For the EF-1α sequences, the introns were removed according to the GT-AG rule and the cDNA region of a *Schizaphis graminum* reference sequence (GenBank accession number AF068479), and the coding regions of EF-1α were used in further phylogenetic analyses.

The Kimura 2-parameter (K2P) model (Kimura 1980) were used to calculate pairwise distances among nucleotide sequences in MEGA 7.0 (Kumar et al. 2016). The optimal nucleotide substitution models were determined based on Akaike Information Criterion (AIC) by using jMODELTEST 2.1.7 (Darriba et al. 2012) for COI (GTR+I), Cytb (GTR), EF-1α (HKY+I) and tRNA/COII (GTR). For each marker, different phylogenetic reconstruction methods (Neighbor-joining, NJ; Maximum likelihood, ML; Bayesian inference, BI) were used to estimate the topologies. MEGA 7.0 was used to build the NJ trees based on the K2P model and 1,000 bootstrap replicates. Based on the estimated models, the ML trees were estimated in RAxML (Silvestro and Michalak 2012) with the settings of ML+ rapid bootstrap, and nodal support was calculated by 1000 replicates. The Bayesian analyses were performed with MrBayes 3.2.6 (Ronquist et al. 2012). Two million generations Markov Chain Monte Carlo (MCMC) were run and sampled every 100 generations, and the first 25% of trees were discarded as burn-in to acquire posterior probability values (PP). The phylogenetic trees were represented and edited using the online tool iTOL (Letunic and Bork 2016).

The haplotype network analysis of COI sequences was also implemented to illustrate the population genetic structure in space based on geographic groups. The COI sequences were imported into DNAsp 5.0 (Librado and Rozas 2009) to analyze the haplotype composition. Then the median-joining network of the haplotypes was computed by using NETWORK 5.0.0.3 (Bandelt et al. 1999) based on default settings.

Results

Sequence characters

Forty-seven COI sequences were aligned to a final length of 556 bp, which included 527 conserved sites, 29 variable sites, and 24 parsimony-informative sites. The nucleotide composition of COI alignment displayed a strong bias toward A+T content (T: 42.6%, C: 12.7%, A: 36.2% and G: 8.5%). The 718 bp long Cytb alignment with 19 sequences included 689 conserved sites, 29 variable sites, and 28 parsimony-informative sites. The nucleotide composition of Cytb alignment was 44.8% T, 12.3% C, 34.2% A, and 8.7% G. After the introns were excluded, sixteen EF-1α sequences were trimmed to a 785 bp long alignment with 769 conserved sites, 16 variable sites, and 13 parsimony-informative sites. The nucleotide composition was 26.2% T, 20.9% C, 27.8% A, and 25.1% G. The tRNA/COII alignment had 626bp with 595 conserved

sites, 31 variable sites and 25 parsimony-informative sites. The nucleotide composition of tRNA/COII alignment was 41.0% T, 11.1% C, 41.1% A, and 6.8% G.

Genetic distances and phylogenetic analyses

The intraspecific and interspecific K2P genetic distances among the samples are shown in Table 2. The maximum genetic distances (1.46%) were between some Indian samples and the other samples. Basically, the COI sequences were able to contribute more informative sites to understand the population structure.

In general, different reconstruction approaches yielded similar phylogenetic trees for the same marker (Figure 1, Suppl. materials 1, 2). Phylogenetic trees showed that all four genes failed to support the monophyly of both *A. bambucifoliae* and *A. bambusae*. Samples of these two species were dispersed in different clades of the phylogenetic trees. Based on the COI tree with more samples (Figure 1), some well-supported clades were distinct. All the samples from the Yunnan and Guizhou plateau of southwestern China as well as all the Indian samples clustered into separate clades. These samples were all morphologically identified as *A. bambusae*. There was also a separate clade including many samples of both morphologically identified species and from different localities of southeastern and southern China, but with low genetic distances.

The network analysis of the COI haplotypes (Figure 2) indicated that all the Indian samples, assigned as haplotypes H6 and H7, were linked together and showed greatest differentiation from the other haplotypes.The samples from southwestern China, including almost all samples from Yunnan and Guizhou Plateau and some from Guangxi, were of haplotype H5. Haplotype H1 with most samples included almost all samples from Fujian in southeastern China. The other samples from southeastern and southern China (Fujian, Guangdong, Hainan) were assigned to several other haplotypes, i.e., H8, H9, H2, H3, H4.

Phylogenetic pattern of morphological variation

The photographs of live specimens that we took during the field work in different localities and at different times indicated the spatial and temporal diversity of all samples (Figure 3). When these photographs were compared with the phylogenetic tree (Figure 1), it was apparent that some key morphological diagnostic characters used to distinguish both species, such as the wax types and the green patches, have no distinct phylogenetic pattern. For example, within the separate clade including many samples of both morphologically identified species from different localities of southeastern China (Figure 3[1–17]), the appearance of these samples based on wax layout and green patches varied greatly, whereas their genetic distances were very low. Moreover, although the samples from Yunnan Plateau with identical COI sequence (Figure 3[21–24]) had relatively similar green patches and were collected at similar times (November 2017), their wax density and distribution were clearly different.

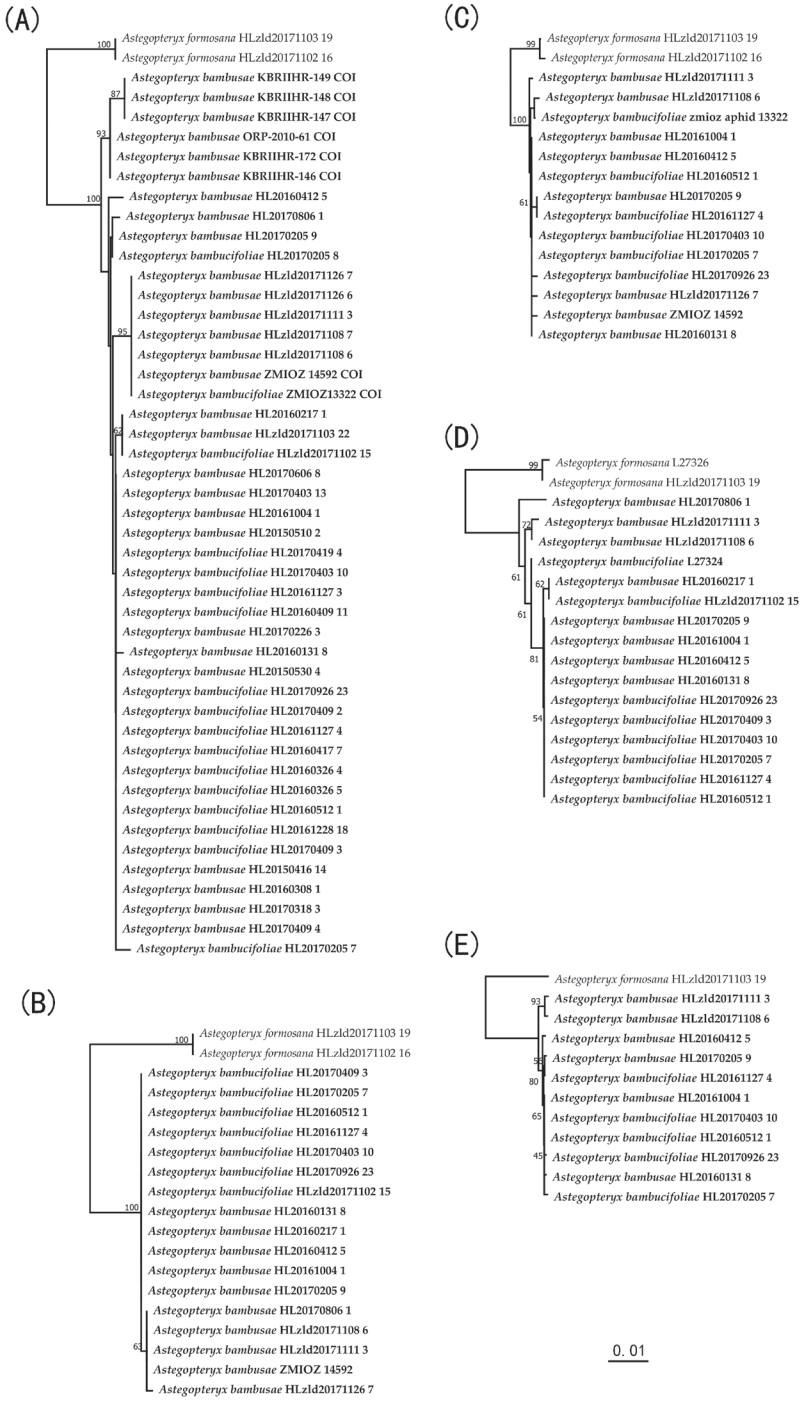

Figure 1. The Neighbor-joining (NJ) trees based on COI (A), Cytb (B), EF-1α (C), tRNA/COII (D), and the combined data of all four genes (E). The ingroup specimens are printed in bold and the bootstrap values higher than 50 are indicated. The sequences are named as putative species name plus specimen voucher number.

Table 2. Genetic distances among *Astegopteryx bambucifoliae* and *A. bambusae* samples based on COI, Cytb, EF-1α, and tRNA/COII sequences.

Genetic distance	Species	Gene	Range (%)	Mean (%)
Intraspecific	*Astegopteryx bambucifoliae*	COI	0–0.91	0.15
		Cytb	0	0
		EF-1α	0–0.26	0.13
		tRNA/COII	0–0.48	0.12
	Astegopteryx bambusae	COI	0–1.46	0.56
		Cytb	0–0.28	0.11
		EF-1α	0–0.38	0.19
		tRNA/COII	0–1.46	0.61
Interspecific	*Astegopteryx bambucifoliae* & *Astegopteryx bambusae*	COI	0–1.46	0.38
		Cytb	0–0.28	0.08
		EF-1α	0–0.38	0.14
		tRNA/COII	0–1.46	0.38

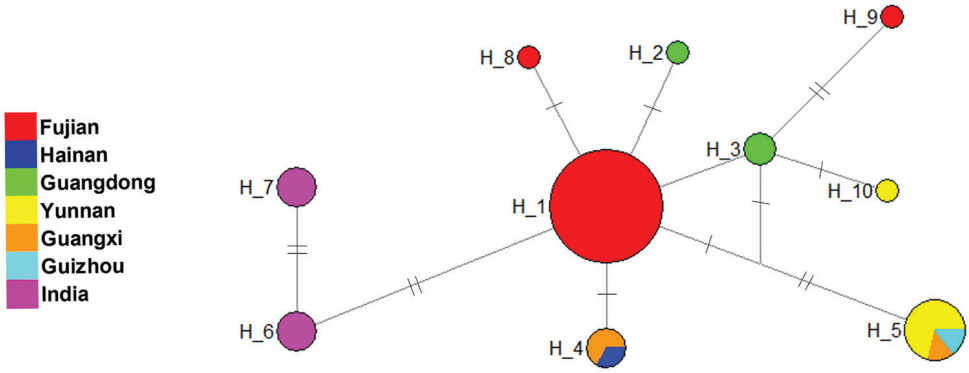

Figure 2. Haplotype networks based on COI sequences. The circles represent different haplotypes, while different colors correspond to the geographical origins of samples and sizes represent relative numbers of sequences (H_1: 23; H_2: 1; H_3: 2; H_4: 3; H_5: 7; H_6: 3; H_7: 3; H_8: 1; H_9: 1; H_10: 1). The short line segments indicate mutated positions between haplotypes.

Discussion

Species descriptions based on limited samples are often unable to represent the whole picture of morphological variation within the species, making it likely that some names will subsequently be synonymised (Winston 1999; Eastop and Blackman 2005). A review of the relevant literature and the results of our present study indicate that *A. bambusae* and *A. bambucifoliae* should be such a case. Based on the molecular data from extensive sampling, our results show that relatively low genetic distances of four genes exist among all samples of both morphologically identified species. In previous DNA barcoding studies of aphids (Foottit et al. 2009; Zhu et al. 2017), 2% has been used as a

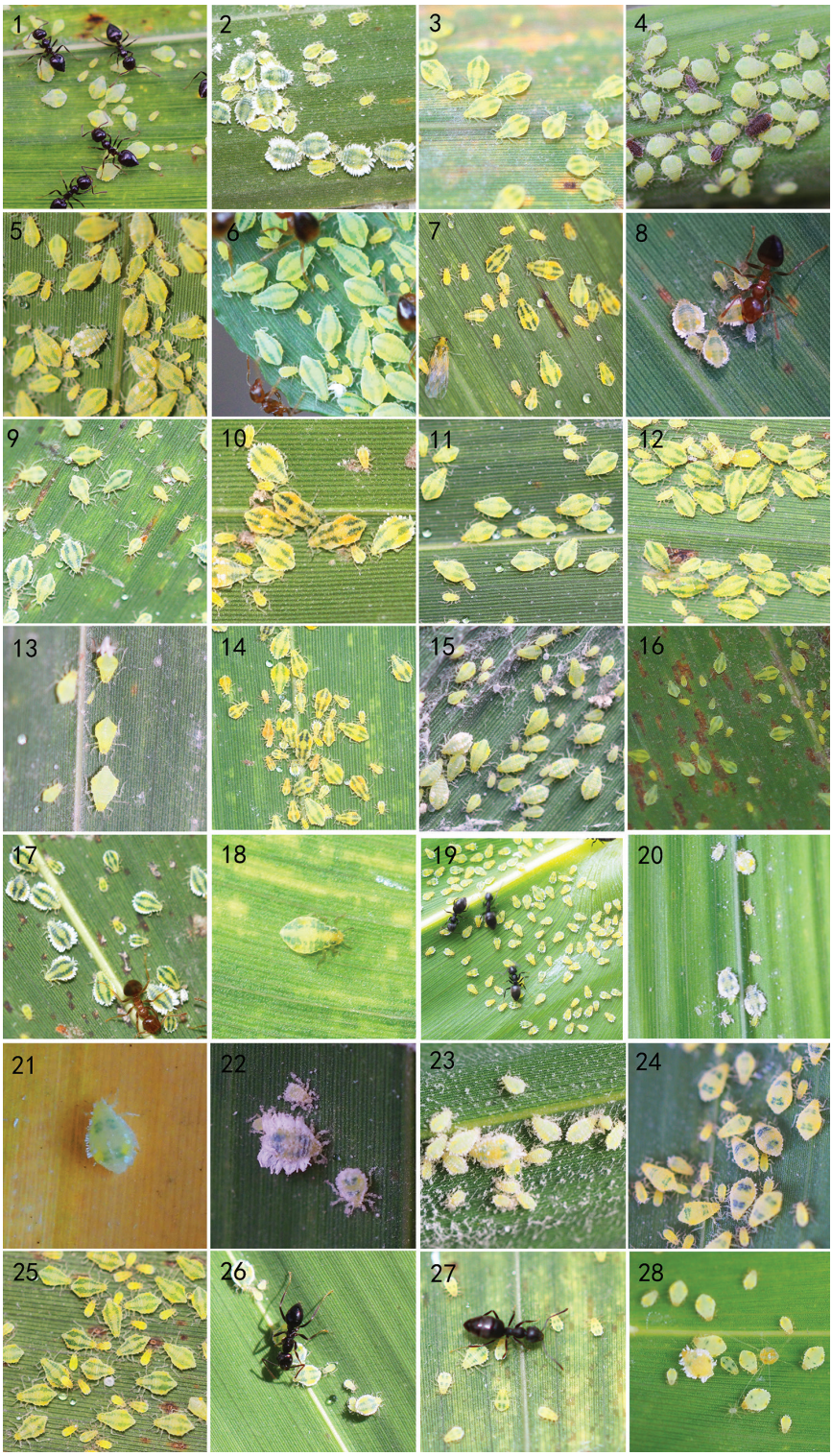
1
2
3
4
5
6
7
8
9
10
11
12
13
14
15
16
17
18
19
20
21
22
23
24
25
26
27
28

threshold value of COI genetic distances for species delimitation. This threshold has also been proposed for other insect groups (Hajibabaei et al. 2006; Zahiri et al. 2014). In the present study, the maximum and mean COI genetic distances (1.46% and 0.56%, respectively; Table 2) among all samples from southern China to India do not reach the 2% threshold value to define separate species. Moreover, no matter what phylogenetic methods were used, the monophyly of neither of the morphologically identified *Astegopteryx* species has been supported by the phylogenetic trees based on any of the four genes. Although all ingroup samples form one well-supported clade, several inner clades with dispersed samples of both species have been less supported with lower bootstrap values. Thus, the molecular data indicate that all samples belong to a single species.

Our study also provides information on the taxonomic significance of variations in appearance in life. Results show that there is no distinct phylogenetic pattern for key diagnostic characters such as green patches on the dorsum and distribution of wax. The high spatial and temporal morphological diversity among all samples used in the present study support our and other colleagues' speculation (Blackman and Eastop 2018) that the stability of these proposed morphological discriminants for the two *Astegopteryx* species is uncertain. The distinct character of a pair of longitudinal dark green patches often interrupted at mid-length on the dorsum of live specimens was proposed by Takahashi (1921) to distinguish *A. bambucifoliae*. However, this character has been described as "uninterrupted longitudinal markings on dorsum" by other taxonomists (Joshi and Poorani 2007), indicating that this character cannot be a stable diagnostic character at species level. Wax gland plates occur widely in the subfamily Hormaphidinae, which *Astegopteryx* belongs to, and have a variety of shapes and sizes as well as complex arrangements (Chen and Qiao 2012). Previous studies showed that characters related to wax gland plates even change ontogenetically, for example, wax gland plates may be present in nymphs and embryos but absent in adults (Shaposhnikov and Gabrid 1987). Considering aphids are producing honeydew and Cerataphidini aphids often live as large colonies in wet subtropical regions (Noordam 1991; Huang et al. 2012; Blackman and Eastop 2018; Qiao et al. 2018), the wax probably has a functional role to protect aphids from possible contamination of honeydew, rain, natural enemies, and other environmental factors (Pope 1983; Heie 1987; Smith 1999; Pike et al. 2002; Moss et al. 2006). Such a functional character may not necessarily be phylogenetically informative for species delimitation, as the appearance and arrangement of wax cells may be easily affected by environmental changes. This is shown by the high wax variation among all samples showed in the present study.

Figure 3. Photographs of live specimens showing high morphological variation among samples. Based on specimen voucher number, these photographs correspond to the following sequences in the phylogenetic trees; **1** HL20170205_7 **2** HL20170606_8 **3** HL20170409_2 **4** HL20170403_13 **5** HL20170226_3 **6** HL20150416_14 **7** HL20160417_7 **8** HL20161004_1 **9** HL20161228_18 **10** HL20150530_4 **11** HL20160326_4 **12** HL20170403_10 **13** HL20160131_8 **14** HL20160512_1 **15** HL20170318_3 **16** HL20170419_4 **17** HL20170926_23 **18** HL20160217_1 **19** HLzld20171102_15 **20** HLzld20171103_22 **21** HLzld20171108_6 **22** HLzld20171108_7 **23** HLzld20171111_3 **24** HLzld20171126_6 **25** HL20170205_8 **26** HL20170806_1 **27** HL20160412_5 **28** HLzld20171102_16.

By integrating the molecular data and morphological information, our results indicate that *A. bambusae* and *A. bambucifoliae* should be regarded as a single species with high intraspecific morphological variation. Based on the history of the two species, we place *A. bambucifoliae* (Takahashi 1921) as a junior synonym of *A. bambusae* (Buckton 1893). Considering the results of our study, as well as published descriptions (Buckton 1893; Takahashi 1921; Noordam 1991; Qiao et al. 2018), it seems that large-scale geographic patterns of population differentiation may exist within the species. For example, the Indian samples we cited seem more genetically divergent. Noordam (1991) reviewed the Javanese *Astegopteryx* species, in which several species originally described by van der Goot (1917) were considered as color varieties of *A. bambusae*. However, based on the color plates (Pl. 1–5) of live specimens in Noordam (1991), the patterns of green bands and wax distribution of those color varieties are quite different from our photographed specimens. This may raise the question of whether the treatment in Noordam (1991) is appropriate. Therefore, future investigation is needed to resolve the identity of populations in Southeast Asia. In addition, considering this species has previously been recorded with facultative host alternation between primary host *Styrax* and secondary host bamboos in Taiwan (Aoki and Kurosu 2010), it will be interesting to have some molecular work done in future on populations from *Styrax*.

Acknowledgments

We thank Fangluan Gao and Lin Wang for providing advice on data analysis. Many thanks to Shigeyuki Aoki, David Stern, and Roger Blackman for providing valuable comments and suggestions to improve the manuscript. This research was supported by National Natural Science Foundation of China (grant number 31772504) and Fujian Provincial Department of Science & Technology (grant number 2015J06005).

References

Aoki S, Kurosu U (1995) Valid name for the aphid *Astegopteryx* "*insularis*" (sensu van der Goot 1917), with notes on its biology (Homoptera, Aphidoidea). Japanese Journal of Systematic Entomology 1: 151–152.

Aoki S, Kurosu U (2010) A review of the biology of Cerataphidini (Hemiptera, Aphididae, Hormaphidinae), focusing mainly on their life cycles, gall formation, and soldiers. Psyche: A Journal of Entomology 2010. https://doi.org/10.1155/2010/380351

Bandelt H-J, Forster P, Röhl A (1999) Median-joining networks for inferring intraspecific phylogenies. Molecular Biology & Evolution 16: 37–48. https://doi.org/10.1093/oxfordjournals.molbev.a026036

Blackman RL, Eastop VF (1994) Aphids on the world's trees: an identification and information guide. 1994. CAB International, Wallingford, United Kingdom.

Blackman RL, Eastop VF (2018) Aphids on the World's Plants: An online identification and information guide. Published online at http://www.aphidsonworldsplants.info [Accessed 25 October 2018]

Buckton GB (1893) Notes on Indian aphids. Indian Museum Notes 3: 87–88.

Chen J, Qiao GX (2012) Wax Gland Plates in Hormaphidinae (Hemiptera: Aphididae): Morphological Diversity and Evolution. Entomological News 122: 27–45. https://doi.org/10.3157/021.122.0104

Darriba D, Taboada GL, Doallo R, Posada D (2012) jModelTest 2: more models, new heuristics and parallel computing. Nature Methods 9: 772. https://doi.org/10.1038/nmeth.2109

Eastop VF, Blackman RL (2005) Some new synonyms in Aphididae (Hemiptera: Sternorrhyncha). Zootaxa 1089: 1–36. https://doi.org/10.11646/zootaxa.1089.1.1

Favret C (2018) Aphid Species File. Version 5.0/5.0. http://Aphid.SpeciesFile.org [Accessed 25 October 2018]

Foottit RG, Maw HE, von Dohlen CD, Hebert PD (2008) Species identification of aphids (Insecta: Hemiptera: Aphididae) through DNA barcodes. Molecular Ecology Resources 8: 1189–1201. https://doi.org/10.1111/j.1755-0998.2008.02297.x

Foottit RG, Maw HEL, Pike KS (2009) DNA barcodes to explore diversity in aphids (Hemiptera: Aphididae and Adelgidae). Redia 92: 87–91.

Hajibabaei M, Janzen DH, Burns JM, Hallwachs W, Hebert PDN (2006) DNA barcodes distinguish species of tropical Lepidoptera. Proceedings of the National Academy of Sciences of the United States of America 103: 968–971. https://doi.org/10.1073/pnas.0510466103

Hall TA (1999) BioEdit: a user-friendly biological sequence alignment editor and analysis program for Windows 95/98/NT. Nucleic Acids Symposium Series 41: 95–98.

Harry M, Solignac M, Lachaise D (1998) Molecular evidence for parallel evolution of adaptive syndromes in fig-breeding *Lissocephala* (Drosophilidae). Molecular Phylogenetics & Evolution 9: 542–551. https://doi.org/10.1006/mpev.1998.0508

Hebert PDN, Cywinska A, Ball SL, Dewaard JR (2003) Biological identification through DNA barcodes. Proceedings of the Royal Society of London Series B, Biological Sciences 270: 313–321. https://doi.org/10.1098/rspb.2002.2218

Heethoff M, Laumann M, Weigmann G, Raspotnig G (2011) Integrative taxonomy: Combining morphological, molecular and chemical data for species delineation in the parthenogenetic *Trhypochthonius tectorum* complex (Acari, Oribatida, Trhypochthoniidae). Frontiers in Zoology 8: 2. https://doi.org/10.1186/1742-9994-8-2

Heie OE (1987) Paleontology and phylogeny. In: Minks AK, Harrewijn P (Eds) Aphids: their biology, natural enemies and control. World crop pests, vol. 2A. Elsevier, Amsterdam, 367–391.

Huang XL, Xiang Yu JG, Ren SS, Zhang RL, Zhang YP, Qiao GX (2012) Molecular phylogeny and divergence times of Hormaphidinae (Hemiptera: Aphididae) indicate Late Cretaceous tribal diversification. Zoological Journal of the Linnean Society 165: 73–87. https://doi.org/10.1111/j.1096-3642.2011.00795.x

Jensen AS, Miller GL, Carmichael A (2010) Host Range and Biology of *Uroleucon* (*Lambersius*) *erigeronense* (Thomas 1878), and its Synonymy with *Uroleucon* (*Lambersius*) *escalantii*

(Knowlton) 1928 (Hemiptera: Aphididae). Proceedings of the Entomological Society of Washington 112: 239–245. https://doi.org/10.4289/0013-8797-112.2.239

Joshi S, Poorani J (2007) Aphids of Karnataka. http://www.nbair.res.in/Aphids/index.php [Accessed 25 October 2018]

Kazutaka K, Standley DM (2013) MAFFT Multiple Sequence Alignment Software Version 7: Improvements in Performance and Usability. Molecular Biology & Evolution 30: 772–780. https://doi.org/10.1093/molbev/mst010

Kimura M (1980) A simple method for estimating evolutionary rates of base substitutions through comparative studies of nucleotide sequences. Journal of Molecular Evolution 16: 111–120. https://doi.org/10.1007/BF01731581

Kumar S, Stecher G, Tamura K (2016) MEGA7: molecular evolutionary genetics analysis version 7.0 for bigger datasets. Molecular Biology and Evolution 33: 1870–1874. https://doi.org/10.1093/molbev/msw054

Kurosu U, Aoki S (1991) The Gall Formation, Defenders and Life Cycle of the Subtropical Aphid *Astegopteryx bambucifoliae* (Homoptera). Japanese Journal of Entomology 59: 375–388.

Letunic I, Bork P (2016) Interactive tree of life (iTOL) v3: an online tool for the display and annotation of phylogenetic and other trees. Nucleic Acids Research 44: W242–W245. https://doi.org/10.1093/nar/gkw290

Librado P, Rozas J (2009) DnaSP v5: a software for comprehensive analysis of DNA polymorphism data. Bioinformatics 25: 1451–1452. https://doi.org/10.1093/bioinformatics/btp187

Madjdzadeh SM, Mehrparvar M (2009) Morphological discrimination of geographical populations of *Macrosiphoniella sanborni* (Gillette, 1908) (Hem.: Aphididae) in Iran. North-Western Journal of Zoology 5: 338–348.

Margaritopoulos JT, Tsitsipis JA, Zintzaras E, Blackman RL (2000) Host-correlated morphological variation of *Myzus persicae* (Hemiptera: Aphididae) populations in Greece. Bulletin of Entomological Research 90: 233–244. https://doi.org/10.1017/S0007485300000353

Meier R (2017) Citation of taxonomic publications: the why, when, what and what not. Systematic Entomology 42: 301–304. https://doi.org/10.1111/syen.12215

Moss R, Jackson RR, Pollard SD (2006) Mask of wax: Secretions of wax conceal aphids from detection by spider"s eyes. New Zealand Journal of Zoology 33: 215–220. https://doi.org/10.1080/03014223.2006.9518448

Noordam D (1991) Hormaphidinae from Java (Homoptera: Aphididae). Zoologische Verhandelingen 270: 1–525.

Palumbi SR (1996) Nucleic acids II : The polymerase chain reaction. Molecular Systematics: 205–247.

Pike N, Richard D, Foster W, Mahadevan L (2002) How Aphids Lose Their Marbles. Proceedings of the Royal Society Biological Sciences 269: 1211–1215. https://doi.org/10.1098/rspb.2002.1999

Pope RD (1983) Some aphid waxes, their form and function (Homoptera: Aphididae). Journal of Natural History 17: 489–506. https://doi.org/10.1080/00222938300770431

Qiao G, Jiang L, Chen J, Zhang G, Zhong T (2018) Hemiptera: Hormaphididae, Phloeomyzidae. Fauna Sinica Insecta 60: 1–414. [+ 8 pls]

Ronquist F, Teslenko M, Van Der Mark P, Ayres DL, Darling A, Höhna S, Larget B, Liu L, Suchard MA, Huelsenbeck JP (2012) MrBayes 3.2: efficient Bayesian phylogenetic in-

ference and model choice across a large model space. Systematic Biology 61: 539–542. https://doi.org/10.1093/sysbio/sys029

Schlick-Steiner BC, Steiner FM, Seifert B, Stauffer C, Christian E, Crozier RH (2010) Integrative taxonomy: a multisource approach to exploring biodiversity. Annual Review of Entomology 55: 421–438. https://doi.org/10.1146/annurev-ento-112408-085432

Shaposhnikov GK, Gabrid NV (1987) Aphids of the family Hormaphididae (Homoptera: Aphidinea) from coniferous trees. Entomologicheskoe Obozrenie 66: 765–772.

Silvestro D, Michalak I (2012) raxmlGUI: a graphical front-end for RAxML. Organisms Diversity & Evolution 12: 335–337. https://doi.org/10.1007/s13127-011-0056-0

Smith RG (1999) Wax glands, wax production and the functional significance of wax use in three aphid species (Homoptera: Aphididae). Annals & Magazine of Natural History 33: 513–530. https://doi.org/10.1080/002229399300227

Stern D, Aoki S, Kurosu S (1997) Determining aphid taxonomic affinities and life cycles with molecular data: a case study of the tribe Cerataphidini (Hormaphididae: Aphidoidea: Hemiptera). Systematic Entomology 22: 81–96. https://doi.org/10.1046/j.1365-3113.1997.d01-20.x

Stern DL (1994) A phylogenetic analysis of soldier evolution in the aphid family Hormaphididae. Proceedings of the Royal Society of London Series B, Biological Sciences 256: 203–209. https://doi.org/10.1098/rspb.1994.0071

Takahashi R (1921) Aphididae of Formosa. Part I. Report of the Department of Agriculture Government Research Institute Formosa 20: 1–97.

Turčinavičienė J, Rakauskas R (2009) *Macrosiphum* on *Knautia* in Central Europe – molecular data support the synonymy of *M. silvaticum* and *M. knautiae* (Hemiptera: Aphididae). Redia-giornale di Zoologia 92: 105–109.

van der Goot P (1917) Zur Kenntnis der Blattlaüse Java's. Contributions Faune Indesnéerlandaises 1(3): 1–301.

von Dohlen CD, Kurosu U, Aoki S (2002) Phylogenetics and evolution of the eastern Asian-eastern North American disjunct aphid tribe, Hormaphidini (Hemiptera: Aphididae). Molecular Phylogenetics & Evolution 23: 257–267. https://doi.org/10.1016/S1055-7903(02)00025-8

Winston JE (1999) Describing Species: Practical Taxonomic Procedure for Biologists. Columbia University Press, New York, 512 pp.

Wool D, Hales DF (1997) Phenotypic Plasticity in Australian Cotton Aphid (Homoptera: Aphididae): Host Plant Effects on Morphological Variation. Annals of the Entomological Society of America 90: 316–328. https://doi.org/10.1093/aesa/90.3.316

Yao I (2012) Ant attendance reduces flight muscle and wing size in the aphid *Tuberculatus quercicola*. Biology Letters 8: 624–627. https://doi.org/10.1098/rsbl.2012.0014

Zahiri R, Lafontaine JD, Schmidt BC, Dewaard JR, Zakharov EV, Hebert PDN (2014) A Transcontinental Challenge – A Test of DNA Barcode Performance for 1,541 Species of Canadian Noctuoidea (Lepidoptera). PLoS ONE 9: e92797. https://doi.org/10.1371/journal.pone.0092797

Zhu XC, Chen J, Chen R, Jiang LY, Qiao GX (2017) DNA barcoding and species delimitation of Chaitophorinae (Hemiptera, Aphididae). ZooKeys 656: 25–50. https://doi.org/10.3897/zookeys.656.11440

Supplementary material 1

The Maximum likelihood (ML) trees based on COI (A), Cytb (B), EF-1α (C), tRNA/COII (D) and the combined data of all four genes (E)

Authors: Qiang Li, Jiamin Yao, Lingda Zeng, Xiaolan Lin, Xiaolei Huang

Data type: molecular data

Explanation note: The ingroup specimens are printed in bold and the bootstrap values over 50 are indicated. The sequences are named as species name plus specimen voucher number.

Copyright notice: This dataset is made available under the Open Database License (http://opendatacommons.org/licenses/odbl/1.0/). The Open Database License (ODbL) is a license agreement intended to allow users to freely share, modify, and use this Dataset while maintaining this same freedom for others, provided that the original source and author(s) are credited.

Link: https://doi.org/10.3897/zookeys.833.30592.suppl1

Supplementary material 2

The Bayesian trees based on COI (A), Cytb (B), EF-1α (C), tRNA/COII (D) and the combined data of all four genes (E)

Authors: Qiang Li, Jiamin Yao, Lingda Zeng, Xiaolan Lin, Xiaolei Huang

Data type: molecular data

Explanation note: The ingroup specimens are printed in bold and the posterior probabilities over 90% are indicated. The sequences are named as species name plus specimen voucher number.

Copyright notice: This dataset is made available under the Open Database License (http://opendatacommons.org/licenses/odbl/1.0/). The Open Database License (ODbL) is a license agreement intended to allow users to freely share, modify, and use this Dataset while maintaining this same freedom for others, provided that the original source and author(s) are credited.

Link: https://doi.org/10.3897/zookeys.833.30592.suppl2

ZooKeys 833: 75–84 (2019)
doi: 10.3897/zookeys.833.31502
http://zookeys.pensoft.net

RESEARCH ARTICLE

A peer-reviewed open-access journal
ZooKeys
Launched to accelerate biodiversity research

Lophorrhinides muellerae (Coleoptera, Scarabaeidae, Cetoniinae): a new genus and species from southern Tanzania

Renzo Perissinotto[1], Lynette Clennell[2], Gerhard Beinhundner[3]

1 *School of Environmental Sciences, Nelson Mandela University, P.O. Box 77000, Port Elizabeth 6031, South Africa* **2** *Macau Anglican College, 109-117 Avenida Padre Tomas Pereira, Taipa-Macau, China* **3** *Am Steigberg 25, D-97502 Euerbach, Germany*

Corresponding author: *Renzo Perissinotto* (renzo.perissinotto@mandela.ac.za)

Academic editor: *Andrey Frolov* | Received 9 November 2018 | Accepted 11 February 2019 | Published 26 March 2019

http://zoobank.org/58964B89-AF20-46CD-8C08-6216782785CE

Citation: Perissinotto R, Clennell L, Beinhundner G (2019) *Lophorrhinides muellerae* (Coleoptera, Scarabaeidae, Cetoniinae): a new genus and species from southern Tanzania. ZooKeys 833: 75–84. https://doi.org/10.3897/zookeys.833.31502

Abstract

A male cetoniine specimen recently submitted for identification from the Ditsong Museum of Natural History (Pretoria, South Africa) has been found to represent a yet unknown species. A review of the recently published book of Beinhundner (2017) has further revealed that one of the specimens mistakenly figured as *Lophorrhina donckieri* Bourgoin, 1913 in that work is most likely the female of this new species. Analysis of the diagnostic characters of the genus *Lophorrhina* Westwood, 1842 shows that the new species differs in several key areas. In particular, the clypeal armature is virtually identical in both sexes, the male protibiae are not typically elongate and narrow as in all the members of *Lophorrhina*, but are remarkably more robust, laterally expanded and with a tridentate margin in both sexes, even though the third tooth in the female and the second and third teeth in the male are virtually obsolete. The general body shape in the new species is also more globose and lacks the typical deplanate and apically tapering elytra of the *Lophorrhina* males. These and other characters are, in our view, sufficient to justify the erection of a new genus, *Lophorrhinides* **gen. n.**, to accommodate the new species, here described as *L. muellerae* **sp. n.** The new genus is presumably a mountain specialist, as both known specimens were collected in the southern highlands of Tanzania, at Manow and Rungwe respectively.

Keywords

Fruit chafers, *Lophorrhina*, East African Rift, Afrotropical region

Copyright *Renzo Perissinotto et al.* This is an open access article distributed under the terms of the Creative Commons Attribution License (CC BY 4.0), which permits unrestricted use, distribution, and reproduction in any medium, provided the original author and source are credited.

Introduction

A male cetoniine specimen from an old collection originating from "Deutsch Ost-Afrika" and submitted for identification in 2016 by the Ditsong Museum of Natural History (Pretoria, South Africa) has revealed unique characteristics, with affinities to *Lophorrhina* Westwood, 1842 and, to a lesser extent, genera such as *Anisorrhina* Westwood, 1842 and *Chlorocala* Kirby, 1828, particularly at the level of the parameres. A female specimen belonging to the same genus and species was also recognised among a series of photographs included under *Lophorrhina donckieri* Bourgoin, 1913, after the publication of the monograph on the "Cetoniinae of Africa" by Beinhundner (2017; p. 990, fig. 18). This has made it possible to complete and substantiate the description of a new species.

The genus *Lophorrhina* Westwood, 1842 currently includes the synonymic genera *Chordodera* Burmeister, 1842, *Daedycorrhina* Bates, 1888 *Aphanesthes* Kolbe, 1892, and *Aphanochroa* Kolbe, 1893. It includes 13 described species, most of which are high altitude endemics of the Tanzanian mountains. The new species described here occurs close to the southern limit of the distribution range of *Lophorrhina* and exhibits several distinct characters that may reflect geographical isolation from the ancestral lineage. In particular, the general body shape is rather globose and not deplanate like in *Lophorrhina*, the scutellum is equilateral triangular and exhibits dense and long setae, while in *Lophorrhina* this is isosceles triangular and virtually asetose. The clypeal shape is also remarkably different to that of *Lophorrhina*, in that the horn is virtually obsolete in both sexes and the clypeal margins are laterally expanded to form a general shape broader but shorter than in *Lophorrhina*.

These and other differences highlighted in the description below make it impossible to include with confidence this species within any existing genera of the African cetoniines, thereby necessitating the erection of a new genus, *Lophorrhinides* gen. n. This adds to the already remarkable diversity observed for this beetle group in the Afrotropical region (excluding Madagascar), where 138 genera and more than 1000 species are currently recognised (Sakai and Nagai 1998, Beinhundner 2017).

Materials and methods

The only two specimens currently known for this new genus and species were analysed after obtaining a loan from the Ditsong Museum of Natural History (TMSA, Pretoria, South Africa) and through direct access to the Private Collection of Gerhard Beinhundner (PCGB, Euerbach, Germany), respectively.

As in previous work, the description of morphological characters of this study follows the terminology used by Krikken (1984) and Holm and Marais (1992). Specimen total length and maximum width were measured using a Vernier calliper, from the anterior margin of the clypeus to the apex of the pygidium and at the widest point of the elytra, respectively.

Photos of the dorsal and ventral habitus were taken with a Nikon CoolPix S9700 and a Nikon CoolPix 990 digital camera with macro setting, while photos of the male genitalia were obtained using a Nikon DigitalSight DS-Fi2 camera attached to a Nikon SMZ25 dissecting microscope. The background was removed from the photos using Microsoft Word 2010 (Picture Tools) and Adobe Photoshop 7.0, in order to increase clarity of resolution. The Combine ZP Image Stacking Software by Alan Hadley (alan@micropics.org.uk) was used to obtain z-stacking composite images.

Results

***Lophorrhinides* gen. n.**
http://zoobank.org/76FA4EC4-214F-499F-9C58-8823A8535E79

Type species. *Lophorrhinides muellerae* gen. et sp. n.

Diagnosis. The new genus is most closely related to *Lophorrhina* Westwood, 1842. It differs from this genus mainly by its generally dense pubescence on the dorsal surface (particularly well-developed in male), the fairly globose rather than deplanate body shape, the hemicircular rather than octagonal pronotal shape, the equilateral rather than isosceles triangular shape of its scutellum, the presence of reduced clypeal armature, which is similar in both sexes, and the reduction of the central horn on head frons to a tubercle. A more comprehensive comparison between the two genera is provided in Table 1 below.

Derivatio nominis. The new genus name clearly refers to its close relationship with the sister genus *Lophorrhina* Westwood, 1842.

***Lophorrhinides muellerae* sp. n.**
http://zoobank.org/89671880-3FD5-4B7D-80C8-D6E838C13938
Fig. 1A–F

Type material. Holotype male: Manow DO Afr, Sammlung Schürhoff (TMSA). Paratype female: Tanzania, Rungwe Mts, 02.2006, leg. V Kayombo (PCGB).

Diagnosis. This is the only species currently recognised within the newly erected genus. Thus, its diagnostic characters are the same as those highlighted above under the description of *Lophorrhinides* gen. n., in comparison to its sister genus *Lophorrhina*. Within *Lophorrhina*, the species that most closely resembles *Lophorrhinides muellerae* sp. n. is *L. donckieri*, but only as far as female superficial characters are concerned. Indeed a photo of the paratype female of *L. muellerae* sp. n. was originally included in a series illustrating that species in the recently published iconographic monograph of Beinhundner (2017: 990, fig. 18). The females of the two species, however, differ remarkably in their clypeal shape, scutellum width/length ratio, body pilosity and general shape, as well as mesometasternal

Table 1. Comparison of diagnostic generic characters of *Lophorrhina* Westwood, 1842 versus *Lophorrhinides* gen. n. The list for *Lophorrhina* includes the key features highlighted in the original description of Westwood (1842) as well as those of the successive synonyms of *Chordodera* Burmeister, 1842, *Daedycorrhina* Bates, 1888, *Aphanesthes* Kolbe, 1892 and *Aphanochroa* Kolbe, 1893.

***Lophorrhina* Westwood, 1842**	***Lophorrhinides* gen. n.**
Clypeal horn flat to concave but truncated in male, drastically reduced in female to a slight elevation	Clypeal horn deeply concave, wide but short in both sexes, only slightly reduced in female compared to male
Presence of flattened, central horn at posterior margin of head frons, between eyes	Presence of central tubercle at posterior margin of head frons, between eyes
Scutellum virtually asetose, isosceles triangular in shape with width/height ratio ≤ 1	Scutellum with dense pilosity, equilateral triangular in shape with width/height ratio > 1
Tridentate protibia in both sexes, but all teeth obsolete in male	Tridentate protibiae in both sexes, but teeth 2-3 obsolete in male and tooth 3 drastically reduced in female
Tibiae and tarsi thin and elongate to hypertrophic in male (especially in prolegs, where tibiae are often arcuate)	Tibiae and tarsi of normal cetoniine length and thickness, with no visible sexual dimorphism
Mesometasternal lobe dilated into a short, round process and protruding forward	Mesometasternal lobe smoothly rounded and not expanded anteriorly or laterally
Body deplanate, with pronotum virtually octagonal and elytra tapering towards apex	Body substantially globose, with hemicircular pronotum exhibiting heavily sinuate posterior margin and elytra smoothly rounded at apex
Ornamentation well developed, with velutinous surface exhibiting longitudinal lines or stripes on pronotum and light-dark maculation on elytra	Ornamentation poorly developed, with pronotum exhibiting only very restricted orange maculation on antero-lateral margin and elytra with dark patches only on umbones and on and around sutural margins
Pilosity absent or drastically reduced on dorsal surface in both sexes	Body surface with dense orange pubescence, which is substantially reduced on female dorsum but still prominent on head and scutellum
Parameres with ventral lobes at apical half wider than dorsal ones and protruding laterally, dorsal lobes arcuate with lateral expansion near apex	Parameres with ventral lobes wider than dorsal ones and protruding laterally, dorsal lobes arcuate with longitudinal groove depression at middle and lateral expansion near apex

process. As sexual dimorphism is very developed in *Lophorrhina*, but barely recognizable in *Lophorrhinides* gen. n., the males of the two genera are drastically different, aside from their aedeagal shape where some similarities can be observed. The key differences between the two genera can be assessed through the comprehensive set of high quality images, illustrating all the diagnostic characters of three species of the genus *Lophorrhina*, i.e. *L. heinkeli* Beinhundner, 2015, *L. macularia* (Bates, 1888), *L. rigouti* (Allard, 1985), published recently by Beinhundner (2015: pls IV, V).

Derivatio nominis. This species is dedicated to Ruth Müller, Senior Curator at the Ditsong Museum of Natural History (Pretoria, formerly Transvaal Museum), who has a long-term record of collaboration with the first author. In 2017, she sent us the male holotype here described, along with other cetoniines currently under study for identification, with the belief that they may represent taxa yet unknown to science.

Description of male holotype. *Size*. Length 17.9 mm; width 9.8 mm.

Body: Black and ochraceous, without cretaceous markings; black areas shiny, but otherwise matte to velutinous; fine to ultrafine punctures covering virtually entire surface, with yellow to brown, long to very long setae emerging at centre of each puncture (Fig. 1A).

Head. Completely black and shiny; clypeus widening anteriorly, deeply concave and sharply upturned at anterior margin to form a horn-like protuberance at middle (Fig. 1C); lateral angles smoothly rounded and clypeo-lateral margins vertically declivous; presence of prominent tubercle at centre of vertex, between supra-ocular tubercles; surface covered in fine and scattered punctures, with yellow-orange setae emerging at centre of most punctures and becoming particularly long towards vertex (Fig. 1C); antenna dark brown, with club slightly longer than flagellum; pedicel dark brown with lighter head attachment and bearing clusters of long, erect yellowish setae.

Pronotum. Black and shiny, with two symmetric ochraceous and oblong maculae on each anterior margin of disc; with numerous but well-spaced fine punctures and long straw-coloured setae emerging at centre of punctures; shape semicircular to hexagonal with lateral margins perfectly rounded; antero-lateral margins smoothly rounded, postero-lateral with pronounced angle; posterior margin strongly sinuate with prescutellar arch smooth (Fig. 1A).

Scutellum. Completely black and shiny; exhibiting identical sculpture and pubescence as pronotum; equilateral triangular in shape with sharp apex; lateral grooves shallow and poorly defined (Fig. 1A).

Elytron. Matte to velutinous; ochraceous to orange, with black sutural margin and dark brown to black maculae on humeral and apical callus as well as on upper and central parts of disc, adjacent to sutural margin; costae barely developed and virtually obsolete; sub-humeral arch with very weak sinuation; humeral and apical calluses prominent and with distinct colouration; ultrafine punctures regularly spaced across entire surface, with medium length and erect brown setae emerging at centre of most punctures; apical margin smoothly rounded, without any signs of proximal spines/protuberances; apical and postero-lateral declivities deep but smooth, imparting rather compact and globose body shape (Fig. 1A).

Pygidium. Triangular in shape, with very wide base; slightly convex; completely black and covered in regularly spaced horseshoe sculpture; fine but long yellow setae scattered throughout surface (Fig. 1D).

Legs. Black and robust, with tarsal segments moderately elongate, with apical tarsal segments at least twice as long as preceding ones; protibia laterally expanded and tridentate, but with second and third teeth virtually obsolete; with longitudinal lines of fine to round punctures and short yellow setae on inner margin; meso- and metatibia with longer and denser yellow setae, densely sculptured and with mid spine on outer carina sharp or moderately developed, respectively; spurs moderately long, slender and acuminate, approximately twice as long in metatibia than in mesotibia (Fig. 1A, B).

Ventral surface. Black to dark brown and shiny; with ultrafine sculpture scattered throughout surface, less dense on mesometasternal lobe and on central area of abdominal sternites; with dense pubescence consisting of long yellow to orange setae, shorter and scattered on abdomen and absent on mesometasternal lobe; mesosternal

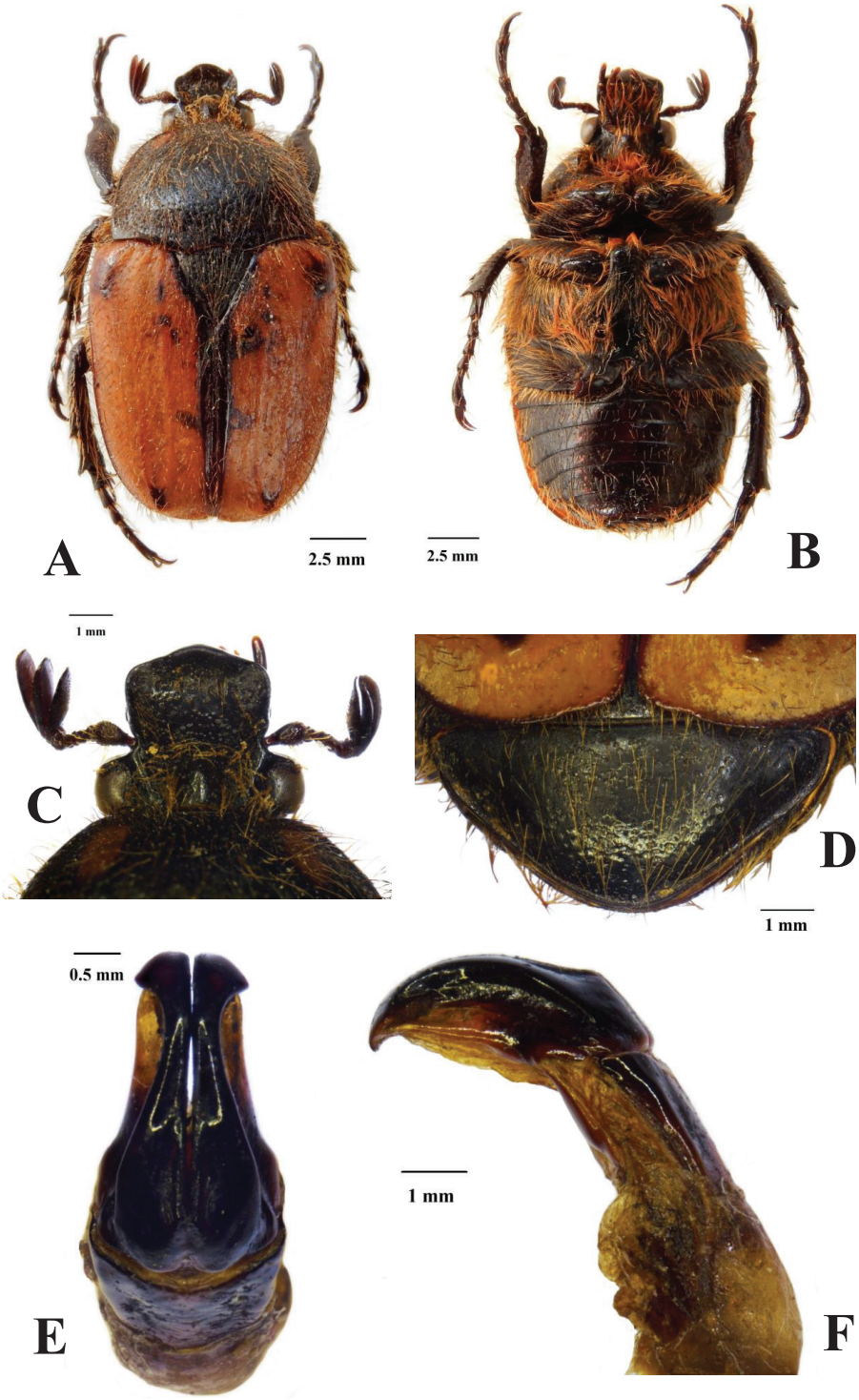

Figure 1. Dorsal (**A**) and ventral (**B**) habitus of male *Lophorrhinides muellerae* gen. et sp. n., with details of clypeus (**C**), pygidium (**D**) and aedeagus in dorsal (**E**) and lateral (**F**) view. Photographs Lynette Clennell.

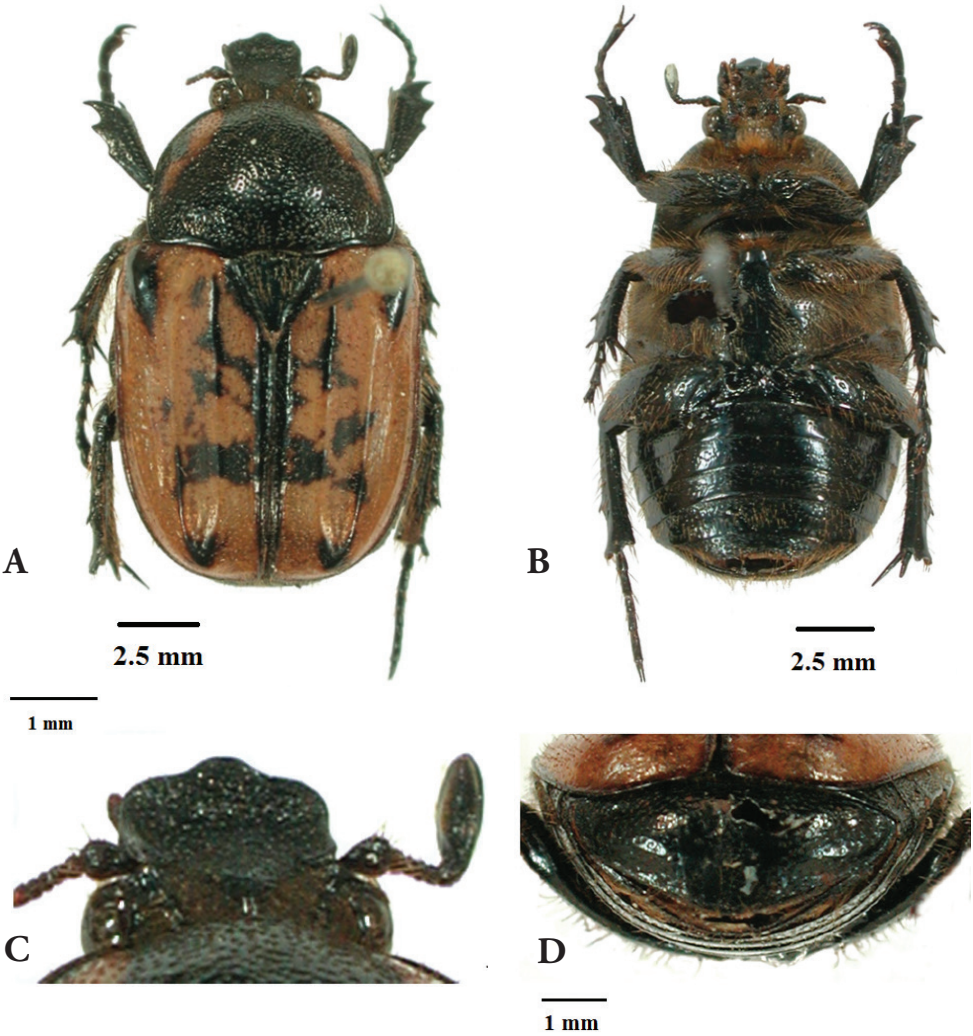

Figure 2. Dorsal (**A**) and ventral (**B**) habitus, with details of clypeal (**C**) and pygidial (**D**) morphology of the female of *Lophorrhinides muellerae* gen. et sp. n. Photographs Gerhard Beinhundner.

lobe smoothly rounded and not expanded anteriorly or laterally; abdominal sternites with visible concavity at centre (Fig. 1B).

Aedeagus. Parameres compact and not particularly elongate; dorsal lobes drastically narrowing anteriorly, with longitudinal groove depression towards mid length and expanding then at apex to form triangular protrusion on each side; apex smoothly rounded and bearing very short scattered setae at margin (Fig. 1E, F); ventral lobes substantially wider and lighter than dorsal lobes (Fig. 1E).

Paratype female. *Size*. Length 18.0 mm; width 9.5 mm.

Differences to male. In comparison to the male, the female specimen exhibits a slightly reduced clypeal armature (Fig. 2C), a shinier and markedly less hairy dorsal surface (Fig. 2A), as well as better-defined teeth on all the tibiae. Both elytral and pro-

Figure 3. Known geographic distribution of *Lophorrhinides muellerae* gen. n. et sp. n. in the southern highlands of Tanzania.

notal ornaments are more expanded than in the male, especially the dark maculae on the elytral disc and umbones (Fig. 2A). As in all closely related species, the abdominal segments of the female show a slight ventral convexity (Fig. 2B, D), rather than the typical grooved concavity of its male counterpart.

Distribution. Both known specimens come from the southern highlands of Tanzania, from Manow and Rungwe respectively (Fig. 3). The two localities are approximately 20 km apart at altitudes of 1700–2900 m asl.

Discussion

The discovery of this new genus and species has come as a surprise, as it clearly represents a novel taxon with at least its male holotype having been available for study in a major museum since its collection in the early 20th century. Interestingly, the only other specimen currently known for this species, a female from Rungwe collected more

recently in 2006, had also been overlooked until now and confused with a female of *Lophorrhina donckieri*, due to a superficial resemblance to that species (cf. Beinhundner 2017: 990, fig. 18). It seems thus likely that other specimens may be "hidden" in other collections around the world. It must also be noted that despite the overwhelming circumstantial evidence in support of the male and female specimens belonging to the same species, there is a margin of doubt regarding this. Molecular phylogenetic analyses could potentially resolve this conclusively, and also help elucidate the relationship with allied genera.

Lophorrhinides muellerae gen. et sp. n. occurs at the southern end of the distribution range of the *Daedycorrhina* Bates, 1888 group, formerly a separate genus but recently synonymised with *Lophorrhina* by Krajcik (1998). As both specimens appear to originate from high altitude areas in the southern Tanzanian highlands of the East African Rift, it is possible that the genus may represent a geographically isolated relic derived from an ancestral lineage shared with *Lophorrhina* and perhaps other genera like *Anisorrhina* and *Chlorocala,* which show some similarities with *Lophorrhinides* gen. n. especially at the level of the parameres and clypeal or head armature.

Virtually nothing is known about the biology of this new genus and species. Given its close relationship with the Tanzanian and Malawian members of the genus *Lophorrhina*, it is likely that *Lophorrhinides* gen. n. shares some ecological characteristics with species of this group. Unfortunately, even in this case, information on the biology of the various species of *Lophorrhina* that occur in these countries is very scarce, but it seems that virtually all specimens collected were either captured in flight or found "drinking" sap running from the bark of different trees, mostly *Acacia* spp. (Thierry Garnier and Alan J. Gardiner, pers. comm.). However, the high altitude montane habitat where *Lophorrhinides muellerae* occurs may suggest a life cycle with a very short life span at the adult stage. This has been shown repeatedly with other genera, particularly in mountainous and/or semiarid environments in southern Africa (e.g., Holm and Marais 1992, Perissinotto et al. 1999, Perissinotto 2017). Here the adults of most cetoniine species emerge from their underground cocoons only after major rainfall events in the late spring or summer and fly and mate during the hottest part of the day. Because they are unable to replenish their energy source through feeding on flowers, sap flows or fermenting fruits, their life span lasts only from several days to a few weeks (Perissinotto et al. 1999).

Acknowledgements

We are very grateful to Ruth Müller of the Ditsong National Museum of Natural History (formerly Transvaal Museum, Pretoria, South Africa) for the proactive submission to the first author of the male specimen here described as new genus and species. Thanks also to Thierry Garnier (Montpellier, France) and Alan Gardiner (Hoedspruit, South Africa) for sharing information on the behaviour of *Lophorrhina* species in the field. The Nelson Mandela University (Port Elizabeth, South Africa) is thanked for providing facilities and funding towards the completion of his work.

References

Allard V (1985) Goliathini 2. Les Coléoptères, du Monde Vol.6. Sciences Nat, Compiegne, 92 pp.

Bates HW (1888) Tropical African Coleoptera; chiefly from the Zanzibar mainland. The Entomologist's Monthly Magazine 24: 237–242. https://doi.org/10.5962/bhl.part.18601

Beinhundner G (2015) Notes on the genus *Lophorrhina* Westwood with description of a new species, and description of a new subspecies of the genus *Pachnoda* Burmeister (Coleoptera, Cetoniidae). Entomologia Africana 20(1): 22–28.

Beinhundner G (2017) The Cetoniinae of Africa. Gerhard Beinhundner, Euerbach, 1199 pp.

Bourgoin A (1913) Description de deux Cétonides nouveaux d'Afrique orientale (Coleoptera: Scarabaeidae). Bulletin de la Société entomologique de France 1913: 495–497.

Burmeister H (1842) Handbuch der Entomologie 3. Coleoptera Lamellicornia Melithophila. TEF Enslin, Berlin, 828 pp.

Holm E, Marais E (1992) Fruit Chafers of Southern Africa (Scarabaeidae: Cetoniini). Ekogilde, Hartbeespoort, 326 pp.

Kirby W (1828) A description of some Coleopterous insects in the collection of the Rev. FW Hope. The Zoological Journal 3: 520–525.

Kolbe HJ (1892) Herr HJ Kolbe sprach über die melitophilen Lamellicornier von Kamerun. Sitzungsbericht der Gesellschaft naturforschender Freunde zu Berlin 1892: 235–261.

Kolbe HJ (1893) Beiträge zur Kenntniss der melitophilen Lamellicornier (Coleoptera). Stettiner entomologische Zeitung 1893: 205–213.

Krajcik M (1998) Cetoniidae of the World. Catalogue Part I. Typos Studio Most, Czech Republic, 96 + 36 pp.

Krikken J (1984) A new key to the suprageneric taxa in the beetle family Cetoniidae, with annotated lists of the known genera. Zoologische Verhandelingen Leiden 210: 3–75.

Perissinotto R (2017) *Neoclita pringlei* (Scarabaeidae, Cetoniinae), a new relict genus and species from the Drakensberg Range of South Africa. European Journal of Taxonomy 279: 1–12. https://doi.org/10.5852/ejt.2017.279

Perissinotto R, Smith TJ, Stobbia P (1999) Description of adult and larva of *Ichnestoma pringlei* n. sp. (Coleoptera Scarabaeidae Cetoniinae), with notes on its biology and ecology. Tropical Zoology 12: 219–229. https://doi.org/10.1080/03946975.1999.10539390

Sakai K, Nagai S (1998) The Cetoniine Beetles of the World. Mushi-Sha's Iconographic Series of Insects 3. Mushi-Sha, Tokyo, 421 pp.

Westwood JO (1842) On the Goliathideous Cetoniidae of Africa. Arcana Entomologica 1: 125–188.

ZooKeys 833: 85–106 (2019)
doi: 10.3897/zookeys.833.30835
http://zookeys.pensoft.net

RESEARCH ARTICLE

A peer-reviewed open-access journal
ZooKeys
Launched to accelerate biodiversity research

Parasitic copepods (Crustacea, Hexanauplia) on fishes from the lagoon flats of Palmyra Atoll, Central Pacific

Lilia C. Soler-Jiménez[1], F. Neptalí Morales-Serna[2], Ma. Leopoldina Aguirre-Macedo[1,3], John P. McLaughlin[3], Alejandra G. Jaramillo[3], Jenny C. Shaw[3], Anna K. James[3], Ryan F. Hechinger[3,4], Armand M. Kuris[3], Kevin D. Lafferty[3,5], Victor M. Vidal-Martínez[1,3]

1 *Laboratorio de Parasitología, Centro de Investigación y de Estudios Avanzados del IPN (CINVESTAV-IPN) Unidad Mérida, Carretera Antigua a Progreso Km. 6, Mérida, Yucatán C.P. 97310, México* **2** *CONACYT, Centro de Investigación en Alimentación y Desarrollo, Unidad Académica Mazatlán en Acuicultura y Manejo Ambiental, Av. Sábalo Cerritos S/N, Mazatlán 82112, Sinaloa, México* **3** *Department of Ecology, Evolution and Marine Biology and Marine Science Institute, University of California, Santa Barbara CA 93106, USA* **4** *Scripps Institution of Oceanography-Marine Biology Research Division, University of California, San Diego, La Jolla, California 92093 USA* **5** *Western Ecological Research Center, U.S. Geological Survey, Marine Science Institute, University of California, Santa Barbara CA 93106, USA*

Corresponding author: *Victor M. Vidal-Martínez* (vvidal@cinvestav.mx)

Academic editor: *Danielle Defaye* | Received 25 October 2018 | Accepted 13 February 2019 | Published 27 March 2019

http://zoobank.org/6F31349B-BF7D-434D-8C06-4128FDD76A56

Citation: Soler-Jiménez LC, Morales-Serna FN, Aguirre-Macedo ML, McLaughlin JP, Jaramillo AG, Shaw JC, James AK, Hechinger RF, Kuris AM, Lafferty KD, Vidal-Martínez VM (2019) Parasitic copepods (Crustacea, Hexanauplia) on fishes from the lagoon flats of Palmyra Atoll, Central Pacific ZooKeys 833: 85–106. https://doi.org/10.3897/zookeys.833.30835

Abstract

We surveyed copepods parasitic on the fishes at Palmyra, a remote atoll in the Central Indo-Pacific faunal region. In total, we collected 849 individual fish, representing 44 species, from the intertidal lagoon flats at Palmyra and recovered 17 parasitic copepod species. The parasitic copepods were: *Orbitacolax williamsi* on *Mulloidichthys flavolineatus*; *Anuretes serratus* on *Acanthurus xanthopterus*; *Caligus confusus* on *Carangoides ferdau*, *Carangoides orthogrammus*, *Caranx ignobilis*, *Caranx melampygus*, and *Caranx papuensis*; *Caligus kapuhili* on *Chaetodon auriga* and *Chaetodon lunula*; *Caligus laticaudus* on *Rhinecanthus aculeatus*, *Pseudobalistes flavimarginatus*, *M. flavolineatus*, *Upeneus taeniopterus*, *Chrysiptera glauca,* and *Epinephalus merra*;

Copyright *Lilia C. Soler-Jiménez* et al. This is an open access article distributed under the terms of the Creative Commons Attribution License (CC BY 4.0), which permits unrestricted use, distribution, and reproduction in any medium, provided the original author and source are credited.

Caligus mutabilis on *Lutjanus fulvus* and *Lutjanus monostigma*; *Caligus randalli* on *C. ignobilis*; *Caligus* sp. on *L. fulvus*; *Caritus serratus* on *Chanos chanos*; *Lepeophtheirus lewisi* on *A. xanthopterus*; *Lepeophtheirus uluus* on *C. ignobilis*; *Dissonus similis* on *Arothron hispidus*; *Nemesis* sp. on *Carcharhinus melanopterus*; *Hatschekia longiabdominalis* on *A. hispidus*; *Hatschekia bicaudata* on *Chaetodon auriga* and *Chaetodon lunula*; *Kroyeria longicauda* on *C. melanopterus* and *Lernanthropus* sp. on *Kyphosus cinerascens*. All copepod species reported here have been previously reported from the Indo-Pacific but represent new geographical records for Palmyra, demonstrating large-scale parasite dispersion strategies.

Keywords
Parasitic copepods, fish, geographical isolation, islands, Indo-Pacific, atoll

Introduction

Although there have been several surveys of copepods parasitic on Indo-Pacific fishes, including the Great Barrier Reef (Australia), New Caledonia, New Guinea, India, Taiwan and the Hawaiian Islands (Yamaguti 1963, Kabata 1966, Lewis 1968, Pillai 1968, 1985, Cressey and Boyle 1973, Cressey and Cressey 1979, Ho and Dojiri 1977, Deets and Dojiri 1990, Ogawa 1991, Ho and Lin 2004, Boxshall and Justine 2005, Tang and Kalman 2005, Palm and Bray 2014), the East Indo-Pacific has received little sampling effort. Lafferty et al. (2008) compared parasite communities, including parasitic copepods, at two coral atolls in the Line Islands chain of the central Pacific (Kiritimati Island and Palmyra Atoll). However, their analysis was limited to broad patterns of richness and abundance of morphospecies, conservatively grouped into broad taxonomic categories. Palm and Bray (2014) listed parasites from Hawaiian fishes, reporting 64 copepod species (13 families) from 298 identified fish species.

Palmyra Atoll is one of the northern Line Islands located in the Indo-Pacific (IP) marine ecoregion (Spalding et al. 2007), 1680 km SSW of Hawaii. It is presently a marine protected area and has not supported regular human settlement since World War II. Palmyra Atoll has a relatively long history with little to no exploitation (DeMartini et al. 2008, Sandin et al. 2008). All fishing has been prohibited at Palmyra since it became a US National Wildlife Refuge in 2000 (before that, its remoteness kept fishing pressure low).

As part of a larger project assembling food webs at Palmyra Atoll, we have been cataloging the parasites found in the system. This paper is a companion to two others examining different fish parasite taxa (Vidal-Martínez et al. 2012, 2017). We recovered a considerable number of parasitic copepods from 44 fish species. As such, our tabulation adds to the few published species descriptions or host records from the Central Indo-Pacific region (Cressey and Boyle 1973, 1979, Cressey 1977, Ho and Lin 2004, Palm and Bray 2014), with an emphasis on describing diversity of the copepod supracommunity (Bush et al. 1997) at this site. The goal of this study is two-

fold. First, we list the copepod species recovered, and note, for each, taxonomic issues and report their prevalence, mean intensity and host species. Second, we then discuss this diversity survey with respect to previously published records for the region.

Material and methods

We collected fish by seine, spear, and hook and line from the intertidal sand flats bordering the lagoon of Palmyra Atoll between October 2009 and July 2012. To avoid loss or mixing of parasites among fishes, immediately after capture, we placed fish in individual plastic bags with lagoon water and transported them to the laboratory facility of the Palmyra Atoll Research Consortium (PARC). We examined only freshly killed fish (and the bag water). Observations were under a stereomicroscope. Skin and fins of each host were carefully examined. The gill arches were removed and examined under a stereomicroscope. The copepods obtained were counted, preliminarily identified, fixed in 95 % EtOH, labelled and stored in vials for later evaluation. Then, in the Laboratory of Aquatic Pathology of CINVESTAV-Mérida, specimens were mounted and cleared with lactophenol to identify species based on morphology using an Olympus BX-53 microscope (Olympus Corporation, Shinjuku, Tokyo, Japan). Prevalence and mean intensity concepts were applied following Bush et al. (1997). Synonyms for each host species and copepod species were obtained from FishBase (Froese and Pauly 2018) and World of Copepods (Walter and Boxshall 2018), respectively. Voucher specimens were deposited in the United States National Parasite Collection, Washington, DC (USNPC), and the Helminthological Collection of the Laboratory of Parasitology, at the Centre for Research and Advanced Studies, National Polytechnic Institute, Mérida, Yucatán, México (CHCM).

Results

Copepods of fishes from Palmyra lagoon flats

During this study, 849 individual fish from 44 species were collected. Fourteen of the 44 fish species examined were parasitized by at least one parasitic copepod species. *Caranx ignobilis* (Forsskål) was host to three copepod species, the most of any fish. *Acanthurus xanthopterus* Valenciennes, *Carcharhinus melanopterus* (Quoy & Gaimard), *Chaetodon auriga* Forsskål, *Chaetodon lunula* (Lacépède), *Lutjanus fulvus* (Forster), *Mulloidichthys flavolineatus* (Lacépède) and *Arothron hispidus* (Linnaeus) served as host for two copepod species. All other infected species hosted a single copepod species. Thirty fish species were found free of any copepod parasite (Table 1). Ten of the 17 copepod species recovered belong to the Caligidae family (Table 2).

Table 1. Fish species examined from the lagoon flats from the Palmyra Atoll. N = number of fish examined; Max = maximum length reported for that fish species in FishBase (http://www.fishbase.se); Range = total length range of the fish examined.

Host examined	Fish common name	N	Infected hosts	Max (cm)	Range (cm)
Acanthuridae					
Acanthurus triostegus (Linnaeus, 1758)	Convict surgeonfish	50	0	27	10–18
Acanthurus xanthopterus Valenciennes, 1835	Yellowfin surgeonfish	20	2	70	20–40
Albulidae					
Albula glossodonta (Forsskål, 1775)	Roundjaw bonefish	24	0	90	37–58
Apogonidae					
Cheilodipterus quinquelineatus Cuvier, 1828	Five-lined cardinalfish	5	0	13	5–6
Balistidae					
Pseudobalistes flavimarginatus (Rüppell, 1829)	Yellowmargin triggerfish	4	0	60	17–53
Rhinecanthus aculeatus (Linnaeus, 1758)	Blackbar triggerfish	18	0	30	8–24
Belonidae					
Platybelone argalus (Lesueur, 1821)	Keeltail needlefish	2	0	50	9–36
Carangidae					
Carangoides ferdau (Forsskål, 1775)	Blue trevally	5	0	75	33–38
Carangoides orthogrammus (Jordan & Gilbert, 1882)	Island trevally	3	0	75	25–35
Caranx ignobilis (Forsskål, 1775)	Giant trevally	4	3	170	56–79
Caranx melampygus Cuvier, 1833	Bluefin trevally	6	2	117	31–66
Caranx papuensis Alleyne & MacLeay, 1877	Brassy trevally	5	2	88	12–41
Carcharhinidae					
Carcharhinus melanopterus (Quoy & Gaimard, 1824)	Blacktip reef shark	5	3	200	46–219
Chaetodontidae					
Chaetodon auriga Forsskål, 1775	Threadfin butterflyfish	13	4	23	12–19
Chaetodon lunula (Lacepède, 1802)	Raccoon butterflyfish	14	6	20	11–16
Chanidae					
Chanos chanos (Forsskål, 1775)	Milkfish	5	1	180	31–57
Gobiidae					
Amblygobius phalaena (Valenciennes, 1837)	Whitebarred goby	18	0	15	1.3–7
Asterropteryx semipunctata Rüppell, 1830	Starry goby	12	0	6	2–4
Gnatholepis anjerensis (Bleeker, 1851)	Eye-bar goby	2	0	8	2–3
Istigobius decoratus (Herre, 1927)	Decorated goby	5	0	13	7–11
Istigobius ornatus (Rüppell, 1830)	Ornate goby	26	0	11	3–6
Istigobius rigilius (Herre, 1953)	Rigilius goby	1	0	11	4
Oplopomus oplopomus (Valenciennes, 1837)	Spinecheek goby	26	0	10	2–7
Psilogobius prolatus Watson & Lachner, 1985	Longjaw shrimpgoby	11	0	6	2–4
Valenciennea sexguttata (Valenciennes, 1837)	Sixspot goby	14	0	14	2–9
Hemiramphidae					
Hemiramphus depauperatus Lay & Bennett, 1839	Tropical half-beak fish	20	0	40	20–34
Kiphosidae					
Kyphosus cinerascens (Forsskål, 1775)	Blue sea chub	2	1	50	35–38
Lutjanidae					
Lutjanus fulvus (Forster, 1801)	Blacktail snapper	26	5	40	7–26
Lutjanus monostigma (Cuvier, 1828)	One spot snapper	6	1	60	17–37
Mugilidae					
Crenimugil crenilabis (Forsskål, 1775)	Fringelip mullet	42	0	60	8–45
Liza vaigiensis (Quoy & Gaimard, 1825)	Squaretail mullet	54	0	63	3–32
Valamugil engeli (Bleeker, 1858)	Kanda	63	0	30	1–20
Mullidae					
Mulloidichthys flavolineatus (Lacepède, 1801)	Yellowstripe goatfish	52	8	43	8–37
Upeneus taeniopterus Cuvier, 1829	Finstripe goatfish	5	3	33	1–30
Muraenidae					
Gymnothorax pictus (Ahl, 1789)	Paintspotted moray	7	0	140	41–70

Host examined	Fish common name	N	Infected hosts	Max (cm)	Range (cm)
Ophichthidae					
Myrichthys colubrinus (Boddaert, 1781)	Harlequin snake eel	3	0	97	33–65
Pinguipedidae					
Parapercis lata Randall & McCosker, 2002	Y-Barred Sandperch	13	0	21	2–3
Pomacentridae					
Abudefduf septemfasciatus (Cuvier, 1830)	Banded sergeant	12	0	23	14–20
Abudefduf sordidus (Forsskål, 1775)	Blackspot sergeant	18	0	24	14–19
Chrysiptera glauca (Cuvier, 1830)	Grey demoiselle	3	0	12	8–10
Stegastes nigricans (Lacepède, 1802)	Dusky farmerfish	10	0	14	8–10
Serranidae					
Epinephelus merra Bloch, 1793	Honeycomb grouper	2	0	32	13–24
Sphyraenidae					
Sphyraena barracuda (Edwards, 1771)	Great barracuda	2	0	200	65–76
Tetraodontidae					
Arothron hispidus (Linnaeus, 1758)	White-spotted puffer	15	9	50	17–49

Table 2. Parasitic copepods of fishes from the lagoon flats of Palmyra Atoll; N = number of fish examined. The authorities for parasites were included in the text.

Copepod species	Hosts	N	Infected hosts	Prevalence (%)	Mean intensity (± SD)
Bomolochidae					
Orbitacolax williamsi	*Mulloidichthys flavolineatus*	52	1	1.9	1
Caligidae					
Anuretes serratus	*Acanthurus xanthopterus*	20	1	5	6
Caligus confusus	*Carangoides ferdau*	5	2	40	2 ± 0.0
	Carangoides orthogrammus	3	1	33.3	6
	Caranx ignobilis	4	3	75	12.7 ± 12.2
	Caranx melampygus	6	2	40	4 ± 0.0
	Caranx papuensis	5	2	33.3	2 ± 0.0
Caligus kapuhili	*Chaetodon auriga*	13	1	7.7	8
	Chaetodon lunula	14	4	28.6	2.5 ± 1.7
Caligus laticaudus	*Rhinecanthus aculeatus*	18		5.6	1
	Pseudobalistes flavimarginatus	4	2	50	21 ± 26.9
	Mulloidichthys flavolineatus	52	7	13.5	1.5 ± 0.5
	Upeneus taeniopterus	5	3	60	2.7 ± 2.1
	Chrysiptera glauca	3	1	3.33	2
	Epinephalus merra	2	1	50	1
Caligus aff. mutabilis	*Lutjanus fulvus*	26	4	15.4	1.75 ± 1.5
	Lutjanus monostigma	6	1	16.6	2
Caligus randalli	*Caranx ignobilis*	4	1	25	1
Caligus sp.	*Lutjanus fulvus*	26	1	3.8	1
Caritus serratus	*Chanos chanos*	5	1	20	4
Lepeophtheirus lewisi	*Acanthurus xanthopterus*	20	1	5	1
Lepeophtheirus uluus	*Caranx ignobilis*	4	1	25	4
Dissonidae					
Dissonus similis	*Arothron hispidus*	15	2	13.3	2 ± 0.0
Eudactylinidae					
Nemesis sp.	*Carcharhinus melanopterus*	5	2	40	2 ± 0.0
Hatschekiidae					
Hatschekia longiabdominalis	*Arothron hispidus*	15	8	53.3	100 ± 329.2
Hatschekia bicaudata	*Chaetodon auriga*	13	3	23.1	7.3 ± 3.1
	Chaetodon lunula	14	2	14.3	5 ± 1.4
Kroyeriidae					
Kroyeria longicauda	*Carcharhinus melanopterus*	5	2	40	16 ± 2.8
Lernanthropidae					
Lernanthropus sp.	*Kyphosus cinerascens*	2	1	50	2

Order Cyclopoida Milne Edwards, 1840
Bomolochidae Claus, 1875
***Orbitacolax* Shen, 1957**

***Orbitacolax williamsi* Cressey & Cressey, 1989**

Type host. *Scolopsis taenioptera* (as *S. dubiosus*) (Cuvier) (Nemipteridae).

Other host and localities. *Scolopsis taenioptera* (as *S. dubiosus*) from Okinawa, Japan (Cressey and Cressey 1989). *Coris batuensis* (Bleeker) (Labridae) from Lizard Island, Australia (Muñoz and Cribb 2006). *Thamnaconus degeni* (Regan) (Monacanthidae) from South Australia (Hayward et al. 2011).

Current host. *Mulloidichthys flavolineatus* (Mullidae).

Site of infection. Gills.

Prevalence and mean intensity. 1.9 and 1 (n = 52).

Specimens deposited. CHCM No. 560 (voucher) (1 vial, 1 specimen ♀).

Remarks. To date, the genus *Orbitacolax* includes 10 valid species, which form two clusters (Venmathi Maran et al. 2014), the *hapalogenyos*-group with four species (*O. hapalogenyos*, *O. pteragogi*, *O. trichiuri*, and *O. unguifer*) and *analogus*-group with six species (*O. analogus*, *O. dactylopterusi*, *O. aculeatus*, *O. leptoscari*, *O. uniunquis*, and *O. williamsi*). This second group is based on the second endopodal segment of leg 2 either no inner seta or having 1 inner seta. Particularly, *O. williamsi* lacks seta on the second endopodal segment of leg 2, as seen in our specimen and the original description provided by Cressey and Cressey (1989). However, Venmathi-Maran et al. (2014) pointed out that *O. williamsi* carries 1 inner seta in that segment, but this is likely inaccurate. *Orbitacolax williamsi* has been found on western Pacific fishes from four families, suggesting that this parasite may have a low host specificity.

Order Siphonostomatoida Burmeister, 1835
Caligidae Burmeister, 1834
***Anuretes* Heller, 1865**

***Anuretes serratus* Shiino, 1954**

Type host. *Prionurus scalprum* (as *Xesurus scalprum*) Valenciennes (Acanthuridae).

Other host and localities. *Prionurus scalprum* (as *Xesurus scalprum*) (Acanthuridae) from Seto, Wakayama Prefecture, Japan (Shiino 1954). *Naso hexacanthus* (Bleeker) (Acanthuridae) from Oahu, Hawaii (Lewis 1964a, Palm and Bray 2014); from Japan and India (Prabha and Pillai 1986). *Prionurus microlepidotus* Lacepède (Acanthuridae) from Australia (Boxshall 2018).

Current host. *Acanthurus xanthopterus* (Acanthuridae).

Site of infection. Gills.

Prevalence and mean intensity. 5 and 6 (n = 20).

Specimens deposited. CHCM No. 561 (voucher) (1 vial, 1 specimen ♀).

Remarks. The validity of the genus *Anuretes* is questionable given the considerable morphological overlap with the members of *Lepeophtheirus* (Dojiri and Ho 2013). Currently, *Anuretes* includes 21 valid species (Boxshall 2018, Walter and Boxshall 2018); of which *A. serratus* may be distinguished by stout spines on distal exopodal segment of leg 1, and a branched spine on first exopodal segment of leg 2 (Shiino 1954, Lewis 1964a), which were clearly observed in our specimens. In addition, *A. serratus* lacks sternal furca. According to Dojiri and Ho (2013), a sternal furca is rarely absent in species of *Anuretes*.

Caligus Müller, 1785

Caligus confusus Pillai, 1961

Type host. *Caranx ignobilis* (as *C. sansun*) (Carangidae).

Other host and localities. *Alepes djedaba* (Forsskål) from Durban; *Caranx caballus* (Günther) and *Caranx caninus* (Günther) from Mexican Pacific and Ecuador; *Caranx djedaba* (Forsskål) from Durban, South Africa and Sri Lanka; *Caranx hippos* (Linnaeus) from Galapagos Islands and Panama; *Caranx ignobilis* from Taiwan, Indian and Australia; *Caranx melampygus* Cuvier from Eniwetok Atoll and Taiwan; *Caranx sexfasciatus* Quoy & Gaimard from South Africa, Taiwan, Indonesia and Australia; *Caranx* sp. from Celebes and New Caledonia (all Carangidae); *Coryphaena hippurus* Linnaeus (Coryphaenidae) from Galapagos Islands and Panama; *Decapterus* sp. (Carangidae) from Tonkin Gulf, Vietnam; *Elagatis bipinnulata* (Quoy & Gaimard) (Carangidae) from Galapagos Islands, Panama, India and Taiwan; *Elagatis* sp. from Celebes; *Epinephelus tauvina* (Forsskål) (Serranidae) from Kuwait; *Rhabdosargus holubi* (Steindachner) (Sparidae) from South Africa; *Seriola dumerili* (Risso) (Carangidae) from Taiwan; *Seriola* sp. (Carangidae) from Colombia (Kabata 1968, Grobler et al. 2003, Ho and Lin 2004, Yuniar et al. 2007, Kazachenko et al. 2014, Morales-Serna et al. 2014, 2015, Boxshall 2018).

Current host. *Carangoides ferdau* (Forsskål), *Carangoides orthogrammus* (Jordan & Gilbert), *Caranx ignobilis*, *Caranx melampygus* and *Caranx papuensis* Alleyne & MacLeay (all Carangidae).

Site of infection. Gills.

Prevalence and mean intensity. 40 and 2 (n = 5) to *Carangoides ferdau*, 33.3 and 6 (n = 3) to *Carangoides orthogrammus*, 75 and 12.7 ± 12.2 (n = 4) to *Caranx ignobilis*; 33.3 and 2 (n = 6) to *Caranx melampygus*; 40 and 4 (n = 5) to *Caranx papuensis*.

Specimens deposited. CHCM No. 562 (voucher) (1 vial, 1 specimen ♀) (from *Caranx ignobilis*), CHCM No. 563 (voucher) (1 vial, 2 specimens ♂ ♀) (from *Caranx papuensis*), USNM No. 1550598 (voucher) (1 vial, 1 specimen ♀) (from *Caranx ignobilis*).

Remarks. The genus *Caligus* contains approximately 250 species. According to Ho and Lin (2004), before the establishment of *C. confusus*, specimens of this species were confused with *Caligus productus* (as *Caligus alalongae*) Dana, 1852 and *Caligus constrictus* Heller, 1865. However, these authors pointed out nine characteristics known only for *C. confusus*. The morphology of our specimens (♂ and ♀) fits with the description of Ho and Lin (2004). Additionally, based on the examination of the present material and also that from previous surveys in the Eastern Pacific (Morales-Serna et al. 2014, 2015), we suggest that the shape of the first segment of the antenna and sternal furca may be useful in identifying *C. confusus*. Clearly, *C. confusus* has high affinity for carangid fish; nonetheless, this parasite can also be found on fish from different families. To date, it is distributed in tropical waters of the Eastern Pacific and Indo-Pacific, with no records for the Atlantic Ocean.

Caligus kapuhili Lewis, 1967

Type host. *Chaetodon miliaris* Quoy & Gaimard (Chaetodontidae).

Other host and localities. *Chaetodon miliaris* Quoy & Gaimard, *Chaetodon fremblii* Bennett from Hawaii (Lewis 1967, Palm and Bray 2014). *Chaetodon auripes* Jordan & Snyder and *Chaetodon vagabundus* Linnaeus from Taiwan (all Chaetodontidae) (Ho and Lin 2007).

Current host. *Chaetodon auriga* and *Chaetodon lunula* (Chaetodontidae).

Site of infection. Gills.

Prevalence and mean intensity. 7.7 and 8 (n = 13) to *Chaetodon auriga*; 28.6 and 2.5 ± 1.7 (n = 14) to *Chaetodon lunula*.

Specimens deposited. CHCM No. 564 (voucher) (1 vial, 1 specimen ♂) (from *C. auriga*). CHCM No. 565 (voucher) (1 vial, 1 specimen ♂) (from *C. lunula*). USNM No. 1550599 (voucher) (1 vial, 1 specimen ♂) (from *C. lunula*).

Remarks. According to Lewis (1967) and Lin and Ho (2007), *C. kapuhili* is morphologically close to *Caligus laticaudus* Shiino, 1960. However, the abdomen is 1-segmented in *C. kapuhili* and 2-segmented in *C. laticaudus*. We found specimens of *C. laticaudus* (see below), which facilitated our morphological analysis. Likewise, we identified *C. kapuhili* based on host preference, since this species has only been found on fish of the genus *Chaetodon* from the North-West Pacific.

Caligus laticaudus Shiino, 1960

Type host. *Pagrus major* (as *Pagrosomus major*) (Temminck & Schlegel) (Sparidae).

Other host and localities. *Pagrus major* (as *Pagrosomus major*) (Sparidae) from Japan (Shiino 1960). *Acanthurus olivaceus* Bloch & Schneider (Acanthuridae) from Eniwetok Atoll; *Dentex tumifrons* (Temminck & Schlegel) (Sparidae) from Korea; *Liza haematocheila* (Temminck & Schlegel) (Mugilidae) from China; *Caranx melampygus*

(Carangidae), *Lutjanus vitta* (Quoy & Gaimard), *Lutjanus russellii* (Bleeker) (Lutjanidae) and *Parapristipoma trilineatum* (Thunberg) (Haemulidae), *Polydactylus plebeius* (Broussonet) and *Polydactylus sextarius* (Bloch & Schneider) (Polynemidae) from Taiwan; *Parastomateus niger* (Bloch) (Carangidae) from Malaysia; *Filimanus heptadactyla* (Cuvier) (Polynemidae) and *Rhabdosargus sarba* (Forsskål) (Sparidae) from India (Ho and Lin 2004, Moon and Kim 2012). *Gnathanodon speciosus* (Forsskål), *Caranx sexfasciatus* Quoy & Gaimard (Carangidae), *Heniochus acuminatus* (Linnaeus) (Chaetodontidae), *Kyphosus bigibbus* Lacepède (Kiphosidae), *Pseudolabrus guentheri* Bleeker (Labridae), *Pagrus auratus* (Forster) (Sparidae) from Australia (Boxshall 2018).

Current host. *Rhinecanthus aculeatus* (Linnaeus), *Pseudobalistes flavimarginatus* (Rüppell) (Balistidae), *Mulloidichthys flavolineatus*, *Upeneus taeniopterus* Cuvier (Mullidae), *Chrysiptera glauca* (Cuvier) (Pomacentridae) and *Epinephalus merra* Bloch (Serranidae).

Site of infection. Gills..

Prevalence and mean intensity. 5.6 and 1 (n = 18) to *Rhinecanthus aculeatus*; 50 and 21 ± 26.9 (n = 4) to *Pseudobalistes flavimarginatus*; 13.5 and 1.5 ± 0.5 (n = 52) to *Mulloidichthys flavolineatus*; 60 and 2.7 ± 2.1 (n = 5) to *Upeneus taeniopterus*; 3.33 and 2 (n = 3) to *Chrysiptera* glauca; 50 and 1 (n = 2) to *Epinephalus merra*.

Specimens deposited. CHCM No. 566 (voucher) (1 vial, 2 specimens ♂ ♀) (from *M. flavolineatus*). USNM No. 1550600 (voucher) (1 vial, 1 specimen ♂) (from *M. flavolineatus*).

Remarks. Ho and Lin (2004) indicated that the female of *C. laticaudus* may be identified by a combination of five characteristics (the corpus of the maxilliped with a large, conical protrusion in the myxal region; the terminal elements on last segment of exopod of leg 1 lack accessory processes; outermost element 1 of the four terminal elements of leg 1 exopod about one third of the length of other three elements which are subequal in length; formula of the 3-segmented exopod of leg 4 as I-0; I-0; III; and the terminal three spines on leg 4 subequal in length). Our results support the view that *C. laticaudus* infects fishes only from the Indo-West Pacific.

Caligus aff. *mutabilis* Wilson, 1905

Type host. *Centropristis striata* (as *Centropristes striatus*) (Linnaeus) (Serranidae).

Other host and localities. *Centropristis striata* (as *Centropristes striatus*) (Serranidae) from North American waters (Wilson 1905). *Acanthocybium* sp., *Euthynnus* sp., *Sarda* sp., *Scomberomorus* sp., and *Thunnus* sp. (all Scombridae) from Colombia; *Archosargus rhomboidalis* (Linnaeus) (Sparidae), *Chaetodipterus faber* (Broussonet) (Ephippidae), *Mycteroperca microlepis* (Goode & Bean), *Scomberomorus brasiliensis* Collette, Russo & Zavala-Camin, *Scomberomorus maculatus* (Mitchill) (Scombridae) and *Trachinotus goodei* Jordan & Evermann (Carangidae) from Brazil; *Balistes* sp. (Balistidae), *Calamus brachysomus* (Lockington) (Sparidae), *Centropomus* sp. (Centropomidae), *Chaetodipterus zonatus* (Girard) (Ephippidae), *Epinephelus labriformis* (Jenyns) (Serranidae),

Hoplopagrus guentherii Gill (Lutjanidae), *Katsuwonus pelamis* (Linnaeus) (Scombridae), *Kyphosus elegans* (Peters) (Kyphosidae), *Lutjanus guttatus* (Steindachner), *Lutjanus peru* (Nichols & Murphy) (Lutjanidae), *Menticirrhus undulatus* (Girard) (Sciaenidae), *Microlepidotus brevipinnis* (Steindachner) (Haemulidae), *Mugil cephalus* (Linnaeus) (Mugilidae), *Paralabrax clathratus* (Girard), *Paralabrax maculatofasciatus* (Steindachner), *Paralabrax nebulifer* (Girard) (all Serranidae), *Sarda chiliensis* (Cuvier), *Scomberomorus sierra* Jordan & Starks (Scombridae) and *Selene orstedii* Lütken (Carangidae) from Mexican Pacific; *S. brasiliensis* from Costa Rica; *Scomberomorus cavalla* (Cuvier) (Scombridae) from Surinam; *S. maculatus* from Florida; *Scomberomorus japonicus* from Campeche (Gulf of Mexico); *E. labriformis*, *Eucinostomus entomelas* Zahuranec (Gerreidae), *Haemulopsis axillaris* (Steindachner) (Haemulidae), *Paralabrax callaensis* Starks (Serranidae), *Chromis cyanea* (Poey) and *Chromis multilineata* (Guichenot) (Pomacentridae) from Ecuador (Cressey and Cressey 1980, Luque and Tavares 2007, Gomes-Sanches et al. 2012, Morales-Serna et al. 2016).

Current hosts. *Lutjanus fulvus* and *Lutjanus monostigma* (Cuvier) (Lutjanidae).

Site of infection. Gills..

Prevalence and mean intensity. 15.4 and 1.75 ± 1.5 (n = 26) to *L. fulvus*; 16.6 and 2 (n = 6) to *L. monostigma*.

Specimens deposited. CHCM No. 567 (voucher) (1 vial, 1 specimen ♂) (from *L. fulvus*), CHCM No. 568 (voucher) (1 vial, 1 specimen ♂) (from *L. monostigma*). USNM No. 1550601 (voucher) (1 vial, 1 specimen ♂) (from *L. monostigma*).

Remarks. Wilson (1905) observed that the genital complex of *C. mutabilis* varies according to the age of the individuals as well as the developmental stage of the eggs. Also, this author described *C. mutabilis* as having a short, 2-segmented abdomen. Later, Cressey and Cressey (1980) redescribed this species based on material collected from scombrid fish. These authors noted an incomplete 2-segmented abdomen and at least two other differences from the type specimens; however, such differences were not considered sufficient to propose a new species. Recently, Morales-Serna et al. (2014, 2015) reported *C. mutabilis* from different host species in the Eastern Pacific, but a molecular analysis revealed relatively high intraspecific genetic divergence among the *C. mutabilis* isolates. Our specimens share the morphological characteristics described by Cressey and Cressey (1980).

Caligus randalli Lewis, 1964

Type host. *Acanthurus triostegus* (Linnaeus) (Acanthuridae).

Other host and localities. To our knowledge, *C. randalli* has not been recorded since its original description (Lewis 1964a). *Acanthurus triostegus* (Acanthuridae) from Hawaii (Lewis 1964a, Palm and Bray 2014).

Current host. *Caranx ignobilis* (Carangidae).

Site of infection. Gills.

Prevalence and mean intensity. 25 and 1 (n = 4).

Specimens deposited. CHCM No. 569 (voucher) (1 vial, 2 specimens ♂♀). USNM No. 1550602 (voucher) (1 vial, 1 specimen ♂).

Remarks. Lewis (1964a) observed that *Caligus randalli* is morphologically close to *C. constrictus* Heller, 1865. According to this author, one of the main differences between both species is the length of the urosome. The urosome of *C. randalli* is one and a half times the length of the urosome of *C. constrictus*. In the present study, we noted that *C. randalli* resembles *Caligus aesopus* Wilson, 1921. However, the urosome in *C. aesopus* is shorter than in *C. randalli*. Hayes et al. (2012) included *C. aesopus* and another nine species of *Caligus* (*C. chorinemy* Kroyer, 1863, *C. tenax* Heller, 1865, *C. spinosurculus* Pearse, 1951, *C. germoi* Pearse, 1951, *C. rectus* Pearse, 1952, *C. confusus*, *C. cordyla* Pillai, 1963, *C. zylanica* Hameed & Pillai, 1986 and *C. equulae* Ho & Lin, 2003) within a cluster of caligid species sharing the following characteristics in the female: bifid postantennal process; bifid posterior process on the maxillule; heavily ornamented apron of the third leg; an inner rosette of large spinules and prominent rib-like structure with a bifid apex, arising near the border with the intercoxal sclerite of leg 3: a massive and strongly incurved spine on the first exopodal segment of leg 3; and a 3-segmented exopod on leg 4 armed with I,I,III spines. *Caligus randalli* also shares these characteristics, and after a detailed examination. We confirmed that the morphological characteristic of our specimens fit with the description Lewis (1964a) for *C. randalli*. This is also supported by records of *C. randalli* in the Central Pacific.

Caligus sp.

Current host. *Lutjanus fulvus* (Lutjanidae).

Site of infection. Gills.

Prevalence and mean intensity. 3.8 and 1 (n = 26).

Specimens deposited. CHCM No. 570 (voucher) (1 vial, 1 specimen ♂).

Remarks. *Caligus* sp. is morphologically close to *Caligus laticaudus*, mainly by the shape and armature of cephalothoracic appendages and legs. However, our specimen differs from *C. laticaudus* in the shape and size of the urosome. Unfortunately, the single specimen of *Caligus* sp. in our collection is not sufficient for a more detailed taxonomic study.

Caritus Cressey, 1967

Caritus serratus Cressey, 1967

Type host:. *Chanos chanos* (Forsskål) (Chanidae).

Other host and localities. *Chanos chanos* (Chanidae) from Nosy Bé, Madagascar (Cressey 1967). Reported as *Caritus tolii* from *Tenualosa toli* (as *Hilsa toli*) (Valenciennes) (Clupeidae) from Sassoon Docks, Bombay (Rangnekar 1984).

Current host. *Chanos chanos* (Chanidae).

Site of infection. Gills.

Prevalence and mean intensity. 20 and 4 (n = 5).

Specimens deposited. CHCM No. 571 (voucher) (1 vial, 1 specimen ♀).

Remarks. Currently, *C. serratus* is the unique valid species included in the genus *Caritus*. Morphological characteristics of our specimens agree well with the redescription provided by Dojiri and Ho (2013).

Lepeophtheirus von Nordmann, 1832

Lepeophtheirus lewisi Hewitt, 1971

Type host. *Acanthurus olivaceus* (Acanthuridae).

Other host and localities. *Acanthurus olivaceus* (Acanthuridae) from Hawaii (Hewitt 1971). *Naso hexacanthus* (Bleeker), *Acanthurus triostegus* (Acanthuridae), *Myripristis* sp., *Fistularia petimba* Lacepède (Fistulariidae) (Lewis 1964a, 1964b, Palm and Bray 2014).

Current host. *Acanthurus xanthopterus* (Acanthuridae).

Site of infection. Gills.

Prevalence and mean intensity. 5 and 1 (n = 20).

Specimens deposited. CHCM No. 572 (voucher) (1 vial, 1 specimen ♂). USNM No. 1550603 (voucher) (1 vial, 1 specimen ♂).

Remarks. *Lepeophtheirus lewisi* was originally described as *Dentigryps bifurcatus* by Lewis (1964a). However, Hewitt (1971) stated that there is not a useful character to separate *Dentigryps* Wilson, 1913 from *Lepeophtheirus* and, therefore, reassigned species of *Dentigryps* to *Lepeophtheirus*. As the name *L. bifurcatus* was preoccupied by *L. bifurcatus* Wilson 1905, Hewitt (1971) renamed Lewis' species as *L. lewisi*. The material of the present study corresponds to a male of *L. lewisi*. The identification of this species was difficult without female specimens; nonetheless, the morphology of our material fits the description provided by Lewis (1964a) for the male of *L. lewisi*. In addition, this copepod has been mainly found in acanthurid fish from the Central Pacific as in the present work.

Lepeophtheirus uluus Lewis, 1964

Type host. *Caranx melampygus* (Carangidae).

Other host and localities. *Caranx melampygus* (Carangidae) from Oahu, Hawaii (Lewis 1964b, Palm and Bray 2014). Reported as *Dentigryps ulua* on *Caranx ignobilis* from Heron Island, Australia (Ho and Dojiri 1977).

Current host. *Caranx ignobilis* (Carangidae).

Site of infection. Gills.

Prevalence and mean intensity. 25 and 4 (n = 4).

Specimens deposited. CHCM No. 573 (voucher) (1 vial, 2 specimens ♂♀).

Remarks. *Lepeophtheirus uluus* was originally described as *Dentigryps ulua* by Lewis (1964b) and then transferred to *Lepeophtheirus* by Hewitt (1971). The morphology of our specimens corresponds to the original description.

Dissonidae Kurtz, 1924
***Dissonus* Wilson, 1906**

***Dissonus similis* Kabata, 1966**

Type host. *Tetractenos hamiltoni* (Richardson) (as *Spheroides hamiltoni*) (Tetraodontidae).

Other host and localities. *Tetractenos hamiltoni* (as *Spheroides hamiltoni*) (Tetraodontidae) from Queensland, Australia (Kabata 1966). *Arothron hispidus* from Philippines; *Arothron meleagris* (Anonymous) from Guam; *Arothron nigropunctatus* (Bloch & Schneider) from Australia, Philippines and New Guinea; and *Arothron stellatus* (Anonymous) (all Tetraodontidae) from New Guinea (Tang and Kalman 2005).

Current host. *Arothron hispidus* (Tetraodontidae).

Site of infection. Gills.

Prevalence and mean intensity. 13.3 and 2 ± 0.5 (n = 15).

Specimens deposited. CHCM No. 574 (voucher) (1 vial, 1 specimen ♀). USNM No. 1550604 (voucher) (1 vial, 1 specimen ♀).

Remarks. The family Dissonidae comprises only two genera, *Innaprokofevnas* Kazatchenko, 2001 with a single species (*I. orientcolae* Kazatchenko, 2001) and *Dissonus* with 12 species (*D. excavatus* Boxshall, Lin, Ho, Ohtsuka, Venmathi Maran & Justine, 2008; D. furcatus Kirtisinghe, 1950; *D. glaber* Kurtz, 1950; *D. heronensis* Kabata, 1966; *D. hoi* Tang & Kalman, 2005; *D. inaequalis* Boxshall, Lin, Ho, Ohtsuka, Venmathi Maran & Justine, 2008; *D. kapuri* (Ummerkutty, 1976); *D. manteri* Kabata, 1966; *D. nudiventris* Kabata, 1965; *D. ruvetti* Nuñes-Ruivo & Fourmanoir, 1956; *D. similis*; and *D. spinifer* Wilson, 1906).

According to Kabata (1966), *D. similis* is morphologically closer to *D. furcatus*. However, *D. similis* may be separated from *D. furcatus* and other congeners by the lack of a sternal furca or stylet and the presence of a genital spinulation extending over the anterior half to two thirds of ventral surface of genital complex (Tang and Kalman 2005, Boxshall et al. 2008). As indicated by Tang and Kalman (2005), *D. similis* is restricted to the tropical western Pacific and is highly host specific to tetraodontid fishes.

Eudactylinidae Wilson C.B., 1932

***Nemesis* sp. Risso, 1826**

Current host. *Carcharhinus melanopterus* (Carcharhinidae).

Site of infection. Gills.

Prevalence and mean intensity. 40 and 2 ± 0.1 (n = 5).

Specimens deposited. CHCM No. 575 (voucher) (1 vial, 1 specimen ♀).

Remarks. *Nemesis* is one of 12 genera in the family Eudactylinidae and includes about nine species (Mangena et al. 2014). *Nemesis* species can be divided into two groups by the relative width of the cephalothorax, free thoracic segments and genital segments (Dippenaar et al. 2008). One group (consisting of most of the species) has a fourth free thoracic segment that is much narrower than the preceding three, whereas the other (consisting of *N. lamna* only) has all four segments of about the same width (Kabata 1979). The identification and comparison of *Nemesis* species belonging to the first group is difficult because of morphological variation among individuals and the inconsistencies in the literature (Hewitt 1969, Kabata 1979).

Hatschekiidae Kabata, 1979
***Hatschekia* Poche, 1902**

***Hatschekia longiabdominalis* Uyeno & Nagasawa, 2013**

Type host. *Arothron hispidus* (Tetraodontidae).

Other host and localities. *Arothron hispidus* (Tetraodontidae) from Japan (Uyeno and Nagasawa 2013). To date, *H. longiabdominalis* has not been recorded from others host and locality.

Current host. *Arothron hispidus* (Tetraodontidae).

Site of infection. Gills.

Prevalence and mean intensity. 53.3 and 100 ± 329.2 (n = 15).

Specimens deposited. CHCM No. 576 (voucher) (1 vial, 1 specimen ♀). USNM No. 1550605 (voucher) (1 vial, 1 specimen ♀).

Remarks. Of the nine genera included in the Hatschekiidae, the most speciose genus is *Hatschekia*, with approximately 140 valid species so far. According to Uyeno and Nagasawa (2013), *H. longiabdominalis* may be separated from other congeners by having a fusiform trunk with posterior lobes, the urosome markedly projecting beyond posterior lobes of the trunk, and unique intercoxal sclerites of legs 1 and 2, which strongly project from the middle of the anterior margin and bear four blunt processes on the posterior margin. We observed all of these characters in our specimens.

***Hatschekia bicaudata* Kabata, 1991**

Type host. *Chaetodon aureofasciatus* Macleay (Chaetodontidae).

Other host and localities. *Chaetodon aureofasciatus* (Chaetodontidae) from Australia (Kabata 1991). *Chaetodon auripes* Jordan & Snyder (Chaetodontidae) from Seto, Wakayama Prefecture, Japan (Izawa 2016).

Current host. *Chaetodon auriga* and *Chaetodon lunula* (Chaetodontidae).

Site of infection. Gills.

Prevalence and mean intensity. 23.1 and 7.3 ± 3.1 (n = 13) to *Chaetodon auriga*; 14.3 and 5 ± 1.4 (n = 14) to *Chaetodon lunula*.

Specimens deposited. CHCM No. 577 (voucher) (1 vial, 1 specimen ♀) (from *Chaetodon auriga*). CHCM No. 578 (voucher) (1 vial, 1 specimen ♀) (from *Chaetodon lunula*). USNM No. 1550606 (voucher) (1 vial, 1 specimen ♀) (from *Chaetodon lunula*).

Remarks. Our samples corresponded to a single mature female from each host, which were not dissected for morphological analysis. Nonetheless, these parasitic copepods resemble *H. bicaudata* in its habitus, antenna, maxilla, and armature of legs 1 and 2, as well as in its preferred hosts, which are butterfly fishes distributed in warm waters from Australia to Japan (see Izawa 2016).

Kroyeriidae Kabata, 1979
***Kroyeria* van Beneden, 1853**

***Kroyeria longicauda* Cressey, 1970**

Type host. *Carcharhinus limbatus* (Müller & Henle) (Carcharhinidae).

Other host and localities. *Carcharhinus limbatus* (Carcharhinidae) from Florida. *Carcharhinus brevipinna* (Müller & Henle) (Carcharhinidae) from Madagascar (Deets 1994).

Current host. *Carcharhinus melanopterus* (Carcharhinidae).

Site of infection. Gills.

Prevalence and mean intensity. 40 and 16 ± 2.8 (n = 5).

Specimens deposited. CHCM No. 579 (voucher) (1 vial, 1 specimen ♀). USNM No. 155607 (voucher) (1 vial, 1 specimen ♀).

Remarks. The family Kroyeriidae comprises three genera, *Kroeyerina* Wilson, 1932 with nine species, *Kroyeria* with 15 species, and *Prokroyeria* Deets, 1987 with a single species (Walter and Boxshall 2018). Within *Kroyeria*, *K. longicauda* can be identified by the lateral tine on the deeply incised, bifid dorsal stylet, the lateral cuticular flange on the caudal rami, and the small number of unusually large endopodal denticulations of legs 1 to 4 that are unique to this species (Deets 1994).

Lernanthropidae Kabata, 1979
***Lernanthropus* de Blainville, 1822**

***Lernanthropus* sp.**

Current host. *Kyphosus cinerascens* (Forsskål) (Kyphosidae).

Site of infection. Gills.

Prevalence and mean intensity. 50 and 2 (n = 2).

Specimens deposited. CHCM No. 580 (voucher) (1 vial, 1 specimen ♀).

Remarks. The genus *Lernanthropus* includes about 120 species and it is one of the commonest genera of parasitic copepods on marine fishes. In this study, a single female of *Lernanthropus* sp. was collected. We were unable to proceed with the species identification because of the lack of specimens for dissection, which is necessary to observe appendages of the cephalothorax as well as legs 1 and 2. Even with enough material, the identification of *Lernanthropus* sp. is quite difficult because many species have not been described with sufficient detail (Koyuncu et al. 2012).

Discussion

The present study is the first detailed survey of the diversity and ecological attributes of the parasitic copepods infecting fishes at Palmyra Atoll. All records we report here are new geographical records. Most copepods (10 of 17) belonged to the family Caligidae. Of these ten caligid species, six were in the genus *Caligus* and two in the genus *Lepeophtheirus*. These finding are in agreement with the fact that *Caligus* copepods are mostly found on warm water fishes, while *Lepeophtheirus* copepod diversity is low in the tropics (Ho and Lin 2004, Suárez-Morales and Gasca 2012, Morales-Serna et al. 2016). However, as far as we know, specific evolutionary or ecological mechanisms underlying this greater diversification *Caligus* species in the tropics are not well understood. On the other hand, in experiments carried out by Bravo et al. 2010, they suggest that species of *Caligus* are more active swimmers than species of *Lepeophtheirus*, which in turns increase transmission between hosts. Clearly, such swimming ability could be contributing to dispersal of *Caligus* and host switching. Several copepods species can parasitize multiple fish species (Dojiri and Ho 2013). This is the case of *C. mutabilis* found on *Lutjanus monostigma* and *L. fulvus* in the present study however, this species has been reported in at least 13 families of marine fishes from the Atlantic and Pacific oceans (Morales-Serna et al. 2015).

Consistent with observations of the monogenean fauna of Palmyra Atoll fishes (Vidal-Martínez et al. 2017), parasitic copepod richness at Palmyra Atoll qualitatively appears low relative to other localities in the Indo-Pacific region. Most of the fish species we examined (30 of 44) were not parasitized by copepods, even with large sample sizes for some fish species (e.g. *Acanthurus triostegus*, n = 50). Several fishes that were unparasitized at Palmyra have copepod records at other sites. For example, *Acanthurus triostegus, Gymnothorax pictus, Epinephelus merra* and *Sphyraena barracuda* have been reported as hosts of at least one species of parasitic copepod in other localities of the Indo-Pacific (Boxshall and Huys 2007, Palm and Bray 2014). Because ectoparasite species richness, host size and age are positively related (Rhode 1993, Muñoz and Cribb 2005), the lack of copepods in some host species could be due to our sampling of only young (*Chanos chanos*) or small individuals (*Sphyraena barracuda*). Furthermore, the intertidal habitat sampled at Palmyra differs from the more often sampled fore-reef and reef flat habitats, making a direct comparison among studies difficult. More generally, Palmyra's remoteness may contribute to its depauperate copepod parasite fauna. The

Line Islands are far from the Austro-Malayan-Philippine region, the presumed center of origin of Indo-West Pacific (IWP) fishes and their parasites. Because we found fewer copepod species than described from Hawaii, which is still further from the presumed center of origin, we suggest that the remote location of the Line Islands and the particularly small size of Palmyra Atoll also contribute to the depauperate nature of the parasitic copepod fauna.

Acknowledgements

We acknowledge and thank the Palmyra Atoll National Wildlife Refuge, U.S. Fish and Wildlife Service, Department of the Interior, The Nature Conservancy and, The United States Geological Survey for their support. We deeply thank The Nature Conservancy staff and US Fish and Wildlife staff who were friendly and helpful. We are particularly indebted to Franklin Viola, Amanda Meyer, Brad Kintz, Aaron Kierzek, Jan Eber, Anthony Wilson, Lynette Williams, Kathy Wilson and Clara Viva-Rodríguez. We also thank Gareth Williams and Ingrid Knapp for sharing their field knowledge. This work also benefitted from a grant from the Marisla Foundation and a U.S. National Science Foundation Grant (DEB-0224565). Any use of trade, product, or firm names in this publication is for descriptive purposes only and does not imply endorsement by the U.S. Government.

References

Boxshall GA (2018) The sea lice (Copepoda: Caligidae) of Moreton Bay (Queensland, Australia), with descriptions of thirteen new species. Zootaxa 4398: 1–172. https://doi.org/10.11646/zootaxa.4398.1.1

Boxshall GA, Huys R (2007) Copepoda of New Caledonia. In: Payri CE, Richer de Forges B (Eds) Compendium of Marine Species of New Caledonia, Doc. Sci. Tech. II7, seconde édition, IRD Nouméa, 259–265.

Boxshall GA, Justine J-L (2005) A new genus of parasitic copepod (Siphonostomatoida: Caligidae) from a razorback scabbardfish, *Assurger anzac* Alexander (Trichiuridae) off New Caledonia. Folia Parasitologica, 52: 349–358. https://doi.org/10.14411/fp.2005.048

Boxshall GA, Lin CL, Ho JS, Ohtsuka S, Venmathi Maran BA, Justine JL (2008) A revision of the family Dissonidae Kurtz, 1924 (Copepoda: Siphonostomatoida). Systematic Parasitology 70: 81–106.

Bravo S, Treasurer J, Sepulveda M (2010). Effectiveness of hydrogen peroxide in the control of *Caligus rogercresseyi* in Chile and implications for sea louse management. Aquaculture 303: 22–27. https://doi.org/10.1016/j.aquaculture.2010.03.007

Bush A, Lafferty K, Lotz J, Shostak A (1997) Parasitology meets ecology on its own terms: Margolis et al. revisited. The Journal of Parasitology 83: 575–583. https://doi.org/10.2307/3284227

Cressey RF (1967) *Caritus* a new genus of caligoid copepod, with a key to the genera of Caliginae. Proceedings of the United States National Museum 123(3623): 1–8. https://doi.org/10.5479/si.00963801.123-3623.1

Cressey RF (1970) Copepods parasites on sharks from the west coast of Florida. Smithsonian Contributions to Zoology 38: 1–30. https://doi.org/10.5479/si.00810282.38

Cressey RF (1977) *Boylea longispican* g., n. sp. and other parasitic copepods from pacific fishes. Transactions of the American Microscopical Society 96(4): 467–476. https://doi.org/10.2307/3225664

Cressey RF, Boyle HB (1973) Five New Bomolochid Copepods Parasitic on Indo-Pacific Clupeid Fishes. Smithsonian Contributions Zoology 161: 1–25. https://doi.org/10.5479/si.00810282.161

Cressey RF, Boyle HB (1979) The Parasitic Copepods of Indo-West Pacific Lizardfishes (Synodontidae). Smithsonian Contributions to Zoology 296: 1–71. https://doi.org/10.5479/si.00810282.296

Cressey RF, Cressey HB (1979) The Parasitic Copepods of Indo-West Pacific Lizardfishes (Synodontidae). Smithsonian Contributions Zoology 296: 1–71. https://doi.org/10.5479/si.00810282.296

Cressey RF, Cressey HB (1980) Parasitic copepods of mackerel – and tuna – like fishes (Scombridae) of the world. Smithsonian Contributions to Zoology 311: 1–86. https://doi.org/10.5479/si.00810282.311.i

Cressey R, Cressey HB (1989) A new species of *Orbitacolax* (Copepoda: Bomolochidae) and redescriptions of additional two species. Canadian Journal of Zoology 67: 2902–2909. https://doi.org/10.1139/z89-411

Deets GB (1987) Phylogenetic analysis and revision of *Kroeyerina* Wilson, 1932 (Siphonostomatoida: Kroyeriidae), copepods parasitic on chondrichthyans, with descriptions of four new species and the erection of a new genus, *Prokroyeria*. Canadian Journal of Zoology 65(9): 2121–2148. https://doi.org/10.1139/z87-327

Deets GB (1994) Copepod-Chondrichthyan coevolution: a cladistics consideration. PhD Thesis, University of British Columbia, Vancouver, 448 pp.

Deets GB, Dojiri M (1990) *Dissonus pastinum* n. sp. (Siphonostomatoida: Dissonidae), a copepod parasitic on a horn shark from Japan. Beaufortia 41: 49–54.

DeMartini EE, Friedlander AM, Sandin SA, Sala E (2008) Differences in fish-assemblage structure between fished and unfished atolls in the northern Line Islands, central Pacific. Marine Ecology Progress Series 365: 199–215. https://doi.org/10.3354/meps07501

Dojiri M, Ho JS (2013) Systematics of the Caligidae copepods parasitic on marine fishes. Koninklijke Brill NV, Leiden. https://doi.org/10.1163/9789004204256

Dippenaar S, van Tonder R, Wintner S, Zungu P (2008) Spatial distribution of *Nemesis lamna* Risso 1826 (Copepoda: Siphonostomatoida: Eudactylinidae) on the gills of white sharks *Carcharodon carcharias* off KwaZulu-Natal, South Africa, African Journal of Marine Science 30(1): 143–148. https://doi.org/10.2989/AJMS.2008.30.1.14.464

Froese R, Pauly D (2018) Editors FishBase. http://www.fishbase.org [10/2018]

Gomes-Sanches E, Kerber CE, Paschoal F, Luque JL (2012) First record of *Caligus mutabilis* (Copepoda: Caligidae), in sea-farmed *Mycteroperca microlepis* (Perciformes: Serrani-

dae) in Brazil. Revista Brasileira de Parasitologia Veterinária 21: 330–333. https://doi.org/10.1590/S1984-29612012000300031

Grobler NJ, Van As JG, Oliver PAS (2003) Additional morphological information on two species of *Caligus* (Copepoda: Caligidae) parasitic on South Africa marine and estuarine fish. African Zoology 38: 139–143. https://doi.org/10.1080/15627020.2003.11657201

Hayes P, Justine JL, Boxshall GA (2012) The genus *Caligus* Müller, 1785 (Copepoda: Siphonostomatoida): two new species from reef associated fishes in New Caledonia, and some nomenclatural problems resolved. Zootaxa 3534: 21–39.

Hayward CJ, Svane I, Lachimpadi SK, Itoh N, Bott NJ, Nowak BF (2011) Sea lice infections of wild fishes near ranched southern bluefin tuna (*Thunnus maccoyii*) in South Australia. Aquaculture 320: 178–182. https://doi.org/10.1016/j.aquaculture.2010.10.039

Hewitt GC (1969) Some New Zealand parasitic Copepoda of the family Eudactylinidae. Zoology Publications from Victoria University of Wellington 49: 1–31.

Hewitt GC (1971) Species of *Lepeophtheirus* (Copepoda, Caligidae) recorded from the ocean sunfish (*Mola mola*) and their implications for the caligid genus *Dentigryps*. Journal of Fisheries Research Board of Canada 28: 323–334. https://doi.org/10.1139/f71-044

Ho JS, Dojiri M (1977) Parasitic copepods on the fishes of the Great Barrier Reef, Australia Part II. Caligoida: *Dissonus*, *Lepeophtheirus* and *Dentigryps*. Publications of the Seto Marine Biological Laboratory 24: 77–97. https://doi.org/10.5134/175956

Ho JS, Lin CL (2003) Three species of *Caligus* (Copepoda: Caligidae) parasitic on fishes of the northeast coast of Taiwan. Journal of the Fisheries Society of Taiwan 30(1): 55–70.

Ho JS, Lin CL (2004) Sea lice of Taiwan (Copepoda: Siphonostomatoida: Caligidae). The Sueichan Press, Keelung.

Ho JS, Lin CL (2007) Two new species of taeniacanthid copepods (Poecilostomatoida) parasitic on marine fishes of Taiwan. Systematic Parasitology 67(1): 73–80. https://doi.org/10.1007/s11230-006-9073-3

Izawa K (2016) Some new and known species of *Hatschekia* Poche, 1902 (Copepoda, Siphonostomatoida, Hatschekiidae) parasitic on the branchial lamellae of Japanese actinopterygian fishes belonging to perciformes, with revision of the known species of the genus. Crustaceana 89: 209–238. https://doi.org/10.1163/15685403-00003503

Kabata Z (1965) Parasitic Copepoda of fishes. Report B.A.N.Z. Antarctic Research Expedition 8(6): 1–16.

Kabata Z (1966) Copepoda parasitic on Australian fishes, V. Genus *Dissonus* (Dissonidae). Annals and Magazine of Natural History 13: 211–226. https://doi.org/10.1080/00222936608656047

Kabata Z (1968) Two species of *Caligus* from New Caledonia. Crustaceana 1: 1–10.

Kabata Z (1979) Parasitic Copepoda of British fishes. The Ray Society, London, 468 pp.

Kabata Z (1991) Copepoda parasitic on Australian fishes, XIII: family Hatschekiidae. Journal of Natural History 25: 91–121. https://doi.org/10.1080/00222939100770081

Kazachenko VN, Kovaleva NN, Ha DN, Nguyen VH, Thanh NV (2014) Redescription of three caligid species of the genus *Caligus* Müller, 1785 (Copepoda: Caligidae), parasites of marine fish *Decapterus* sp. (Perciformes: Carangidae) from Tonkin Gulf, Vietnam. Tap Chi Sinh Hoc 36: 1–11.

Koyuncu CE, Castro-Romero R, Karaytug S (2012) *Lernanthropus indefinitus* n. sp. (Copepoda, Siphonostomatoida, Lernanthropidae) parasitic on *Argyrosomus regius* (Asso, 1801) (Pisces, Sciaenidae). Crustaceana 85: 1409–1420. https://doi.org/10.1163/15685403-00003138

Lafferty KD, Shaw JC, Kuris AM (2008) Reef fishes have higher parasite richness at unfished Palmyra Atoll compared to fished Kiritimati Island. EcoHealth 5: 338–345. https://doi.org/10.1007/s10393-008-0196-7

Lewis AG (1964a) Caligoid copepods (Crustacea) of the Hawaiian Islands: Parasitic on fishes of the family Acanthuridae. Proceedings of the United States National Museum 11: 137–244. https://doi.org/10.5479/si.00963801.115-3482.137

Lewis AG (1964b) The caligid copepod genus *Dentigryps* (Crustacea: Caligoida). Proceedings of the United States National Museum 115: 347–380. https://doi.org/10.5479/si.00963801.115-3487.347

Lewis AG (1967) Copepod crustaceans parasitic on teleost fishes of the Hawaiian Islands. Proceedings of the United States National Museum 121: 1–204. https://doi.org/10.5479/si.00963801.121-3574.1

Lewis AG (1968) Copepod crustaceans parasitic on the fishes of Enewetok Atoll. Proceedings of the United States National Museum 125: 1–78. https://doi.org/10.5479/si.00963801.125-3656.1

Lin CL, Ho JS (2007) Six species of sea lice (Copepoda, Caligidae) new to Taiwan. Journal of the Fisheries Society of Taiwan 34: 41–67.

Luque JL, Tavares LER (2007) Checklist of Copepoda associated with fishes from Brazil. Zootaxa 1579: 1–39. https://doi.org/10.11646/zootaxa.1579.1.1

Mangena T, Jordaan BP, Dippenaar SM (2014) Phylogenetic relationships and genetic diversity of *Nemesis* Risso, 1826 species found on different elasmobranch host species off the KwaZulu-Natal coast, South Africa. African Journal of Marine Science 36(2): 163–173. https://doi.org/10.2989/1814232X.2014.912992

Moon SY, Kim IH (2012) Sea lice (Copepoda, Siphonostomatoida, Caligidae) new to Korea, including three new species. Journal of Species Research 1: 175–217. https://doi.org/10.12651/JSR.2012.1.2.175

Morales-Serna FN, Caña-Bozada V, Mera-Loor G, Loor-Andrade P, Fajer-Ávila EJ, Ho JS (2015) New records of sea lice (Copepoda: Caligidae) from marine fishes in Jaramijó, an area with potential for sea-cage aquaculture in Ecuador. Zootaxa 3920: 366–380. https://doi.org/10.11646/zootaxa.3920.2.8

Morales-Serna FN, Medina-Guerrero RM, Fajer-Ávila EJ (2016) Sea lice (Copepoda: Caligidae) parasitic on fishes reported from the Neotropical region. Neotropical Biodiversity 2(1): 141–150. https://doi.org/10.1080/23766808.2016.1236313

Morales-Serna FN, Pinacho-Pinacho CD, Gómez S, Pérez-Ponce de León G (2014) Diversity of sea lice (Copepoda: Caligidae) parasitic on marine fishes with commercial and aquaculture importance in Chamela Bay, Pacific coast of Mexico by using morphology and DNA barcoding, with description of a new species of *Caligus*. Parasitology International 63: 69–79. https://doi.org/10.1016/j.parint.2013.09.005

Muñoz G, Cribb TH (2005) Infracommunity structure of parasites of *Hemigymnus melapterus* (pisces: labridae) from lizard island, australia: the importance of Habitat and parasite body size. Journal of Parasitology 91(1): 38–44. https://doi.org/10.1645/GE-3321

Muñoz G, Cribb TH (2006) Parasite communities and diet of *Coris batuensis* (Pisces: Labridae) from Lizard Island, Great Barrier Reef. Memoirs of the Queensland Museum 52: 191–198.

Ogawa K (1991) Ectoparasites of sawfish, *Pristis microdon*, caught in fresh waters of Australia and Papua New Guinea. University Museum, University of Tokyo, Nature and Culture 3: 91–101.

Palm HW, Bray RA (2014) Marine Fish Parasitology in Hawaii. Westarp and Partner Digitaldruck, Hohenwarsleben XII, Germany, 320 pp.

Pillai NK (1961) Copepods parasitic on South Indian Fishes. Part I, Caligidae. Bulletin of the Research Institute, University of Kerala (C) 8: 87–130.

Pillai NK (1963) Copepods parasitic on South Indian fishes: Family Caligidae. Journal of the Marine Biological Association of India 5(1): 68–96.

Pillai NK (1968) Additions to the copepod parasites of South Indian fishes. Parasitology 58: 9–36. https://doi.org/10.1017/S0031182000073388

Pillai NK (1985) Parasitic copepods of Marine fishes. The Fauna of India. Zoological Survey of India, Calcutta, 900.

Prabha C, Pillai NK (1986) Additions to the copepods parasitic on the marine fishes of India. 4. on twenty-six species of Caligidae. Records of the Zoological Survey of India 79: 1–139.

Rangnekar MP (1984) Parasitic copepods from marine fishes of Bombay. In: Vervoort W (Ed.) Studies on Copepoda II. Proceedings of the First International Conference on Copepoda, Amsterdam, The Netherlands, 24–28 August 1981. Crustaceana 7: 344–351.

Sandin SA, Smith JE, DeMartini EE, Dinsdale EA, Donner SD, Friedlander AM, Konotchick T, Malay M, Maragos JE, Obura D, Pantos O, Paulay G, Richie M, Rohwer F, Schroeder RE, Walsh S, Jackson JBC, Knowlton N, Sala E (2008) Baselines and Degradation of Coral Reefs in the Northern Line Islands. PLoS One 3(2): 1548. https://doi.org/10.1371/journal.pone.0001548

Shiino SM (1954) Copepods parasitic on Japanese fishes 3. On two new species of the genus *Anuretes*. Report of Faculty of Fisheries 1: 260–272.

Shiino SM (1960) Copepods parasitic on the fishes collected on the coast of Province Shima, Japan. Reports of the Faculty of Fisheries, Prefectural University of Mie 3(3): 471–500.

Spalding MD, Fox HE, Allen GR, Davidson N, Ferdaña ZA, Finlayson M, Halpern BS, Jorge MA, Lombana A, Lourie SA, Martin KD, McManus E, Molnar J, Recchia CA, Robertson J (2007) Marine ecoregions of the world: a bioregionalization of coastal and shelf areas. BioScience 57: 573–583. https://doi.org/10.1641/B570707

Suárez-Morales E, Gasca RA (2012). New *Lepeophtheirus* (Copepoda: Siphonostomatoida: Caligidae) from Isla del Coco National Park, Costa Rica, Eastern Tropical Pacific. Revista de Biología Tropical 60: 235–242.

Tang D, Kalman JE (2005) A new caligiform copepod (Siphonostomatoida: Dissonidae) parasitic on *Seriola hippos* from western Australian waters, with new records and morphological

variation for *Dissonus nudiventris* and *Dissonus similis* and an updated key to the species of *Dissonus*. Journal of Parasitology 91: 427–437. https://doi.org/10.1645/GE-3370

Uyeno D, Nagasawa K (2013) The genus *Hatschekia* (Copepoda: Hatschekiidae) from pufferfishes (Tetraodontiformes: Tetraodontidae) off the Ryukyu Islands, Japan, with descriptions of four new species and a redescription of *H. pholas*. Folia Parasitologica 60: 61–74. https://doi.org/10.14411/fp.2013.008

Venmathi-Maran BA, Moon SY, Adday TK, Khamees NR, Myoung JG (2014) A new species of parasitic copepod *Nothobomolochus* and redescription of *Orbitacolax hapalogenyos* (Yamaguti & Yamasu, 1959) (Cyclopoida: Bomolochidae) off Iraq. Acta Parasitologica 59: 675–685.

Vidal-Martínez VM, Aguirre-Macedo ML, McLaughlin JP, Hechinger RF, Jaramillo AG, Shaw JC, James AK, Kuris AM, Lafferty KD. (2012) Digenean metacercariae of fishes from the lagoon flats of Palmyra Atoll, Eastern Indo-Pacific. Journal of Helminthology 5: 1–17. https://doi.org/10.1017/S0022149X11000526

Vidal-Martínez VM, Soler-Jiménez LC, Aguirre-Macedo ML, McLaughlin J, Jaramillo AG, Shaw JC, James A, Hechinger RF, Kuris AM, Lafferty KD (2017) Monogenea of fishes from the lagoon flats of Palmyra Atoll in the Central Pacific. ZooKeys 713: 1–23. https://doi.org/10.3897/zookeys.713.14732

Walter TC, Boxshall G (2018) World of Copepods database. http://www.marinespecies.org/copepoda [2018-10-02]

Wilson CB (1905) North American parasitic copepods belonging to the family Caligidae, part I: the Caliginae. Proceedings of the United States National Museum 28: 479–672. https://doi.org/10.5479/si.00963801.28-1404.479

Wilson C.B (1906) Report on some parasitic Copepoda collected by Professor Herdman, at Ceylon, in 1902. In: Herdman WA (Ed.) Report to the Government of Ceylon on the Pearl Oyster Fisheries of the Gulf of Manaar 5(34). 189–210.

Wilson CB (1913) Crustacean parasites of West Indian fishes and land crabs, with descriptions of new genera and species. Proceedings of the United States National Museum 44(1950): 189–227. https://doi.org/10.5479/si.00963801.44-1950.189

Wilson CB (1921) Report on the parasitic Copepoda collected during the survey of the Juan Fernandez Islands, 1916–1917. Natural History of the Juan Fernandez & Easter Islands 3: 69–74.

Wilson CB (1932) The copepods of the Woods Hole region, Massachusetts. Bulletin of the United States National Museum 158: 1–635. https://doi.org/10.5479/si.03629236.158.i

Yamaguti S (1963) Parasitic Copepoda and Branchiura of fishes. New York: Interscience Publishers, 1104 pp.

Yuniar AT, Palm HW, Walter T (2007) Crustacean fish parasites from Segara Anakan Lagoon, Java, Indonesia. Parasitology Research 100: 1193–1204. https://doi.org/10.1007/s00436-006-0391-9

ZooKeys 833: 107–119 (2019)
doi: 10.3897/zookeys.833.30936
http://zookeys.pensoft.net

RESEARCH ARTICLE

A peer-reviewed open-access journal
ZooKeys
Launched to accelerate biodiversity research

Pentaneurella katterjokki Fittkau & Murray (Chironomidae, Tanypodinae): redescription and phylogenetic position

Fabio Laurindo da Silva[1,2], Elisabeth Stur[1]

1 *Department of Natural History, NTNU University Museum, Norwegian University of Science and Technology, NO-7491 Trondheim, Norway* **2** *Department of Zoology, Institute of Biosciences, University of São Paulo, CEP: 05508-090, São Paulo, Brazil*

Corresponding author: *Elisabeth Stur* (elisabeth.stur@ntnu.no)

Academic editor: *G. Kvifte* | Received 30 October 2018 | Accepted 19 February 2019 | Published 1 April 2019

http://zoobank.org/3246F2A6-4529-4314-8B9F-75743F2DE7FF

Citation: Silva FL, Stur E (2019) *Pentaneurella katterjokki* Fittkau & Murray (Chironomidae, Tanypodinae): redescription and phylogenetic position. ZooKeys 833: 107–119. https://doi.org/10.3897/zookeys.833.30936

Abstract

The monotypic genus *Pentaneurella* Fittkau & Murray was originally described based on larvae, pupal exuviae and pharate males. The latter prevented the observation of key features, such as wing dimensions, abdominal coloration pattern, and hypopygial apodemes (sternapodeme and phallapodeme), and the description of the adult male was considered incomplete by the authors. Herein, the adult female of *Pentaneurella katterjokki* is described for the first time, and the adult male, pupa and larva are redescribed and figured based on specimens recently collected in Germany and Norway. We also discuss the phylogenetic position of *Pentaneurella*.

Keywords

DNA barcodes, immature stages, non-biting midges, Palearctic, Pentaneurini, taxonomy

Introduction

Fittkau (1962), in his reclassification of the subfamily Tanypodinae (Diptera: Chironomidae), separated the genus *Pentaneura* Philippi (*sensu lato* Edwards 1929, Freeman 1955, 1956) into eighteen genera within the tribe Pentaneurini. The only non-

Copyright *Fabio Laurindo da Silva, Elisabeth Stur.* This is an open access article distributed under the terms of the Creative Commons Attribution License (CC BY 4.0), which permits unrestricted use, distribution, and reproduction in any medium, provided the original author and source are credited.

South American species assigned to *Pentaneura* sensu Fittkau (1962) was a specimen from northern Sweden, *Pentaneura* spec. Katterjokk (Fittkau 1962), which was later placed in its own monotypic genus, and named *Pentaneurella katterjokki* (Fittkau & Murray, 1983).

Non-biting midges of the genus *Pentaneurella* are medium-sized dipterans with a Palearctic distribution. Larvae are only known from springs and spring-fed streams in Swedish Lapland and from a mountain stream in northern Norway (Cranston and Epler 2013), although the genus has been consistently recorded through Europe (Sæther and Spies 2013). Fittkau and Murray (1983) described *Pentaneurella* based on larvae, pupal exuviae and pharate males. The latter prevented the observation of key features, such as wing dimensions, wing venation, abdominal coloration pattern, and hypopygial apodemes (sternapodeme and phallapodeme), which are considered essential for male distinction in the subfamily Tanypodinae. Therefore, *Pentaneurella katterjokki* is redescribed and figured below as adult male, pupa and larva based on specimens recently collected in Germany and Norway. In addition, the adult female is described for the first time. Finally, the phylogenetic position of *Pentaneurella* is discussed.

Material and methods

Fourth instar larvae and pupae were sampled with hand nets, while adults were collected using emergence- and Malaise traps. Associations between different life stages were established using DNA barcoding. Alcohol-preserved specimens were dissected, the bodies cleared in 8% KOH, and slide-mounted in Euparal®. Measurement methods are according to Epler (1988). Morphological terminology and abbreviations follow Roback (1971) and Sæther (1980), supplemented by Kowalyk (1985) for larval cephalic setation and Silva et al. (2011, 2014) for larval terminology. The color is described based on the specimens preserved in alcohol. The examined specimens are deposited in the NTNU University Museum insect collection (NTNU-VM) and Zoologische Staatssammlung München (ZSM), Germany. One leg was dissected off each specimen and submitted to the Canadian Centre for DNA Barcoding. Metadata, photos, sequences and trace-files are available in the Barcode of Life Data Systems (BOLD, www.boldsystems.org) through the dataset DS-PKATTER with doi: 10.5883/DS-PKATTER. GenBank accessions are HM421431, HM421434, HM421436, HM421438, HM421441 and MK402317 to MK402322. DNA extracts and partial COI gene sequences were generated using standard primers and bi-directional Sanger sequencing with BigDye 3.1 termination at the Canadian Centre for DNA Barcoding in Guelph. Protocols and original trace-files are available through the dataset DS-PKATTER in BOLD. Alignments were done on amino acid sequences and were trivial as indels were absent; only sequences > 300bp were used in the final alignment.

Taxonomy

Pentaneurella katterjokki Fittkau & Murray, 1983

Pentaneura spec. Katterjokk Fittkau, 1962: 372 (description of male)
Pentaneurella katterjokki Fittkau & Murray, 1983: 62 (description of male and immature stages)

Material examined. ***Type material:*** Holotype pharate male (ZSM slide A and B), SWEDEN, Katterjokk, Swedish Lappland, leg. L. Brundin. Two paratypes: pharate female and larva data as for holotype.

Additional material: NORWAY, Oppland, Rondane National Park: Adult male (NTNU-VM slide 201765), Skranglehaugen (P4), 1110 m asl, 61.98270N, 9.80360E, 14–21.vii.2008, leg. T. Ekrem, [BOLD ID: ATNA328]. Adult male (NTNU-VM slide 201767), as previous except for Skranglehaugen (P3), 1115 m asl, 61.98219N, 9.80451E, [BOLD ID: ATNA333]. Adult female (NTNU-VM slide 201768), as previous except for 07–14.vii.2008, leg. T. Hoffstad, [BOLD ID: ATNA335]. Adult female (NTNU-VM slide 201766), Skranglehaugen (P2), 1119 m asl, 61.98141N, 9.80480E, 14–21.vii.2008, leg. T. Ekrem, [BOLD ID: ATNA 331]. Pupa (NTNU-VM slide 201769), Skranglehaugen (P5), 1105 m asl, 61.98346N, 9.80384E, 07–14.vii.2008, leg. T. Hoffstad, [BOLD ID: ATNA338]. Larva (NTNU-VM slide 201764) Skranglehaugen, 1117 m asl, benthos, 61.99186N, 9.80454E, 23.vi.2008, leg. E. Stur, [BOLD ID: ATNA122]. Pupa (NTNU-VM slide 201771) Dørålseter, 1032 m asl, kick sample 3, 61.99347N, 9.80343E, 10.viii.2015, leg. K. Hårsaker, T. Ekrem and M. Majaneva, [BOLD ID: EBAI-Ch122]. Larva (NTNU-VM slide 201770) as previous, [BOLD ID: EBAI-Ch66]. GERMANY, Bayern, Berchtesgaden National Park: Adult male, (NTNU-VM slide 201774), Herrenrointquelle 308, 1250 m asl, 47.57778N, 12.97222E, 26.vii-09.viii.2005, leg. F. Eder, [BOLD ID: ES147]. Adult male, (NTNU-VM slide 201772), Schapbachquelle 360a, 1140 m asl, 47.58278N, 12.95806E, 27.v.-14.vi.2005, leg. F. Eder, [BOLD ID: ES46]. Adult male, (NTNU-VM slide 201773), as previous except for 28.vi-12.vii.2005, leg. F. Eder & A. Schellmoser [BOLD ID: ES82].

Diagnostic characters. *Pentaneurella katterjokki* differs from other Pentaneurini species by the combination of the following characters. ***Adult male:*** thorax with a scutal tubercle, tibial spur on fore leg with long outer tooth and shorter side teeth, anal point apically notched. ***Adult female:*** gonapophysis VIII triangular, tergite IX without setae, coxosternapodeme strongly curved, postgenital plate broadly rounded, labia with inconspicuous microtrichia. ***Pupa:*** plastron plate moderately large, corona absent, anal macrosetae with adhesive sheaths, genital sac symmetrically tapered. ***Larva:*** dorsally DP absent, peg sensilla large, firmly fused with the margin of antennal segment 2, forming a fork-like process.

Description. ***Adult male*** **(n = 3, except where otherwise stated).** *Size*. Total length 5.2 (1) mm. Wing length 3.0–3.1 mm. Total length/wing length 1.75 (1). Wing length/profemur length 2.09–2.22 (2).

General coloration. Head pale brown with darker occipital margin; pedicel and antenna brown; maxillary palp pale brown. Thorax pale brown. Wing membrane transparent without marks. Legs brown to pale brown. Abdominal tergite I–VI white, T VII with continuous pale brown transverse band near proximal margin, VIII pale brown; hypopygium pale brown.

Head. Temporal setae 17–19, uniserial. Eye ratio 0.47–0.59. Tentorium 235–289 µm long. Clypeus 132–189 µm long, 97–111 µm wide at widest part, bearing 12–22 setae. Cibarial pump 284–301 µm long. Lengths of palpomeres 1–5 (in µm): 77–82; 84–97; 163–178; 171–207; 324–342. Antenna 1250–1297 µm long, diameter of pedicel 185–188 (2) µm. AR 1.22–1.31.

Thorax. Antepronotals 6–10. Acrostichals 30–52, double staggered row which diverges posteriorly to join the dorsocentral row; dorsocentrals 24–38, biserial anteriorly and uniserial posteriorly; prealars 11–12 (2); supraalar 1 (1). Anapleural suture ratio 0.48–0.55. Scutellars 10–14. Scutal tubercle present.

Wing (Fig. 1A). Width 0.85–0.86 (4) mm. Membrane densely covered with macrotrichia. Costa 2.9–3.1 (4) mm long without extension ending proximal to R_{4+5}; MCu almost at FCu; R_{2+3} present, R_3 not reaching costa. VR 0.91–1.05. WW 0.27–0.29. Brachiolum with 3 setae. Squama with 18–26 (2) setae. Anal lobe moderately developed.

Legs (Fig. 1B–E). Fore leg: width at apex of tibia 70 (2) µm, tibia with single, apical and pectinate spur 36–37 (2) µm long (Fig. 1B), with 4 (2) lateral teeth; ta_{1-4} without preapical pseudospurs. Mid leg: width at apex of tibia 64–72 µm, tibia with two apical spurs 22–27; 32–40 µm long (Fig. 1C), with 4–5 lateral teeth; ta_{1-4} with preapical pseudospurs. Hind leg: width at apex of tibia 62–72 µm, tibia with two apical spurs 22–29; 25–29 µm long (Fig. 1D), with 4 lateral teeth; comb not observed; ta_{1-4} without preapical pseudospurs. Claws slender, distally recurved and pointed and with large basal protuberance (Fig. 1E). Pulvilli absent. Lengths and proportion of leg segments as in Table 1.

Hypopygium (Fig. 1F). Tergite IX slightly concave posteriorly, without posterior setae. Membranous anal point broad, apically notched. Phallapodeme 106–130 (2) µm long. Sternapodeme with reduced anterior process. Gonocoxite cylindrical, 235–285 µm long, 103–131 µm wide. GcR 2.02–2.44. Gonostylus slender, 166–176 µm long, megaseta cochleariform, 14–17 µm long. HR 1.44–1.62. HV 3.04 (1).

***Adult female* (n = 2, except where otherwise stated)**. *Size*. Total length 5.2 (1) mm. Wing length 3.3–3.4 mm. Total length/wing length 1.02–1.14. Wing length/profemur length 2.55–2.74.

Table 1. Lengths (in µm) and proportions of leg segments in *Pentaneurella katterjokki* Fittkau & Murray, male (n = 2 or 3).

	fe	**ti**	**ta_1**	**ta_2**	**ta_3**
p_1	1385–1487	1433–1634	616–630	551–568	385–409
p_2	1246–1503	1414–1757	935–1110	577–693	420–510
p_3	1279–1304	1434–1519	1025–1163	684–732	471–507
	ta_4	ta_5	LR	BV	SV
p_1	225–240	146–155	0.38–0.44	2.59–2.78	4.63–4.90
p_2	241–284	154–182	0.63–0.75	2.34–2.77	2.22–3.12
p_3	268–295	167–186	0.71–0.77	2.28–2.35	2.42–2.65

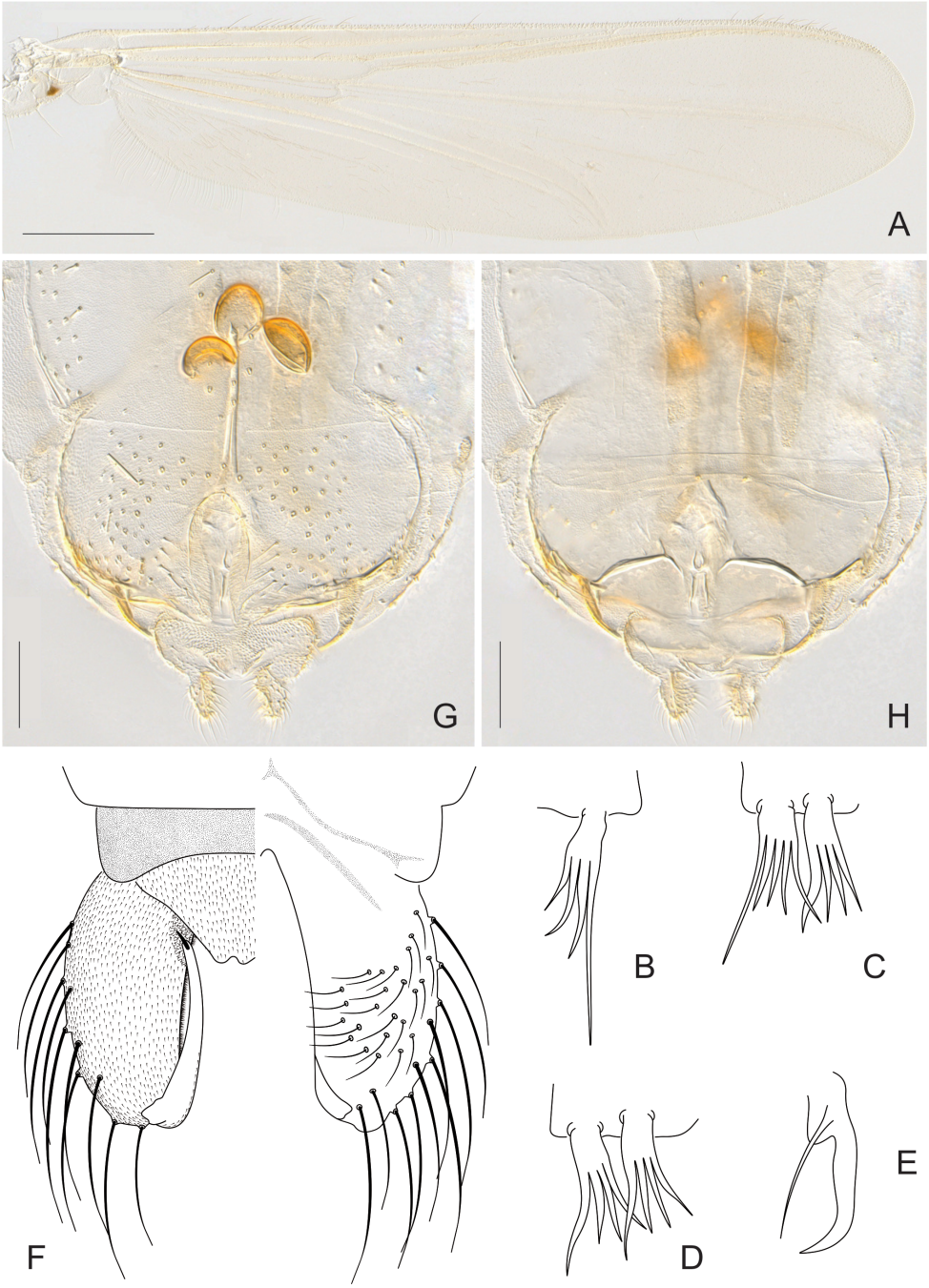

Figure 1. *Pentaneurella katterjokki* Fittkau & Murray, adult male (**A–F**), adult female (**G–H**). **A** Wing **B** fore tibial spur **C** mid tibial spurs **D** hind tibial spurs **E** tarsal claw **F** hypopygium, left: ventral aspect, right: dorsal aspect **G** female genitalia, dorsal aspect **H** female genitalia, ventral aspect. Scale bars: 500 µm (**A**); 100 µm (**G, H**).

Table 2. Lengths (in μm) and proportions of leg segments in *Pentaneurella katterjokki* Fittkau & Murray, female (n = 2).

	fe	ti	ta_1	ta_2	ta_3
p_1	1235–1343	1539–1625	1149–1151	745–747	508–512
p_2	1349–1414	1520–1621	822–1165	586–729	417–515
p_3	1238–1448	1596–1879	837–1171	583–765	421–553
	ta_4	ta_5	LR	BV	SV
p_1	290–306	175–196	0.71–0.75	2.28–2.34	2.41–2.58
p_2	232–317	165–188	0.54–0.72	2.36–2.68	2.55–3.57
p_3	258–286	158–182	0.52–0.62	2.40–2.74	2.66–3.64

General coloration. Head pale brown with darker occipital margin; pedicel and antenna brown; maxillary palp pale brown. Thorax pale brown. Wing membrane transparent without marks. Legs brown to pale brown. Abdominal tergites and genitalia pale brown.

Head. Temporal setae 22–24, irregularly uniserial. Eye ratio 1.12–1.33. Tentorium 186–287 μm long. Clypeus 157–176 μm long, 108–121 μm wide at largest part, bearing 25–28 setae. Cibarial pump 281–305 μm long. Lengths of palpomeres 1–5 (in μm): 52–57; 98–102; 180–181; 188–193; 333–334. Antenna 897–920 μm long, diameter of pedicel 98–100 μm. AR 0.36–0.39.

Thorax. Antepronotals 7. Acrostichals 44–48, double staggered row which diverges posteriorly to join the dorsocentral row of setae; dorsocentrals 36–48, biserial anteriorly and uniserial posteriorly; prealars 15–16; supraalars 2. Anapleural suture ratio 0.49 (1). Scutellars 8–10. Scutal tubercle present.

Wing. Width 1.00–1.10 mm. Costa 3.3–3.4 mm long. VR 0.96–0.98. WW 0.30–0.31. Brachiolum with 3 setae. Squama with 22–25 setae.

Legs. Fore leg: width at apex of tibia 71–74 μm, tibia with single, apical and pectinate spur 27–28 μm long, with 4 lateral teeth; ta_{1-4} without preapical pseudospurs. Mid leg: width at apex of tibia 54–68 μm, tibia with two apical spurs 27–28; 29–32 μm long, with 4–5 lateral teeth; ta_{1-4} with preapical pseudospurs. Hind leg: width at apex of tibia 65–67 μm, tibia with two apical spurs 30–35; 44–48 μm long, with 4 lateral teeth; comb not observed; ta_{1-4} without preapical pseudospurs. Claws slender, distally recurved and pointed and with large basal protuberance. Lengths and proportion of leg segments as in Table 2.

Genitalia (Fig. 1G–H). Gonapophysis VIII triangular, 84–85 μm long. Tergite IX without setae. Coxosternapodeme 142–159 μm long. Postgenital plate broadly rounded. Cerci oval-quadrate, 55–63 μm long, 24–31 μm wide; with 20 elongated setae. Labia with inconspicuous microtrichia. Notum 196–199 μm long. Seminal capsules oblong, 74–75 μm long, 55–69 μm wide, with conical shaped necks. Length ratio SCa/No 0.37–0.38.

***Pupa* (n = 2, except where otherwise stated).** *Size*. Abdomen 3.5–4.3 mm long in male.

General coloration. Exuviae mostly pale brown without any distinctive patterns; thoracic horn brown.

Cephalothorax (Fig. 2A). Wing sheath smooth, 1.5–1.6 mm long. Thoracic horn 322–336 μm long and 111–115 μm wide (Fig. 2A). THR 2.89–2.93. Respiratory

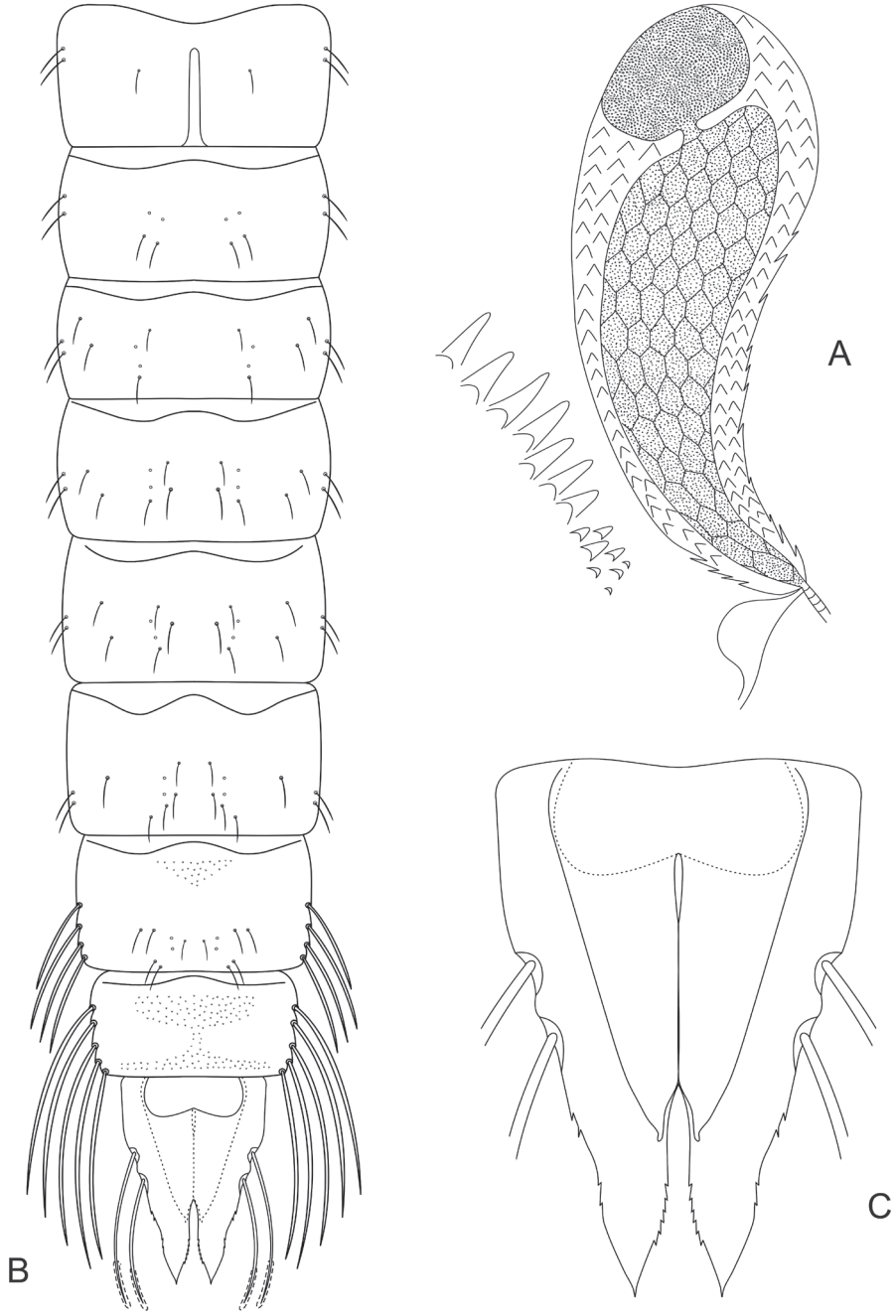

Figure 2. *Pentaneurella katterjokki* Fittkau & Murray, pupa. **A** Thoracic horn with basal lobe and thoracic comb **B** abdominal segments with chaetotaxy, dorsal aspect **C** anal lobe and male genital sac, ventral aspect.

atrium almost filling the lumen cavity, apically constricted into a narrow, short and straight neck, connected basally to a large rounded plastron plate. External membrane with spinules basally interconnected, forming scales. Basal lobe large apically round. Thoracic comb with 14 or 15 conical tubercles (Fig. 2A).

Abdomen (Fig. 2B, C). Tergite I with scar 217–238 µm long. Shagreen on tergites very sparse, spinules only present on the anterior median border of tergite VII, anterior and posterior borders of tergite VIII and sparsely on the anal lobe. Sternites I and VIII without shagreen, S II–VI with lateral longitudinal narrow bands or shagreen, S VII almost entirely covered with shagreen. Abdominal chaetotaxy as in figure 2B. Abdominal segment VII with 4 LS-setae. A VIII with 5 LS-setae. Anal lobe 516–533 µm long, 319–331 µm wide (Fig. 2C). ALR 1.60–1.62. Male genital sac not surpassing apex of anal lobe.

***4th instar larva* (n = 2, except where otherwise stated).** *General coloration*. Head golden yellow, postoccipital margin brown. Ligula pale yellow, with apex brown. Abdomen pale yellow. Procercus pale brown along anterior margin.

Head (Fig. 3A). Length 808–873 µm, 495–518 µm wide; IC 0.59–0.61. Dorsally DP absent, S5 and S8 postero-mesal to S7. Ventrally S9, S10 and SSm forming a gently curved line (Fig. 3A).

Antenna (Fig. 3B–C). Length 374–383 µm, A_1 274–276 µm long, with ring organ located 0.44–0.54 from base, A_2 86–93 µm long. Peg sensilla large, firmly fused with margin of antennal segment 2, forming a fork-like process (Fig. 3C). AR 2.57–2.73. Blade 104–106 µm long.

Maxilla (Fig. 3D). Basal palp segment 59–60 µm long, 12–13 wide at middle, with ring organ located 0.40–0.68 from base. PR 4.44–4.45. APR 4.59–4.66.

Mandible (Fig. 3E). Length 95–115 µm. Sensillum campaniformium located 0.72 from apex. AMD 2.38– 2.89.

Mentum and M appendage (Fig. 3F). Dorsomentum sclerotised, without teeth. Labial vesicles oblong. Pseudoradula with fine granulation, not arranged in distinct longitudinal rows, 115 (1) µm long.

Hypopharyngeal complex (Fig. 3G–H). Ligula with 5 teeth, 86–98 µm long, 44–52 µm wide at base; row of teeth slightly concave, middle and inner teeth subequal in size, outer slightly larger; inner teeth curved outward (Fig. 3G). IO 0.98–1.02, MO 0.98–1.00. Paraligula bifid, 36–47 µm long, inner tooth 29–36 µm long. Pecten hypopharyngis with 14–15 subequal teeth, corner tooth and middle teeth slightly broader than remainder (Fig. 3H).

Body (Fig. 3I). Without fringe of swim-setae. Procercus 153–182 µm long, 54–71 µm wide, with 6 anal setae 680–760 µm long. L/W 2.56–2.83. Anal tubules slender, 311–341 µm long. Posterior parapod 671–695 µm long. Claws simple (Fig. 3I), some with small spines on inner and/or outer margin.

Systematics. In their comprehensive analyses of the Chironomidae subfamily Tanypodinae, Silva and Ekrem (2016) considered morphological characters across all life stages for all nine tribes within the subfamily, involving 54 genera and 115 species. In their study, Silva and Ekrem suggested that *Paramerina* Fittkau, *Reomyia* Roback and *Schineriella* Murray & Fittkau should be subgenera in *Zavrelimyia*. In addition,

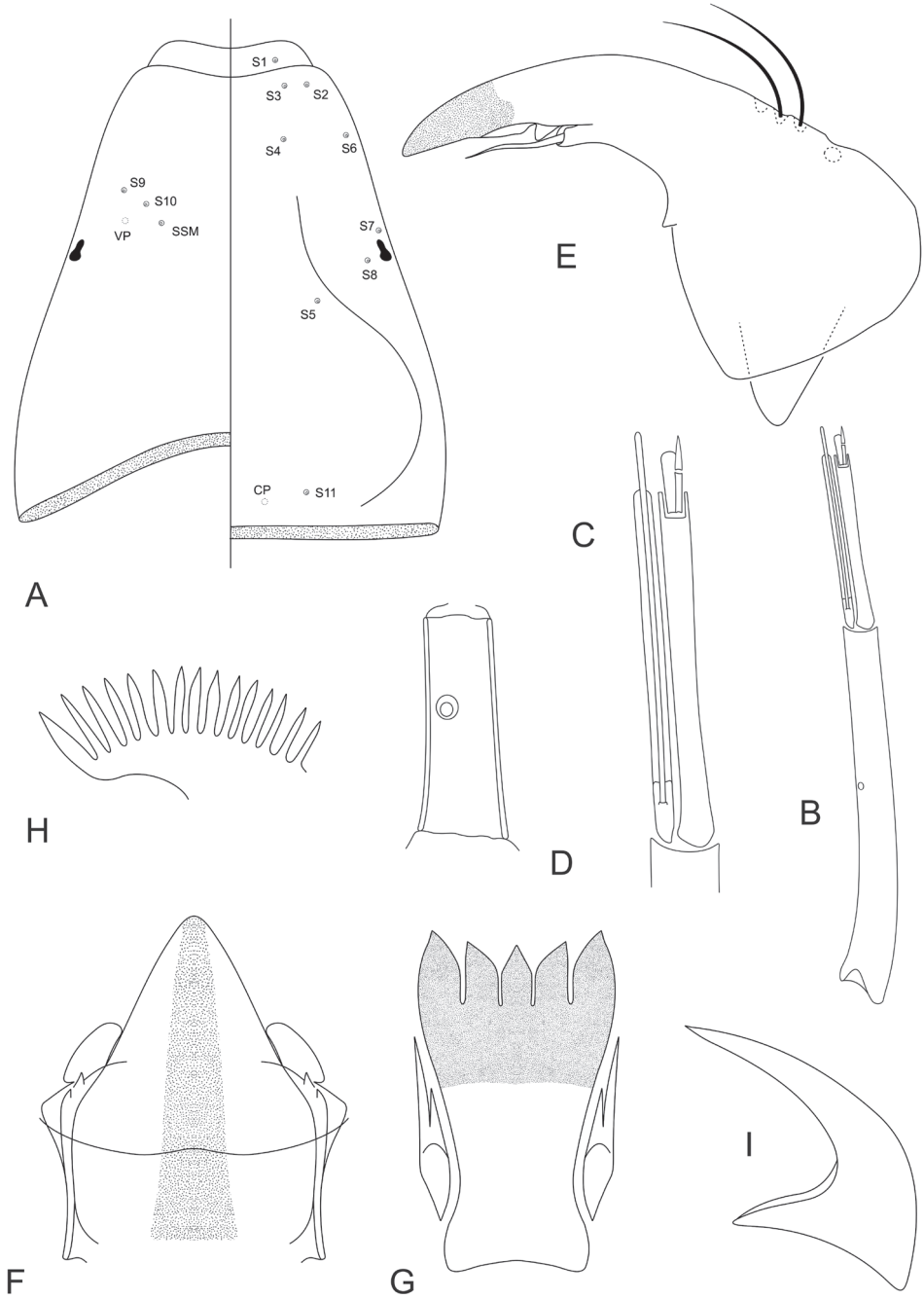

Figure 3. *Pentaneurella katterjokki* Fittkau & Murray, larva. **A** Head with chaetotaxy. Left: ventral aspect, right: dorsal aspect **B** antenna **C** apex of antenna **D** maxillary palp **E** mandible **F** mentum and M-appendage **G** ligula and paraligula **H** pecten hypopharyngis **I** simple claw of posterior parapod.

Pentaneurella was recovered as sister to *Trissopelopia* Kieffer in both analyses of equally weighted characters and by using implied weights. However, in an ongoing phylogenetic study of the subfamily Tanypodinae, which includes morphological evidence from modern and fossil chironomids (Silva and Baranov unpub. data), *Pentaneurella* turned out to be more closely related to the subgenera *Reomyia*, *Schineriella* and *Zavrelimyia*, within *Zavrelimyia* sensu Silva and Ekrem (2016), than to *Trissopelopia*, although with low support.

The male of *Pentaneurella* is morphologically similar to *Larsia* Fittkau, *Pentaneura* Philippi, *Trissopelopia*, and *Zavrelimyia* Fittkau. The bases of the lyrate tibial spurs are similar to the ones of *Larsia* and *Pentaneura*, and the absence of setae on tergite IX resembles *Trissopelopia* (Murray and Fittkau 1989). Nonetheless, *Pentaneurella* differs from *Larsia* in the presence of a distinctively notched, membranous anal point, while the presence of a distinct scutal tubercle separates adults of *Pentaneurella* from both *Trissopelopia* and *Pentaneura*. Moreover, *Pentaneurella* appears to be similar to *Zavrelimyia* sensu lato, only differing from the latter by having a scutal tubercle.

Regarding the immature stages, the pupa of *Pentaneurella* shows certain similarities to *Krenopelopia* Fittkau and *Monopelopia* Fittkau (Fittkau and Murray 1986). *Monopelopia* was recovered by Silva and Ekrem (2016) as sister to *Nilotanypus* Kieffer, and these two taxa as sister to *Monopelopia* (*Cantopelopia*) Roback. The presence of a basal lobe and thoracic comb, and anal macrosetae with adhesive sheaths, however, may be used to distinguish *Pentaneurella* from *Krenopelopia* and *Monopelopia* (Fittkau and Murray 1986). Larvae of *Pentaneurella* and *Krenopelopia* differ from *Pentaneura* and *Trissopelopia* by possessing a large peg sensilla which is firmly fused with the margin of antennal segment 2, forming a tuning-fork-like process. In both *Pentaneurella* and *Krenopelopia* the ligula has a lower middle tooth and inner teeth are curved outward. The absence of a dorsal pore, however, separates *Pentaneurella* from this genus (Cranston and Epler 2013). In addition, larvae of *Pentaneurella* appear to have cephalic setation and fork-like Lauterborn organs similar to those of *Zavrelimyia* sensu lato.

Remarks on distribution and ecology. In the Palaearctic, the subfamily Tanypodinae is represented by 29 genera, of which *Anatopynia*, Johannsen, *Telmatopelopia* Fittkau and *Pentaneurella* currently are unique to the region. The latter is a relatively common genus of non-biting midges initially recorded from northern Scandinavia. Currently, the genus has been recorded in Finland (Paasivirta 2014), France (Brown et al. 2007, Moubayed-Breil et al. 2012), Germany (Stur and Wiedenbrug 2006), Norway (Fittkau and Murray 1983), Russia (Ashe and O'Connor 2009), Slovakia (Šporka 2003), Spain (Hjorth-Andersen 2002), Sweden (Fittkau and Murray 1983, Bylén and Ronny-Larsson 1994), Switzerland (Lods-Crozet 1998) and Turkey (Özkan 2006, Kazanci et al. 2008). Herein, we record *Pentaneurella* from Central Norway. Several specimens were collected in the Rondane National Park, located in typical high mountain area, with large plateaus and several lentic and lotic systems.

Little is known about the ecology of *Pentaneurella*. Immature stages seem to be cold stenothermic rheophiles and krenophiles. Larvae of *Pentaneurella* have been recorded inhabiting springs and spring-fed streams in Sweden and the Bavarian Alps

as well as mountain streams in northern and Central Norway (Fittkau and Murray 1983, Stur and Wiedenbrug 2006, own data). Moubayed-Breil et al. (2012) found *Pentaneurella* in low and middle mountain streams located in the eastern Pyrenees and Corsica, while Bylén and Ronny-Larsson (1994) recorded larvae of *Pentaneurella* being parasitized by the microsporidium *Pernicivesicula gracilis* Bylén & Ronny-Larsson, in a sample of midge larvae collected from a small river in southern Sweden. Furthermore, larvae of *Pentaneurella* were also recorded from a sand bed stream from insular Turkey (Özkan 2006).

Acknowledgements

Thanks to the team at the Canadian Centre for DNA Barcoding for help with DNA barcode analysis. We would also like to thank Martin Spies, Torbjørn Ekrem, Karstein Hårsaker and Markus Majaneva for supplying us with the material examined in this study. Thanks to Torbjørn Ekrem for comments on the manuscript. F.L. Silva was supported by fellowships from the Coordination for the Improvement of Higher Education Personnel (CAPES - 2014/9239-13-8) and São Paulo Research Foundation (FAPESP - 2016/07039-8). We are indebted to the reviewers for their valuable comments on the manuscript. DNA barcode data in this publication were generated in collaboration with the Norwegian Barcode of Life Network (NorBOL) funded by the Research Council of Norway and the Norwegian Biodiversity Information Centre.

References

Ashe P, O'Connor JP (2009) A World Catalogue of Chironomidae (Diptera). Part 1. Buchonomyiinae, Chilenomyiinae, Podonominae, Aphroteniinae, Tanypodinae, Usambaromyiinae, Diamesinae, Prodiamesinae and Telmatogetoninae. Irish Biogeographical Society & National Museum of Ireland, Dublin, 445 pp.

Brown LE, Milner AM, Hannah DM (2007) Groundwater influence on alpine stream ecosystems. Freshwater Biology 52: 878–890. https://doi.org/10.1111/j.1365-2427.2007.01739.x

Bylén EKC, Ronny-Larsson JI (1994) Ultrastructural study and description of *Pernicivesicula gracilis* gen. et sp. nov. (Microspora, Pereziidae), a rod-shaped microsporidium of midge larvae, *Pentaneurella* sp. (Diptera, Chironomidae), in Sweden. European Journal of Protistology 30: 139–150. https://doi.org/10.1016/S0932-4739(11)80024-6

Cranston PS, Epler JH (2013) The larvae of Tanypodinae (Diptera: Chironomidae) of the Holarctic Region – Keys and diagnoses. In: Andersen T, Cranston PS, Epler JH (Eds) The larvae of Chironomidae (Diptera) of the Holarctic Region – Keys and diagnoses. Insect Systematics and Evolution Supplement 66: 39–136.

Edwards FW (1929) British non-biting midges (Diptera, Chironomidae). Transactions of the Entomological Society of London 77: 279–430. https://doi.org/10.1111/j.1365-2311.1929.tb00692.x

Epler JH (1988) Biosystematics of the genus *Dicrotendipes* Kieffer, 1913 (Diptera: Chironomidae: Chironominae) of the world. Memoirs of the American Entomological Society 36: 1–214.

Fittkau EJ (1962) Die Tanypodinae (Diptera: Chironomidae). Die Tribus Anatopyniini, Macropelopiini und Pentaneurini. Abhandlungen zur Larvalsystematik der Insekten 6: 1–453.

Fittkau EJ, Murray DA (1983) *Pentaneurella katterjokki*, eine neue Gattung und Art der Tanypodinae (Diptera, Chironomidae). Nachrichtenblatt der Bayerischen Entomologen 32: 57–63.

Fittkau EJ, Murray DA (1986) The pupae of Tanypodinae (Diptera: Chironomidae) of the Holarctic Region – Keys and Diagnoses. In: Wiederholm T (Ed.) The adult males of Chironomidae (Diptera) of the Holarctic region – Keys and diagnoses. Entomologica scandinavica, Supplement 28: 31–113.

Freeman P (1955) A study of African Chironomidae, Part I. Bulletin of the British Museum (Natural History) Entomology 4: 1–67.

Freeman P (1956) A study of African Chironomidae, Part II. Bulletin of the British Museum (Natural History) Entomology 4: 287–368.

Hjorth-Andersen MCT (2002) Catálogo de los Diptera de España, Portugal y Andorra (Insecta). Monografías S.E.A, Zaragosa, 323 pp.

Kazanci N, Dügel M, Girgin S (2008) Determination of indicator genera of benthic macroinvertebrate communities in running waters in western Turkey. Review of Hydrobiology 1: 1–16.

Kowalyk HE (1985) The larval cephalic setae in the Tanypodinae (Diptera: Chironomidae) and their importance in generic determinations. Canadian Entomologist 117: 67–106. https://doi.org/10.4039/Ent11767-1

Lods-Crozet B (1998) Chironomidae. In: Merz B, Bächli G, Haenni, JP, Gonseth Y (Eds) Diptera – Check-list. Fauna Helvetica 1: 92–101.

Moubayed-Breil J, Langton PH, Ashe P (2012) *Rheotanytarsus dactylophoreus*, a new mountain species from streams in the Eastern Pyrenees and Corsica (Diptera: Chironomidae). Fauna Norvegica 31: 167–173. https://doi.org/10.5324/fn.v31i0.1375

Murray DA, Fittkau EJ (1989) The adult males of Tanypodinae (Diptera: Chironomidae) of the Holarctic Region – Keys and Diagnoses. In: Wiederholm T (Ed.) The adult males of Chironomidae (Diptera) of the Holarctic region – Keys and diagnoses. Entomologica scandinavica, Supplement 34: 37–124.

Özkan N (2006) The Larval Chironomidae (Diptera) Fauna of Gökçeada (Imbroz). Gazi University Journal of Science 19: 69–75.

Paasivirta L (2014) Checklist of the family Chironomidae (Diptera) of Finland. Zookeys 441: 63–90. https://doi.org/10.3897/zookeys.441.7461

Roback SS (1971) The adults of the subfamily Tanypodinae (=Pelopiinae) in North America (Diptera: Chironomidae). Monograph of the Academy of Natural Sciences of Philadelphia 17: 1–410.

Silva FL, Fonseca-Gessner A, Ekrem T (2011) Revision of *Labrundinia maculata* Roback, 1971, a new junior synonym of *L. longipalpis* (Goetghebuer, 1921) (Diptera: Chironomidae: Tanypodinae). Aquatic Insects 33: 293–303. https://doi.org/10.1080/01650424.2011.640434

Silva FL, Fonseca-Gessner AA, Ekrem T (2014) A taxonomic revision of genus *Labrundinia* Fittkau, 1962 (Diptera: Chironomidae: Tanypodinae). Zootaxa 3769: 1–185. https://doi.org/10.11646/zootaxa.3769.1.1

Silva FL, Ekrem T (2016) Phylogenetic relationships of nonbiting midges in the subfamily Tanypodinae (Diptera: Chironomidae) inferred from morphology. Systematic Entomology 41: 73–92. https://doi.org/10.1111/syen.12141

Šporka F (2003) Vodné bezstavovce (makroevertebráta) Slovenska, súpis druhov a autekologické charakteristiky. Slovenský hydrometeorologický ústav, Bratislava, 590 pp.

Stur E, Wiedenbrug S (2006) Familie Zuckmücken (Chironomidae) In: Gerecke R, Franz H (Eds) Quellen im Nationalpark Berchtesgaden. Lebensgemeinschaften als Indikatoren des Klimawandels. Forschungsbericht 51: 183–194.

Sæther OA (1980) Glossary of Chironomid morphology terminology (Diptera: Chironomidae). Entomologica scandinavica, Supplement 14: 1–51.

Sæther OA, Spies M (2013) Fauna Europaea: Chironomidae. In: de Jong H, Pape T (Eds) Fauna Europaea: Diptera: Nematocera. Fauna Europaea version 2017.06. http://www.faunaeur.org/

ZooKeys 833: 121–132 (2019)
doi: 10.3897/zookeys.833.32413
http://zookeys.pensoft.net

RESEARCH ARTICLE

A peer-reviewed open-access journal
ZooKeys
Launched to accelerate biodiversity research

A new species of the millipede genus *Cryptocorypha* Attems, 1907, from northern Thailand (Polydesmida, Pyrgodesmidae)

Natdanai Likhitrakarn[1], Sergei I. Golovatch[2], Ruttapon Srisonchai[3], Chirasak Sutcharit[3], Somsak Panha[3]

1 *Division of Plant Protection, Faculty of Agricultural Production, Maejo University, Chiang Mai 50290, Thailand* **2** *A.N. Severtsov Institute for Problems of Ecology and Evolution, Russian Academy of Sciences, Leninsky pr. 33, Moscow 119071, Russia* **3** *Animal Systematics Research Unit, Department of Biology, Faculty of Science, Chulalongkorn University, Bangkok, 10330, Thailand*

Corresponding author: *Somsak Panha* (somsak.pan@chula.ac.th); *Sergei I. Golovatch* (sgolovatch@yandex.ru)

Academic editor: *Robert Mesibov* | Received 14 December 2018 | Accepted 22 January 2019 | Published 1 April 2019

http://zoobank.org/DAC73643-A75B-4F6B-8C93-17AFA890D5F8

Citation: Likhitrakarn N, Golovatch SI, Srisonchai R, Sutcharit C, Panha S (2019) A new species of the millipede genus *Cryptocorypha* Attems, 1907, from northern Thailand (Polydesmida: Polydesmida: Pyrgodesmidae) ZooKeys 833: 121–132. https://doi.org/10.3897/zookeys.833.32413

Abstract

The millipede family Pyrgodesmidae and the genus *Cryptocorypha* are recorded from Thailand for the first time, being represented there by *C. enghoffi* **sp. n.** The new species is distinguished by the evident apicodorsal trichostele on the last tibia of both sexes and the gonopodal telopodite being particularly complex, quadripartite, consisting of the longest, mesal, suberect solenomere branch; a slightly shorter, similarly slender, acuminate endomere branch tightly appressed to the solenomere; a somewhat shorter, caudal, strongly curved, armed exomere process; and a very distinct, low, lateral, sac-shaped velum at their base. This situation strongly resembles the one observed in the geographically closest *C. perplexa* Golovatch & VandenSpiegel, 2015, from Myanmar, but the shapes and armament of all outgrowths of the gonopodal telopodite are clearly different. A key to all three *Cryptocorypha* pecies known from Indochina or Myanmar and an updated checklist of all 21 species of the genus are provided.

Keywords

Chiang Mai, Diplopoda, Henrik Enghoff, Huai Hong Khrai Royal Development Study Centre

Copyright *Natdanai Likhitrakarn et al.* This is an open access article distributed under the terms of the Creative Commons Attribution License (CC BY 4.0), which permits unrestricted use, distribution, and reproduction in any medium, provided the original author and source are credited.

Introduction

The genus *Cryptocorypha* Attems, 1907, is one of the few relatively speciose genera of the mainly tropical millipede family Pyrgodesmidae which is among the largest in the entire class Diplopoda. The family Pyrgodesmidae currently comprises more than 170 genera and nearly 400 species (Minelli 2015, Golovatch et al. 2017). *Cryptocorypha* has recently been reviewed, rediagnosed (Golovatch et al. 2011b, 2013, 2017, Golovatch and VandenSpiegel 2015), and shown to encompass 20 species ranging from central and eastern tropical Africa, through India, Sri Lanka and Myanmar, to East Asia, southern China, Indochina, western Indonesia, and even Melanesia (Table 1).

Most of the congeners tend to show very narrow distributions, with only a single species, *C. ornata* (Attems, 1938), being extremely widespread on tropical islands and archipelagos in the Indian and Pacific oceans, apparently due to anthropo- and/or ornithochory (Minelli 2015, Golovatch et al. 2017).

The present paper puts on record a new species of this genus, the first to be found in Thailand. An updated checklist of all 21 species of *Cryptocorypha* known to date and a key to all three congeners from Indochina or Myanmar are also provided.

Materials and methods

The specimens were hand-collected from Huai Hong Khrai Royal Development Study Centre during the rainy season (during the months of April to October in 2015 and 2016). Live animals were photographed in their habitats and then taken for photography in the laboratory using a Canon 70D digital camera with a Canon EF-S 60mm f/2.8 Macro USM lens. After that, the specimens were preserved in 75% ethanol. The morphological characters were studied in the laboratory using uncleaned specimens and an Olympus stereo microscope. The terminology used follows that accepted in the most recent publications (Golovatch et al. 2011b, 2013, 2017, Golovatch and VandenSpiegel 2015). Scanning electron micrographs (SEM) were taken with a JEOL, JSM–5410 LV microscope with gold coating, and the material returned from stubs to alcohol after examination. Images of the holotype habitus were taken in the laboratory and assembled using the "CellD" automontage software of the Olympus Soft Imaging Solution package and the gonopods of a paratype were dissected and illustrated under Euromex iScope microscopes. The holotype and most of the paratypes are housed in the Museum of Zoology, Chulalongkorn University (CUMZ), Bangkok, Thailand. A few paratypes have also been donated to the collections of the Zoological Museum, State University of Moscow, Russia (ZMUM), Natural History Museum of Denmark, University of Copenhagen, Denmark (ZMUC), Naturhistorisches Museum Wien, Austria (NHMW), and Natural History Museum, London, Great Britain (NHML), as indicated in the text.

The Animal Care and Use Protocol Review No. 1723018 was applied.

Table 1. Described *Cryptocorypha* arranged in alphabetic order and supplied with geographical details.

No.	Species	Locality or localities
1	*C. areata* (Carl, 1932)	India, Upper Palnis, Kodaikanal and environs, 2,200 m; Maryian-shola, 2,300 m; Kukkal-shola, 1,900 m; near Pumberai, 1,900 m; Lower Palnis, Thandikudi, 1,500 m; Travancore, between Palni and Anaimala Hills, 1,850 m (Carl 1932)
2	*C. bocal* Golovatch, Nzoko Fiemapong & VandenSpiegel, 2017	Congo D.R., South Kivu Province, Itombwe, Uvira District, road-km 10 from Katobo to Kahololo, 03°12'S, 28°51'E, 2,400–2,800 m (Golovatch et al. 2017)
3	*C. chernovi* Golovatch, Geoffroy & VandenSpiegel, 2013	Vanuatu, Espiritu Santo Island, Rotal, near Rotal hole, 15°15'10.1"S 167°03'30.5"E, 250 m; Boutmas, near the entrance to Fapon Cave, 15°19'51.7"S 166°57'53.6"E, 380 m; Malo Island off Espiritu Santo, Avorani, 15°42'22.1"S 167°07'43.5"E, 110 m (Golovatch et al. 2013)
4	*C. diffusa* (Brolemann, 1920)	East Africa, Mt. Kilimanjaro, a small series near a forest, 2,700–2,800 m (Brolemann 1920); Kenya, Taita Hills, Mbololo Forest, 03°19'S, 38°27'E, 1,800–1,900 m; Yale Forest, 03°39'S, 38°33'E; Fururu Forest, 03°26'S, 38°20'E; Ngangao Forest, 03°22'S, 38°21'E; Saga Forest, 03°50'S, 38°58'E; Mwachora Forest, 03°24'S, 38°22'E (Golovatch and VandenSpiegel 2014); Mission Zoolg. I.R.S.A.C en Afrique Orientale, Tanganyika terr. (= Tanzania), Ngorongoro, Bocagere Region, 2,300 m; Mt. Oldeani versant Est, mountain forest with *Bambusa*, 2,350–1,950 m; mountain forest, 1,880–1,950 m; Mt. Oldeani versant N.O, etrepage sous *Hagenia*, 2,600 m (Golovatch et al. 2017)
5	*C. dimorpha* Golovatch, Nzoko Fiemapong & VandenSpiegel, 2017	Congo D.R., Kivu, Maniema Province, Mwenga, 03°03'S, 28°26'E (Golovatch et al. 2017)
6	*C. enghoffi* sp. n.	Thailand, Chiang Mai Province, Doi Saket District, Huai Hong Khrai Royal Development Study Centre, 18°52'47"N, 99°13'22"E, 445 m
7	*C. hoffmani* Golovatch, Semenyuk, VandenSpiegel & Anichkin, 2011	Vietnam, Dong nai Province, Nam Cat Tien National Park, ca. 150 m (Golovatch et al. 2011a, 2011b)
8	*C. japonica* (Miyosi, 1957)	Japan, Tokyo, Futako Tamagawa (Miyosi 1957)
9	*C. kandyana* (Carl, 1932)	Sri Lanka (Ceylon), Kandy (Carl 1932)
10	*C. kumamotensis* (Murakami, 1966)	Japan, Ehime Prefecture, Niihama, Oshima; Iyo-Mishima, Kinsha (Murakami 1966)
11	*C. leia* Chamberlin, 1945	Indonesia, Java, Goenong Malabar, 1,600 m (Chamberlin 1945)
12	*C. leleupi* Golovatch, Nzoko Fiemapong & VandenSpiegel, 2017	Congo D.R., South Kivu Province, Itombwe, Uvira District, road-km 10 from Katobo to Kahololo, 03°12'S, 28°51'E, 2,800 m (Golovatch et al. 2017)
13	*C. monomorpha* Golovatch, Nzoko Fiemapong & VandenSpiegel, 2017	Congo D.R., Kivu, Dorsale de Lubero, Mt Muleke, versant Sud, village Itala, 00°17'S, 29°15'E, 1,820 m (Golovatch et al. 2017)
14	*C. nympha* Loksa, 1967	Republic of the Congo (Congo-Brazzaville), ORSTOM-Park (Loksa 1967)
15	*C. ornata* (Attems, 1938)	Nearly pantropical anthropo- and/or ornithochore species (Adis et al. 1998; Golovatch et al. 2017). Hawaiis (Attems 1938, 1940); Saint Helena Island (Hoffman 1977); Cook Islands; Marquesas Islands; Tahiti Island; Hong Kong (Adis et al. 1998); Taiwan (Golovatch et al. 2011a)

The geographical coordinates and elevation were recorded by means of a Garmin GPSMAP 60 CSx using the WGS84 datum and subsequently double-checked with Google Earth.

Taxonomic part

Family Pyrgodesmidae Silvestri, 1896

Genus *Cryptocorypha* Attems, 1907

Diagnosis. The genus is characterized within Pyrgodesmidae by an unusually flat body with 19 or 20 segments (either in both sexes or 19 solely in the male) and only a slightly convex dorsum, coupled with 6+6 faint lobulations or 11 radii at a regularly rounded anterior margin of a flabellate collum that fully covers the head from above; usually three or four (rarely five) more distinct lobulations at the lateral margins of poreless and pore-bearing paraterga, respectively; a normal pore formula (5, 7, 9, 10, 12, 13, 15–18(19)) with the ozopores not borne on porosteles, but opening flush on the dorsal surface at the base of the penultimate lobulation; the absence of anterior and the presence of only very few (1–2) caudal lobulations; the development of 2–3 transverse, often irregular rows of small and non-differentiated knobs/tuberculations on each postcollum metatergum; and a dorsally fully exposed epiproct. The last tibia in the male or even in both sexes is often, but not always, with a conspicuous, long, setigerous, apicodorsal cylinder (= trichostele). The gonopods are with relatively small coxae and a shallow gonocoel that leaves the telopodites very strongly exposed and in situ held (sub)parallel to each other; each telopodite is 2-, 3- or 4-partite, with a strongly developed, slender, often fimbriate, mesal solenomere branch (usually the longest) and a typically sac-shaped velum at its base, sometimes also with 1–2 adjacent processes (exo- and/or endomere, depending on position) (Golovatch et al. 2017).

Cryptocorypha enghoffi sp. n.

http://zoobank.org/D2E1D3D0-3968-41B0-AD60-7D610F34F832
Figs 1–4

Holotype. ♂ (CUMZ), Thailand, Chiang Mai Province, Doi Saket District, Huai Hong Khrai Royal Development Study Centre, 445 m a.s.l., 18°52'47"N, 99°13'22"E, 06/05/2015, leg. N. Likhitrakarn. **Paratypes.** 2 ♂, 3 ♀, 1 subadult (19 segments), 1 juvenile (18 segments) (CUMZ), 1 ♂, 1 ♀ (ZMUM), same locality, together with holotype. 1 ♂, 1 ♀, 2 subadult (19 segments) (CUMZ), 1 ♂, 1 ♀ (ZMUC), 1 ♂, 1 ♀ (NHMW), 1 ♂, 1 ♀ (NHML), same locality, 09/06/2016, leg. N. Likhitrakarn.

Name. Honours Henrik Enghoff, a globally renowned specialist in Diplopoda and one of the pioneers of diplopodological research in Thailand.

Diagnosis. Differs from other species of the genus by the presence of 20 body segments in both sexes, coupled with an evident apicodorsal trichostele on the last tibia of both sexes (Fig. 4F) and in the gonopod structure being particularly complex, similar to that of *C. perplexa* Golovatch & VandenSpiegel, 2015, but differs clearly in the shapes and armament of all four main outgrowths of the telopodite (Fig. 4A–D).

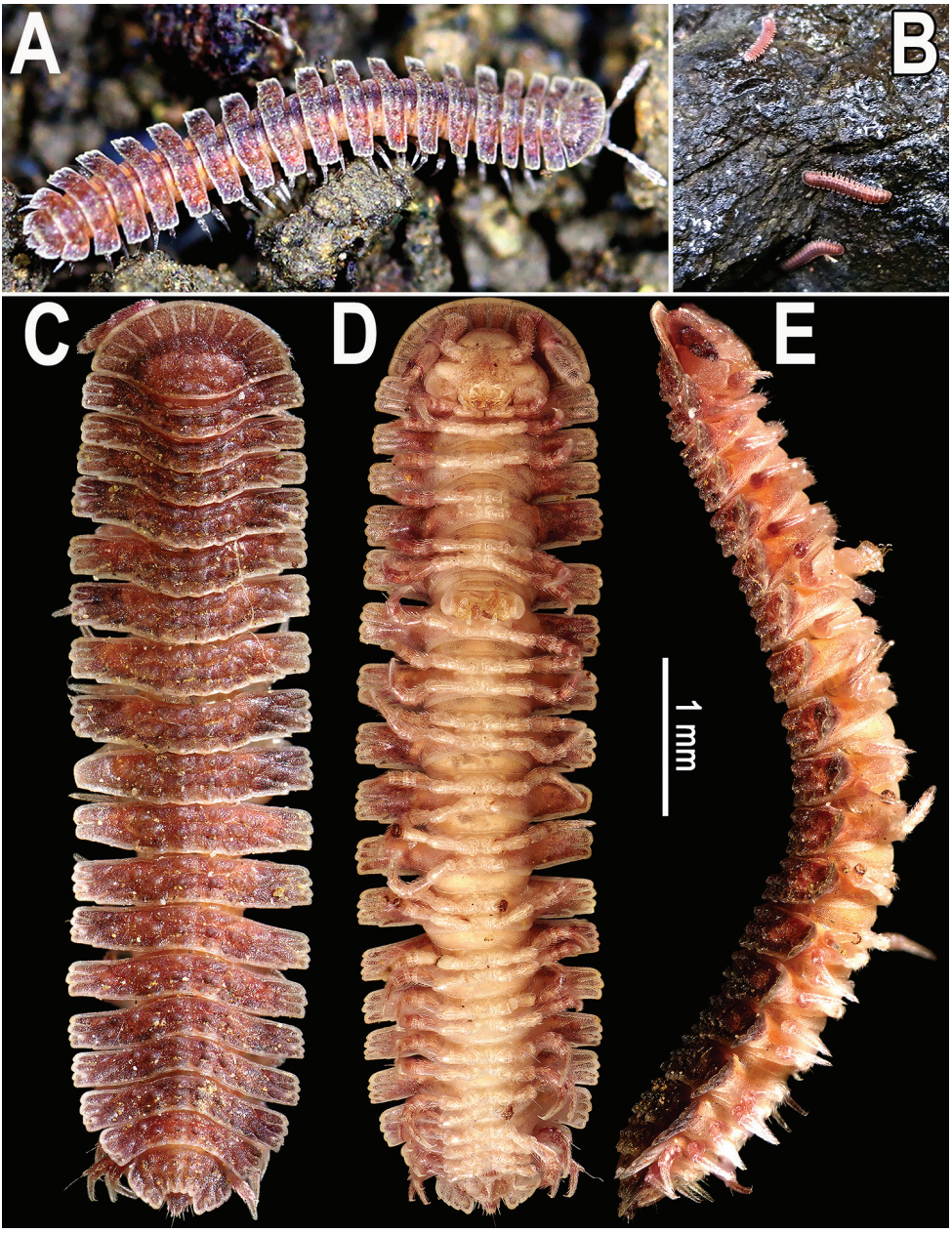

Figure 1. *Cryptocorypha enghoffi* sp. n., **A** ♀ paratype **B** a few paratypes **C, D** holotype **A, B** habitus, live coloration in their habitat **C–E** habitus and coloration in alcohol, dorsal, ventral and lateral views, respectively.

Description. Length ca. 12.1 mm, width of midbody segments 2.95 and 1.55 mm on pro- and metazonae, respectively (holotype). Length of adults ca. 11.5–12.8 mm (♂ paratypes) and 14.5–15.2 mm (♀ paratypes), width of midbody pro- and meta-

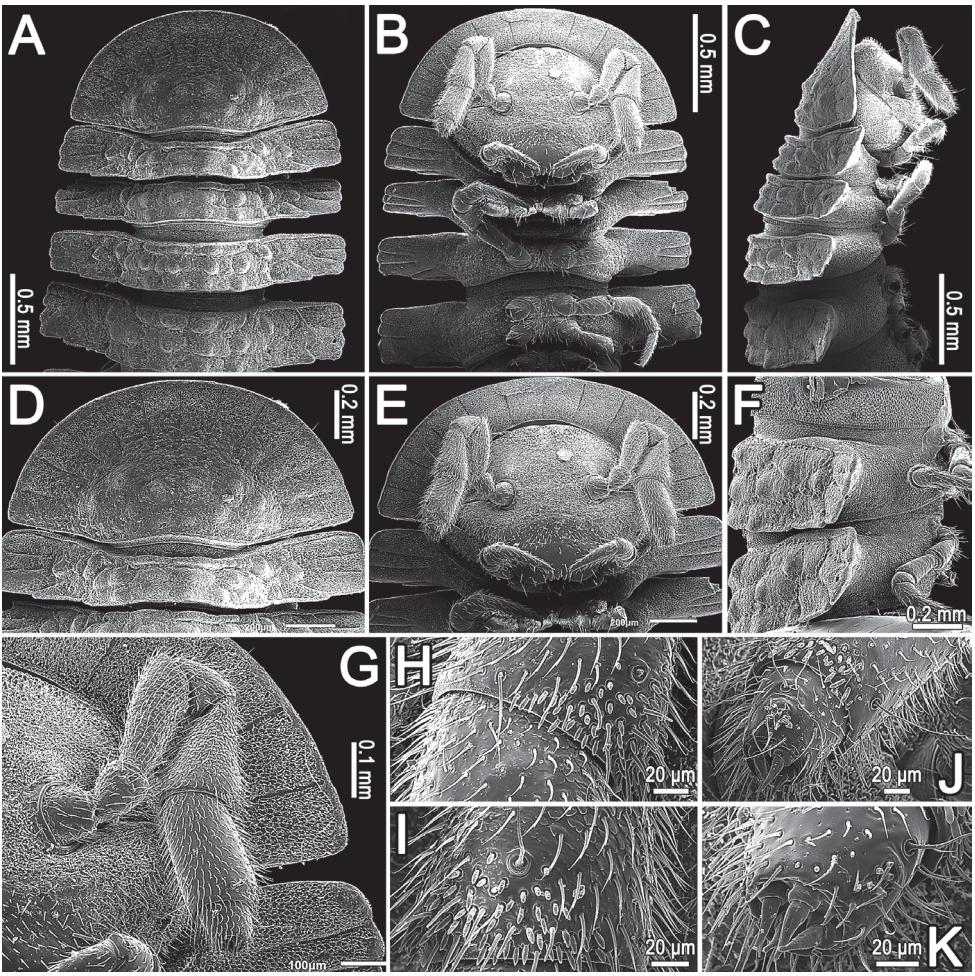

Figure 2. *Cryptocorypha enghoffi* sp. n., ♂ paratype. **A–C** anterior part of body, dorsal, ventral and lateral views, respectively **D** collum, dorsal view **E** head, ventral view **F** segments 8, 9, lateral view **G** antenna, ventral view **H–K** right antenna **H** bacilliform sensilla on antennomere 5, sublateral view **J, I** bacilliform sensilla on antennomere 6, subventral and sublateral views, respectively **K** tip of right antenna, sublateral view.

zonae 0.8–1.2 and 2.2–2.6 mm (♂ paratypes) or 1.2–1.8 and 2.8–3.4 mm (♀ paratypes), respectively.

Coloration of live animals uniformly reddish to purplish red (Fig. 1A, B), antennae, legs, and venter mainly lighter, yellowish to reddish (Fig. 1A); coloration in alcohol, after three years of preservation, faded to reddish (Fig. 1C–E) or light brown, antennae and legs light red to light brown, while venter yellowish to nearly pallid (Fig. 1D, E).

Body robust, with 20 segments (♂, ♀). Pro- to metazonum width ratio close to 1:2. In width, head << collum < segment 3 = 4 < 2 < 5 < 6–14(15) (♂, ♀), thereafter

body rapidly tapering towards telson (Figs 1C, D, 3G, H). Head subovoid (Fig. 2B, C, E), slightly transverse, densely setose in clypeolabral region, micropapillate; epicranial suture superficial. Interantennal isthmus approximately twice as large as either diameter of antennal socket or antennomere 1 (Fig. 2B, E).

Antennae short and clavate (Figs 1A, D, 2B, C, E, G), in situ reaching body segment 3 (♂, ♀) when stretched laterally or ventrolaterally; in length, antennomere 1 < 2 < 4 <7 < 3 < 5 < 6; antennomeres 5–7 each with a more or less compact apicodorsal group of bacilliform sensilla (Fig. 2G–K).

Collum flabellate (Figs 1A, C, 2A–E), completely covering the head from above, anterior margin regularly rounded, with 11 equal, long and evident radii (Figs 1C, 2A); middle and caudal parts with two transverse, arched, rather faint rows of low bosses (Figs 1C, 2A, C, D). Paraterga set at approximately upper 1/3 (♂, ♀) of body height, subhorizontal to faintly declivous (♂, ♀) (Figs 1E, 2C). Dorsum moderately convex, its outline smoothly extending onto paraterga (Fig. 2C).

Tegument encrusted with a microspiculate cerotegument, dull, beset with microvilli (Figs 2A, C, D, F, 3A, C–G, I, J). Prozonae and strictures between pro- and metazonae very delicately microgranulate, also beset with microvilli (Fig. 3F), conforming to the pattern observed in *C. ornata* and several other genera and species of Pyrgodesmidae (cf. Akkari and Enghoff 2011). Metaterga with three transverse rows of non-differentiated tuberculations and distinct rows of usually transversely oblong, polygonal to rounded, low bosses (Figs 2A, 3A, J), except for collum and segments 2–4 showing two transverse rows of such tuberculations (Fig. 2A, D), each of the latter typically surmounted by minute, setigerous, spherical knobs (Fig. 3D). Paraterga areolate-rugose, beset with microvilli arranged in a polygonal alveolate pattern (Fig. 3E; see also Akkari and Enghoff 2011 for comparison). Tergal setae mostly abraded, retained ones inconspicuous and very short.

Postcollum paraterga very broad, thin and slightly, but clearly lobulate laterally (Figs 1A, C, 2A, B, 3A, B, D, G, H, J), with three lobulations in all poreless segments, four lobulations in all pore-bearing ones, all also delimited by very long, rather evident radii both dorsally and ventrally; anterior marginals absent, but two caudal marginals evident.

Pore formula normal: 5, 7, 9, 10, 12, 13, 15–19, ozopores being very small, round, discernible dorsally at base of 3rd lobulation (Figs 2A, F, 3A, D, E, G, J).

Limbus microspiculate, each caudal crenulation being very finely and sharply spinulose (Fig. 3F).

Epiproct readily visible from above, not hidden under 19th segment (Figs 1A, 3G, J), with four strong setae on top (Fig. 3K).

Hypoproct subtriangular, caudal edge with 1+1 strong and widely separated setae on evident knobs (Fig. 3K).

Sterna wide, approximately twice as broad as diameter of coxal socket (Figs 1D, 2B, 3B, H, K), moderately setose, without modifications, superficially impressed along main axis. Epigynal ridge behind ♀ legs 2 low and inconspicuous. Gonopod aperture transversely oblong-oval, caudal and lateral margins thin and slightly elevated.

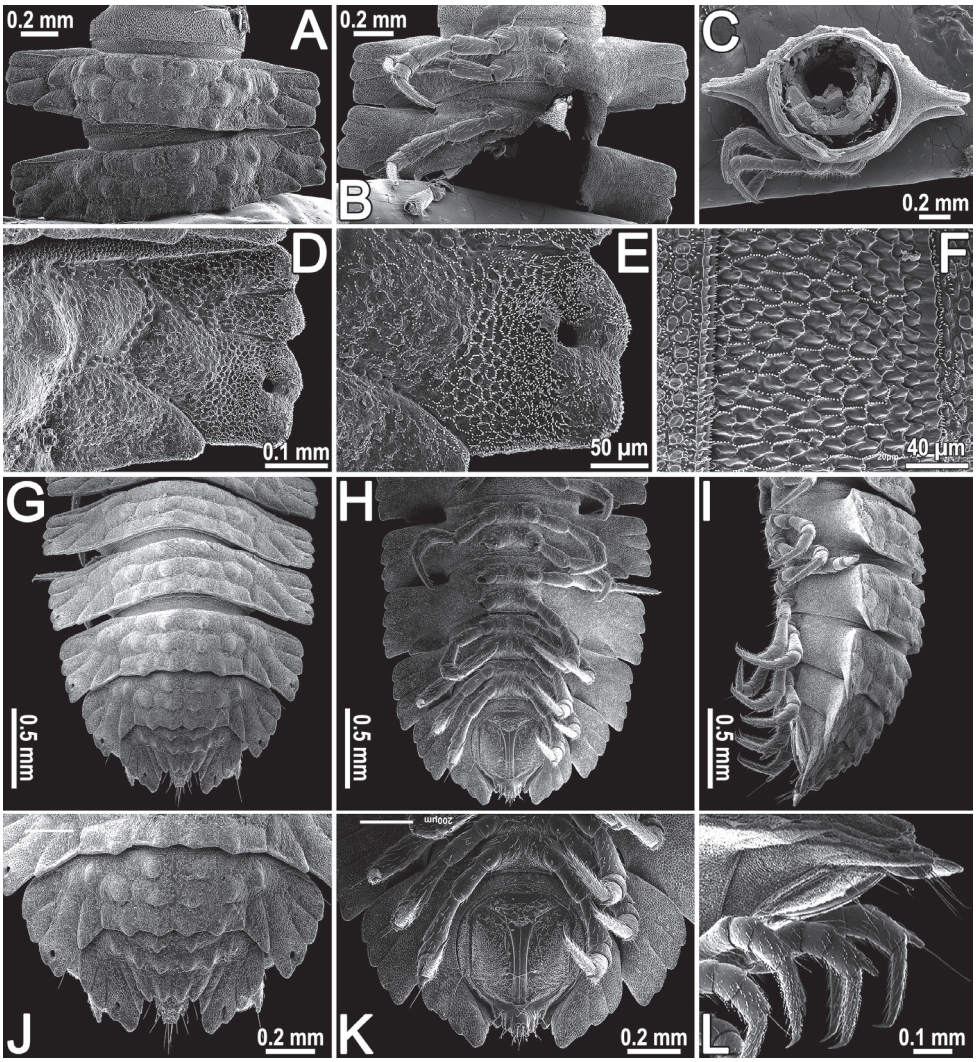

Figure 3. *Cryptocorypha enghoffi* sp. n., ♂ paratype. **A**, **B** segments 8, 9, dorsal and ventral views, respectively **C** cross-section of segment 8, caudal view **D** paraterga of segment 9, dorsal view **E** poriferous paratergum of segment 9 **F** tegument texture in the region of a stricture between pro- and metazonae, dorsal view **G–L** posterior part of body, dorsal, ventral, lateral, dorsal, ventral and lateral views, respectively.

Legs long and slender (Fig. 4E), longer than width of paraterga, densely setose, last tibiae with evident apicodorsal trichosteles in both sexes (Figs 3I, K, L, 4F); in length, tarsi > femora > prefemora >> tibiae > coxae > postfemora (♂, ♀), neither adenostyles nor tarsal brushes. Claws simple, slightly curved ventrad.

Gonopods (Fig. 4A–D) very complex, in situ held parallel to each other; coxite rather small, boat-shaped, gonocoel shallow, cannula simple. Each telopodite grossly

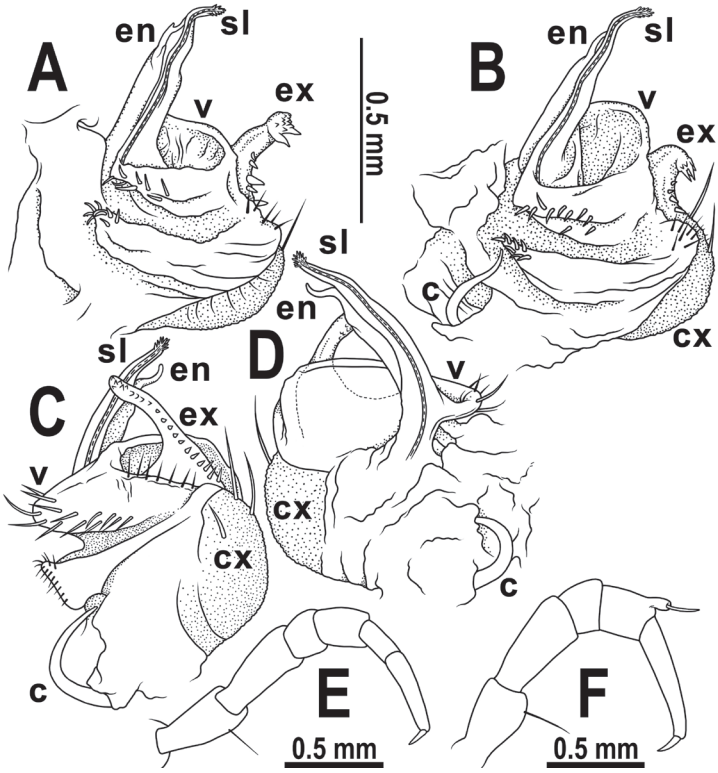

Figure 4. *Cryptocorypha enghoffi* sp. n., ♂ paratype. **A–D** left gonopod, sublateral, submesal, suboral, lateral and mesal views, respectively **E** midbody leg, lateral view **F** last leg, lateral view. Abbreviations: **c**, cannula **cx**, coxite **en**, endomere **ex**, exomere **sl**, solenomere **v**, velum.

quadripartite: (1) an evident, long, suberect, rod-shaped, apically unequally bifid and acuminate endomere tightly appressed to and starting at base of (2) the longest, suberect, rod-shaped, distally curved, apically conspicuously and densely fringed/fimbriate solenomere, followed first (3) by a sac-shaped, mesally irregularly membranous, low velum and then (4) by a conspicuous, long, clearly papillate/dentate, strongly curved, apically slightly clavate and rounded exomere .

Remarks. This new species was found walking on a rock surface (Fig. 1B). The air was very humid, this being characteristic of the rainy season. The specimens were found in the Dry Dipterocarp Forest at the Huai Hong Khrai Royal Development Study Centre. This study centre was established under the royal initiative in 1982 in the area of Khun Mae Kuang National Forest Reserve, Chiang Mai Province for conducting research and experimentation using appropriate progressive methods which suited the development needs of the Northern Region, especially the conservation of watersheds, reforestation and agricultural development. It covers approximately 8,500 rai (1,360 hectares).

Key to the species of *Cryptocorypha* currently known to occur in Indochina or Myanmar, chiefly based on ♂ characters

1 Body larger, 10–15.2 mm long. Gonopods complex, telopodite clearly quadripartite (Fig. 4A–D).....**2**

– Body smaller, 4.0–4.5 mm long. Gonopods simple, telopodite bipartite, with only an evident solenomere branch protruding above a hypertrophied sac-shaped velum (Golovatch et al. 2011b: figs 39–44). Vietnam..... ..... ***C. hoffmani***

2 Body smaller, 10–11 mm long, width of midbody metazonae 1.9–2.0 mm. Velum shorter and smaller, exomere suberect, nearly as long as endomere, with an evident stump-shaped outgrowth caudally at base (Golovatch and Vandenspiegel 2015: figs 3C–F, 4B–D). Myanmar .....***C. perplexa***

– Body larger, 11.5–15.2 mm long, width of midbody metazonae 2.2–3.4 mm. Velum a prominent sac, exomere strongly curved, clearly shorter than endomere, without an outgrowth at base (Fig. 4A–D). Northern Thailand..... .....***C. enghoffi* sp. n.**

Conclusions

The diplopod diversity in Thailand has hitherto been reported to total 228 species (Likhitrakarn et al. 2017, Srisonchai et al. 2018a, b, c, d, Pimvichai et al. 2018). Given that only a single species, *C. enghoffi* sp. n., of the very large micropolydesmid (= small-bodied) family Pyrgodesmidae has been reported from Thailand, there can be no doubt whatsoever that many more micropolydesmids, including those representing not only the Pyrgodesmidae, but also such taxonomically relatively poorly assessed families as Cryptodesmidae, Opisotretidae, Trichopolydesmidae, and Haplodesmidae still await discovery and description in Thailand and the adjacent countries of Southeast Asia.

Acknowledgements

This project was partly funded by grants received from the Office of the Royal Development Projects Board (RDPB), while most of the financial support was obtained from TRF Strategic Basic Research BDG 6080011 (2017–2019) to CS and NL, and TRF Senior Research Scholar RTA 5880002 (2015–2018) and BDC-PG2-161012 to SP. We thank the members of the Animal Systematics Research Unit for their technical assistance in the laboratory. We are most grateful to all reviewers who have provided constructive criticism and thus considerably improved our paper.

References

Adis J, Golovatch SI, Hoffman RL, Hales DF, Burrows FJ (1998) Morphological adaptations of the semiaquatic millipede *Aporodesminus wallacei* Silvestri 1904 with notes on the taxonomy, distribution, habitats and ecology of this and a related species (Pyrgodesmidae, Polydesmida, Diplopoda). Tropical Zoology 11: 371–387. https://doi.org/10.1080/03946975.1998.10539372

Akkari N, Enghoff H (2011) On some surface structures of potential taxonomic importance in families of the suborders Polydesmidea and Dalodesmidea (Polydesmida, Diplopoda). In: Mesibov R, Short M (Eds) Proceedings of the 15th International Congress of Myriapodology, 18–22 July 2011, Brisbane, Australia. ZooKeys 156: 1–24. https://doi.org/10.3897/zookeys.156.2134

Attems C (1907) Javanische Myriopoden, gesammelt von Direktor Dr. K. Kraepelin im Jahre 1903. Mitteilungen aus dem Naturhistorischen Museum in Hamburg 24: 77–142. https://biodiversitylibrary.org/page/10278476

Attems C (1938) Myriapoda 3, Polydesmoidea II. Fam. Leptodesmidae, Platyrhachidae, Oxydesmidae, Gomphodesmidae. Das Tierreich 69: 1–486.

Attems C (1940) Myriapoda 3. Polydesmidea III. Fam. Polydesmidae, Vanhoeffeniidae, Cryptodesmidae, Oniscodesmidae, Sphaerotrichopidae, Peridontodesmidae, Rhachidesmidae, Macellolophidae, Pandirodesmidae. Das Tierrerich 70: 1–577.

Brolemann HW (1920) Myriapodes III. Diplopoda. In: Shultz A (Ed.) Voyage de Ch. Alluaud et R. Jeannel en Afrique Orientale (1911–1912). Résultats scientifiques, Librairie des Sciences Naturelles Léon Lhomme, Paris: 49–298. https://biodiversitylibrary.org/page/56511877

Carl J (1932) Diplopoden aus Süd-Indien und Ceylon. 1. Teil. Polydesmoidea. Revue Suisse de Zoologie 39(17): 411–529. https://doi.org/10.5962/bhl.part.118948

Chamberlin RV (1945) On some diplopods from the Indo-Australian Archipelago. American Museum Novitates 1282: 1–42.

Golovatch SI, VandenSpiegel D (2014) Notes on Afrotropical Pyrgodesmidae, 1 (Diplopoda: Polydesmida). Arthropoda Selecta 23(4): 319–335. http://kmkjournals.com/upload/PDF/ArthropodaSelecta/23/23_4_319_335_Golovatch_VandenSpiegel_for_Inet.pdf

Golovatch SI, VandenSpiegel D (2015) A new species of the millipede genus *Cryptocorypha* Attems, 1907, from Myanmar (Diplopoda: Polydesmida: Pyrgodesmidae). Arthropoda Selecta 24(1): 27–31. http://kmkjournals.com/upload/PDF/ArthropodaSelecta/24/24_1_027_031_Golovatch_VandenSpiegel_for_Inet.pdf

Golovatch SI, Mikhaljova E, Chang HW (2011a) The millipede families Cryptodesmidae, Haplodesmidae, Pyrgodesmidae, Opisotretidae and Xystodesmidae in Taiwan (Diplopoda, Polydesmida). Tropical Natural History 11(2): 119–134. https://tci – thaijo.org/index.php/tnh/article/view/102999

Golovatch SI, Geoffroy JJ, VandenSpiegel D (2013) A new species of the millipede genus *Cryptocorypha* Attems, 1907, from Vanuatu, Melanesia, southwestern Pacific (Diplopoda: Polydesmida: Pyrgodesmidae). Arthropoda Selecta 22(4): 333–337. http://kmkjournals.com/upload/PDF/ArthropodaSelecta/22/22_4%20333_337%20Golovatch%20Cryptocorypha%20for%20Inet.pdf

Golovatch SI, Nzoko Fiemapong AR, VandenSpiegel D (2017) Notes on Afrotropical Pyrgodesmidae, 3 (Diplopoda: Polydesmida). Arthropoda Selecta 26(3): 175–215. http://kmkjournals.com/upload/PDF/ArthropodaSelecta/26/26_3_175_215_Golovatch_et_al_for_Inet.pdf

Golovatch SI, Semenyuk II, VandenSpiegel D, Anichkin AE (2011b) Three new species of the millipede family Pyrgodesmidae from Nam Cat Tien National Park, southern Vietnam (Diplopoda: Polydesmida). Arthropoda Selecta 20(1): 1–9. http://kmkjournals.com/upload/PDF/ArthropodaSelecta/20/20_1%20001_009%20Golovatch.pdf

Hoffman RL (1977) Diplopoda. La faune terrestre de l'Île de Sainte-Hélène, 4ème partie. Annales du Musée Royal de l'Afrique Centrale 220: 360–377.

Likhitrakarn N, Golovatch SI, Panha S (2017) The first record of the pantropical millipede, *Chondromorpha xanthotricha* (Attems, 1898) (Diplopoda: Polydesmida: Paradoxosomatidae), from Thailand. Arthropoda Selecta 26(4): 281–287. http://kmkjournals.com/upload/PDF/ArthropodaSelecta/26/26_4_281_287_Likhitr_et_al_for_Inet.pdf

Loksa I (1967) The Scientific Results of the Hungarian Soil Zoological Expedition to the Brazzaville-Congo. 32. Diplopoda, I. Opuscula Zoologica, Budapest 7(2): 205–220. http://opuscula.elte.hu/PDF/Opuscula7_1/Loksa,%20I_7_1_10.pdf

Minelli A (Ed.) (2015) The Myriapoda. Volume 2. Treatise on Zoology. Anatomy, Taxonomy, Biology. Brill, Leiden & Boston, 482 pp.

Miyosi Y (1957) Beiträge zur Kenntnis japanischer Myriopoden. 19. Aufsatz: Über eine neue Gattung und zwei neue Arten von Diplopoden. Zoological Magazine 66(1): 29–33 [in Japanese with German abstract].

Murakami Y (1966) Postembryonic development of the common Myriapoda of Japan. XXI. A new genus of the family Oniscodesmidae and a new species of the genus *Archandrodesmus* (Cryptodesmidae). Zoological Magazine 75(2): 30–33 [in Japanese with English abstract].

Pimvichai P, Enghoff H, Panha S, Backeljau T (2018) Morphological and mitochondrial DNA data reshuffle the taxonomy of the genera *Atopochetus* Attems, *Litostrophus* Chamberlin and *Tonkinbolus* Verhoeff (Diplopoda: Spirobolida: Pachybolidae), with descriptions of nine new species. Invertebrate Systematics 32: 159–195. https://doi.org/10.1071/IS17052

Srisonchai R, Enghoff H, Likhitrakarn N, Panha S (2018a) A revision of dragon millipedes I: Genus *Desmoxytes* Chamberlin, 1923, with the description of eight new species (Diplopoda, Polydesmida, Paradoxosomatidae). ZooKeys 761: 1–177. https://doi.org/10.3897/zookeys.761.24214

Srisonchai R, Enghoff H, Likhitrakarn N, Panha S (2018b) A revision of dragon millipedes II: The new genus *Nagaxytes*, with the description of three new species (Diplopoda, Polydesmida, Paradoxosomatidae). European Journal of Taxonomy 462: 1–44. https://doi.org/10.5852/ejt.2018.462

Srisonchai R, Enghoff H, Likhitrakarn N, Panha S (2018c) A revision of dragon millipedes III: The new genus *Gigaxytes*, with the description of three new species (Diplopoda, Polydesmida, Paradoxosomatidae). European Journal of Taxonomy 463: 1–43. https://doi.org/10.5852/ejt.2018.463

Srisonchai R, Enghoff H, Likhitrakarn N, Panha S (2018d) A revision of dragon millipedes IV: The new genus *Spinaxytes*, with the description of nine new species (Diplopoda, Polydesmida, Paradoxosomatidae). ZooKeys 797: 19–69. https://doi.org/10.3897/zookeys.797.29510

Zhang CZ, Li ZY (1981) Eine neue Art vom *Archandrodesmus* (Cryptodesmidae, Diplopoda) aus China. Acta Zootaxonomica Sinica 63: 250–252 [in Chinese with German abstract].

ZooKeys 833: 133–150 (2019)
doi: 10.3897/zookeys.833.32736
http://zookeys.pensoft.net

RESEARCH ARTICLE

A peer-reviewed open-access journal
ZooKeys
Launched to accelerate biodiversity research

Four new species of the trapdoor spider genus *Conothele* Thorell, 1878 (Araneae, Halonoproctidae) from China

Hao Liu[1], Xin Xu[1,2], Zengtao Zhang[1], Fengxing Liu[1], Daiqin Li[3]

1 *State Key Laboratory of Biocatalysis and Enzyme Engineering, Centre for Behavioural Ecology and Evolution (CBEE), School of Life Sciences, Hubei University, 368 Youyi Road, Wuhan 430062, Hubei Province, China*
2 *College of Life Sciences, Hunan Normal University, 36 Lushan Road, Changsha 410081, Hunan Province, China*
3 *Department of Biological Sciences, National University of Singapore, 14 Science Drive 4, 117543, Singapore*

Corresponding author: *Xin Xu* (xuxin_09@163.com); *Daiqin Li* (dbslidq@nus.edu.sg)

Academic editor: *C. Hamilton* | Received 29 December 2018 | Accepted 30 January 2019 | Published 1 April 2019

http://zoobank.org/EDCF57EA-B7D9-4C8F-98F4-6AB6A8F6FDD4

Citation: Liu H, Xu X, Zhang Z, Liu F, Li D (2019) Four new species of the trapdoor spider genus *Conothele* Thorell, 1878 (Araneae, Halonoproctidae) from China. ZooKeys 833: 133–150. https://doi.org/10.3897/zookeys.833.32736

Abstract

Herein four species of the trapdoor spider genus *Conothele* Thorell, 1878 collected from China are described as new to science based on the female genital morphology: *C. baisha* **sp. n.** (Hainan Province), *C. baoting* **sp. n.** (Hainan Province), *C. linzhi* **sp. n.** (Tibet), and *C. jinggangshan* **sp. n.** (Jiangxi Province). For two Hainan species, *C. baisha* **sp. n.** and *C. baoting* **sp. n.**, between which it is difficult to distinguish solely based on female genital morphology, additional diagnoses derived from species-specific nucleotide substitution information and genetic distances using the mitochondrial gene, cytochrome c oxidase subunit I are provided.

Keywords

Araneae, China, COI, DNA barcode, Mygalomorphae, taxonomy

Introduction

Conothele Thorell, 1878 is a genus of trapdoor spiders belonging to the family Halonoproctidae Pocock, 1901 (Opisthothelae: Mygalomorphae) that was recently elevated from the family Ctenizidae based on molecular-based evidence (Godwin et al. 2018).

Copyright *Hao Liu et al.* This is an open access article distributed under the terms of the Creative Commons Attribution License (CC BY 4.0), which permits unrestricted use, distribution, and reproduction in any medium, provided the original author and source are credited.

Like many poor-dispersal, ground-dwelling trapdoor spiders (although some species of *Ummidia* Thorell, 1875 disperse by ballooning (Coyle 1985; Fisher et al. 2014)), *Conothele* spiders construct underground burrows which are lined with silk and opened to the surface with a trapdoor. The trapdoor is usually covered with a layer of soil, leaf litter, and/or moss, which blend well in the surrounding environment, making them difficult to locate in nature (Fig. 1; Bond and Coyle 1995; Xu et al. 2017a; Yang and Xu 2018).

Conothele was previously placed in the family Ctenizidae. However, the two Ctenizidae subfamilies, Ctenizinae and Ummidiinae (Raven 1985; Ortiz 2007), and even the entire family were not monophyletic (Hedin and Bond 2006; Ayoub et al. 2007; Bond et al. 2012; Opatova et al. 2013). Recently, Godwin et al. (2018) relimited the whole family and subfamilies based on molecular phylogenetic evidence, and split it into two families, Halonoproctidae and Ctenizidae. Halonoproctidae now comprises six genera and 87 species belonging to two subfamilies, Ummidiinae Ortiz, 2007 (*Conothele*, *Latouchia* Pocock, 1901, and *Ummidia*) and Halonoproctinae Pocock 1901 (*Bothriocyrtum* Simon, 1891, *Cyclocosmia* Ausserer, 1871, and *Hebestatis* Simon, 1903) (Godwin et al. 2018; World Spider Catalog 2019).

The two ummidiin genera *Conothele* and *Ummidia* share some common morphological and behavioral characters, thus they were considered as undistinguishable (Main 1985; Decae 2010). One of the most obvious shared features by two genera is the presence of a saddle depression on tibia III (Gertsch 1979; Coyle 1981; Ortiz 2007), leading some authors to consider both genera as synonyms (Decae 2010). However, these two genera are completely separated geographically, with *Conothele* being distributed in the Orient and Australasian regions, and *Ummidia* being found in the New World and Mediterranean regions (Xu et al. 2017a; Godwin et al. 2018; Yang and Xu 2018). In addition, they are reciprocally monophyletic, and currently considered as valid genera based on phylogenetic analyses (Godwin et al. 2018).

Conothele contains 26 described species that are widely distributed in the Orient (China, India, Japan, Laos, Myanmar, Sumatra) and Australasia (World Spider Catalog 2019). Until now, only seven species have been described from China primarily based on either female or male morphology (World Spider Catalog 2019), including *C. taiwanensis* (Tso, Haupt & Zhu, 2003) (♂♀; Taiwan Province), *C. baiyunensis* (Xu, Xu & Liu, 2017) (♀; Guangzhou Province), *C. daxinensis* (Xu, Xu & Li, 2017) (♀; Guangxi Province), *C. sidiechongensis* (Xu, Xu & Liu, 2017) (♀; Yunnan Province), *C. yundingensis* (Xu, Xu & Li, 2017) (♀; Yunnan Province), *C. cangshan* (Yang & Xu, 2018) (♂; Yunnan Province) and *C. deqin* (Yang & Xu, 2018) (♂; Yunnan Province).

In this study, we diagnosed and described four new *Conothele* species collected in China based on female morphology as we were unable to obtain adult males (Fig. 2). As in other halonoproctid studies (Xu et al. 2017a; Yang and Xu 2018), both male and female morphology should be described for a new species; however, often it is impractical or impossible to collect adult males by direct searching or by excavating burrows. The standard DNA alignment of the mitochondrial cytochrome *c* oxidase subunit (COI), which provides the species-specific nucleotide substitution information in the animal barcoding gene region, has been widely used to diagnose species

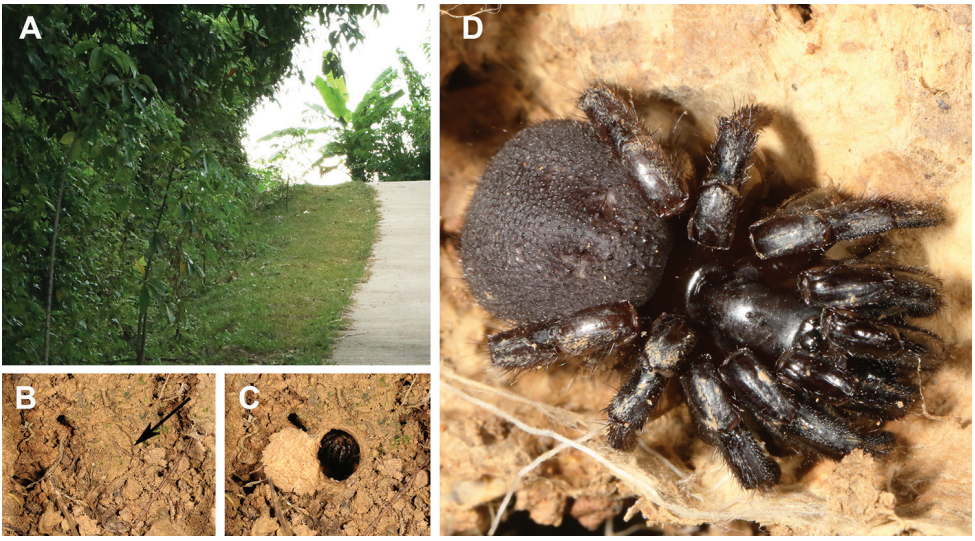

Figure 1. Microhabitat, burrow with a trapdoor, and general somatic morphology of *Conothele baisha* sp. n. **A** microhabitat **B, C** burrow exterior **B** the trapdoor with the door closed **C** the trapdoor with door open **D** female (LH-2017-089; Jishi Village, Changjiang County, Hainan Province, China).

(Brower 2010; Cook et al. 2010; Planas and Ribera 2015; Xu et al. 2015, 2017b). Therefore, for the two new species from Hainan Province (*Conothele baisha* sp. n. and *C. baoting* sp. n.) that show similar morphology and considerable intraspecific variations in female genitalia, we provided additional evidence of species-specific nucleotide substitutions and genetic distances based on COI to support our identifications and for future verification of males.

Materials and methods

All specimens were collected from Tibet, Hainan, Jiangxi Provinces, China (Fig. 2). The right four legs of adult females were removed and stored in 100% ethanol at -80 °C for the molecular work. The rest of each specimen was stored as a voucher in 75–80% ethanol for morphological examination. All the voucher specimens were examined under an Olympus SZX16 stereomicroscope, and they were photographed using a Leica M205C digital microscope. Genitalia were cleaned by Protease K digest for 3 hrs at 56 °C. All the voucher specimens were deposited at the **CBEE** (Centre for Behavioural Ecology and Evolution), School of Life Sciences, Hubei University, Wuhan, China. All measurements were carried out under a Leica M205C digital microscope and given in millimeters. Standard measurements were made following Decae (2010). Measurements of legs and palps are given in the following order: Leg total length (femur + patella + tibia + metatarsus + tarsus), palp total length (femur + patella + tibia + tarsus).

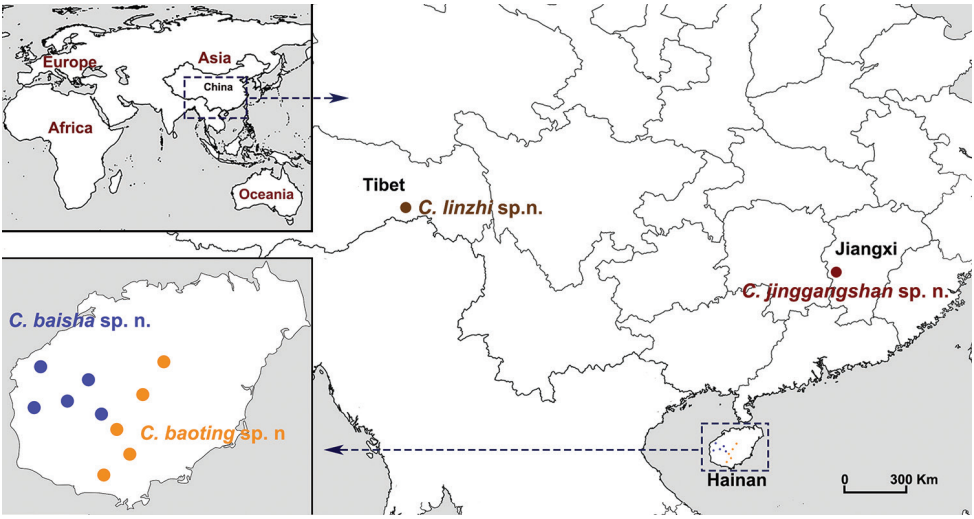

Figure 2. A map showing the distribution of four new species.

Abbreviations used are:

ALE anterior lateral eye;
AME anterior median eye;
PLE posterior lateral eye;
PME posterior median eye;
MOA median ocular area;
PMS posterior median spinneret;
PLS posterior lateral spinneret;
TL total length (including chelicerae but excluding spinnerets).

We extracted the total genomic DNA using the universal genomic DNA extraction kit (CWBIO) from one or two right legs per specimen depending on the size of the legs. The 25 µL PCR reaction included 12.5 µl 2 × TaqMaster Mix (TIANGEN), 9.5 µl double-distilled H_2O (ddH_2O), 1 µl genomic DNA and 1 µl of each forward and reverse primer (10 µM). The primer pairs of COI were LCO1490 (5'-GGTCAACAAATCATAAAGATATTGG-3') and HCO2198 (5'-TAAACTTCAGG GTGACCAAA AAATCA-3') (Folmer et al. 1994). The PCR reaction protocol: initial denaturation at 94 °C for 5 min; 35 cycles of denaturation at 94 °C for 30 s, annealing at 40 °C for 45s and elongation at 72 °C for 1 min, and final extension at 72 °C for 10 min. The PCR products were visualized by agarose gel electrophoresis (1% agarose). All PCR products were purified and sequenced at the TSINGKE Biological Technology (Wuhan China) or Sunny Biological (Shanghai China). The species-specific nucleotide substitutions in the standard DNA barcode alignment and genetic distances were identified using MEGA v6 (Tamura et al. 2013; Xu et al. 2017b).

Taxonomy

Genus *Conothele* Thorell, 1878

Type. *Conothele malayana* (Doleschall 1859): 5, pl. 5, fig. 8 (described female).

Diagnosis. The genus *Conothele* can be distinguished from all other Halonoproctidae genera other than *Ummidia* by the presence of a saddle depression on tibia III (Coyle 1981; Ortiz 2007; Decae 2010). *Conothele* differs from *Ummidia* by their burrowing habits. The former constructs a short, parallel to the surface of ground, superficial burrow, whereas the latter digs a several centimeters long burrow in the soil (Haupt 2006). Moreover, the geographical ranges of *Ummidia* and *Conothele* are completely separated, with *Conothele* being distributed in the Orient and Australasian regions, and with *Ummidia* being distributed in the New World and Mediterranean regions (Xu et al. 2017a; Godwin et al. 2018; Yang and Xu 2018; World Spider Catalog 2019).

Conothele linzhi sp. n.

http://zoobank.org/93117D0B-1A52-4CC3-9E67-044B44BB7DAF
Fig. 3

Holotype. Female (LH-2017-051), collected in Baishuwang Garden Roadside, Bayi Town, Linzhi City, Tibet, China, 29.6106N, 94.4040E, 2980 m a.s.l., 14 July 2017, collected by FX Liu, ZT Zhang, J Chen and J Liu (CBEE).

Paratypes. 3 females (LH-2017-046, LH-2017-048, LH-2017-050), collected at the same locality as the holotype (CBEE).

Diagnosis. Females of *C. linzhi* sp. n. can be distinguished from those of the other *Conothele* species by an obviously large irregularly duct-like sigillum in the sternum center (Fig. 3C); by the terminal lobes of spermathecae hemisphere-shaped; by the distal part of stalks Z-shaped and tilted slightly anteriorly (Fig. 3G-J).

Description. TL 19.26; chelicerae length 2.51, carapace 7.39 long, 7.15 wide; opisthosoma 9.43 long, 7.38 wide. Carapace brownish black, glabrous, with a few slender setae on or behind the eye tubercle. Caput arched. Fovea deep and darker (Fig. 3A). Eight eyes in two rows, with the anterior eye row procurved, and the posterior eye row straight (Fig. 3E); eye group 0.93 long, 1.48 wide; ALE-AME 0.29, AME-AME 0.18, PLE-PME 0.08, PME-PME 0.38; MOA 0.64 long, front width 0.56, back width 0.82; ALE: AME: PLE: PME (0.48: 0.19: 0.33: 0.21). Many slender setae on clypeus (Fig. 3E). Chelicerae black (dorsal view); inner margin with 6 teeth, outer margin with 9 teeth. Labium, coxae of palp and sternum brownish black (Fig. 3C). Labium 1.27 long, 1.47 wide, with 19 conspicuous cuspules. Coxae of palp 2.78 long, 1.86 wide, with approx. 68 conspicuous cuspules (the right one, ventral view) (Fig. 3C). Sternum 4.60 long, 4.65 wide, with an obviously large, irregularly shaped sigillum in the center and with many setae (Fig. 3C).

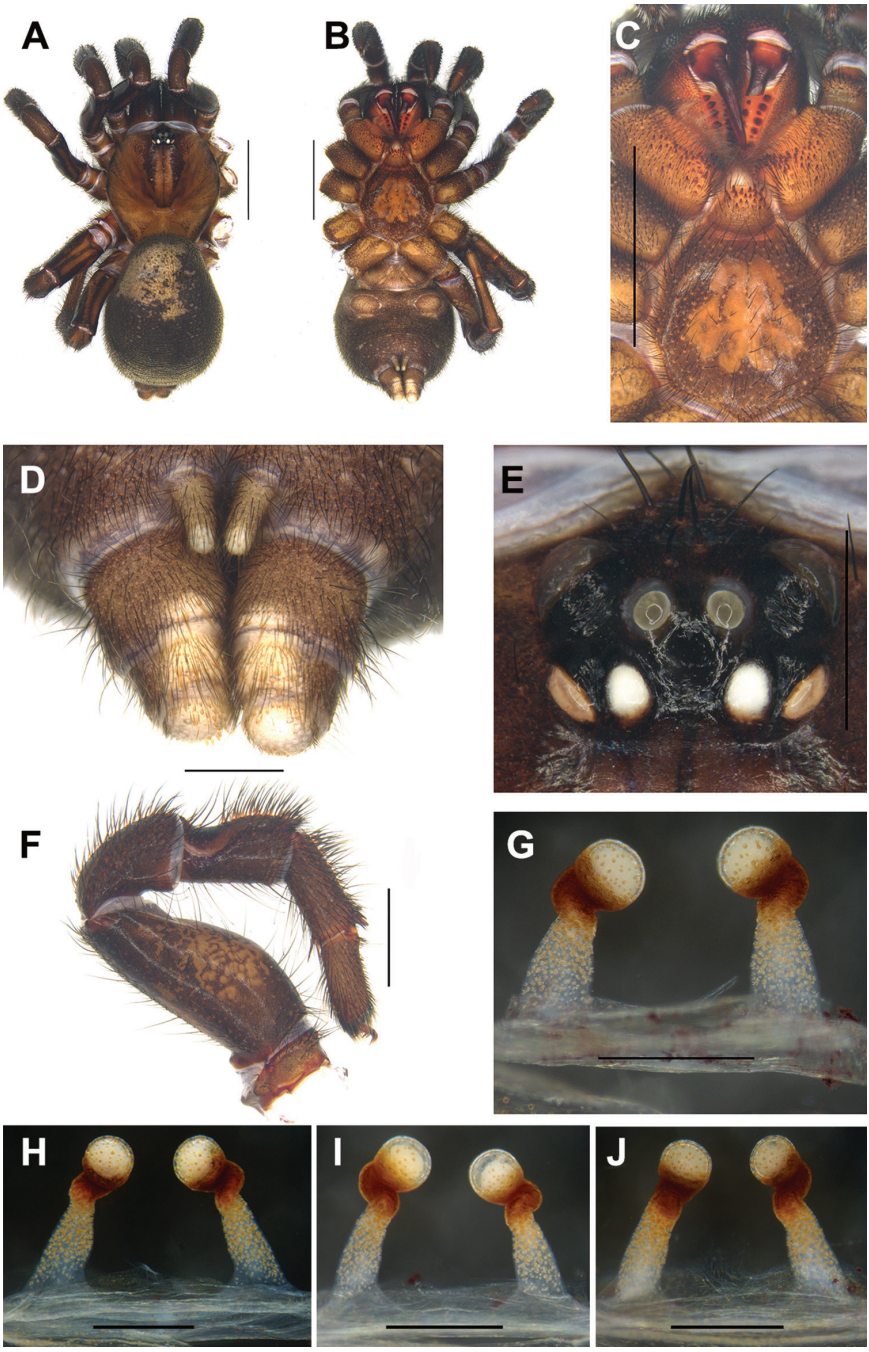

Figure 3. General somatic morphology and female genitalia of *Conothele linzhi* sp. n. **A–G** holotype (LH-2017-051) **A** dorsal view **B** ventral view **C** chelicerae, labium, coxae of palp and sternum, ventral view **D** spinnerets, ventral view **E** eyes, dorsal view **F** left leg III, prolateral view **G–J** female genitalia, dorsal view **H–J** paratypes **H** (LH-2017-046) **I** (LH-2017-048) **J** (LH-2017-050). Scale bars: 5 mm (**A–C**); 1 mm (**D, E**); 2 mm (**F**); 0.5 mm (**G–J**).

Legs brownish black, with long and short black dense setae. Tibia III with a saddle-like depression dorsally on the basal part, and the depression is smaller than that of the other *Conothele* species (Fig. 3F). Palp with a single tarsal claw and a denticle on the claw. Legs each with three tarsal claws, paired claws with one denticle. Leg formula: IV, I, II, III. Measurements of palp and legs: palp 13.25 (4.99+2.02+3.51+2.73), leg I 15.25 (5.65+2.66+3.61+2.12+1.21), leg II 12.74 (4.52+2.13+2.65+2.06+1.38), leg III 12.70 (4.52+1.84+2.33+2.00+2.01), leg IV 16.22 (5.22+2.24+2.77+3.13+2.86).

Opisthosoma ellipsoid and black, scattered with thick and slender black setae. Spinnerets brown (Fig. 3D), PMS one-segmented, 0.86 long, PMS-PMS 0.23; PLS divided into three sections, 2.17 long. Female genitalia with a pair of spermathecae slightly tilted to the middle; the terminal lobes of spermathecae hemisphere-shaped; stalks sclerotized and Z-shaped distally, and tilted slightly anteriorly (Fig. 3G-J).

Male. Unknown.

Etymology. The species epithet, a noun in apposition, refers to the type locality.

Distribution. Tibet (Linzhi City).

***Conothele jinggangshan* sp. n.**
http://zoobank.org/B259FF23-9B58-40C0-8F4B-11905347CDA9
Fig. 4

Holotype. Female (LH-2017-225), collected in Revolutionary Martyrs Cemetery, Ciping Town, Jinggangshan City, Jian City, Jiangxi Province, China, 26.5881N, 114.1599E, 910 m a.s.l., 12 September 2017, collected by FX Liu, F Li (CBEE).

Diagnosis. Female of *C. jinggangshan* sp. n. can be distinguished from those of the other *Conothele* species by the sternum with a pair of obvious elliptic sigilla (Fig. 4C); by the distal part of stalks which are outwardly and then inwardly bend, somewhat semi-circle-like (Fig. 4G).

Description. TL 13.74; chelicerae length 1.77, carapace 6.62 long, 5.40 wide; opisthosoma 6.89 long, 5.70 wide. Carapace dark brown, glabrous, with a few slender setae on or behind the eye tubercle (Fig. 4A). Caput arched. Fovea deep and dark (Fig. 4A). Eye tubercle black. Eight eyes in two rows, with the anterior eye row procurved, and the posterior eye row slightly recurved (Fig. 4E); eye group 0.73 long, 1.38 wide; ALE-AME 0.20, AME-AME 0.14, PLE-PME 0.02, PME-PME 0.46; MOA 0.51 long, front width 0.48, back width 0.86; ALE: AME: PLE: PME (0.34: 0.17: 0.30: 0.19). Four slender setae on clypeus (Fig. 4E). Chelicerae dark brown (dorsal view); inner margin with five teeth, outer margin with seven teeth. Labium, coxae of palp and sternum brown (Fig. 4C). Labium 0.82 long, 1.00 wide, with four conspicuous cuspules. Coxae of palp 2.03 long, 1.31 wide, with approx. 41 conspicuous cuspules (the right one, ventral view) (Fig. 4C). Sternum 3.09 long, 2.74 wide, with a pair of obvious elliptic sigilla and with small number of setae (Fig. 4C).

Legs brown, light brown ventrally, with long and short brown sparse setae. Basal part of tibia III with saddle-like depression dorsally (Fig. 4F). Palp with a single tar-

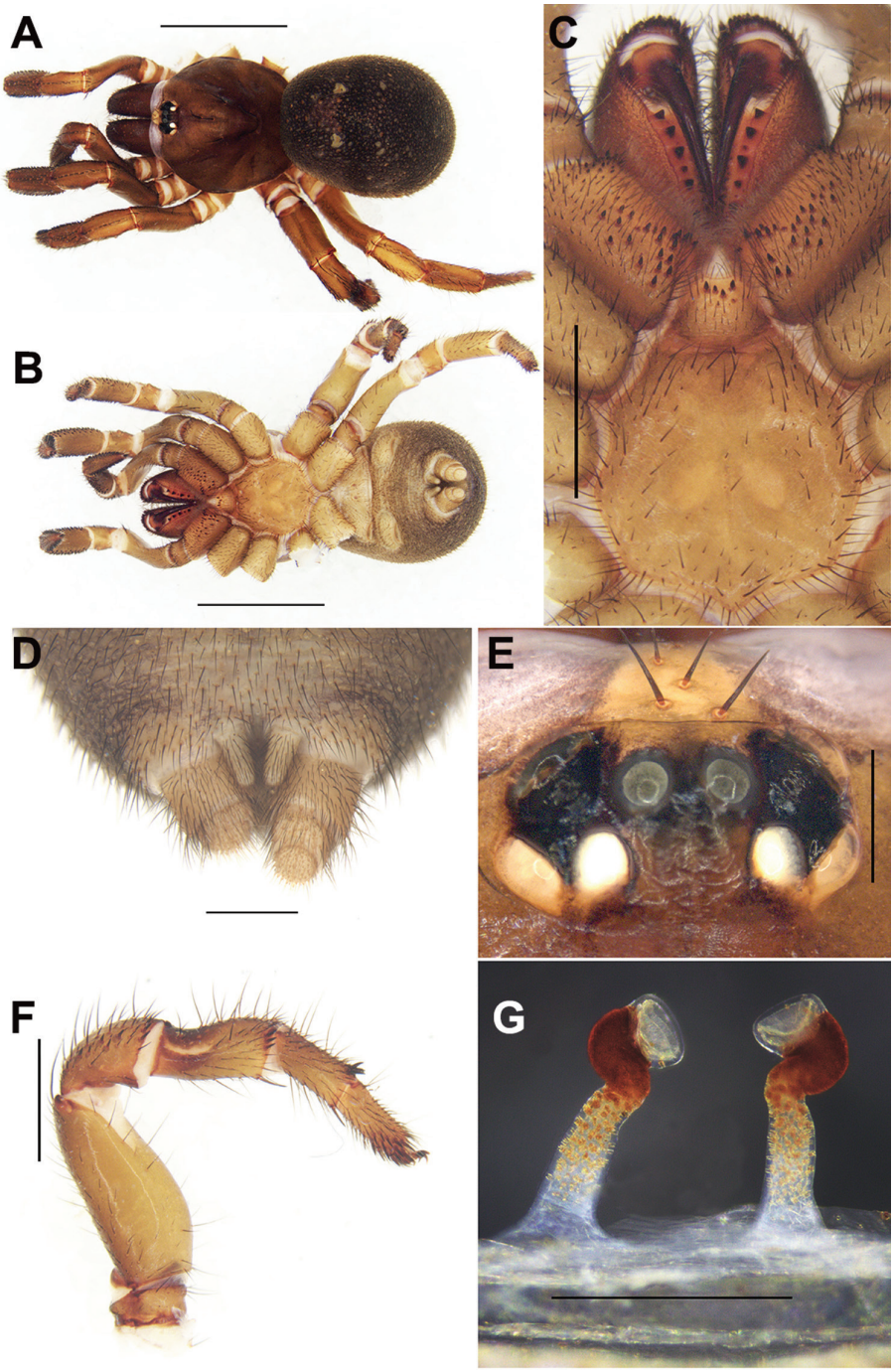

Figure 4. General somatic morphology and female genitalia of *Conothele jinggangshan* sp. n. (holotype, LH-2017-225) **A** dorsal view **B** ventral view **C** chelicerae, labium, coxae of palp and sternum, ventral view **D** spinnerets, ventral view **E** eyes, dorsal view **F** left leg III, prolateral view **G** female genitalia, dorsal view. Scale bars: 5 mm (**A, B**); 1 mm (**D**); 2 mm (**C, F**); 0.5 mm (**E, G**).

sal claw and with two denticles on the claw. Legs each with three tarsal claws, paired claws with one denticle. Leg formula: IV, I, II, III. Measurements of palp and legs: palp 9.07 (3.40+1.42+2.27+1.98), leg I 9.89 (3.65+1.93+2.41+1.04+0.86), leg II 9.40 (3.21+1.66+2.13+1.23+1.17), leg III 9.35 (3.20+1.29+2.01+1.36+1.49), leg IV12.09 (4.14+1.74+2.50+2.16+1.55).

Opisthosoma ellipsoid, black, scattered with slender short black setae. Spinnerets brown (Fig. 4D), PMS short and one-segmented, 0.64 long, PMS-PMS 0.19; PLS divided into three sections, 1.38 long. Genitalia with a pair of spermathecae, each stalk slender, long, distally sclerotized and folded, which is first bent outwards and then inwards, semi-circle-like; with bowl-shaped lobes (Fig. 4G).

Male. Unknown.

Etymology. The species epithet, a noun in apposition, refers to the type locality.

Distribution. Jiangxi Province (Jinggangshan City).

***Conothele baisha* sp. n.**
http://zoobank.org/464B6E9B-B04A-49F8-8516-AE79A33A12A7
Figs 5, 6

Holotype. Female (LH-2017-136), collected in Nanmeiling, Yacha Town, Baisha County, Hainan Province, China, 19.1075N, 109.4227E, 250 m a.s.l., 10 August 2017, collected by FX Liu, D Li, ZT Zhang, X Xu (CBEE).

Paratypes. 2 females (LH-2017-128, LH-2017-135) collected at the same locality as the holotype (CBEE); 1 female (LH-2017-080), collected in Yalong Village, Tianan Township, Donghe Town, Dongfang City, Hainan Province, China, 18.9947N, 108.8976E, 170 m a.s.l., 5 August 2017; 1 female (LH-2017-089), collected in Jishi Village, Changjiang County, Hainan Province, China, 19.2305N, 109.0730E, 170 m a.s.l., 6 August 2017; 1 female (LH-2017-090), collected in Bawangling National Forest Park, Baoshan village, Changjiang County, Hainan Province, China, 19.0757N, 109.0822E, 210 m a.s.l., 7 August 2017; 1 female (LH-2017-161), collected in Shiyixinyi Village, Wuzhishan City, Hainan Province, China. 18.9122N, 109.5118E, 290 m a.s.l., 11 August 2017, all collected by FX Liu, D Li, ZT Zhang, X Xu (CBEE).

Diagnosis. Female genitalia of *C. baisha* sp. n. resembles *C. daxinensis* (Xu, Xu & Li, 2017), but can be distinguished from the latter by the spermathecae with each stalk sturdy, short, simple and direct (Fig. 5G). It can be also distinguished from *C. baoting* sp. n. by short stalks without the trench between the distal part of the stalks and the lobes. Moreover, *C. baisha* sp. n. can be distinguished from *C. baoting* sp. n. by the following unique nucleotide substitutions in the standard DNA barcode alignment: A (13), G (97), A (134), T (157), A (172), G (196), C (205), A (223), T (224), A (253), G (280), C (302), G (304), C (322), A (421), G (424), A (502), G (520), A (592), A (634), G (637).

Description. TL10.35; chelicerae length 1.49, carapace 4.76 long, 4.28 wide; opisthosoma 4.83 long, 4.22 wide. Carapace brown, glabrous, with a few slender setae on or behind the eye tubercle (Fig. 5A). Caput arched. Fovea deep and brown (Fig. 5A).

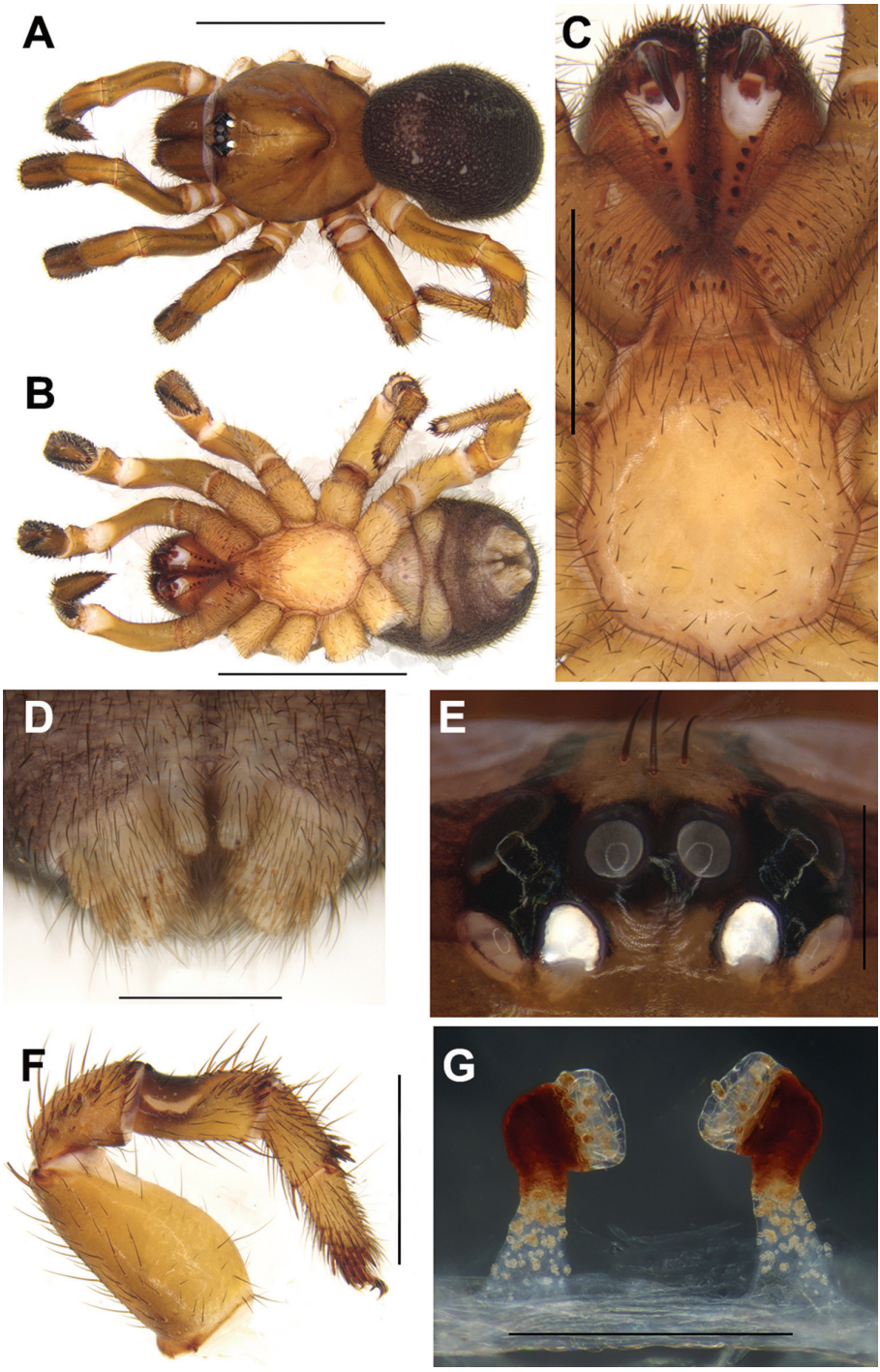

Figure 5. General somatic morphology and female genitalia of *Conothele baisha* sp. n. holotype (LH-2017-136) **A** dorsal view **B** ventral view **C** chelicerae, labium, coxae of palp and sternum, ventral view **D** spinnerets, ventral view **E** eyes, dorsal view **F** left leg III, prolateral view **G** female genitalia, dorsal view. Scale bars: 5 mm (**A, B**); 1 mm (**D**); 2 mm (**C, F**); 0.5 mm (**E, G**).

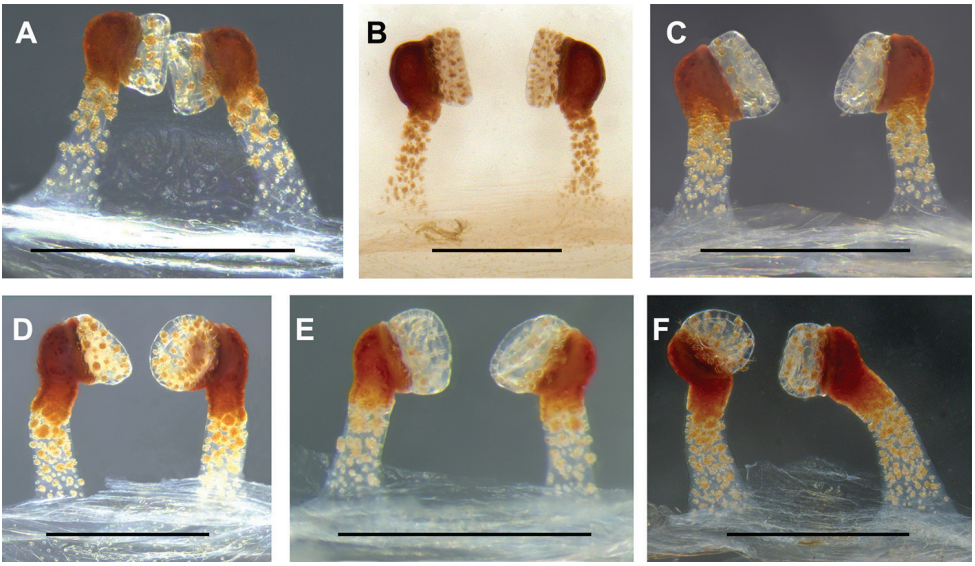

Figure 6. Female genitalia of the paratypes of *Conothele baisha* sp. n. showing the intraspecific variations in spermathecae. **A** (LH-2017-080) **B** (LH-2017-089) **C** (LH-2017-090) **D** (LH-2017-128) **E** (LH-2017-135) **F** (LH-2017-161), dorsal view. Scale bars: 0.5 mm.

Eye tubercle black. Eight eyes in two rows, with the anterior eye row slightly procurved, and the posterior eye row slightly recurved (Fig. 5E); eye group 0.56 long, 1.18 wide; ALE-AME 0.14, AME-AME 0.10, PLE-PME 0.04, PME-PME 0.36; MOA 0.43 long, front width 0.43, back width 0.70; ALE: AME: PLE: PME (0.34: 0.19: 0.23: 0.16). Three slightly thick setae on clypeus (Fig. 5E). Chelicerae dark brown (dorsal view); inner margin with three teeth, outer margin with seven teeth. Labium, coxae of palp and sternum brown (Fig. 5C). Labium 0.53 long, 0.80 wide, with four conspicuous cuspules. Coxae of palp 1.50 long, 1.10 wide, with approx. 13 conspicuous cuspules (the right one, ventral view) (Fig. 5C). Sternum 2.97 long, 2.35 wide, with a large smooth area which lacks setae in the center, but many setae outside this area (Fig. 5C).

Legs brown, with long and short brown sparse setae. Basal part of tibia III with saddle-like depression dorsally (Fig. 5F). Palp with a single tarsal claw, with two denticles on the claw. Legs each with three tarsal claws, paired claws with one denticle. Leg formula: IV, I, III, II. Measurements: palp 6.86 (2.63+1.25+1.42+1.56), leg I 8.11 (2.97+1.46+1.83+0.99+0.86), leg II 7.18 (2.55+1.36+1.54+0.84+0.89), leg III 7.46 (2.92+0.92+1.45+0.92+1.25), leg IV 8.64 (3.07+1.22+1.62+1.42+1.31). Leg II and leg III are almost the same length.

Opisthosoma ellipsoid and black, scattered with many slender, short black setae. Spinnerets brown (Fig. 5D), PMS short and one-segmented, 0.48 long, PMS-PMS 0.08; PLS divided into three sections, 0.78 long. Genitalia with a pair of spermathecae, terminating with face-to-face bowl-shaped lobes; stalks sclerotized distally, each stalk sturdy, short, simple and direct, without the trench between the distal part of the stalks and the lobes (Fig. 5G).

Variation. The female genitalia show considerable intraspecific variations: the spermathecae stalks of the holotype (Fig. 5G) and some paratypes are unbent (Fig. 6A–C, E), or slightly curved (Fig. 6D), or the stalk on the left is tilted to the right by ca. 30°, and the right stalk is curled distally (Fig. 6F). The spermathecae of all samples are face to face, except for one (Fig. 6F).

Male. Unknown.

Etymology. The species epithet, a noun in apposition, refers to the type locality.

Distribution. Hainan Province (Baisha County, Changjiang County, Dongfang City, Wuzhishan City).

GenBank accession numbers. LH-2017-080: MK454955; LH-2017-089: MK454956; LH-2017-090: MK454957; LH-2017-128: MK454958; LH-2017-135: MK454959; LH-2017-136: MK454960; LH-2017-161: MK454961.

Remarks. The mean intraspecific genetic distance of *C. baisha* sp. n. is 1.25 % and 1.23 % using Kimura 2-parameter (K2P) model and *p*-distance model, respectively. The interspecific genetic distance between *C. baisha* sp. n. and *C. baoting* sp. n. is 5.78 % and 5.49 % using K2P and *p*-distance, respectively. This interspecific genetic distance in *Conothele* is comparable to other mygalomorphs identified at 5–6% (Hamilton et al. 2011, 2014).

Conothele baoting **sp. n.**

http://zoobank.org/BB49CB7D-E6A6-4994-A5F3-3F63720DFFA5
Figs 7, 8

Holotype. Female (LH-2017-205), collected in Maoding Village, Shiling Town, Baoting County, Hainan Province, China, 18.6987N, 109.7563E, 160 m a.s.l., 20 August 2017, collected by FX Liu, D Li, X Xu (CBEE).

Paratypes. 1 female (LH-2017-209), collected at the same locality as the holotype (CBEE); 5 females (LH-2017-165, LH-2017-166, LH-2017-167, LH-2017-168, LH-2017-169), collected in Wuzhishan City, Hainan Province, China, 18.8147N, 109.5124E, 260–470 m a.s.l., 12 August 2017, collected by FX Liu, D Li, ZT Zhang, X Xu (CBEE); 4 females (LH-2017-179, LH-2017-180, LH-2017-196, LH-2017-198), collected in Qiongzhong County, Hainan Province, China, 18.9899N, 109.6720E, 190–380 m a.s.l., 14–17 August 2017, collected by FX Liu, D Li, X Xu (CBEE); 1 female (LH-2017-187), collected in Wupo Town, Tunchang County, Hainan Province, China, 19.1380N, 110.0625E, 90 m a.s.l., 15 August 2017, collected by FX Liu, D Li, X Xu (CBEE); 3 females (LH-2017-211, LH-2017-212, LH-2017-213), collected in Baoqian Village, Tianya District, Sanya Ciy, Hainan Province, China, 18.3931N, 109.4224E, 90 m a.s.l., 22 August 2017, collected by FX Liu, D Li, X Xu (CBEE).

Diagnosis. Females of *C. baoting* sp. n. can be distinguished from those of other *Conothele* species by the spermathecae with plate-shaped lobes, each stalk slender, long, distally sclerotized and thickened, and narrowest in the middle. It can be distinguished from *C. baisha* sp. n. by long stalks each with an obvious trench between the distal part of the stalk and the lobe (Fig. 7G). Moreover, *C. baoting* sp. n. can be diagnosed from

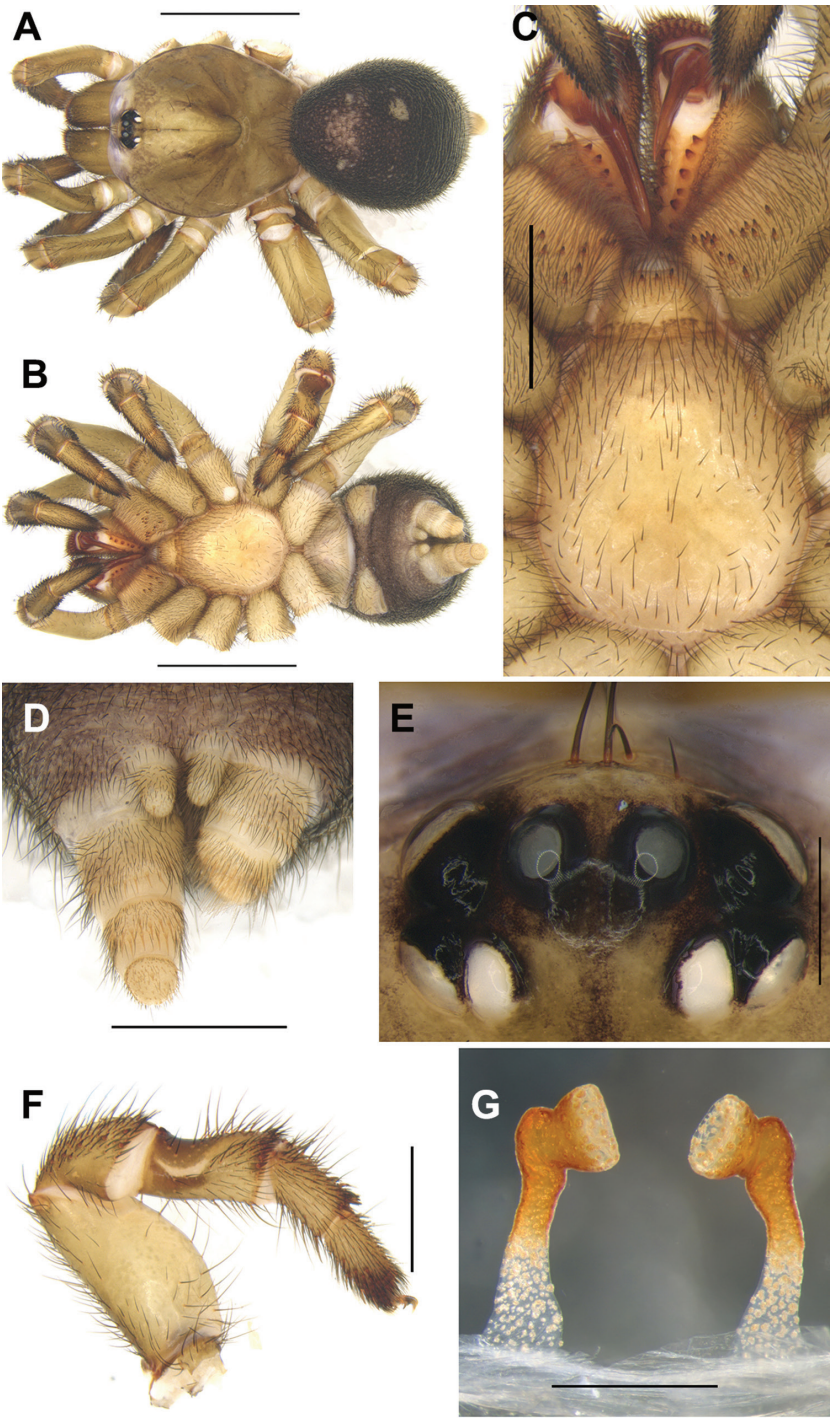

Figure 7. General somatic morphology and female genitalia of *Conothele baoting* sp. n. holotype (LH-2017-205) **A** dorsal view **B** ventral view **C** chelicerae, labium, coxae of palp and sternum, ventral view **D** spinnerets, ventral view **E** eyes, dorsal view **F** left leg III, prolateral view **G** female genitalia, dorsal view. Scale bars: 5 mm (**A, B**); 2 mm (**C, D, F**); 0.5 mm (**E, G**).

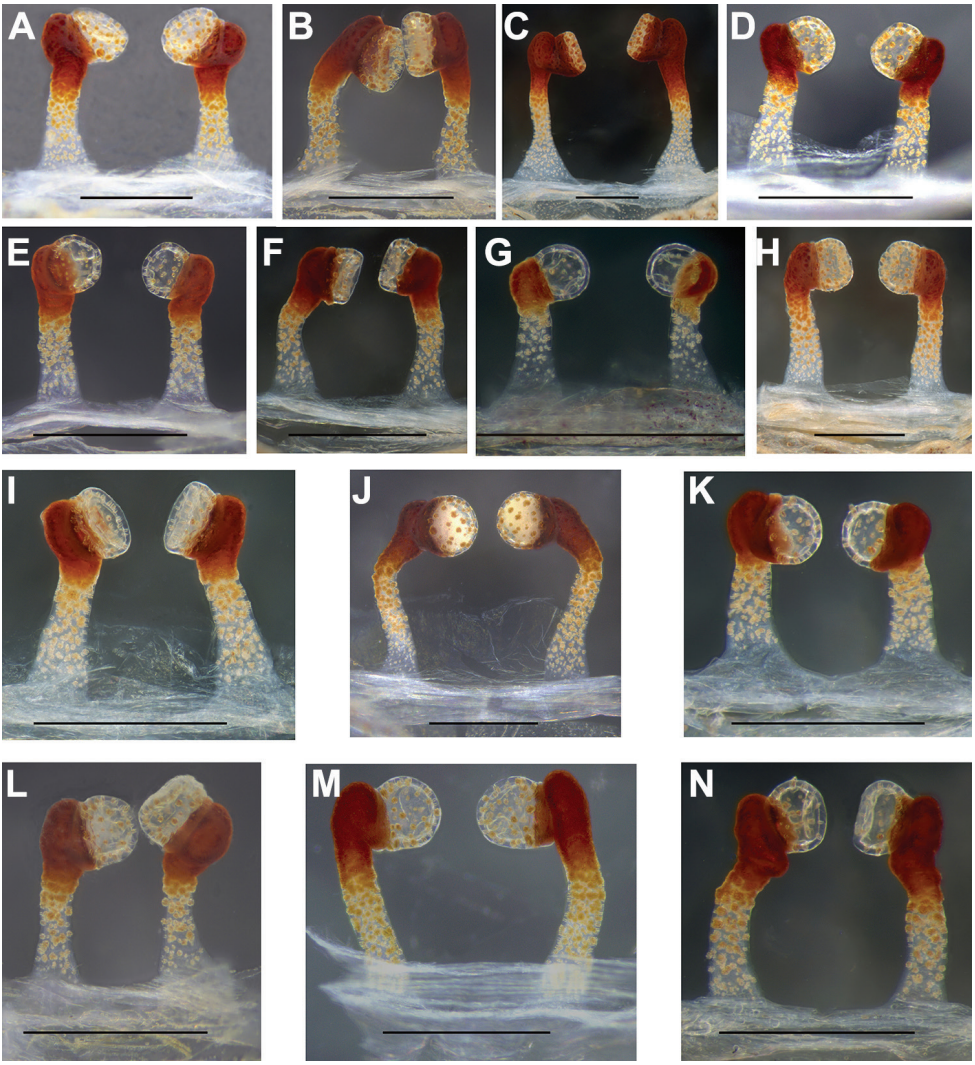

Figure 8. Female genitalia of the paratypes of *Conothele baoting* sp. n. showing the intraspecific variations in spermathecae **A** (LH-2017-165) **B** (LH-2017-166) **C** (LH-2017-167) **D** (LH-2017-168) **E** (LH-2017-169) **F** (LH-2017-179) **G** (LH-2017-180) **H** (LH-2017-187) **I** (LH-2017-196) **J** (LH-2017-198) **K** (LH-2017-209) **L** (LH-2017-211) **M** (LH-2017-212) **N** (LH-2017-213) dorsal view. Scale bars: 0.5 mm.

C. baisha sp. n. by the following unique nucleotide substitutions in the standard DNA barcode alignment: G (13), T (97), G (134), A (157), G (172), A (196), T (205), G (223), C (224), T (253), A (280), T (302), A (304), T (322), C (376), G (421), A (424), G (502), A (520), G (592), G (634), A (637).

Description. TL 14.71, chelicerae length 1.80, carapace 6.92 long, 6.20 wide; opisthosoma 6.52 long, 5.40 wide. Carapace light brown, glabrous, with a few slender setae on or behind the eye tubercle (Fig. 7A). Caput arched. Fovea deep and brown (Fig. 7A). Eye tubercle black. Eight eyes in two rows, with both two eye rows straight (Fig. 7E);

eye group 0.76 long, 1.39 wide; ALE-AME 0.19, AME-AME 0.25, PLE-PME 0.03, PME-PME 0.57; MOA 0.66 long, front width 0.56, back width 0.90; ALE: AME: PLE: PME (0.38: 0.14: 0.32: 0.15). Three slightly thick setae on clypeus (Fig. 7E). Chelicerae light brown (dorsal view); inner margin with five teeth, outer margin with seven teeth. Labium, coxae of palp and sternum brown (Fig. 7C). Labium 0.84 long, 1.41 wide, with three conspicuous cuspules. Coxae of palp 2.04 long, 1.54 wide, with approx. 18 conspicuous cuspules (the right one, ventral view) (Fig. 7C). Sternum 3.91 long, 3.23 wide, with a large smooth area which has a few setae in the center and many setae outside (Fig. 7C).

Legs brown, with long and short brown dense setae. Basal part of tibia III with saddle-like depression dorsally (Fig. 7F). Palp with a single tarsal claw, with two denticles on the claw. Legs each with three tarsal claws, paired claws with two denticles. Leg formula: IV, I, II, III. Measurements: palp 8.73 (3.20+1.58+2.03+1.92), leg I 11.15 (3.99+2.17+2.49+1.49+1.01), leg II 10.37 (3.58+2.11+2.20+1.22+1.26), leg III 9.81 (3.26+1.41+2.10+1.40+1.64), leg IV 11.94 (4.13+1.72+2.25+2.17+1.67).

Opisthosoma ellipsoid, black, scattered with sparse slender, short black setae. Spinnerets brown (Fig. 7D). PMS one-segmented and short, slightly thick, 0.62 long, PMS-PMS 0.12; PLS divided into three sections, 2.23 long. Genitalia with a pair of spermathecae; spermathecae with plate-shaped lobes, each stalk slender, long, distally sclerotized and thickened, and narrowest in the middle. There is an obvious trench between the distal part of the stalk and lobe (Fig. 7G).

Variation. The female genitalia show considerable intraspecific variations: the stalks of some specimens are unbent (Fig. 8A, D, E, G, H, I, K, L), while others are slightly curved (Fig. 8B, C, F, J, M, N); there are three different shapes of lobes of spermathecae, slightly globular (Fig. 8D, E, G, J, K, M, N), bowl-shaped (Fig. 8A, B, F, H, I, L), and plate-shaped (Figs 7G, 8C).

Male. Unknown.

Etymology. The species epithet, a noun in apposition, refers to the type locality.

Distribution. Hainan Province (Baoting County, Qiongzhong County, Sanya Ciy, Tunchang County, Wuzhishan City).

GenBank accession numbers. LH-2017-165: MK454962; LH-2017-166: MK454963; LH-2017-167: MK454964; LH-2017-168: MK454965; LH-2017-169: MK454966; LH-2017-179: MK454967; LH-2017-180: MK454968; LH-2017-187: MK454969; LH-2017-196: MK454970; LH-2017-198: MK454971; LH-2017-205: MK454972; LH-2017-209: MK454973; LH-2017-211: MK454974; LH-2017-212: MK454975; LH-2017-213: MK454976.

Remarks. The mean intraspecific genetic distance of *C. baoting* sp. n. is 0.77 % in K2P and 0.76 % in *p*-distance.

Acknowledgements

This study was supported by the grants from the National Natural Sciences Foundation of China (NSFC) (31272324; 31601850), the Hunan Provincial Natural Science Foundation of China (2017JJ3202), and the Singapore Ministry of Education AcRF

Tier 1 grant (R-154-000-A52-114). We thank Fan Li, He Zhang, Xuan Huang, and also the staff of the Centre for Behavioural Ecology and Evolution (CBEE, Hubei University) for all their help and support throughout this study. We also thank Wenjin Gan for her help in the logistics in the field. We value the positive feedback from Chris Hamilton, Vera Opatova, and Rebecca Godwin.

References

Ayoub NA, Garb JE, Hedin M, Hayashi CY (2007) Utility of the nuclear protein-coding gene, elongation factor-1 gamma (EF-1g), for spider systematics, emphasizing family level relationships of tarantulas and their kin (Araneae: Mygalomorphae). Molecular Phylogenetics and Evolution 42: 394–409. https://doi.org/10.1016/j.ympev.2006.07.018

Bond JE, Coyle FA (1995) Observations on the natural history of an *Ummidia* trapdoor spider from Costa Rica (Araneae, Ctenizidae). The Journal of Arachnology 23: 157–164.

Bond JE, Hendrixson BE, Hamilton CA, Hedin M (2012) A reconsideration of the classification of the spider infraorder Mygalomorphae (Arachnida: Araneae) based on three nuclear genes and morphology. PLoS ONE 7(6): e38753. https://doi.org/10.1371/journal.pone.0038753

Brower AVZ (2010) Alleviating the taxonomic impediment of DNA barcoding and setting a bad precedent: names for ten species of '*Astraptes fulgerator*' (Lepidoptera: Hesperiidae: Eudaminae) with DNA-based diagnoses. Systematics and Biodiversity 8: 485–491. https://doi.org/10.1080/14772000.2010.534512

Cook LG, Edwards RD, Crisp MD, Hardy NB (2010) Need morphology always be required for new species descriptions? Invertebrate Systematics 24: 322–326. https://doi.org/10.1071/IS10011

Coyle FA (1981) Notes on the behaviour of *Ummidia* trapdoor spiders (Araneae, Ctenizidae): burrow construction, prey capture, and the functional morphology of the peculiar third tibia. Bulletin of British Arachnological Society 5: 159–165.

Coyle FA (1985) Ballooning behavior of *Ummidia* spiderlings (Araneae, Ctenizidae). The Journal of Arachnology 13: 137–138.

Decae AE (2010) The genus *Ummidia* Thorell 1875 in the western Mediterranean, a review (Araneae: Mygalomorphae: Ctenizidae). The Journal of Arachnology 38: 328–340. https://doi.org/10.1636/A09-85.1

Doleschall L (1859) Tweede Bijdrage tot de kennis der Arachniden van den Indischen Archipel. Acta Societatis Scientiarum Indica-Neerlandica 5: 1–60.

Fisher JR, Fisher DM, Skvarla MJ, Dowling APG (2014) Pre-ballooning in *Ummidia* Thorell 1875 (Araneae: Ctenizidae) from the Interior Highlands, USA: second account from the region and review of mygalomorph ballooning. The Journal of Arachnology 42: 318–321. https://doi.org/10.1636/B14-43.1

Folmer O, Black M, Hoeh W, Lutz R, Vrijenhoek R (1994) DNA primers for amplification of mitochondrial cytochrome c oxidase subunit I from diverse metazoan invertebrates. Molecular Marine Biology and Biotechnology 3: 294–299.

Gertsch WJ (1979) American spiders. Van Nostrand Reinhold, New York, 274 pp.

Godwin RL, Opatova V, Garrison NL, Hamilton CA, Bond JE (2018) Phylogeny of a cosmopolitan family of morphologically conserved trapdoor spiders (Mygalomorphae, Ctenizidae) using Anchored Hybrid Enrichment, with a description of the family, Halonoproctidae Pocock 1901. Molecular Phylogenetics and Evolution 126: 303–313. https://doi.org/10.1016/j.ympev.2018.04.008

Hamilton CA, Formanowicz DR, Bond JE (2011) Species delimitation and phylogeography of *Aphonopelma hentzi* (Araneae, Mygalomorphae, Theraphosidae): cryptic diversity in North American tarantulas. PLoS ONE 6: e26207. https://doi.org/10.1371/journal.pone.0026207

Hamilton CA, Hendrixson BE, Brewer MS, Bond JE (2014) An evaluation of sampling effects on multiple DNA barcoding methods leads to an integrative approach for delimiting species: A case study of the North American tarantula genus *Aphonopelma* (Araneae, Mygalomorphae, Theraphosidae). Molecular Phylogenetics and Evolution 71: 79–93. https://doi.org/10.1016/j.ympev.2013.11.007

Haupt J (2006) On the taxonomic position of the East Asian species of the genus *Ummidia* Thorell, 1875 (Araneae: Ctenizidae). In: Deltshev C, Stoev P (Eds) European Arachnology 2005, Acta Zoologica Bulgarica Supplement 1: 77–79.

Hedin M, Bond JE (2006) Molecular phylogenetics of the spider infraorder Mygalomorphae using nuclear rRNA genes (18S and 28S): conflict and agreement with the current system of classification. Molecular Phylogenetics and Evolution 41: 454–471. https://doi.org/10.1016/j.ympev.2006.05.017

Main BY (1985) Further studies on the systematics of ctenizid trapdoor spiders: A review of the Australian genera (Araneae: Mygalomorphae: Ctenizidae). Australian Journal of Zoology (Supplementary Series) 108: 1–84. https://doi.org/10.1071/AJZS108

Opatova V, Bond JE, Arnedo MA (2013) Ancient origins of the Mediterranean trap-door spiders of the family Ctenizidae (Araneae, Mygalomorphae). Molecular Phylogenetics and Evolution 69: 1135–1145. https://doi.org/10.1016/j.ympev.2013.08.002

Ortiz D (2007) Ummidiinae, a new replacement name for Pachylomerinae Simon, 1889 (Araneae: Ctenizidae). Boletín Sociedad Entomológica Aragonesa 40: 395–396.

Planas E, Ribera C (2015) Description of six new species of *Loxosceles* (Araneae: Sicariidae) endemic to the Canary Islands and the utility of DNA barcoding for their fast and accurate identification. Zoological Journal of the Linnean Society 174: 47–73. https://doi.org/10.1111/zoj.12226

Raven RJ (1985) The spider infraorder Mygalomorphae (Araneae): cladistics and systematics. Bulletin of American Museum of Natural History 182: 1–180.

Siliwal M, Nair MV, Molur S, Raven R (2009) First record of the trapdoor spider genus *Conothele* (Araneae, Ctenizidae) from India, with a description of two new species. The Journal of Arachnology 37: 1–9. https://doi.org/10.1636/A07-86.1

Tamura K, Peterson D, Peterson N, Stecher G, Nei M, Kumar S (2013) MEGA6: Molecular evolutionary genetics analysis version 6.0. Molecular Biology and Evolution 28: 2731–2739. https://doi.org/10.1093/molbev/msr121

World Spider Catalog (2019) World spider catalog. Natural History Museum Bern, version 20.0. http://wsc.nmbe.ch [Accessed on 30 January 2019]

Xu X, Liu FX, Chen J, Li D, Kuntner M (2015) Integrative taxonomy of the primitively segmented spider genus *Ganthela* (Araneae: Mesothelae: Liphistiidae) – DNA barcoding gap agrees with morphology. Zoological Journal of the Linnean Society 175: 288–306. https://doi.org/10.1111/zoj.12280

Xu X, Xu C, Liu F, Zhang Z, Li D (2017a) Four new species of the trapdoor spider genus *Conothele* Thorell, 1878 from Mainland China and Laos (Araneae, Ctenizidae). ZooKeys 643: 63–74. https://doi.org/10.3897/zookeys.643.10543

Xu X, Liu F, Ono H, Chen J, Kuntner M, Li D (2017b) Targeted sampling in Ryukyus facilitates species delimitation of the primitively segmented spider genus *Ryuthela* (Araneae: Mesothelae: Liphistiidae). Zoological Journal of the Linnean Society 181: 867–909. https://doi.org/10.1093/zoolinnean/zlx024

Yang Z, Xu X (2018) Two new species of the trapdoor spider genus *Conothele* Thorell, 1878 (Mygalomorphae: Halonoproctidae) from China. Zootaxa 4442: 171–180. https://doi.org/10.11646/zootaxa.4442.1.10